SUBSURFACE INVESTIGATION OF PARTS OF BENUE TROUGH AND BORNU BASIN, NORTHEAST NIGERIA, USING AEROMAGNETIC DATA

By

SALAKO, Kazeem Adeyinka
Ph.D/SSSE/2007/219

DEPARTMENT OF PHYSICS

FEDERAL UNIVERSITY OF TECHNOLOGY

MINNA

FEBRUARY, 2014

SUBSURFACE INVESTIGATION OF PARTS OF BENUE TROUGH AND BORNU BASIN, NORTHEAST NIGERIA, USING AEROMAGNETIC DATA

By

SALAKO, Kazeem Adeyinka
Ph.D/SSSE/2007/219

THESIS SUBMITTED TO THE POSTGRADUATE SCHOOL, FEDERAL UNIVERSITY OF TECHNOLOGY, MINNA, NIGERIA IN PARTIAL FULFILLMENT OF THE REQUIREMENTS FOR THE AWARD OF THE DEGREE OF DOCTOR OF PHILOSOPHY (PH.D) IN APPLIED GEOPHYSICS

FEBRUARY, 2014

DECLARATION

I hereby declare that this thesis titled: **Subsurface Investigation of parts of Benue Trough and Bornu Basin, Northeast Nigeria, Using Aeromagnetic Data** is a collection of my original research work and it has not been presented for any other qualification anywhere. Information from other sources (published or unpublished) has been duly acknowledged.

____

SALAKO, Kazeem Adeyinka SIGNATURE/DATE
Ph.D/SSSE/2007/219
FEDERAL UNIVERSITY OF TECHNOLGY, MINNA, NIGERIA.

DEDICATION

This thesis is dedicated to Almighty Allah and to the memory of my late father, Alhaji Jamiu Abefe Afolabi Salako.

CERTIFICATION

The thesis titled: **Subsurface Investigation of parts of Benue Trough and Bornu Basin, Northeast Nigeria, Using Aeromagnetic Data,** by SALAKO, Kazeem Adeyinka (Ph.D/SSSE/2007/219), meets the regulations governing the award of the degree of Doctor of Philosophy (Ph.D) of the Federal University of Technology, Minna, Nigeria and it is approved for its contribution to scientific knowledge and literary presentation.

Prof. E. E. Udensi Major Supervisor	…………………... Signature & Date
Prof. M. A. Daniyan Co-Supervisor	…………………... Signature &Date
Prof. P. I. Olasehinde Co-Supervisor	…………………… Signature &Date
Dr. K. U. Isah Head, Physics Department	…………………… Signature & Date
Prof. G. N. Nsofor Dean, School of Natural and Applied Science	……..……………... Signature & Date
Prof. (Mrs.) S. N. Zubairu Dean, Postgraduate School	………………….. Signature & Date

ACKNOWLEDGEMENTS

All praises and adorations are solely due to Allah, who out of His Mercy actualized this work. It is part of His work and destiny upon me that have made everything possible for me to accomplish this great task of life.

I wish to thank my supervisor, Prof. E.E. Udensi and his wife Dr. (Mrs.) J. Udensi for all the encouragement and understanding and for being such a friend and father to me. I have not just only learnt Geophysics from him, but with humility, perseverance, act of being focused, setting goals as well as other vital virtues of life. Sir, you have left in me an indelible mark of being courageous, purposeful and to make something out of nothing. I remain ever grateful.

Other members of the supervisory committee, who are not just my supervisors but like my father; Prof. M.A. Daniyan and Prof. P.I. Olasehinde, are appreciated for their invaluable contributions and assistances that have helped to make this research work successful.

I wish to appreciate the contribution of my lovely wife Mrs. Sekinat Omobola Salako, for her encouragements, patience and her support morally and spiritually for the realization of this work. I also appreciate my children, Ruqayyat, Hamidat and Ikram for their patience and understanding for the critical times I subjected them to in pursuance of this work.

My profound gratitude goes to my brothers and sisters, Alh. Tia'miyu A. Salako, Mal. Mushafa'u, Mrs. Bintu, Mrs. Wuleimat, Mrs. Hidayat, and Mrs. Simia't for all their prayers and encouragement, and understanding.

I wish to appreciate all members of Islamic Brotherhood Forum (IBF), FUT Minna, Prof. O.K. Abubakre, Prof. A.M. Junaid, Prof. Y.A. Sanusi, Dr. Y.A. Iyaka, Dr, A.I.

Gambari, Dr. S.K. Abdulkareem, Mal. Ganiyu Shefiu (Don Jos) and Mr. A.A. Oke. Jazakumu llahu khaeran katheeran.

I feel very much indebted to my fathers and colleague in the Department of Physics, FUT Minna, the HOD, Dr. K.U. Isah, Prof. O.D. Oyedum, Prof. O.B. Awojoyegbe, Prof. A.N. Baba-Kutigi, Dr. Uno E. Uno, Dr. A. Umaru, Mr. M.K. Kolo, Mr. S.A.S Jonah, Mr. A.A. Adetona, Mr. A.A. Rafiu, Mr. I.O. Olarinoye, Mr. K. Igwe, Mr. J. Ezenwora, Miss J.O. Eichie, Mr. M. Agida, Mal. M.I. Kimpa, Mr. G.I. Aku, Mal. M. Bature, Mal. U.D. Alhassan, Mr. O.M. Dada, Mr. M. Abiodun, all Technical staff, Mrs M. Lori, and Mr. Musa for all the encouragements, assistance and advices offered me.

My special thanks go to Mr. A.A. Adetona who is not only a colleague but had contributed greatly in actualizing this work. Also my appreciation goes to Mr. D. Olaniyan (formerly NGSA), Mr. A.A. Rafiu, Mr. Eletta Bolaji and Mrs. N.P. Ofor for their support and encouragements at all times. My special appreciation goes to the staff and management of Nigerian Geological Survey Agency for the use of their facilities in processing the data and for other personal helps.

I also appreciate all the prayers, concerns and supports of all my students both past and present. I appreciate you all.

ABSTRACT

The geophysical investigation of the subsurface structures of parts of Benue Trough and Bornu Basin, northeast Nigeria, using aeromagnetic data was carried out in this study. The area under investigation is bounded by latitude 9.5^0 N to 12.0^0N and longitude 9.5^0 E to 12.0^0 E. It is covered by 25 aeromagnetic maps. The aeromagnetic maps were digitized on a 3 km by 3 km grid and later compiled to produce a combined aeromagnetic data file of the study area. The 3 km spacing interval imposed a Nyquist frequency of 0.167 km^{-1} while the data file generated comprised of 7921 data points. The data obtained were subjected to filtering process so as to obtain residual data necessary for interpretation. The residual data were subjected to structural analysis using Centre for Exploration Targeting (CET) grid plug-ins, 2D subsurface modelling and depth analysis using spectral analysis and source parameter imaging. The filtering process separated the deep seated (long wavelength) anomaly from the shallow (short wavelength) anomaly. The low magnetic values tend towards northern portion of the study area. The magnetic (structural) trends in the study area were east-west, northeast-southwest, and northwest-southeast trends with the dominating structural trend in the area as northwest-southeast. There were various magnetic lineaments in the study area. These lineaments were suggested to be extension of landward Oceanic fracture zones. The results of CET structural analysis showed that the two basins (Bornu and Benue Trough) had similar structural relationship with more structural activities in Bornu Basin, the basement complex region and the volcanic areas at the eastern part. It also showed that structural similarities exist between the surface geology and the surface lineament map of the area. The maximum sedimentary thickness obtained with spectral analysis was 3.72 km. This occurred in the central part around Gombe and south of Damaturu and Bulkachuwa. The result of the Source Parameter Imaging (SPI) has its maximum sedimentary thickness of about 5.0 km around Gombe, Ako Gombe, Bulkachuwa and Damaturu areas. The result of 2D modelling showed that the sedimentary thicknesses ranged from 0.0 km to a maximum of 4.60 km. The maximum sedimentary thicknesses were found around Gombe, Ako Gombe, Bulkachuwa and Damaturu areas, with a value of about 3.00 km to 4.60 km. The maximum sedimentary thicknesses obtained, which range between 3.72 km to about 4.60 km are adequate for the hosting of hydrocarbons. The minimum sedimentary thickness delineated by these methods could be found around Bauchi axis in the basement complex region, Kaltungo and the volcanic areas in the eastern part of the survey area. The results of these analytical methods were all in agreement. The boundary between the Bornu Basin and the Upper Benue Trough was successfully delineated through trend analysis of the total magnetic intensity, upward continuation filter and 2D modelling of the subsurface structures. The end results of these methods showed that Upper Benue Trough was separated from the Bornu Basin at about latitude 11.0^0 N. This area corresponds to "Dumbulwa-Bage High". However, the subsurface lithology obtained from 2D modelling of the residual field showed the presence of two lithological units. The sedimentary rock unit underlined by the basement rock consists of shales, sandstones, limestones, siltstones, clay and non-marine facies, while the Basement rock units were composed of pegmatite, granite gneiss and migmatites.

TABLE OF CONTENTS

LIST OF FIGURES

LIST OF TABLE

LIST OF ABBREVIATION

Abbreviation	Meaning
CET	Centre for Exploration Targeting
TMI	Total Magnetic Intensity
FFT	Fast Fourier Transform
RTE	Reduce to magnetic equator
RTP	Reduce to Magnetic Pole
SPI	Source Parameter Imaging
SRTM	Shuttle Radar Topographic Mission
UTM	Universal Transverse Mercator
nT	nano Tesla

CHAPTER ONE

1.0 INTRODUCTION

1.1 Background to the Study

1.1.1 Field of Applied Geophysics

The science of Geophysics applies the principles of physics to the study of the Earth. Geophysical investigations of the interior of the Earth involve taking measurements at or near the Earth's surface that are influenced by the internal distribution of physical properties. Analysis of these measurements can reveal how the physical properties of the Earth's interior vary vertically and laterally. By working at different scales, geophysical methods may be applied to a wide range of investigations from studies of the entire Earth to exploration of a localised region of the upper crust for engineering or other purposes (Kearey, Brooks and Hill, 2004).

The cardinal point in applied geophysics is to add a third dimension to geological maps. The trained eye of the field geologist is replaced with the scientific instrument whose function is to detect changes in the physical properties of the rocks which lie concealed beneath the surface of the earth. Thus, geophysics involves the study of those parts of the earth hidden from direct view by measuring their physical properties with appropriate instruments, usually on the surface. It also includes interpretation of the measurements to obtain useful information on the structure and composition of the concealed zones.

The initial step in the application of geophysics to the search for minerals probably was taken in 1843 when von Wrede pointed out that the magnetic theodolite used by Lamont to measure variations in the earth's magnetic field, might also be employed to discover magnetic ore bodies (Telford, Geldart, Sherrif and Keys, 2001). The continued increase in the demand for metals of all kinds and the enormous increase in the use of oil and natural gas during the past few decades have led to the development of many geophysical techniques of ever-increasing sensitivity for the detection and mapping of unseen deposits and structures. Advances have been especially rapid during the past three decades or so, because of the development of new electronic devices for field equipment and the wide spread application of the digital computer in the interpretation of geophysical data.

Geophysical surveying provides a relatively rapid and cost effective means of deriving aerially distributed information on subsurface geology. In the exploration for subsurface resources, the geophysical methods are capable of detecting and delineating local features of potential interest. Since the majority of mineral deposits are beneath the surface, their detection depends upon those characteristics which differentiate them from the surrounding media. Methods based upon variations in the elastic properties of rocks have been developed for determining structures associated with oil and gas, such as faults, anticlines and synclines, though these are often thousands of meters below the surface. The variations in the electrical conductivity and natural currents in the earth, the rates of decay in the artificial potential differences introduced into the ground, local changes in gravity, magnetism and radioactivity- all provide information to the geophysicist about the nature of the structures below the surface, thus permitting him to determine the most favourable places for locating the mineral deposits he seeks.

Geophysical techniques can therefore only detect a discontinuity, that is, where one region differs sufficiently from another in some property. Applied geophysics in the search for minerals, oil and gas may be divided into the following general methods of exploration: gravity, magnetic, electrical, electromagnetic, seismic, radioactivity, well logging and miscellaneous chemical, thermal and other methods. The choice of technique or techniques to locate a certain mineral depends upon the nature of the mineral and the surrounding rocks.

1.1.2 **Geophysical Methods**

There are broad divisions of geophysical survey methods from those that make use of natural fields of the Earth and to those that require the input into the ground of artificially generated energy. The natural field methods utilize the gravitational, magnetic, electrical and electromagnetic fields of the Earth, searching for local perturbations in these naturally occurring fields that may be caused by concealed geological features of economic or other interest. Artificial source methods involve the generation of local electrical or electromagnetic fields that may be used analogously to natural fields, or, in the most important single group of geophysical surveying methods, the generation of seismic waves whose propagation velocities and transmission paths through the subsurface are mapped to provide information on the distribution of geological boundaries at depth (Kearey, Brooks and Hill, 2004).

Generally, natural field methods can provide information on Earth properties to significantly greater depths and are logistically simpler to carry out than artificial source methods. The latter, however, are capable of producing a more detailed and better resolved picture of the subsurface geology.

Several geophysical surveying methods can be used at sea or in the air. The higher capital and operating costs associated with marine or airborne work are offset by the increased speed of operation and the benefit of being able to survey areas where ground access is difficult or impossible. A wide range of geophysical surveying methods exists, for each of which there is an operative physical property to which the method is sensitive. The type of physical property to which a method responds clearly determines its range of applications. Thus, for example, the magnetic method is very suitable for locating buried magnetic ore bodies because of their magnetic susceptibility. Similarly, seismic or electrical methods are suitable for the location of a buried water table because, saturated rock may be distinguished from dry rock by its higher seismic velocity and higher electrical conductivity (Kearey, Brooks and Hill, 2004).

1.2 **Magnetic Method**

The magnetic and gravity methods have much in common, but magnetic interpretation is generally more complex and variations in the magnetic field are more erratic and localised. This is partly due to the difference between the dipolar magnetic field and the monopolar gravity field, partly due to the variable directions of the magnetic field, whereas the gravity field is always in the vertical direction, and partly due to the time-dependence of the magnetic field, whereas the gravity field is time-invariant (ignoring small tidal variations). A gravity map is usually dominated by regional effects; a magnetic map generally shows a multitude of local anomalies.

The aim of a magnetic survey is therefore to investigate subsurface geology on the basis of anomalies in the Earth’s magnetic field resulting from the magnetic properties of the underlying rocks. Although most rock-forming minerals are effectively non-magnetic, certain rock types contain sufficient magnetic minerals to produce significant magnetic anomalies. Similarly, man-made ferrous objects also generate magnetic anomalies.

The aeromagnetic method of geophysical surveying has been established for more than five decades as a powerful method in mining and petroleum exploration (Reford and Sumner, 1964). Many important discoveries can be either directly or indirectly be credited to aeromagnetic method. The data collection method is also very fast and cheaper than other methods.

1.2.1 **The Aeromagnetic Survey**

The study of the earth's magnetism is the oldest branch of the subject of geophysics. Sir William Gilbert (1540-1603) made the first scientific investigation of the terrestrial magnetism when he showed that the earth's magnetic field was equivalent to that of a permanent magnet, lying in a general north-south direction, near the earth's rotational axis (Telford, Geldart, Sherrif and Keys, 2001). In 1843, Von Wrede first used variations in the magnetic field to locate deposits of magnetic ore. The publication of the Examination of Iron Ore Deposits by Magnetic Measurements by Thalen in 1879 marked the beginning of applied geophysics (Telford, Geldart, Sherrif and Keys, 2001).

The cardinal point of a magnetic survey is to find the distribution of magnetized material whose magnetic field is given on a plane surface. Magnetic prospecting thus involves the measurement of variations in the earth's magnetic field. It is a natural source method in which local variations introduced by magnetic properties of rock near the surface causes minute changes in the main field. Determination of the structure and nature of the magnetized material is therefore an *inverse* problem of potential field theory. That is, the source is determined from its potential (Grant and West, 1965).

Magnetic exploration is carried out on land, at sea and air. Until the middle 1940s, all magnetic exploration was carried out on the ground using field methods similar to those in gravity surveys. Today, virtually all magnetic survey for oil is done from the air or ships. This is also true for most reconnaissance surveys for minerals. The speed, economy and convenience of aeromagnetic surveys are the main factors for this trend. Aeromagnetic interpretation is the drawing of inferences about the geology and ore potential of a given region from aeromagnetic survey data.

Aeromagnetic surveys simply map the distribution of magnetic minerals in the earth's crust. The major magnetic minerals are magnetite, titanhematite, maghemite, pyrotite, and native iron ore Fe-Ni-Co alloys. These minerals give rise to magnetic anomalies, either because of their abnormally large magnetic susceptibilities or because they have high remanent magnetization.

Of the magnetic minerals that occur in nature, magnetite is the most abundant. On a global basis, the others can probably be ignored. Thus aeromagnetic surveys, in particular terms, map the magnetite in the rocks below the aircraft. While aeromagnetic surveys are extensively used as reconnaissance tools, there has been an increasing recognition of their value for evaluating prospective areas by virtue of the unique information they provide. Sharma (1987) outlined the roles of aeromagnetic survey as follows:

i. Delineation of volcano-sedimentary belts under sand or other recent cover, or in strongly metamorphosed terrains when recent lithologies are otherwise unrecognizable.

ii. Recognition and interpretation of faulting, shearing and fracturing not only as potential hosts for a variety of minerals, but also an indirect guide to epigenetic, stress related mineralization in the surrounding rocks.

iii. Identification and delineation of post-tectonic intrusive. Typical of such targets are zoned syenite or carbonatite complexes, kimberlites, tin-bearing granites and mafic intrusions.

iv. Direct detection of deposits of certain iron ores.

v. Identification of environments favourable for groundwater exploitation including fracture systems in crystalline rocks and bedrock aquifers under alluvial covers.

vi. In prospecting for oil, aeromagnetic data can give information from which one can determine depths to basement rocks and thus locate and define the extent of sedimentary basins. Sedimentary rocks however exert such a small magnetic effect compared with igneous rocks that virtually all variations in magnetic intensity measurable at the surface result from topographic or lithologic changes associated with the basement or from igneous intrusions (Dobrin, 1976).

1.3 Statement of the Problem

The Benue Trough is generally known to contain numerous mafic and felsic intrusives, sub- basinal structures with a bright prospect for hydrocarbon accumulation. Benue Trough is also close to the Niger Delta, where most of the hydrocarbon mining activities in the country are taking place. Due to the location of the basin and the expected basement depth predicted by previous researches, has drawn attention to the area due to the possibility of hydrocarbon potential of the Trough. This work will explore the possibility of hydrocarbon potentialities of the Upper Benue Trough and southern Bornu Basin in other to expand the petroleum base of the Country (Nigeria).

1.4 Justification of the Study

The use of modern digital processing tools (conversion of aeromagnetic data from space domain (wavelength) to frequency domain (wave-number) for proper handling and better interpretation) on the aeromagnetic data of the study area is expected to shed more light in unfolding the historical evolution and tectonic settings of the survey area. These digital tools would be combined in such a manner to investigate and interpret the aeromagnetic data covering the survey area and thus the emerging picture is expected to yield better resolution than ever known. The following are the outlines of the objectives that justify this research work:

1. The origin and tectonic evolution of the Benue Trough and Bornu Basin have been the subject of several suggestions. Most of the suggestions are based on qualitative interpretation of data and inferences from regional surveys carried out in the adjacent Benue Trough. While working on the central part of Nigeria, Ajakaiye, Hall, Ashiekaa and Udensi (1991) and Ajakaiye, Hall, Millar, Verhejen, Award and Ojo (1986) noted that magnetic features in the area are mainly magnetic lineaments with definite characteristics which exist within the Nigerian landmass. The lineaments they noted coincided with the major structural trends such as the Benue Trough in Nigeria and fractures in the oceanic crust of West Africa. They stated that onshore lineaments in West Africa are extensions of St. Paul, Romanche, Chain and Charcot fracture zones in the Mid-Atlantic Ocean.

   The lineaments are believed to be part of the major zones of weakness in the crust that predate the opening of the Atlantic Ocean and were reactivated in the early stages of continental drift. Three of these fracture zones, St. Paul, Romanche and Chain are believed to pass through the study area (Latitude 9.5^0 - 12.0^0 and Longitude 9.50 - 12.0^0). By reason of the detailed nature of the present study, qualitative and quantitative analysis of magnetic trends will be made. Suggestions will be put forward in respect of the nature of the magnetic lineaments and their relationship with the St. Paul, Romanche and Chain fracture zones of the Mid- Atlantic.

2. The boundary delineation and mapping of the geological structures within the study area have mostly been done by geologists (Ojo and Pinna, 1982; Whiteman, 1982; Dessauvagie, 1974; Benkhelil (1988 and 1989) and Zaborski, 1998 among others). Detailed geophysical examination has not been carried out

to a large extent as compared to geological survey in the study area which would have correlated the geological results/findings. The present work is expected to achieve this through the use of CET grid analysis.

3. The Benue Trough is of interest due to its large area of coverage, it forms a regional structure which is exposed from the northern frame of the Niger Delta and runs northeast-wards for about l000 km to underneath Lake Chad, where it terminates. For this reason, researches conducted within the area are usually restricted to a section of the basin either the lower, upper or the middle Benue basin. The location of the basin and the expected basement depth predicted by previous researches drawn attention to the area due to the possibility of hydrocarbon potential of the Trough. The Benue Basin is close to the Niger Delta, where most of the hydrocarbon exploration activities in the country are taking place. The average depth estimate by Likkasson, Ajayi and Shemang (2005) was 4.6 km while 5.6 km was obtained by Onwuemesi (1995). These had shown that the depth can be within the range of expected depth for the curie temperature expected for thermal saturation for crude oil. The present work would probably confirm this.

4. The dynamism observed in geophysical data interpretation due to advent of the computer, had opened up a lot of room for more research even within areas that had been investigated. Today we have more efficient analyzing software which can reveal features that might have escaped the sensitivity of previous tools employed. Thus re-evaluating previous studies with more advanced techniques may be useful.

1.5 Aim and Objectives of the Present Study

This study is expected to generate and upgrade the existing geophysical knowledge of the survey area that had been previously made available by other researchers. The primary aim of this study is to produce information (database) that could be a guide to both magnetic mineralisation and hydrocarbon potentialities of the study area and to also serve as a guide to future geological mapping of the study area.

1.5.1 Objectives of the Study

The objectives of this study include:

a) to carry out a surface mapping of the study area and qualitatively analyse the trend to determine prominent structural features of the area;

b) to enhance location of prominent deep seated (long wavelength) anomalies within the study area through the use of upward continuation filter control on the total magnetic intensity data;

c) to delineate the two basins and determine their structural relationship through the use Centre for Exploration Targeting (CET) Grid Analysis;

d) to estimate and analyse depth to magnetic source bodies through spectral depth analysis and Source Parameter Imaging (SPI);

e) to carry out detail modelling of the residual magnetic field anomalies to determine the subsurface structures of the study area, particularly the thicknesses of the two basins (thickness of the sedimentary rocks); and

f) to determine the economic potentials of the study area in terms of hydrocarbon potentials.

1.6 The Study Area (Location and Extent)

The Benue Trough is commonly subdivided into three main domains corresponding to both geological and geomorphologic partitions. These include the Southern (Lower) Benue Trough which covers areas within the south-eastern Nigeria, the central (Middle) Benue Trough which covers Gboko, Makurdi and Lafia areas and the Northern (Upper) Benue Trough that covers Gombe-Yola areas.

The present study area covers extensively the Upper Benue Trough, the southern part of the Chad Basin (also known as lower Bornu Basin), the Keri - Keri Formation around Gombe and part of the Younger Granites region of the Jos and Bauchi areas. This area is situated at the North-Eastern part of Nigeria (Figure 1.1). The area is bounded by Latitude 9.5^0N to 12.0^0N and Longitude 9.5^0E to 12.0^0E. The physiological features recognized in the area are the river Benue and its tributaries like river Gongola, Amumma, Rowai, Ruhu, Misau and so on.

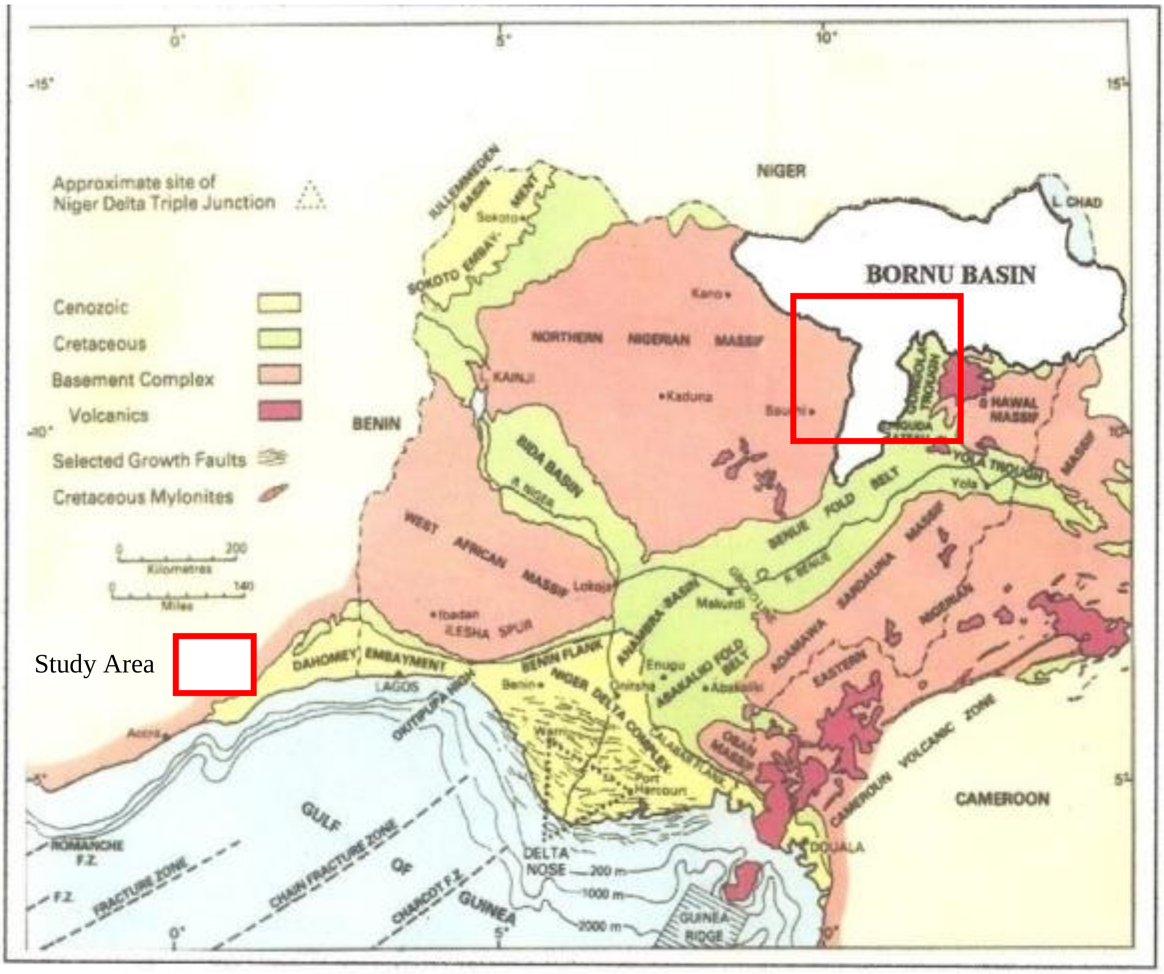

Figure 1.1: Location of the Study Area (parts of Upper Benue Trough and southern Bornu Basin). Adapted from Whiteman (1982).

CHAPTER TWO

2.0 LITERATURE REVIEW

2.1 Overview of Geology of the Study Area

The study area covers extensively the Upper Benue Trough, some parts of Chad Basin (Southern part of Bornu Basin), the Younger Granites (province of Bauchi area) and the Basement Complex (Figure 2.1a). Figure 2.1b is the geological sequence of Figure 2.1a showing the ages of formations and depositions. All the rocks in the area belong either to the Upper Cretaceous or to the Precambrian. All the above mentioned units have already been described in detail by various workers (Buchanan, Macleod, Turner, Berridge, and Black (1971); McCurry (1976); Ajibade (1976); Eborall (1976); Wright (1976); Bowden and Turner (1974)). The sandstones of the Upper Benue Trough and the lower part of the Bornu Basin belong to the Upper Cretaceous and they are underlain by the Precambrian rocks of the Basement Complex.

2.2 General Geology of the Basement Complex

The Basement Complex is exposed over nearly half of Nigeria (Figure 2.2). It extends in the west into the Dahomeyan of the Benin Republic and in the east into the Cameroon. In the remaining half of the country Cretaceous and younger sediments cover the Basement Complex. The Nigeria Basement Complex is believed to be mostly Precambrian in age. However, it probably contains intrusions of Paleozoic age (Oyawoye, 1964). The earliest study of the Basement Complex was made by Falconer (1911) who recognized the age distinction between the Precambrian Older Granites and the Jurassic “Younger” Granites of Jos Plateau. He also introduced these terms.

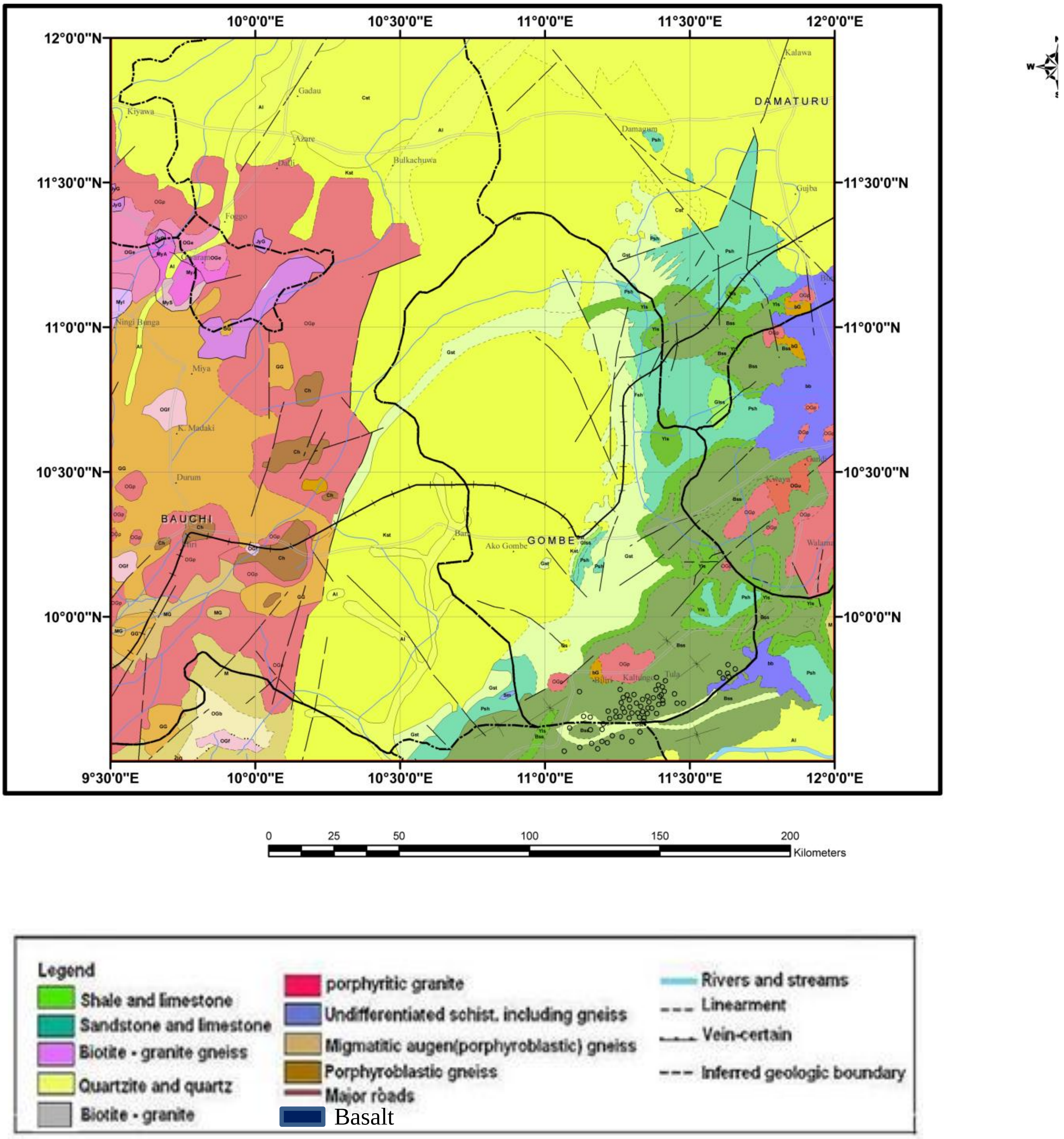

Figure 2.1a: The geological map of parts of Upper Benue Trough and southern Bornu Basin (Adapted from Nigeria Geological Survey Agency, 2006).

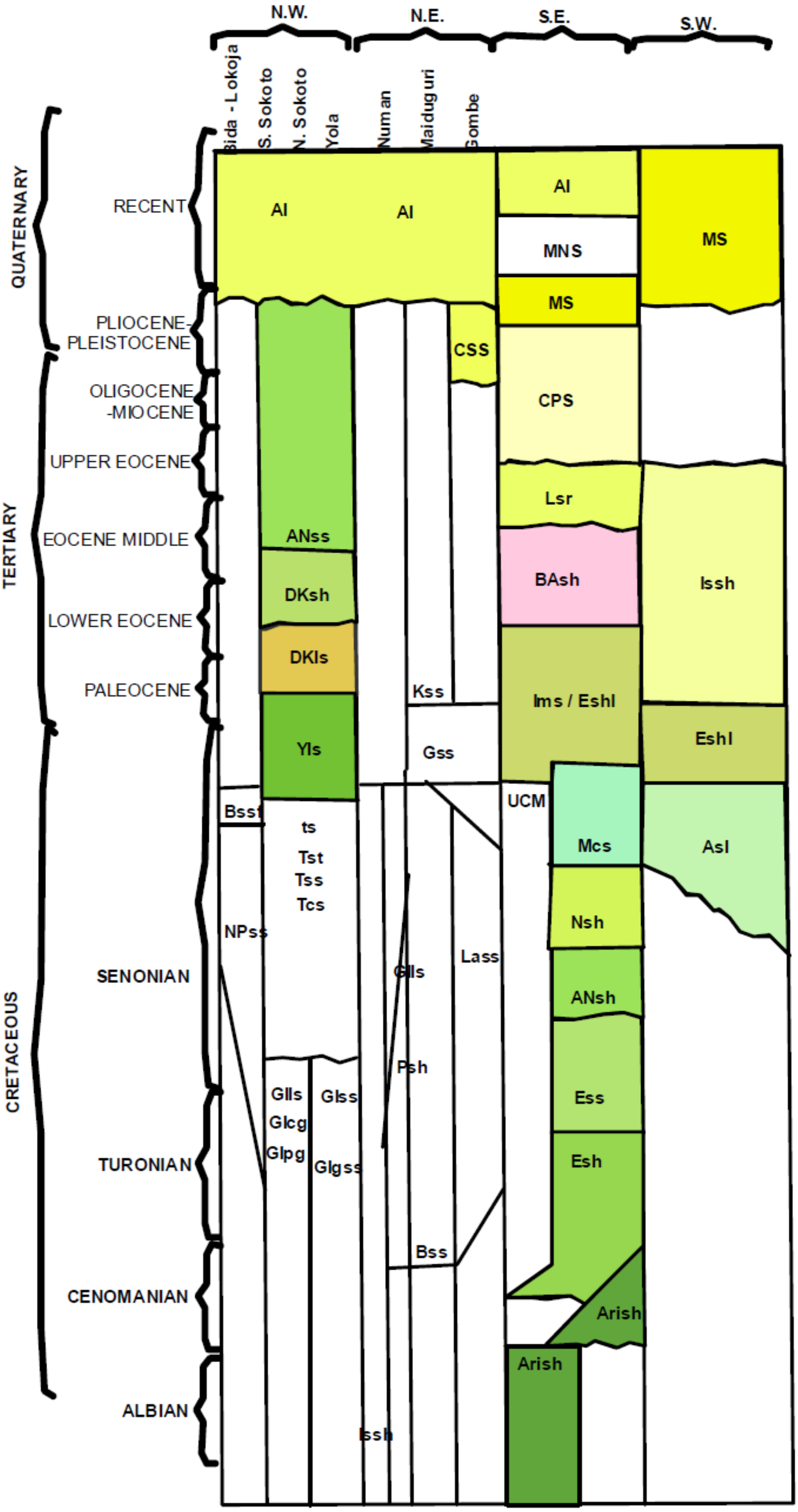

Figure 2.1b: The geological sequence of Upper Benue Trough and southern Bornu Basin. Adapted from Nigeria Geological Survey Agency (2006)

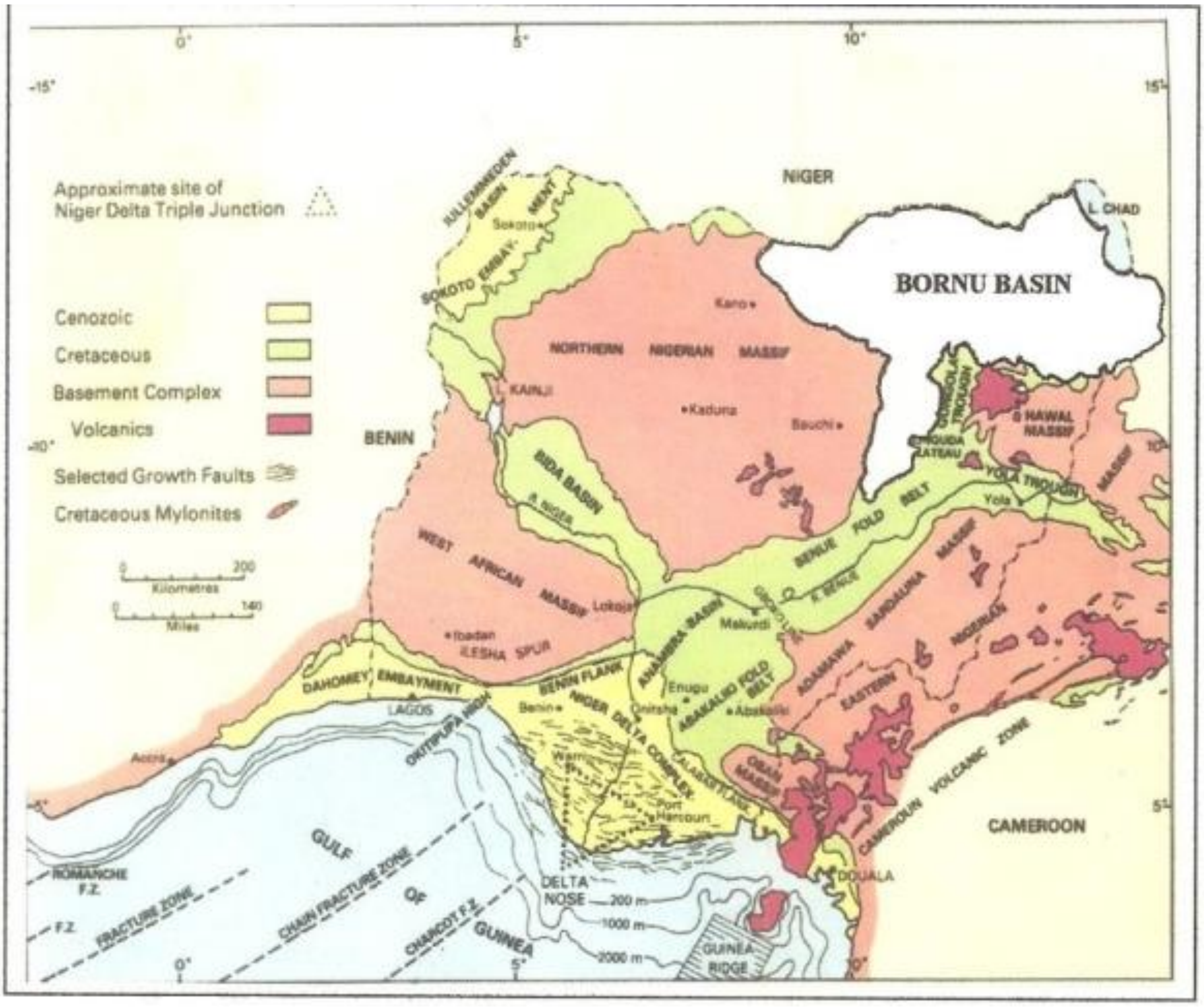

Figure 2.2: The Basement Complex and Cretaceous sediments of Nigeria (Adapted from Whiteman, 1982)

The geology of the Basement Complex is quite complicated. The terrain involved represents a level at considerable depth in the earth which has now been exposed through erosion over several million years (Russ, 1957 and Oyawoye, 1964). The rocks have been involved in multiple folding, fracturing and igneous activities. The rocks of the Nigeria Basement Complex can be grouped into three lithological units (Ajibade, 1980). These are:

(i) The migmatite-gneiss complex which covers about 70% of the whole Basement Complex.

(ii) The metasediments and metavolcanics which form the schist belts and

(iii) The Older Granites which intruded both the migmatite-gneiss complex and the schist belts.

The migmatite-gneiss complex is the largest unit in the Basement Complex and consists essentially of migmatites, quartzo-feldsparthic-biotite-hornblende gneiss with relict meta-sedimentary rocks. It is considered to be the oldest unit in the Complex and probably evolved by sedimentation followed by successive migmatization, granitization and igneous intrusions (Russ, 1957).

Following the formation of the gneisses, a period of sedimentation intervened and predominantly fine-grained rocks were deposited, probably in moderately deep water (Russ, 1957). During the episode of compression which followed sedimentation, these beds were iso-clinically folded and largely converted to schist. The metasediments and metavolcanics form the schist belts. Mapped outcrops of these are mainly found in western half of the country. They consist of low grade metamorphosed sedimentary rocks with associated volcanic rocks. Their age is believed to be between 1000 and 800 Myrs (McCurry, 1976). The metasediments are thought to have once covered the whole

Basement Complex area. They have been removed by subsequent erosion and are now preserved in synclinal troughs (McCurry, 1976).

After the folding of the sediments; the formation of the meta-sediments and the meta-volcanic, there followed a period of granitic intrusion. This was the Older Granite cycle, known throughout Nigeria (Falconer, 1911; Russ, 1957; Truswell and Cope, 1963). The Older Granites are bodies of igneous rock of various compositions, ranging from true granites to tonalites and charnochitic rocks which intruded both the migmatite-gneiss complex and the schist belts. They occur as elongated Batholiths or small circular plutons. Age determinations on the Older Granites all over Nigeria have yielded Pan-African age- 600 Myrs (Grant, 1978).

2.2.1 **Geology of the Younger Granite of Jos and Bauchi Area**

The origin and evolution of the Younger Granites has been a subject of controversy between those who favour a plume hypothesis and others who support lithospheric controls. For example, the magmatism responsible for the alkaline ring complexes has been related to either the action of mantle plumes beneath the lithosphere or to intraplate deformation with reactivation of deep fractures (Ajakaiye and Verheijen, 1983). Also, an inverse correlation between periods of alkaline magmatism, the periods of rapid displacements of the African plate has been noted and has been interpreted as indicating that intraplate magmatism occurs where there is interference and collision along the African plate (Black, Caby, Moussine-Pauchkie, Bayer, Bartrand, Bovillier, ... and Lesquer, 1979). In addition, alkaline ring complexes have been interpreted as being related to rifting and to transform faults (Ajakaiye, 1970). They have also been found to align along directions corresponding to an early arc of rotation and are thought either to precede and predetermine the oceanic transform faults or to have occurred later during reactivation of fractures situated at the ends of the oceanic transform faults (Black *et al.*, 1979). The Nigerian ring complexes are a few million years older than the onset of seafloor spreading in the South Atlantic (Bellion, 1989).

2.3 The Geology of the Cretaceous Sediments in the North-East Nigeria

Nigeria contains some of the most extensively developed and best studied Cretaceous successions known from Africa. The Cretaceous sediments almost everywhere lie directly upon crystalline basement rocks which belong to the Pan-African mobile belts (McCurry, 1976; Ajibade, Woakes and Rahaman, 1989). Previous reviews of the Cretaceous system in Nigeria were provided by Reyment (1965) and Whiteman (1982). A bibliography was given by Zaborsky (1996). Entries for Nigeria in editions of the Lexique Stratigraphique International were compiled by the Geological Survey of Nigeria (1956) and Reyment and Tait (1983). Geological maps of the country were prepared by the Geological Survey of Nigeria (1974) and, with explanatory notes, by Dessauvagie (1974, 1975). The most important of the Cretaceous sedimentary basins is the Benue Trough, an integral part of the "West and Central Africa Rift System" (WCARS) of Fairhead (1986) and subsequent authors (Guiraud, Binks, Fairhead and Wilson (1992); Genik (1993); Keller, Wendlandt and Bott, 1995).

2.3.1 Geology of the Upper Benue Trough

The Upper Benue Trough comprises the area extending from the Bashar-Mutum Biyu line as far north as the "Dumbulwa-Bage high" of Zaborski, Ugodulunwa, Idornigie Nnabo and Ibe (1998), which separates it from the Bornu Basin. Early studies of the Upper Benue Trough and Southern Bornu Basin were carried out by Falconer (1911), Jones (1932), Raeburn and Jones (1934) and Barber (1965). The basis for all later work was provided by Carter, Barber, Tait and Jones (1963) who undertook a regional study of the area covered by the Geological Survey of Nigeria 1/250,000 Series map sheets 25 (Potiskum), 36 (Gombe) and 47 (Lau). The Upper Benue Trough has since become known in greater detail and has been almost entirely remapped through the work of Allix (1983), Benkhelil (1985, 1986, 1988), Popoff (1988), Guiraud (1989, 1990a, 1991a, 1993) and Zaborski, Ugodulunwa, Idornigie Nnabo and Ibe (1998).

2.3.2 Geology of the Bornu Basin

The Bornu Basin (or “Maiduguri Subbasin” of Avbovbo, Ayoola and Osahon, 1986) is the south-western part of the Chad Basin (Figure 1). The Cretaceous sediments in the Bornu Basin are almost entirely concealed by the continental Pliocene to Pleistocene Chad Formation (Carter, Barber, Tait and Jones, 1963; Barber, 1965; Miller, Johnston, Oluwa and Uzoma, 1968) which reaches a thickness of over 1500 m (Olugbemiro, 1997). Descriptions of the Bornu Basin have been given by Raeburn and Jones (1934), Matheis (1976); Avbovbo, Ayoola and Osahon (1986); Okosun (1995a) and Olugbemiro (1997). Those parts of the Chad Basin to the north and east were reviewed by Bellion (1989) with important subsequent accounts having been given by Schneider, Wolff and Genik (1992, 1993). The latter provided detailed descriptions of the concealed east Niger, Bongor, Doba, Dosco and Salamat rifts. The Southern part of the Bornu Basin is covered by the Geological Survey of Nigeria 1/250,000 Series map sheets 25 (Potiskum). Raeburn and Jones (1934); Barber (1965) and Miller, Johnston, Oluwa and Uzoma (1968) produced the geological maps of parts of the area to the north.

2.3.3 The Structural Setting of Benue Trough and Southern Bornu Basin and their Tectonic Evolution

The Upper Benue Trough includes an E-W trending Yola arm and a N-S trending Gongola arm of Gongola Basin. These two branches are separated by an area structurally dominated by four major NE-SW trending sinistral strike-slip faults, the Gombe, Bima-Teli, Kaltungo and Burashika faults; basement inliers, notably the

Kaltungo inlier, are associated with them (Figure 2.3a). Figure 2.3b is the legend explaining features in the lineament map of Figure 2.3a.

Benkhelil (1988, 1989) regarded this median zone as the partially exposed basement high characterizing the axis of the Benue Trough. Carter, Barber, Tait and Jones (1963) referred to it as the "Zambuk Ridge". This term has frequently been applied to a line marked by a single fault which passes just south of Zambuk village. Guiraud (1993), referred to the axial zone as the "Wuyo-Kaltungo basement high". The present terms "Yola arm", "Wuyo-Kaltungo high" and "Gongola Basin", correspond to the "Benue Basin", "Zambuk Ridge" and southern "Chad Basin" respectively of Carter, Barber, Tait and Jones (1963). A series of N-S to NNE-SSW trending faults control the trend of the Gongola Basin (Zaborski, Ugodulunwa, Idornigie Nnabo and Ibe, 1998) while deep-seated E-W trending fractures appear to characterise the Yola arm (Benkhelil, 1988; Maurin and Guiraud (1989, 1990) and Braide, 1992a). The highest thickness sedimentary successions occur in the western part of the Gongola Basin to which Campano-Maastrichtian and Cenozoic deposits are restricted. Over 5 km of sediments occur in the "Dukku", "Ako" and "Bashar" sub-basins; thinner successions occur in the "Lau" and "Numan" sub-basins of the Yola arm (Benkhelil, 1988, 1989). The Yola arm extends eastwards into Cameroun where it is known as the Garoua Basin.

Similarly, Cratchley (in Avbovbo, Ayoola and Osahon, 1986) recognized an ovoid-shaped negative Bouguer gravity anomaly north of Maiduguri. Combining the gravity data with seismic refraction studies, Cratchley, Louis and Ajakaiye (1984) identified a "Maiduguri Trough", thought to contain some 3000 m of Cretaceous and Quartenary sediments, running NNE from near Maiduguri and connecting with the Termit rift. A positive regional gravity anomaly of about 45 mgal amplitude was associated with the

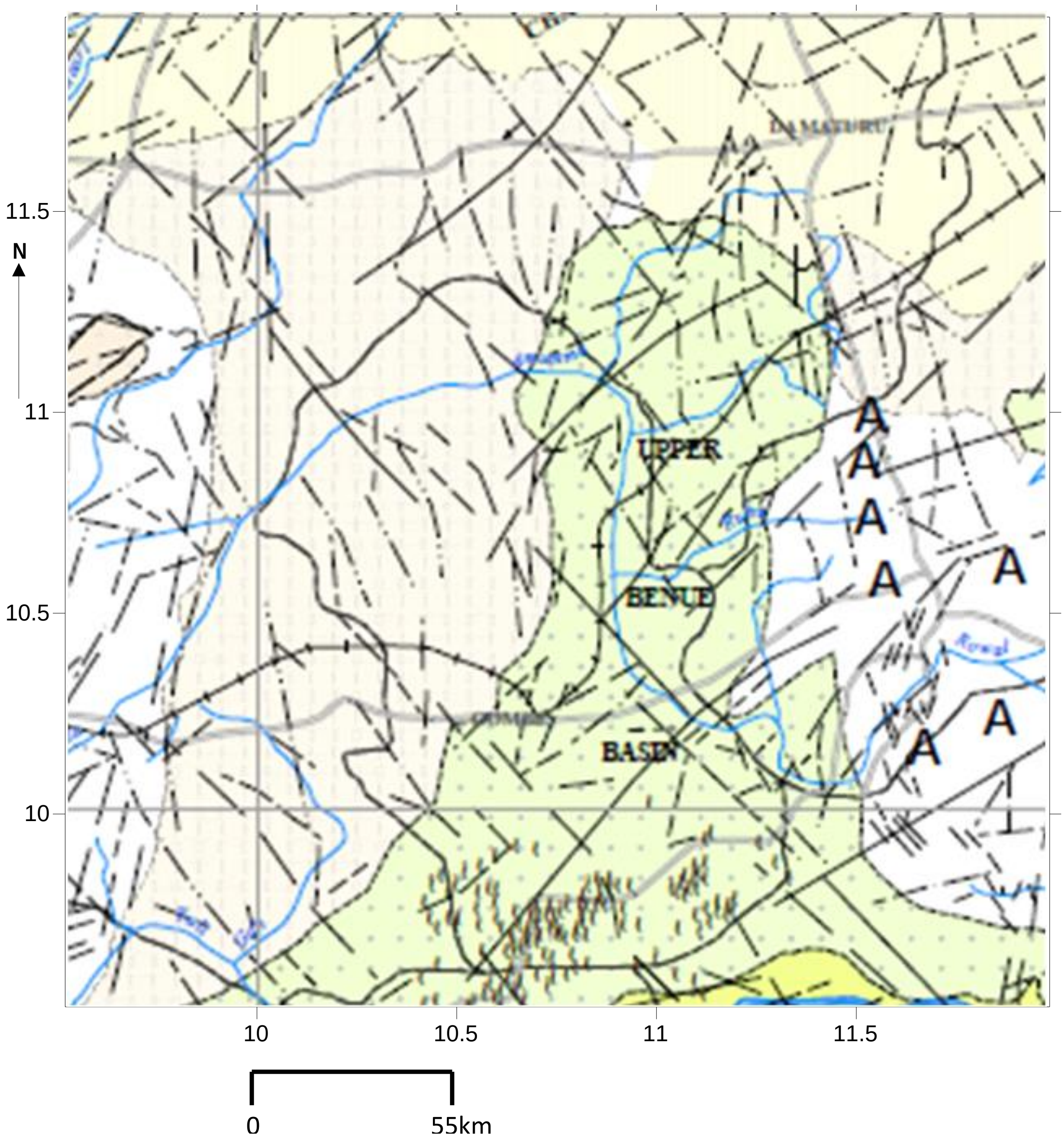

Figure 2.3a: Lineament map of parts of Upper Benue Trough and southern Bornu Basin.

Adapted from Nigerian Geological Survey Agency, 2006

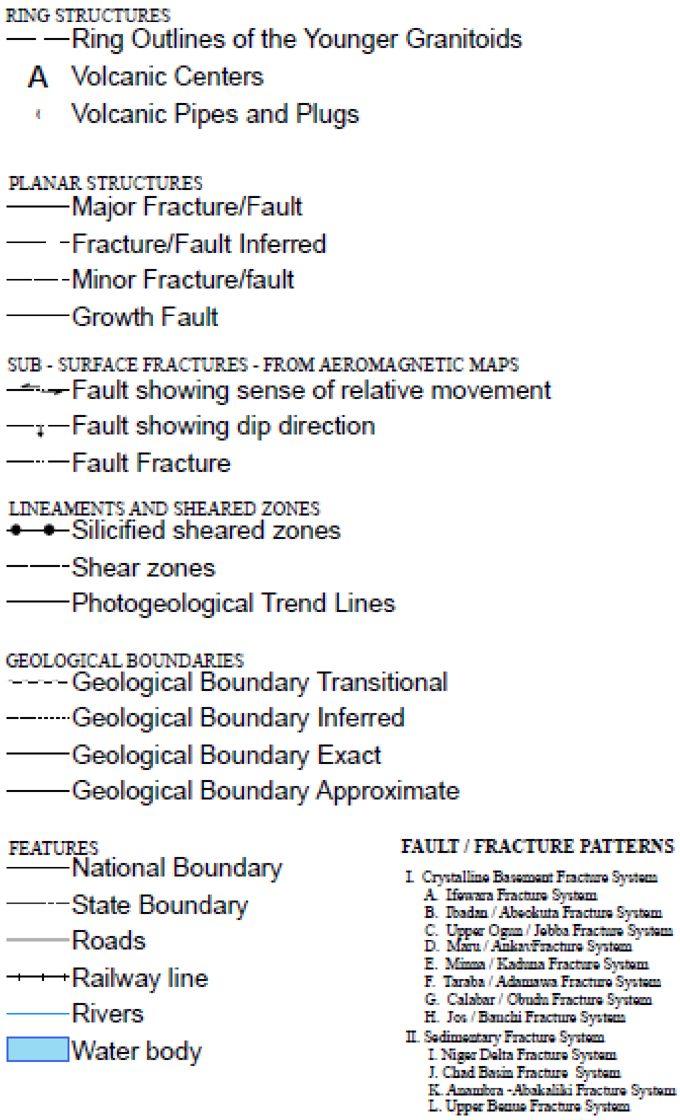

Figure 2.3b: Major keys on the Lineament map of parts of Upper Benue Trough and southern Bornu Basin. (Adapted from Nigeria Geological Survey Agency, 2006)

Maiduguri Trough, by comparison with the Benue Trough, this anomaly was interpreted in terms of crustal thinning. Seismic reflection data of Avbovbo, Ayoola and Osahon (1986) inferred a total thickness of over 10 km of Cretaceous to Quaternary sediments in the “Maiduguri depression”.

Two main faults were identified, a dominant NE-SW trending and a subsidiary NW-SE trending set. The former involve the Precambrian basement, high-angle normal faults delimiting horst graben-like features. The latter affect only the sediments. Nearly all faults terminate at an angular unconformity separating Cretaceous from younger beds (Figure 2.3a).

Two stages in basin evolution were suggested, an Albian - Maastrichtian to Danian with concomitant crustal sagging and compressional tectonics; and a Cenozoic-Recent quiescent phase. Olugbemiro (1997) reported terminal Cretaceous to earliest Cenozoic folding, uplift and erosion, believing that this event was of greater importance than any Santonian deformation that might have occurred. The Chad Formation has been attributed to a thermal sag stage of basin development subsequent to rifting in the WCARS (Fairhead (1986, 1988a, 1988b); Fairhead and Okereke (1987, 1990)). Sahagian (1993) and Hartley and Allen (1994) believed that uplift of its periphery, notably that of the Hoggar, Air, Tibesti and Darfur domes, was the most important control on Neogene-Recent sedimentation in the Chad basin.

2.4 Stratigraphy and Sedimentation

The stratigraphy of the Bornu Basin has largely been interpreted by comparison with the Upper Benue Trough. The Cretaceous succession in the Upper Benue Trough comprises Early Cretaceous continental classics, the Bima Group, and a dominantly marine Late Cretaceous succession. The former include the oldest sediments known in the Benue

Trough, deposited during active rifting. During the Late Cretaceous, thermo-tectonic sag conditions prevailed and sedimentation was strongly influenced by transgressive - regressive events. The Upper Cretaceous may be divisible into discrete pre- Santonian and Campano - Maastrichtian parts, the latter deposited during a renewed phase of rifting (Figure 2.4).

Carter, Barber, Tait and Jones (1963) referred the outcropping sediments in the south-west (previously described by Jones (1932) and Raeburn and Jones (1934)) to the Gongila Formation, Fika Shales and Gombe Sandstones. At Damagum and Maiduguri, to the north, 100 m and 450 m respectively of beds belonging to the Fika Shales were identified in boreholes which bottomed within the unit. On the northern flank of the Dumbulwa-Bage high, Zaborski, Ugodulunwa, idornigie Nnabo and Ibe (1998) subdivided the Cretaceous outcrops into the Kanawa, Dumbulwa and Fika members of the Pindiga Formation. The Fika member contains Coniacian ammonites and to the east, where the Dumbulwa member wedges out, its basal part includes calcareous sandstones with Coilopoceras. Dolerite sills intrude the Fika member. Obi (1995, 1998) described a Cretaceous succession about 50 m thick outcropping along the central southern margin of the Bornu Basin, an area referred to as “Hawal Basin”.

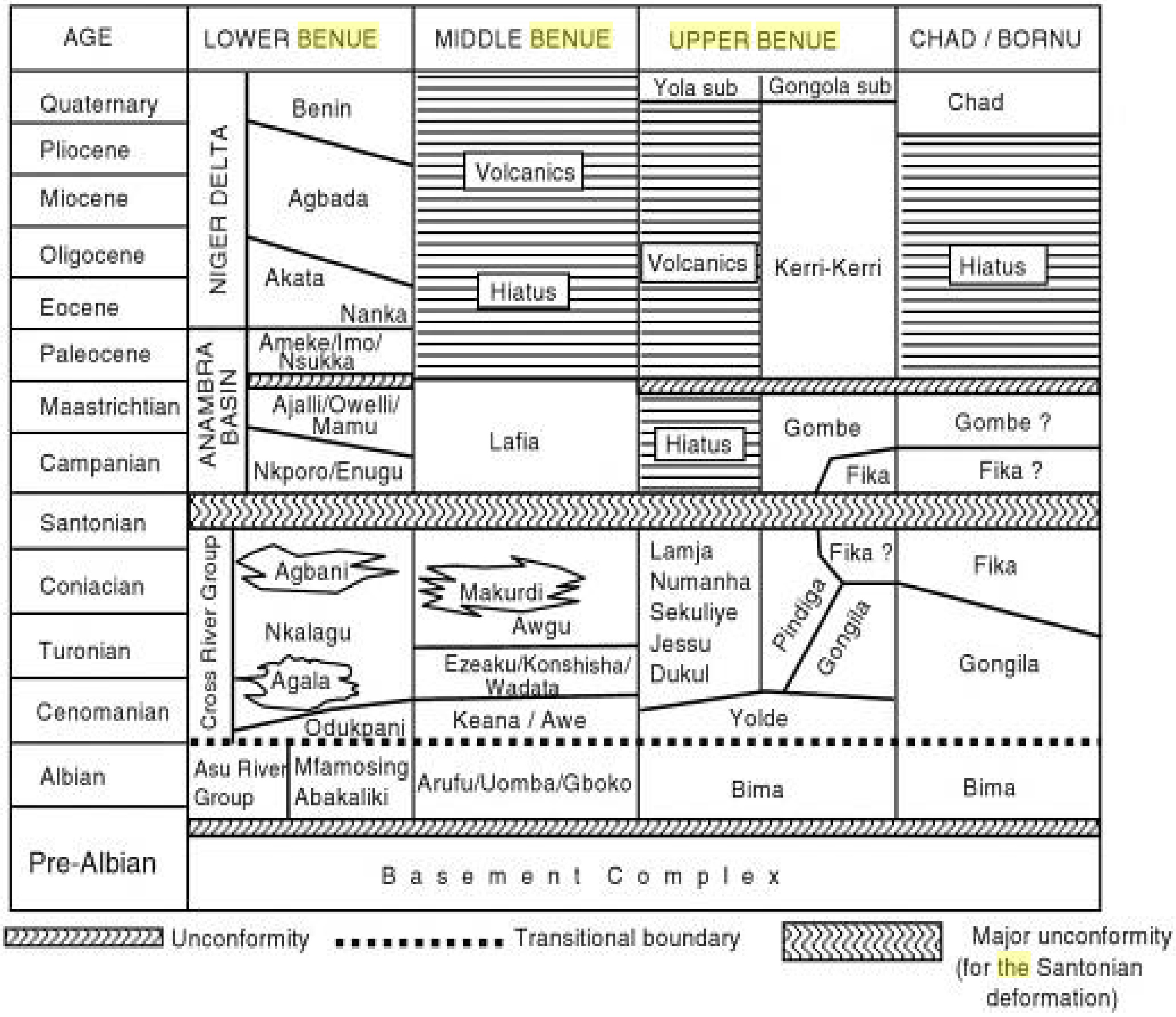

Figure 2.4: Idealised N-S stratigraphic cross section across the Chad Basin — Benue Trough (BT), Nigeria (after Obaje, 2009).

The following units were identified:

i. a coarsening-upwards succession divisible into: an upper part comprising about 13 m of bioturbated, calcareous fine-grained sandstones and siltstone, gypsum-bearing clay shale with small bivalves and gastropods and fine to medium-grained, laminated or cross–bedded sandstone with *Ophiomorpha, Thalassinoides* and *Skoilithos;* and a lower part comprising 12 m of alternating fine to medium-grained sandstones' bioturbated siltstone and shale;

ii. 16 m gypsum-bearing blue-grey clay shale with intercalated limestones;

iii. about 4 m of medium to coarse-grained, calcacereous often nodular sandstones and sandy claystones; and

iv. at least 5 m of pebbly sandstones directly overlying the Precambrian basement.

Unit i was referred to the Bima Group, ii to the Yolde Formation and iii and iv to the Gongila Formation.

Knowledge of the subsurface Cretaceous stratigraphy of the Bornu Basin derives from seismic and boreholes studies. Avbovbo, Ayoola and Osahon (1986) identified seven "seismic sequences" in the Maiduguri depression interpreted as:

1. The Chad Formation;
2. The Keri-Keri Formation, lying uncomformably upon the older folded and faulted succession;
3. The Gombe Sandstone;
4. The Fika Shale;
5. The Gongila Formation;
6. The upper Bima Group;

a unit regarded as distinct from the Bima Group, divisible into 1b above, seismically transparent and believed to be made up of marine shales; and 1a below, an inferred fault scarp fan and fluvial facies.

Okosun (1995a) and Olugbemiro (1997) provided direct lithological data from boreholes located to the north of Maiduguri. The Cretaceous sediments are directly overlain by the Chad Formation; Keri-Keri Formation and Gombe Sandstone are absent. Three or four Cretaceous units were identified:

i. a marine grey or blue-black shale, occasionally gypsum-bearing, with thin limestone intercalations and black shale horizons, referred to the Fika Shale. Diorite sills occur in places. A lectostratotype 890 m thick was proposed for the unit in the Kanadi-1 well by Okosun (1995a) Dating of the Cretaceous sediments is imprecise. Okosun (1992) assigned an age within the range of Turonian to Santonian to ostracods recovered from beds referred to the Fika Shale.

ii. Correlation of the Cretaceous successions in the Bornu Basin and Upper Benue Trough remains inexact. Okosun (1995a) and Olugbemiro (1997) respectively suggested Albian to Turonian and Albian to Cenomanian ages for beds referred to the Bima Group in the Bornu Basin; Lower Turonian and Turonian ages for the Gongila Formation; and Turonian to Maastrichtian and Turonian to Santonian ages for the Fika Shale. Okosun (1995a) indicated the Kanadi well as bottoming in basement rocks, Olugbemiro (1997) reported only the Kinasar well as penetrating the full thickness of the Bima Group and “pre-Bima” beds. A notable feature of the succession in the latter well in contrast to the Upper Benue Trough is relatively greater importance of the Upper Cretaceous marine beds compared to the equivalents of the Bima Group. Olugbemiro (1997) reported *Heterohelix* from the upper part of the Bima Group in the Mbeji well and arenaccous foraminifers were recovered from “Bima” deposits in this, the Kanadi and Albarka wells.

iii. The earliest Cretaceous marine beds in the Upper Benue Trough and the Chad Basin to the north (Bellion, 1989; Genik, 1993) are Cenomanian. It is unlikely that the “pre-Bima” shales of Avbovbo, Ayoola and Osahon (1986) are Albian marine deposits as these authors supposed. Olugbemiro (1997) suggested that sedimentation in the Bornu Basin began only during the Albian to Cenomanian. This also conflicts with the Upper Benue Trough and Termit rift where sediments as old as latest Jurassic occur (Genik, 1993). Further data, including detailed dating of the Bornu Basin sediments, is required to resolve these apparent discrepancies; the lower part of the succession may contain argillaceous deposits, as suggested for the Benue Trough by Popoff (1988).

2.5 Economic Geology of the Study Area

The potential of the Benue Trough (Figure 2.5) for resources of raw materials of economic significance is related to its form, origin and history as a rift which failed to develop into an ocean basin, and is compared to similar geological environments in other parts of the world. Deposits of limestone, brick and fire clay, construction stone, laterite and coal, some are being worked, while others are being investigated and new ones sought. Lignite is found with the highest rocks of the stratigraphic sequence at the seaward end of the trough, which could also be regarded as the earliest deposits of the present Niger Delta. Significant occurrences of base metal sulphides (lead and zinc, with smaller amounts of copper), cadmium and silver, and the associated minerals barites and fluorspar, are known to occur locally in spatial, and probably genetic, relation to salt water springs. The possibility of finding larger lower grade deposits of base metals is encouraging. Sources of glass sand and mineral (juvenile) water could have been valuable in more populated and otherwise developed parts of the country.

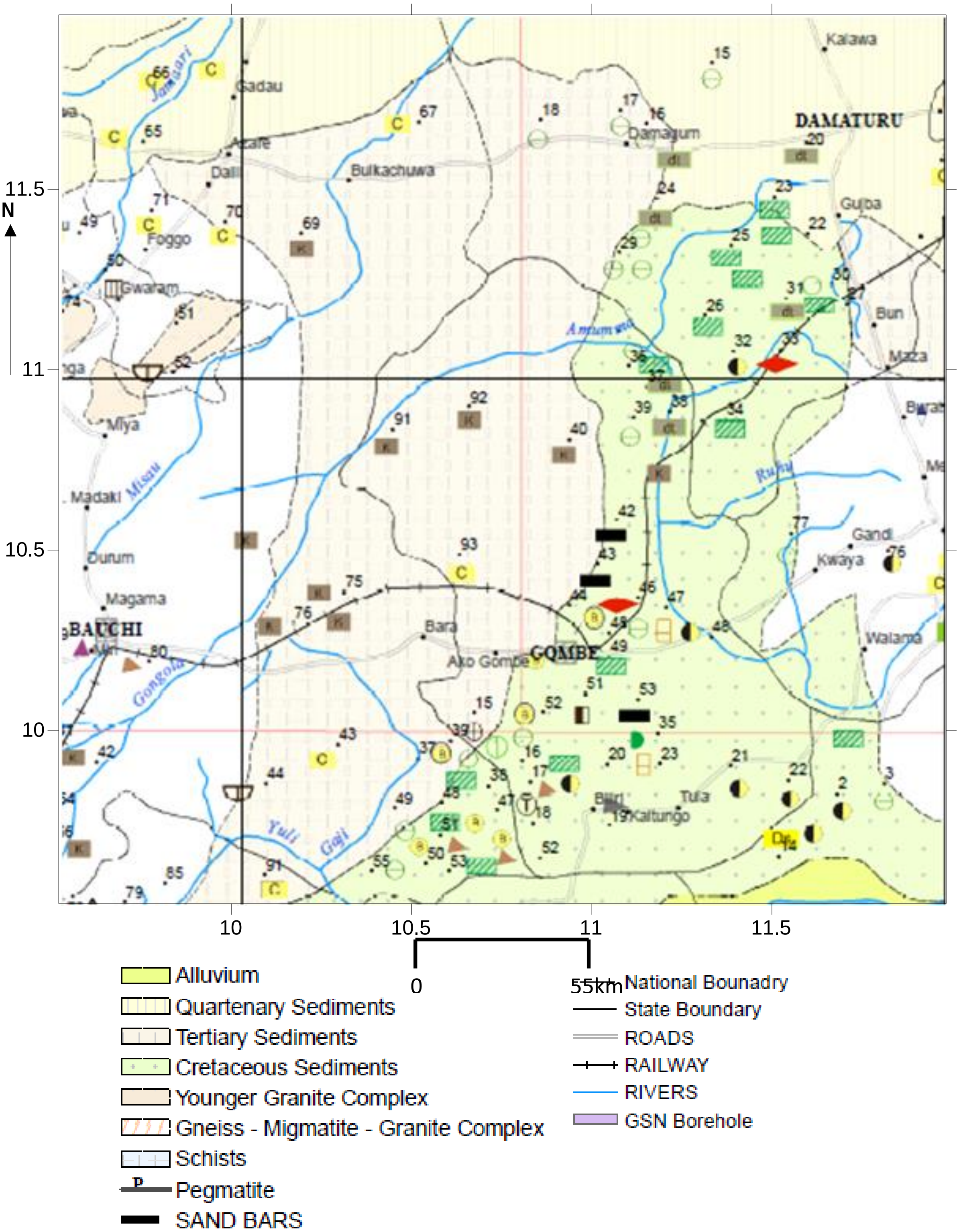

Figure 2.5: Geological and Mineral map of parts of Upper Benue Trough and southern Bornu Basin. Adapted from Nigerian Geological Survey Agency, 2006

The potential for large economic deposits of rock-salt (halite) is considered to be very good but other evaporate deposits such as gypsum and anhydrite, which may also occur, are likely to be too deep for commercial exploitation. The possibilities for oil and natural gas are also worth further investigation, as is the potential for radioactive minerals within the sediments. The indication for large reserves of ground (meteoric) water is doubtful, most of the sedimentary formations lacking the necessary porosity and permeability.

The rift structure is too senile to yield any presently usable geothermal energy although there has been some fairly recent (Quaternary) volcanic activity and there are many warm springs; combustible gases in these springs are only of importance as a hazard to underground mining, while the presence of rare gases has yet to be checked, but is unlikely to be in productive quantities (Ford, 1981).

2.6 Review of Previous Geophysical Studies in the Area

In Nigeria extensive geophysical investigations have been largely confined to sedimentary formations with proven natural resource potentials. The Niger Delta area of southern Nigeria has witnessed extensive gravity, magnetic and in particular seismic surveys in connection with oil and gas by oil industries operating in Nigeria. The Chad Basin has also attracted some attention in the last decade mainly for oil and ground water purposes. In comparison to other Cretaceous systems aforementioned, fewer numbers of geophysical investigations have also been done in the Benue Trough (Figure 2.1a).

The Benue Trough being generally regarded as a rift structure is noted to have many features in common with other intra-continental rifts. According to Shemang, Jacoby and Ajayi (2005), the Benue rift can be compared with some well-known rift systems such as the East African, the Rhine Graben, the Baikal rift and the Rio Graande rift. These rift systems are all associated with volcanism and regional uplift. Mareschal (1983) indicated the basic geophysical characteristics of a rift as having a thin crust, low velocity and density upper mantle and higher than normal heat flow. Owing to these, many workers and researchers have focused a lot of attention on the trough. These were aimed at depicting the nature and characteristics of the structure. The earliest studies in the Benue Trough were mainly aimed at exploring its origin and tectonic evolution.

The earliest geophysical investigations in the Benue Trough were mainly centred on the measurement and rather qualitative study of its gravity field. The occurrence of lead-zinc mineralization, salt deposits and bright prospects of finding oil and uranium deposits in the trough have turned the area into one of great economic importance. Therefore, there has been more extensive and intensive geological activity in the trough with renewed attempts at more detailed geophysical studies in the past few years. This has led not only to a better understanding of the structure of the Benue Trough, but also its origin and evolution. However, there are limited numbers of geophysical work as compared with that of the geological work in the study area.

Cratchley and Jones (1965) carried out the first gravity survey in the middle and upper Benue Trough. They showed that the Bouguer isogals are generally parallel or sub-parallel to the margins of the trough. Two fundamental features were identified: a positive regional anomaly, with an amplitude of approximately 50 mGal and a mean width in excess of 150 km, interpreted as indicating a thinner crust below the basin compared to the flanking basement; and shorter-wavelength residual anomalies, comprising an axial positive anomaly flanked either side by negative anomalies, interpreted as representing an axial zone of shallow basement rocks containing basic to intermediate intrusive flanked by zones where the sedimentary infill reaches thicknesses of up to 6 km. Subsequent estimates of the amount of crustal thinning below the Benue Trough have varied from as little as 1.5 km (Adighije, 1979 and 1981) to over 10 km (Artsybashev and Kogbe, 1974). The short-wavelength axial gravity high has been interpreted as representing a dense intrusive “mantle diaper” (Adighije, 1979, 1981) or a zone of shallow basement rocks intruded to a greater or lesser extent by basic to intermediate magmatic bodies (Osazuwa, Ajakaiye and Verheijen, 1981; Ajayi and Ajakaiye, 1981, Ofoegbu and Onuoha, 1990).

Based on the assumed density contrast of 170 kgm^{-3} between the crust and mantle, Cratchley and Jones (1965) suggested a mantle uplift of 10-12 km having a width of 190-220 km. In his preliminary interpretation of gravity anomalies associated with some prominent salt springs in the middle Benue, Ajayi (1979) suggests that the magnitudes of the gravity anomalies locally associated with the prominent salt springs in Nigeria's Middle Benue range from -1.1 to -5.7111 gals. The preliminary interpretations of these anomalies suggest the possible existence of small to medium sized salt domes buried at a moderate to intermediate depths of 0.5 to 1.8 km.

In the upper Benue Trough, Osazuwa, Ajakaiye and Verheijen (1981) have also interpreted the regional anomaly in terms of an up-arching of the mantle-crust interface. In 1985, ELF Nigeria limited gave a detailed analysis of the regional gravity field over the trough. Their two dimensional models of the Bouguer anomaly over different sections of the Trough confirm a crustal thickness varying between 22 – 32 km. Cratchley and Jones (1965) also correlated the local positive residual anomalies in the Benue Trough with some outcrops of cretaceous rocks. Ajakaiye (1981) interpreted locally occurring negative anomalies whose values hardly exceed 100g.u. in terms of brine springs occurring at different depths of 300 – 800 m. In 1987, Ajayi (1979) identified similar brine springs at moderate depths of 0.56 - 1.64 km in the Middle

Benue Trough. Ofoegbu and Onuoha (1990) accounted for some of the locally occurring anomalies in terms of dyke-like bodies that are known to abound within the Trough and associated with volcanic centres in the area.

Following the release of aeromagnetic data collected over the Benue Trough and surrounding regions by the Geological Survey of Nigeria, there has been a reasonable measure of interest in the qualitative interpretation of these data. Ofoegbu (1984a) was able to produce a comprehensive aeromagnetic map of the Middle and Lower Benue Trough. The magnetic field over the Benue Trough is made up of contributions from short, medium and long wavelength anomalies. The basement complex bordering the trough and outcropping in some places within it is characterised by short wavelength anomalies, which arise from either susceptibility changes within the basement, near surface intrusive in the basement or their combined effects (Ofoegbu, 1984).

The gravity field over the Benue Trough according to Ofoegbu and Onuoha (1990) was characterised by a prominent axial positive anomaly of 200 – 400 g.u. which continues over the entire length of the trough but for a slight eastward shift over the southern Benue Trough. Ajakaiye (1981) suggested that the Bouguer anomalies observed in the trough ranges in value from 60 to 400 g.u. According to her, the Free Air anomaly values are close to zero except for the local attainment of values of 300g.u. Superimposed on these anomalies is a pronounced regional positive anomaly, which has been independently interpreted in terms of an uplifted mantle and the thinning of the crust underneath the trough (Cratchley and Jones, 1965; Artsybashey and Kogbe, 1974; Adighije, 1981; Ajayi and Ajakaiye**,** 1981; Fairhead and Okereke, 1987).

Ofoegbu (1985) has subjected the aeromagnetic anomalies over the Benue Trough and adjacent regions to a power spectrum analysis in an effort to eliminate the anomaly components due to shallow sources. The conclusion he drew from the resultant long wavelength anomalies is that these anomalies are essentially due to variable curie isotherm or to morphological variations at the top of a magnetized lower crust. The curie isotherm underneath the trough he found to vary between 18- 27km, is of immense interest, and can be related to the thermal history of the area.

Stuart, Fairhead, Dorbath and Dorbath (1985) carried out seismic refraction studies. His studies indicated that a crustal thickness of 23 km below the Garoua Basin (Eastern Yola arm) compared to a normal thickness of 34 km to the south, and a density contrast between the crust and anomalously low-density mantle of 0.17 gcm^{-3}.

In 1986, Ofoegbu also transformed several aeromagnetic profiles over the Benue Trough to the corresponding pseudo gravimetric profiles using the equivalent layer method. A joint analysis of the magnetic, gravity and pseudo gravimetric anomaly profiles confirmed that:

a) The short wavelength anomalies on the aeromagnetic profiles are caused by variation in magnetization due to existence of very thin intrusions occurring at shallow depths.
b) The medium and long wavelength anomalies on the aeromagnetic and pseudo gravimetric profiles are due to magnetization from deeply seated intrusive bodies to asthenospheric origin.

In addition to gravity and magnetic methods, other geophysical techniques have been applied in the investigation for structures and economic resources in the Benue Trough. Workers like Orajaka and Nwachukwu (1968); Eze (1985) and Okoye (1988) have successfully applied electromagnetic and induced polarization methods in determining the extent of lead-zinc mineralization in parts of Abakaliki and Ishiagu areas of Ebonyi state.

Ajakaiye, Hall, Millar, Verhejen, Award and Ojo (1986) interpreted aeromagnetic anomalies and tectonic trends in and around the Benue Trough; Nigeria, shows that magnetic lineaments with definite characteristics exist within the Nigerian continental landmass. The study shows that the Benue Trough is part of a large-scale continental feature of global importance because its boundary faults can be linked to the Chain and Charcot feature zones in the mid-Atlantic.

Avbovbo, Ayoola and Osahon (1986) inferred a total thickness of over 10 km of Cretaceous to Quaternary sediments in the "Maiduguri depression" (less than 5 km was subsequently proved) from their seismic reflection data. Two main fault systems were identified, a dominant NE-SW trending and a subsidiary NW-SE trending set. The former involve the Precambrian basement, high-angle normal faults delimiting horst and graben-like features. The latter affects only the sediments. Nearly all the faults terminate at an angular unconformity separating Cretaceous from younger beds.

Fairhead and Okereke (1987) carried out a new gravity survey to investigate the nature and cause of the Bouguer gravity field associated with the Cretaceous West African rift system in Nigeria and Cameroon. The new gravity measurements included data collected over the basement area between the Benue Trough and the Cameroon border and filled an important gap in the gravity coverage. After removal of the long wavelength negative anomaly from the observed gravity field, the remaining positive gravity anomaly, associated with the rift system, was interpreted in terms of two and three dimensional crustal models. These models were constrained by crustal thicknesses derived from a seismic refraction study carried out across and to the south of the Yola rift. The results of simple three dimensional gravity modelling indicate the crust beneath the lower and middle Benue is approximately 20 km thick while beneath the Gongola rift the crust is approximately 25 km thick relative to a normal crustal thickness of 34 km away from the rift.

Fairhead and Okereke (1988) estimated the depth to major density contrasts within the lithosphere over the West African Rift System and adjacent basement areas in Nigeria and Cameroon, based on the spectral analysis of the Bouguer gravity field. The study revealed that three main density discontinuities occur in the depth ranges 7 to 12 km, 19 to 30 km and 80 to 93 km. The shallow crustal density discontinuities reflect a range of geological structures associated with the rift zones, shear zones and cratonic margins. The 19 to 30 km depth range is in good agreement with the Moho depths determined by seismic refraction studies beneath and to the south of the Yola Rift in Cameroon and by East-West gravity modelling profiles across the Benue Trough in Nigeria. The deepest density discontinuities observed at 80 to 93 km depth are compatible with the presence of an anomalous low velocity upper mantle structure at these depths deduced from the inversion of tele-seismic travel time residuals.

Fairhead and Green (1989) carried out a gravity modelling to determine the African rifting system and tectonic model for Nigeria and East Niger rift basins. They discovered that since early Mesozoic times, three phases of rifting have occurred in Africa and are related to distinct phases of break-up of Gondwana. These contrasting rift episodes have provided an insight to the extent to which plate tectonic processes and more localised mechanical anisotropy processes within the African lithosphere have influenced rifting. The result shows the extent and nature of the broad (regional) positive Bouguer anomaly associated with these rifts. The removal of this regional anomaly allows the delineation of the (residual) negative Bouguer anomaly which reflects the lateral extent and thickness of Mesozoic and Cenozoic sediments. This residual anomaly is interpreted using iterative three dimensional modelling, by incorporating a density-depth function derived from well logs. Results indicate that an extensive basin complex exists in eastern Niger with sedimentary sections greater than 7 km in depth and are in good agreement with the aeromagnetic data.

Ajakaiye, Hall, Asiekaa and Udensi (1991) interpreted the aeromagnetic survey of substantial part of Nigeria carried out by the Geological Survey of Nigeria between 1974 and 1980. The results of their analysis reveal magnetic lineation and regions of distinct magnetic interpretations character and field level which are interpreted as expressions of tectonic features related to igneous intrusive of various ages. The total field magnetic intensity data derives from the crystalline shield area with its characteristics Jurassic granitic ring complexes and Neogene volcanic, and the Benue trough which is considered to be a failed-rift arm. Major intrusive and fault zones were clearly delineated. The results of the analyses also revealed the aspects of the regional tectonic framework of West Africa and its relationship with major structures in the adjacent Atlantic basins.

Nur, Onuoha and Ofoegbu (1994) carried out the spectral analysis of aeromagnetic data over the Middle Benue Trough. The research indicated a two depth model with depth to deeper sources ranging from 1600 m to 5000 m while depth to shallow sources ranges from 60 m to 1200 m.

Nwogbo (1997) mapped shallow magnetic sources in the Upper Benue Basin of Nigeria in order to determine their structures, distribution and location at depths by employing techniques based on the Fourier analysis of aeromagnetic fields. Spectral depth determination to magnetic source in the region yielded two distinct magnetic depth ranges. Mean depth (depth to magnetic deeper source) values in the range of 2.00 - 2.62 km and mean depth to shallower magnetic sources in the region vary between 0.07 -

0.63 km. Some deeper intrusives occur within the basement at depths of up to 2.45 km. The numerous shallow intrusions in the basin however occur substantially outside the basement.

Udensi (2000) carried out the interpretation of total magnetic field over the Nupe Basin using aeromagnetic data. The study indicated an average depth to burial of 3.39 km with anomalies indicating probable hydrocarbon occurrence.

Nur (2000) carried out the analysis of aeromagnetic data over the Yola arm of the Upper Benue Trough, Nigeria. The study indicated a two depth source model with the depth to deeper sources varying between 625 m to 2219 m and an average depth to shallow source is 414 m.

Nur (2001) carried out the spectral analysis and Hilbert transform of gravity data over the southwest of the Chad Basin, Nigeria. The results obtained from the spectral analysis indicated sedimentary thicknesses ranging from 420 m to 8000 m in the southwest of the Chad Basin.

Nur (2003) carried out the interpretation of pseudo-gravimetric data over the Middle Benue Trough, Nigeria. The study used the two dimensional spectral analysis of the pseudo-gravimetric data to determine the average sedimentary thickness in the study area. The analysis indicated a two depth model, with the depth to deeper sources ranging from 1345 m to 6530 m while the depth to shallow sources ranges from 444 m to 1000 m.

Nur**,** Ofoegbu and Onuoha (2003) carried out the spectral analysis and Hilbert transform of aeromagnetic data over the Upper Benue Trough, Nigeria. The study revealed a sedimentary thickness of about 3.3 km around Bashar-Futuk. The research also, suggested that the sub-basin in the southwest of the study area may provide good prospects for hydrocarbon exploration.

Udensi and Osazuwa (2003) carried out spectral analysis of the residual magnetic field values over ten sections of the Nupe Basin. The study revealed that the average depth to the basement rocks under the Basin is 3.39 km. The study also revealed the existence of two areas with sedimentary thickness greater than 4.5 km which may have possible hydrocarbon potential.

Estimates of the thickness of sedimentary rocks in the Benue 'Trough obtained from the interpretation of magnetic anomalies agree fairly with those obtained through the analysis of the gravity field. Osazuwa, Ajakaiye and Verheijen (1981) working in the Yola arm of the upper Benue Trough estimated the thickness of sedimentary rocks at between 0.9 and 4.9 km while Ofoegbu (1988) working in the same area put his own between 0.5 and 4.6 km. Ofoegbu (1984), working in the lower Benue Trough found the thickness of sediments to vary between 0.5 and 7 km. Ajakaiye (1981) and Ofoegbu (1984), analysed the small amplitude, medium wavelength anomalies of general regular shapes and gentle gradients on which are superimposed several locally occurring high frequency anomalies. This characterises the trough in terms of deep lying basement and highly magnetic intrusive bodies either within the sediments or basement or both. Osazuwa, Ajakaiye and Verheijen (1981) have also estimated the thickness of igneous intrusive bodies in the Yola arm of the upper Benue Trough as being about 10 km and occurring at depths of l km or less. Ofoegbu (1985) interpreted a linear anomaly, which runs continuously for about 60 km from Kambari to Bimari as being due to a dyke-like body having an average width of 0.71 m, depth of 0.36 km and magnetization of 0.38 A/m. He equally in 1984 interpreted an anomaly near Bukuru in terms of a volcanic plug of thickness 0.46 km and depth 0.6 km.

Many other workers have analysed the aeromagnetic anomalies over igneous intrusions in the lower parts of the Benue Trough. Njoku (1985) was able to delineate the nature and subsurface morphology that are responsible for the striking magnetic anomaly pattern that occurs in the Ndi - Akparata area northeast of Abakaliki. Madu and Onuoha (1984) combined the results of limited gravity studies and the analysis of aeromagnetic data and were able to map the nature of the basement-sediment boundary in the Gbokolo area of Benue state.

Shemang, Jacoby and Ajayi (2005) investigated the gravity anomalies over the Gongola arm of the Upper Benue Trough. In their findings, they concluded that the results of the interpretation of gravity anomalies suggest the existence of intra basement intrusive of high densities in the trough at depths between about 0.5 and 2 km**.** The existence of intrusive suggests the existence of deeply penetrating fractures within the area. This according to them conforms to basic intrusive which has been inferred from results of geophysical studies in different parts of the world over major rift systems such as the Rhine Graben and Baikal rift (Logatchev, 1993). They went further to suggest that the width of the rift was acquired early in the evolution of the rift. The buried basic intrusions at depths of 0.5 - 2 km suggests the existence of deep fissures in the crust beneath the area of their study, which might have originated during rifting and parts of which became the foci of intrusive into the crust.

Likkasson, Ajayi and Shemang (2005) interpreted the 24 aeromagnetic maps covering the Middle Benue Basin. He subjected the data from the middle of the Basin to map and profile analysis using analytic signal, matched filtering and forward/inverse modelling as processing tools to the aeromagnetic total-field intensity anomaly of the Middle Benue Trough. Magnetic depth to geology contrast or faults for the sedimentary cover gives a maximum of 3.30 km from the ground level. The spectral matching yielded three dipole equivalent source layers at 0.89, 4.33 and 18.22 km depth. Depth of 4.33 km corresponds to max thickness of sediment, while that of 0.89 km may be attributable to effects of survey terrain clearance and other shallow plate sources. They attributed the magnetic layer of 18.22 km to correspond to the base of the curve depth in the area. Results obtained from selected values of susceptibility from the sediments, metamorphic and granite basement and basic intrusions give sedimentary thickness along the three profiles across the area up to 4.5km with more fitting depth on the River Benue zone. They observed that prominent faults exist over Amar, Mutum Buyu, Ibi-Wukari, Donga and Wase, such faults could be responsible for basement projections in the Middle Benue Basin.

The Steel Raw Materials Exploration Agency and the Nigeria Coal Corporation had also used electromagnetic methods in delineating faults and fracture patterns especially in the coalfields of the Lafia area (Akubue, 1986). Abaneme (1983) and Aneke (1984) have used the electrical methods extensively for mineral exploration purposes while Onuoha and Aka (1983) and Nwodo (1985) applied the method for groundwater investigations.

Oil exploration activities have been going on for a long time in parts of the lower Benue Trough, the Gongola arm and the Chad Basin. The seismic reflection method has been used extensively in these studies, but as is usual with such data, much of it is largely unpublished and remains the property of the Nigerian National Petroleum Company (NNPC) or of the company that acquired them.

The Nigeria Geological Survey Agency (NGSA) and some mining companies in their search for uranium and other associated deposits in the Benue Trough also carried out radiometric measurements. On the basis of these surveys, a background radioactivity of

100 - 300 c.p.s. was established for the Benue Trough (Ajakaiye, 1981) with the Cretaceous sediments having values of between 50 - 150 c.p.s. Local occurrence of values as high as 500 - 20,000 c.p.s. have been interpreted as indicating the occurrence of rocks rich in uranium, potassium and thorium (Ajakaiye, 1981).

All the studies described above are limited in coverage and depth with respect to the various methods used. They however, indicate the need for a detailed study of the middle and upper Benue Trough (as much more detailed work had been carried out in the lower Benue Trough) so as to assess its economic potentialities with respect to other Cretaceous systems.

CHAPTER THREE

3.0 MATETRIALS AND METHODS

3.1 Materials

3.1.1 Data Acquisition

The study area is covered by twenty five aeromagnetic maps of total-field intensity in half-degree sheets. These are numbers 83 - 87, 106 - 110, 128 - 132, 149 - 153 and 170 - 174. These are obtainable from the Nigerian Geological Agency (NGSA) which carried out an aeromagnetic survey of substantial part of Nigeria between 1974 and 1980. The magnetic information consists of profiles or flight lines plotted on continuous strip chart or tape records. The data were collected at a nominal flight altitude of 152.4 m along N-S flight lines spaced approximately 2 km apart. The data were later published in the form of ½º by ½º aeromagnetic maps on scale 1:100,000. The magnetic values were plotted at 10 nT (nano Tesla) interval. The maps were numbered and named according to the places covered for easy referencing. The actual magnetic values were reduced by 25,000 gammas before plotting the contour maps (Huntings, 1976). This means that the value of 25,000 gammas should be added to the contour values so as to obtain the actual magnetic field at a given point. A correction based on the International Geomagnetic Reference Field, IGRF, and epoch date January 1, 1974 was included in all the maps.

3.1.2 Map Digitization Techniques

The method of extracting magnetic field intensity values from an aeromagnetic map is referred to as digitization. Principal methods that can be applied to achieve this include the Visual Interpolation Method (i.e. Digitization on Grid Layout) and Digitization along Flight Line Method. Today, there are computer based methods for digitizing aeromagnetic data. Popular among these software is Integrated Land and Water Information System (ILWIS).

3.1.2.1 **Digitisation on Grid Layout (Visual Interpolation Method)**

This method involves the drawing of a given number of straight lines vertically and horizontally at equal spacing on a tracing paper to form a grid layout. The boundaries of the layout must coincide with the boundaries of the aeromagnetic map to be digitised. The layout is overlain on the aeromagnetic map and magnetic values are read at the junctions or cross points on the grid system. At grid points where contour lines do not cross, visual interpolation to the closest contour line is made to estimate the magnetic value at the grid point. Since the grid points are evenly spaced, it is easier to determine the longitude and latitude of each grid point. The grid layout may be rectangular or square depending on the wish of the interpreter and the nature of the area concerned. This method is referred to as the visual interpolation method. This method is better applied in areas with dense magnetic contours such that most of the grid points are crossed by contours or are in close proximity to contours. Experience and carefulness substantially reduced the error of human judgment.

3.1.2.2 **Digitisation along Flight Lines**

Airborne magnetic surveys are usually done along flight lines. These flight lines are also indicated in the aeromagnetic maps. Thus a digitiser may decide to pick magnetic field values at points where contour lines cross the flight lines. In this method, no visual interpolation is needed. A major advantage of this method is the fact that the values read along flight lines are very close to the actual magnetic values measured during the survey. Reading along flight lines also reduces the error of human judgment since no visual interpolation is done. The two main disadvantages of this method are:

(i) The latitude and longitude values of each data point must be read directly or calculated by directly measuring the x and y distances of each data point. This must be done since the data points are randomly spaced. Either way of calculating the longitude and latitude in this method can introduce human error of judgment.

(ii) The randomly spaced data are not suitable for most available methods of magnetic data analysis and interpretation. Thus, before the data can be used, a two-dimensional interpolation of the data must be carried out to obtain data values on a regular grid. Ojo and Kangkolo (1997) noted that each of the interpolation methods taken singly presents disadvantages.

Today, most data from NGSA have already been digitised. However, the data used for this work were acquired much earlier before the release of the new data by NGSA in 2010. The data used were digitised on a 19 x 19 grid systems using Integrated Land and Water Information Systems (ILWIS). The spacing imposes a Nyquist wavelength of 1/2.894 km, approximately 3.0 km. Thus, the magnetic feature that can be defined by the digitised data has a narrowest width of 6.0 km. This gridding system was supported by previous studies with crustal magnetic anomalies (Ajakaiye, Hall and Millar (1985); Udensi, 2000; Udensi and Osazuwa (2002)), which shows that the spacing is suitable for the portrayal and interpretation of magnetic anomalies arising from regional crustal structure. They noted that, crustal anomalies are much wider than 6 km and therefore lie in a frequency range for which computational errors arising from aliasing do not occur with 3 km digitizing grid.

3.1.3 **Production of Composite Dataset**

Production of a unified aeromagnetic map of the study area is the ultimate aim, as this composite map would represent the entire study area and it is on this map that the interpretation was based. The computer program used to realize the dataset was designed to work on a square or rectangular blocks of small maps. The maps represented in this study form a square block.

The problem that has to be solved is that of the boundary (edge) effect, as adjourning sheet has similar coordinate and values as the one next to it for the boundary data. This problem has to be overcome before a unified dataset is produced. Each small map contains 19 by 19 digitise values. At the boundary of two maps, the field values in the last column of the first map have the same coordinates (latitude and longitude) as the field values at the first column of the second map. To have a unified dataset, all magnetic values with the same coordinates must be added and averaged so that there would be no rows and columns of magnetic points with the same coordinates. A data file containing the magnetic values of the small maps formed the input file for the merger program. The program will read in the number of each map one after the other, placing them in a row and merging their column boundary values. It will merge the upper row boundary values of the first map with the lower row boundary values of the second map. The program continues this process until all maps are read and merged in. The output from this program is the dataset or unified aeromagnetic map in 89 by 89 square grid system.

3.1.4 Production of Composite Aeromagnetic Map (TMI/Super Map)

The unified composite dataset for the study area was produced and edge-matched to remove duplication of data for corresponding edge point from adjourning sheet map. This composite dataset was imported into the Surfer 8 environment and saved as a '*.xls' or '*.csv' file format. The data was arranged in three columns having field northing (latitude), easting (longitude) and the corresponding magnetic values extracted from the digitised maps. This dataset was then gridded in the Surfer environment using Kriging system of grid method and a composite aeromagnetic map of the study area (Figure 3.1) was produced. Similarly, the composite aeromagnetic map of the study area was also produced using Oasis montaj. Figure 3.2 is the coloured version of Figure 3.1.

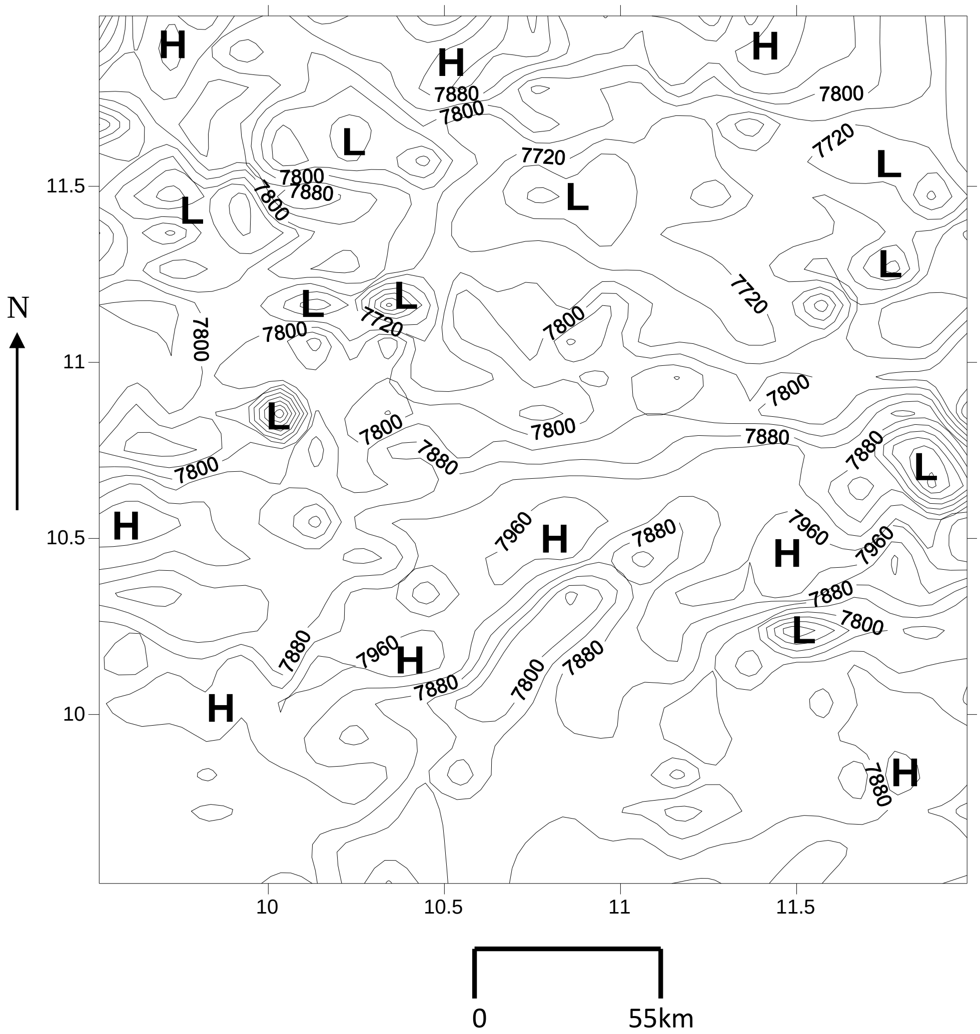

Figure 3.1: Total magnetic intensity contour map of parts of Upper Benue Trough and southern Bornu Basin. Magnetic ‘highs’ and ‘lows’ are represented with ‘H’ and ‘L’ respectively. (Contour Interval is 40 nT). A value of 25000 nT must be added to get the total field value.

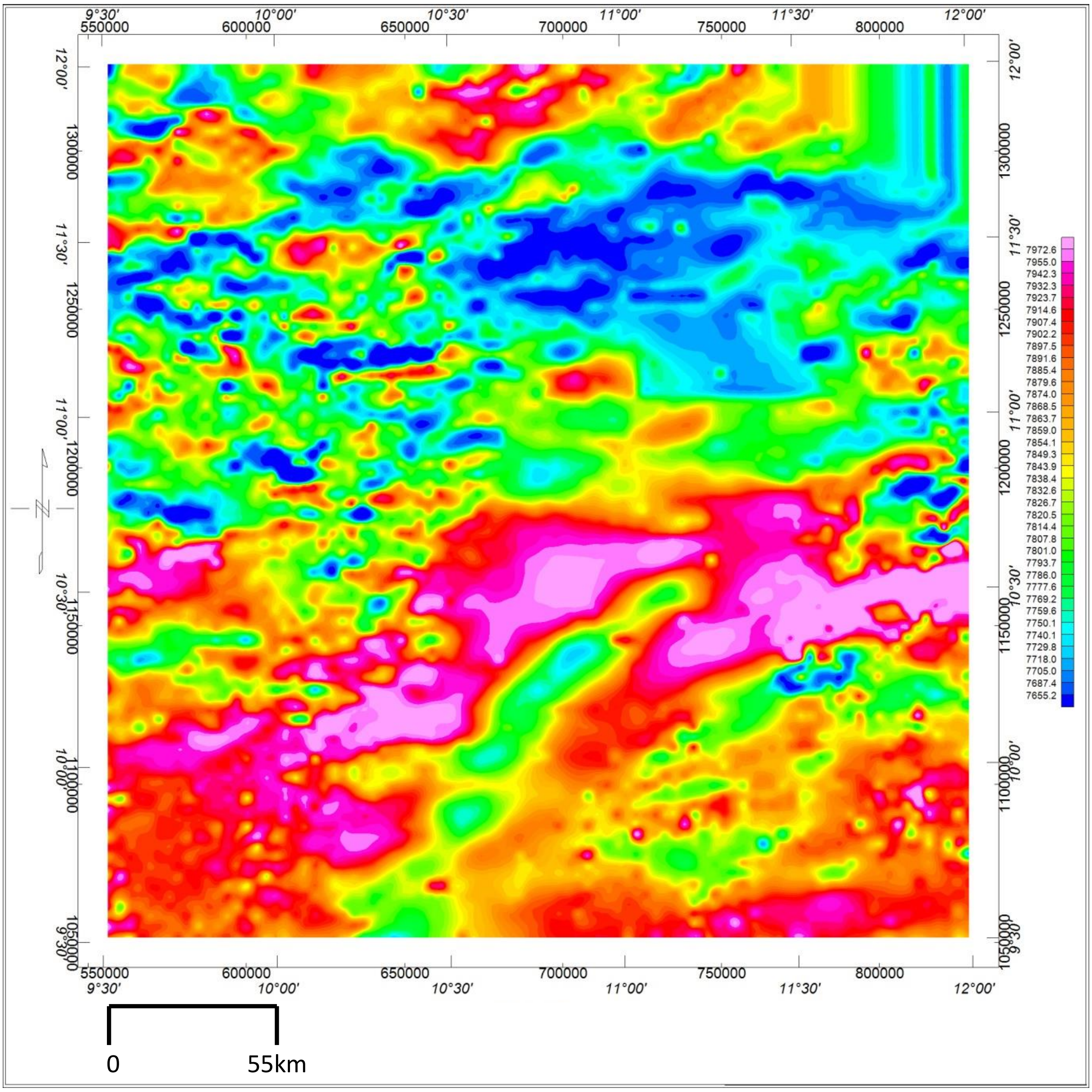

Figure 3.2: Colour-shaded Total Magnetic Intensity (TMI) Map of parts of Upper Benue Trough and southern Bornu Basin. Unit of total magnetic intensity is nano tesla (nT). A value of 25000 nT must be added to get the total field value.

3.2 Data Processing Methods

The data obtained in this study were processed in different ways for easy and effective interpretations of the sub-surface structure of the study area both qualitatively and quantitatively. These data were processed in three major ways as stated below:

a. Filtering process
b. CET (Centre for Exploration Targeting) grid analyses
c. Depth analysis techniques and
d. Magnetic modelling techniques

The filtering process and CET grid analyses would aid the qualitative interpretation while both depth analysis and magnetic modelling techniques would aid the subsurface magnetic interpretation quantitatively.

3.3 Filtering of the Magnetic Data (Regional - Residual Separation)

This is an essential process prior to analysis and interpretation. The objective of the filter is to condition the data set and to render the resulting presentation in such a way to make the magnetic anomalies easier to interpret in terms of their geological sources (Bird, 1997). Therefore, the most effective way to filter the data is with the understanding of the geologic control and the desired filtered results. Several filtering techniques can be performed in the frequency domain (i.e. wavenumber domain). However, one of the most traditional filters, used in the potential field, is the separation of long (deep) and short (shallow) wavelength anomalies (i.e. regional - residual separation). The success of this technique depends on the proper choice of cut-off wavelength used in the filter design. The cut-off wavelengths and information about the contribution of the short and long wavelengths in the spectrum can be obtained from the calculated radially–averaged power spectrum of the data (e.g. using Butterworth filtering method).

Regional - Residual Separation

The Total Magnetic Intensity (TMI) map is one that shows the superposition of disturbances of noticeably different order of sizes. The larger features show up as trends, which continue smoothly over considerable distances. They are caused by the deeper heterogeneity of the earth's crust. These trends are called the 'regional trends'. Superimposed on the regional fields, but frequently camouflaged by them, are the smaller local disturbances which are secondary in size but of primary importance. These are the residual anomalies and they may provide direct evidence of the existence of reservoir-type structures or mineral ore bodies.

All anomalies occur as local variations imposed upon (a) other local variations, (b) regional variations and (c) noise. In another sense, potential field data usually has energy in the profile or grid data from a large range of wavenumbers. All possible precautions should be taken to establish a reasonable regional field or base level for each anomaly. In the field, for example, an isolated profile should be extended to a reasonable distance from the source so that the interpreter will have a chance to estimate the asymptotic level of the anomaly. The regional may be defined as the value of the field which would exist if there were no local disturbance due to the source we are trying to interpret. The regional is actually unknown and may become quite subjective. It can be treated as an additional variable in an interpretation, but reasonable limits may be set from common sense provided by human intervention (Reeves, 2005).

For potential field data to be interpreted, the residual anomalies must be separated from the regional (background) field. In some respects, the problem usually conceived is analogous to filtering, but with the difference that is seen (the part ordinarily removed by filtering). This residual is of importance in the several methods of removing the unwanted regional from the total field data. The following are one of the various way of separating regional field from residual field, these are:

a. Graphical (smoothing) method and

b. Analytical method

3.3.1 **Graphical (Smoothing) Method**

One of the oldest and most traditional methods of making the regional-residual separation is by visually smoothing the contour lines on a number of profiles. The process is based on successive approximations (Grant and West, 1965). The process works roughly by approximations in the following way: the trend of the regional field is assumed and profiles are drawn along that trend. The set of profiles which emerge from this exercise is then examined with a view to further smoothing, and so on, until an acceptable regional map is achieved. This method has the merit of being flexible, since it allows the interpreter to incorporate into the process his personal judgment or sense of 'rightness' about the forms of residual anomalies. This method will be satisfactory when the regional trend is fairly evident from the beginning. However, this method requires considerable work by expertise or experience which might not be readily available. Similarly, there are circumstances when smoothing method cannot be applied, these are:

i. When the ground is very hilly and the subsurface material are inhomogeneous

ii. If the regional trend is very strong, residual anomalies are easily missed by visual methods

iii. Even when the ground is not hilly, but residual anomalies are very large, the regional trends are often very difficult to isolate. This is more obvious in large scale surveys.

3.3.2 **Analytical Method**

The analytical method uses numerical operations on the observed data to isolate anomalies. Such techniques generally require that the magnetic values be spaced in a regular array, as done in this study. Four analytical approaches are common in use, they are:

i. Direct calculation of residual by techniques such as the centre-point-and-ring method

ii. Determination of first vertical derivatives

iii. Upward and downward continuation and

iv. Polynomial fitting

Computation of the first vertical derivative in an aeromagnetic survey is equivalent to observing the vertical gradient directly with a magnetic gradiometer and has the same advantages, namely, enhancing shallow sources, suppressing deeper ones, and giving a better resolution of closely-spaced sources. Second, third and higher order vertical derivatives may also be computed to pursue this effect further, but usually the noise in the data becomes more prominent than the signal above the second vertical derivative. The equation of the wavenumber domain filter to produce nth derivative is:

$$F(w) = w^n \qquad (3.1)$$

Horizontal derivatives may also be calculated, noting that a direction (azimuth) needs to be chosen, giving another element of choice for optimum presentation. Alternatively, the maximum horizontal gradient at each grid point can be displayed, regardless of direction (Reeves, 2005).

Upward and Downward Continuation - A potential field measured on a given observation plane at a constant height can be calculated as though the observations were made on a different plane, either higher (upward continuation) or lower (downward continuation). The equation of the wavenumber domain filter to produce upward continuation is simply:

$$F = e^{-hw} \tag{3.2}$$

Where h is the continuation height. This function decays steadily with increasing wavenumber, attenuating the higher wavenumbers more severely, thus producing a map in which more regional features predominate

The equation of the wavenumber domain filter to produce downward continuation is:

$$F = e^{hw} \tag{3.3}$$

This is a curve which is zero at zero wavenumber and increases exponentially at higher wavenumbers, thus emphasizing the effect of shallow sources and noise. Noise removal is thus an essential first step before downward continuation, and continuation depths should not exceed real source depths. Some careful experimentation is usually necessary to obtain acceptable results (Reeves, 2005).

The polynomial fitting method - is about the most flexible and most applied of the analytical method for determining regional magnetic field (Skeels, 1967; Johnson, 1969 and Dobrin, 1976). In this method, the matching of regional by a polynomial surface of low order exposed the residual features as a random error. The treatment is based on statistical theory. The observed data are used to compute, usually by least squares, the mathematically describable surface giving the closest fit to the magnetic field that can be obtained within a specified degree of detail. This surface is considered to be the regional field and the residual is the difference between the magnetic field value as actually mapped and the regional field value thus determined (Udensi, 2000).

The polynomial fitting was done using the least square method. The method becomes handy and adequate because of the simple nature of the geology of the area and its limited spatial extent. It was assumed reasonably that the regional field is a first degree polynomial surface. All the regional fields were therefore calculated as two dimensional (2-D) first degree polynomial surfaces.

A computer program was used to derive the residual magnetic values by subtracting values of the regional fields from the total magnetic values at the grid cross point. The regional and residual magnetic maps of the area are shown in Figures 3.3 and 3.4 respectively.

3.4 Structural Analysis of the Residual Map of Study Area Using CET Grid Analysis

The CET grid analysis is a new technique developed by Centre for Exploration Targeting (CET), released in the year 2011. It included two workflows. The first method is suitable for analysing regions of subdued magnetic responses (like sedimentary areas) where texture analysis can first enhance the local data contrast. The second method, edge detection, is useful in identifying linear discontinuities.

The CET grid analysis extension provides a rapid unbiased workflow that reduces time when interpreting large volumes of grid data. This extension contains tools for texture analysis, phase analysis, and structure detection. These are versatile algorithm useful for grid texture analysis, lineament detection, edge detection and thresholding (Kovesi (1991, 1997), Lam, Lee and Suen (1992); Holden, Dentith and Kovesi (2008) and Holden, Kovesi, Dentith, Wedge, Wong and Fu (2010)).

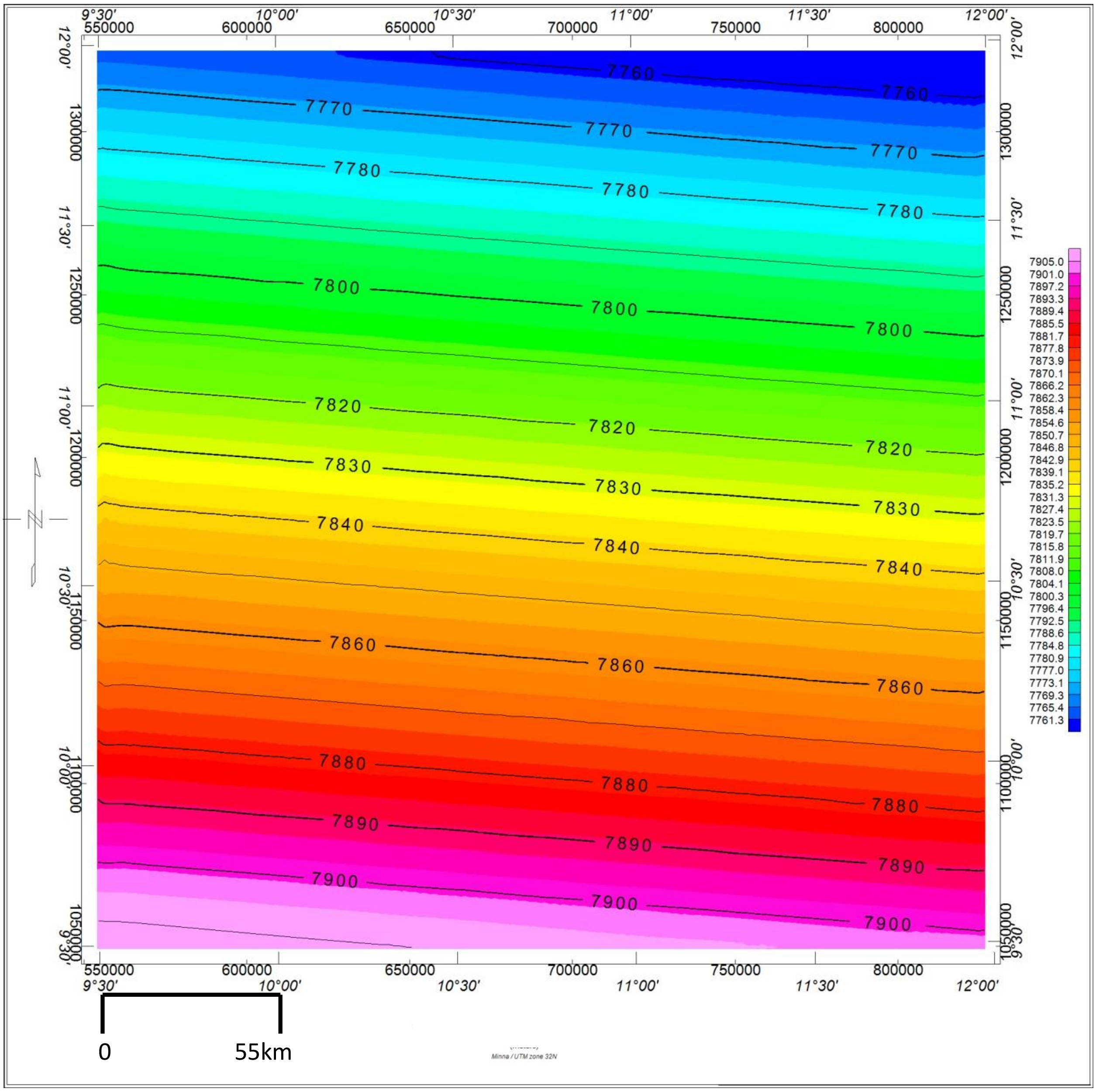

Figure 3.3: Regional-Magnetic contour map of parts of Upper Benue Trough and southern Bornu Basin (contour interval is 10 nT).

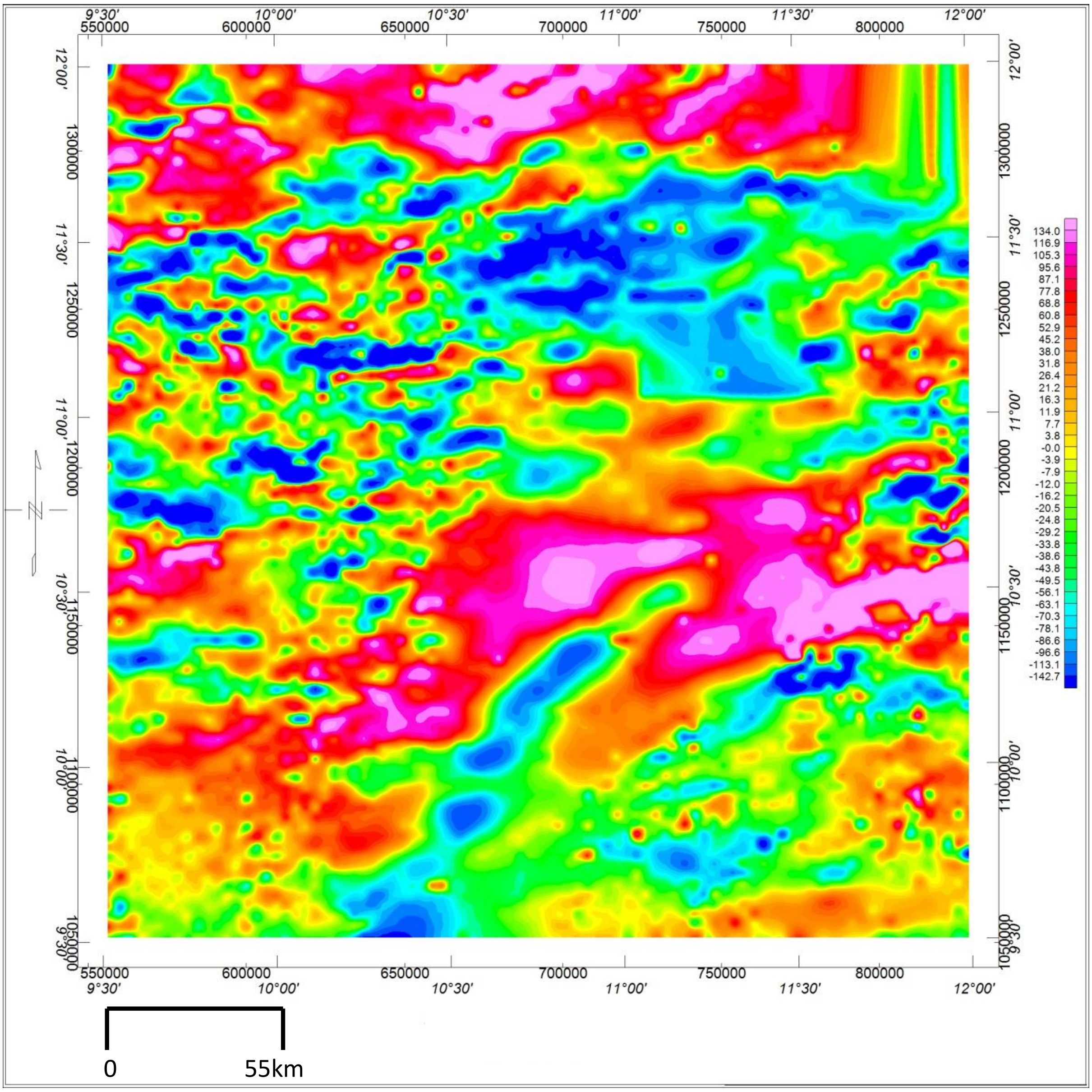

Figure 3.4: Colour - Shaded Residual-Magnetic map of the study area. Unit of total magnetic intensity is nano tesla (nT).

The CET grid analysis uses three successive grid methods, these are:

1. Texture analysis- this is based on image enhancement, it is useful for highlighting local intensity variations. It enhances regions of discontinuity within aeromagnetic data sets. Trends are found in the data by identifying regions of textural complexity in the local magnetic response before looking for axes of symmetry. Such axes are likely to be distinct linear discontinuities in the signal. Regions of magnetic discontinuity usually correspond with and can reveal, lithology boundaries, faults and dykes, which are critical to understanding the geology of an area. The texture analysis output, finds the skeletal structure of the regions of the magnetic discontinuity. The output is a set of binary skeletal line segments that belong to each of the discontinuity regions, early showing the changes of orientations and offsets within the structure. In summary, texture analysis, highlights the locations of complex local textures often associated with discontinuities in magnetic data (Lam, Lee and Suen (1992), Holden, Dentith and Kovesi (2008) and Holden, Kovesi, Dentith, Wedge, Wong and Fu (2010)).
2. Phase symmetry- This uses the results of the texture analysis to detects any laterally continuous line-like regions of discontinuity (Kovesi (1991, 1997)).
3. Structural detection- this uses the phase symmetry results to reduce the regions containing discontinuities into skeletal structures detailed as a binary grid.
4. Discontinuity structure detection- This approach applies phase-based edge detection directly to data to find edges whose noise characteristics and poor contrast limit the effectiveness of traditional gradient based approaches. As an alternative method of identifying linear discontinuities, edge detection can be performed directly on magnetic or gravity data. Using phase-based approach

will ensure that even features lying in low contrast regions will be detected (Holden, Dentith and Kovesi (2008) and Holden, Kovesi, Dentith, Wedge, Wong and Fu (2010)).

The structural analysis is better done when the residual grid is first reduced to the equator (RTE) before being transformed to the pole (RTP). The structures in the original data/grid if not transformed would not show as the initial data was taken too close to the equator (i.e. Nigeria is closer to the equator than to the pole). Another reason for necessary transformation was that the tool for the analysis and most other processing tools were developed with the ideas that the data collected (to be used for processing) were closed to the pole. This is because, the environment in which most of these software were developed are very close to the pole.

Therefore, to put the software into better use and for adequate and appropriate analysis, our data needed to be transformed from its initial state (first reduced to the equator-RTE) and then reduced to pole- RTP. This process emulates the traditional manual drawing of interpretive lines along the discontinuity. This includes:

i. Phase Congruency- this find edges in magnetic or gravity data irrespective of their orientation or contrast with the background (Kovesi, 1991 and 1997).
ii. Structure Detection- This generates trend line estimates from the edge information detected by the phase congruency transform (Holden, Dentith and Kovesi (2008) and Holden, Kovesi, Dentith, Wedge, Wong and Fu (2010)).

3.5 Depth Analysis

3.5.1 Spectral Analysis

Spectral analysis involves a plot of a radially-averaged power spectrum on a natural logarithmic scale. In general, it is found that potential field anomalies analysed in this way display something approaching a natural power-law spectrum, such that, much energy comes from large, deep sources (at a low wavenumbers) and relatively little (orders of magnitude less) from small, shallow ones (high wavenumbers) with an approximately exponential decay with wavenumber. Beyond the Nyquist wavenumber, the spectrum is meaningless, (any energy originally here will be aliased or folded-back into lower wavenumbers), but usually noise predominates at wavenumbers approaching the Nyquist wavenumber if a sound sampling regime was established for the survey.

3.5.1.1 Theory of Spectral Analysis (Spectral Depth-Determination Methods)

The Fourier transform of the potential filed due to a prismatic body has a broad spectrum whose peak location is a function of the depth to the top and bottom surfaces and whose amplitude is determined by its density or magnetization. The peak wavenumber (ω') can be related to the geometry of the body according to the following expression.

$$w' = \frac{ln\left({}^{h_0}/_{h_t}\right)}{h_b - h_t} \qquad (3.4)$$

where:

w' is the peak wavenumber in radian /ground unit

h_t is the depth to the top

h_b is the depth to the bottom

for a bottomless prism, the spectrum peak at the zero wavenumber according to the expression:

$$f(\omega) = e^{-h\omega} \tag{3.5}$$

where ω is the angular wavenumber in radians/ground unit and h is the depth to the top of the prism.

For a prism with top and bottom surface, the spectrum is:

$$f(\omega) = e^{-h_t\omega} - e^{-h_b\omega} \tag{3.6}$$

where h_t and h_b are the depths to the top and bottom surface respectively. As the prism bottom moves closer to the observation point at the surface, the peak moves to a higher wavenumber (Figure 3.5).

Considering the spectrum of a fixed size prism, as the prism depth increases, the peak of the spectrum shifts to lower wavenumbers (the space domain anomaly becomes broader) and the amplitude of the spectrum decreases.

When looking at the spectrum, it is important to note that the amplitude of a deep prism does not exceed the amplitude of the same prism at shallow depth at any wavenumber. The effect of increasing the depth is to shift the peak to lower wavenumbers.

Because of this characteristic, there is no way to separate the effect of deep sources from shallow sources of the same type by using wavenumber filters. The sources can only be distinguished if the deep sources have greater amplitude or if the shallow sources have less depth extent. When considering a line that is long enough (or area large enough) to include many sources, the log spectrum of this data can be used to determine the depth to the top of a statistical ensemble of sources using the relationship.

$$Log\ E(k) = 4\pi hk \tag{3.7}$$

where h is the depth in ground units and k is the wavenumber in cycles / ground unit.

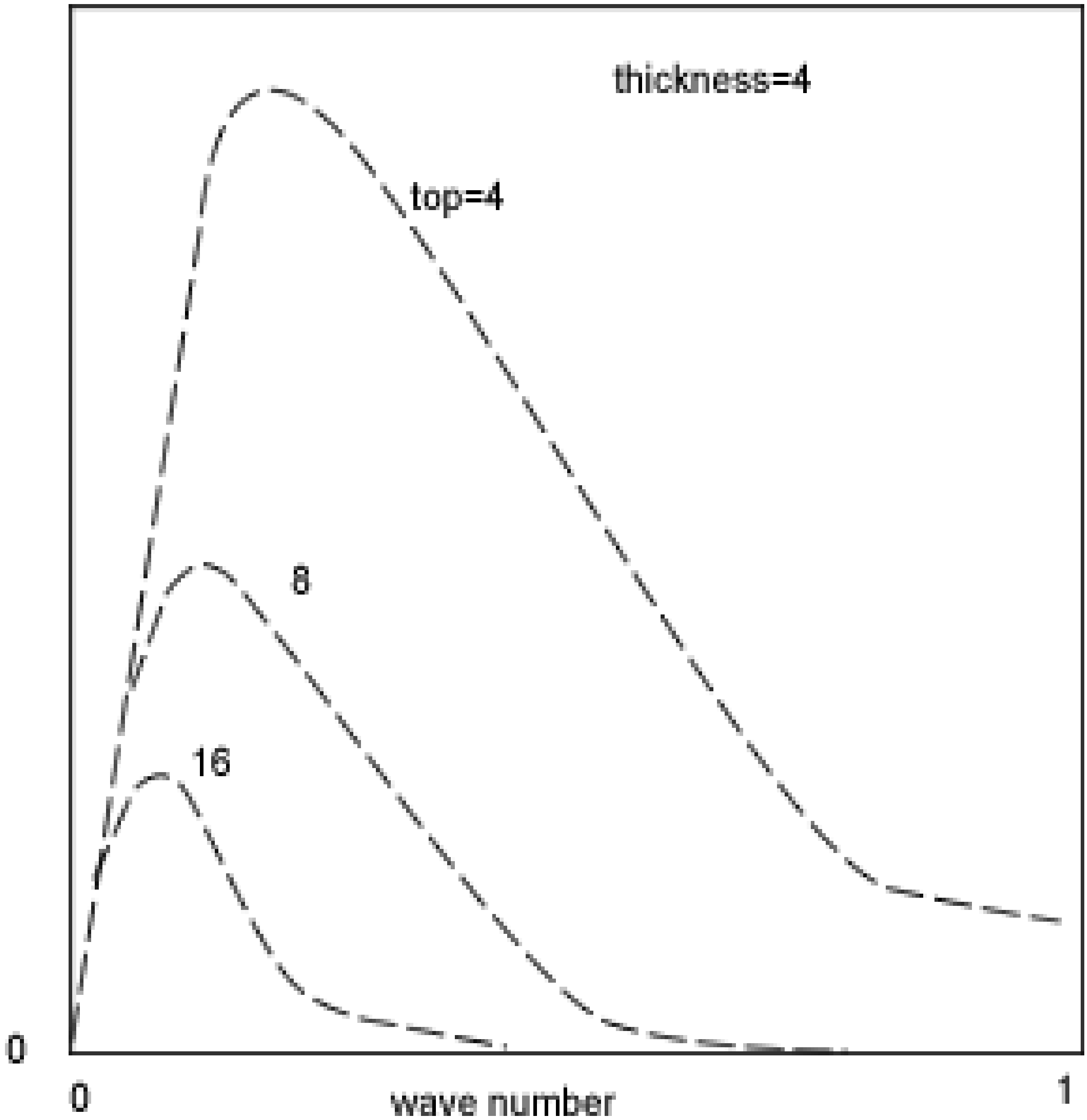

Figure 3.5: A sample spectrum of a prism. The number units are in cycle/km.

The depth of an 'ensemble' of source can be determined by measuring the slope of the energy (power) spectrum and dividing by 4π. A typical energy spectrum for magnetic data may exhibit three parts – a deep source component, a shallow source component and a noise component. Figure 3.6 illustrates the interpretation of an energy spectrum into those three components.

As well as having a form in the space domain, magnetic anomalies have a form in the frequency domain and, in theory, can be interpreted in the frequency domain. In practice, the spectra of single sources and multiple sources are much more complicated in the frequency domain than their space domain equivalents (e.g. Bhattacharyya, 1966) and no routine interpretation is attempted with such representations. The main attempts to use spectral data for depth estimates stem from a publication by Spector and Grant (1970) which was based on the unpublished thesis of Spector (1968). Spector (1968) showed that for an ensemble of prismatic blocks with infinite depth extent the logarithmic radial energy spectrum of the total magnetic intensity consists of a straight line whose gradient is related to the average depth to the tops of the prisms.

Furthermore, in the case of a double ensemble of prisms, two gradients would normally be obvious in the spectrum, with the steep gradient related to the deeper sources and the low gradient related to the shallow sources. It is important to realize, however, that the slope of spectra can only be used to calculate average depths when the sources are an ensemble of uncorrelated magnetic poles. Significant corrections for the average width of the prismatic bodies and their depth extent must be applied before any accurate depth estimation can be attempted for the spectra of ensembles of prismatic blocks. According to Spector (1968), these corrections can modify depth estimates to the order of 50 per cent.

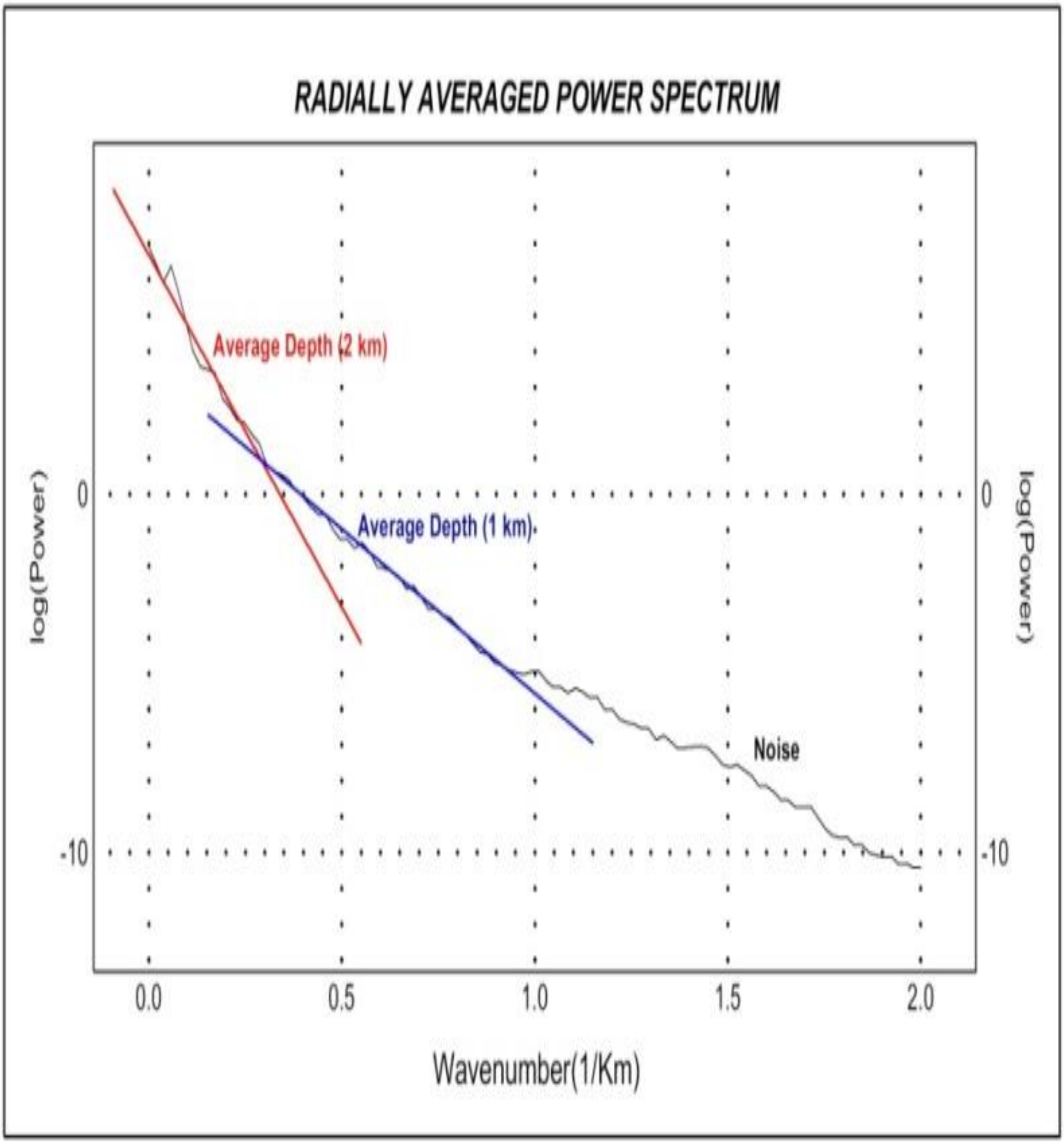

Figure 3.6: A typical spectral plot

3.5.2 Source Parameter Imaging (SPI)

The Source Parameter Imaging ™ (SPI™) function is a quick, easy, and powerful method for calculating the depth of magnetic sources. Its accuracy has been shown to be ± 20% in tests on real data sets with drill hole control. This accuracy is similar to that of Euler deconvolution, however SPI has the advantage of producing a more complete set of coherent solution points and it is easier to use.

A stated goal of the SPI method (Thurston and Smith, 1997) is that the resulting images can be easily interpreted by someone who is an expert in the local geology. The SPI method (Thurston and Smith, 1997) estimates the depth from the local wavenumber of the analytical signal. The analytical signal $A_1(x, z)$ is defined by Nabighian (1972) as:

$$A_1(x,z) = \frac{\partial M(x,z)}{\partial x} - j\frac{\partial M(x,z)}{\partial z} \qquad (3.8)$$

where $M(x,z)$ is the magnitude of the anomalous total magnetic field, j is the imaginary number, z and x are Cartesian coordinates for the vertical direction and the horizontal direction respectively. Nabighian (1972) shows that the horizontal and vertical derivatives comprising the real and imaginary parts of the 2D analytical signal are related as follows:

$$\frac{\partial M(x,z)}{\partial x} \Leftrightarrow -\frac{\partial M(x,z)}{\partial z} \qquad (3.9)$$

where ⇔ denotes a Hilbert transformation pair. The local wavenumber k_1 is defined by Thurston and Smith (1997) to be

$$k_1 = \frac{\partial}{\partial x}\tan^{-1}\left[\frac{\partial M}{\partial z}\Big/\frac{\partial M}{\partial x}\right] \qquad (3.10)$$

The concept of an analytic signal comprising second-order derivatives of the total field, if used in a manner similar to that used by Hsu, Herman, Bhartia, Seftor, Torres, Thompson, …. and Holben (1996), the Hilbert transform and the vertical-derivative operators are linear, so the vertical derivative of (3.9) will give the Hilbert transform pair,

$$\frac{\partial^2 M(x,z)}{\partial z \partial x} \Leftrightarrow -\frac{\partial^2 M(x,z)}{\partial^2 z} \qquad (3.11)$$

Thus the analytic signal could be defined based on second-order derivatives, $A_2(x, z)$, where

$$A_2(x,z) = \frac{\partial^2 M(x,z)}{\partial z \partial x} - j\frac{\partial^2 M(x,z)}{\partial^2 z} \qquad (3.12)$$

This gives rise to a second-order local wavenumber k_2, where

$$k_2 = \frac{\partial}{\partial x} \tan^{-1}\left[\frac{\partial^2 M}{\partial^2 z} \Big/ \frac{\partial^2 M}{\partial z \partial x}\right] \qquad (3.13)$$

The first- and second-order local wavenumbers are used to determine the most appropriate model and a depth estimate independent of any assumptions about a model.

Nabighian (1974) gives the expression for the vertical and horizontal gradient of a sloping contact model as:

$$\frac{\partial M}{\partial x} = 2KFc \sin d \; \frac{h_c cos(2I-d-90)+x sin(2I-d-90)}{h_c^2+x^2} \qquad (3.14)$$

$$\frac{\partial M}{\partial z} = 2KFc \sin d \; \frac{x cos(2I-d-90)+h_c sin(2I-d-90)}{h_c^2+x^2} \qquad (3.15)$$

where K is the susceptibility contrast at the contact, F is the magnitude of the earth's magnetic field (the inducing field), $c = 1 - cos^2 i sin^2 \alpha$, α is the angle between the positive x-axis and magnetic north, *i* is the ambient-field inclination,

$\tan I = \sin i / \cos\alpha$, d is the dip (measured from the positive x-axis), h_c is the depth to the top of the contact and all trigonometric arguments are in degrees. The coordinate system has been defined such that the origin of the profile line (x = 0) is directly over the edge.

The expression for the magnetic-field anomaly due to a dipping thin sheet is

$$M(x,z) = 2KF_{cw}\ \frac{h_1 sin(2I-d) - x cos(2I-d)}{h_c^2 + x^2} \tag{3.16}$$

(Reford, 1964), where w is the thickness and h_1 the depth to the top of the thin sheet. The expression for the magnetic-field anomaly due to a long horizontal cylinder is given by Murthy and Mishra (1980) as

$$M(x,z) = 2KFS\ \frac{\sin i}{sinI}\ \frac{\left(h_h^2 - x^2\right)cos(2I-180) + 2xh_h \sin(2I-180)}{\left(h_c^2 + x^2\right)^2} \tag{3.17}$$

where S is the cross-sectional area and h_h is the depth to the centre of the horizontal cylinder.

Substituting (3.14), (3.15), (3.16) and (3.17) into the expression for the first- and second-order (i.e. (3.10) and (3.13) respectively) local wavenumbers, we obtain, after some simplification, a remarkable result as:

$$k_1 = \frac{(n_k + 1)h_k}{h_k^2 + x^2} \tag{3.18}$$

and

$$k_2 = \frac{(n_k + 2)h_k}{h_k^2 + x^2} \tag{3.19}$$

where n_k is the SPI structural index (subscript k = c, t or h), and $n_c = 0$, $n_t = 1$ and $n_h = 2$ for the contact, thin sheet and horizontal cylinder models, respectively. From (3.18) and (3.19) above, it is evident that the first- and second-order local wavenumbers are independent of the susceptibility contrast, the dip of the source and the inclination, declination, and the strength of the earth's magnetic field.

The contact, thin sheet and horizontal cylinder are all two-dimensional models (infinite strike extent), so it is an implicit assumption of the SPI method that the geology is two dimensional. If the body is two-dimensional and there is no interference from nearby bodies, the depth estimate will be reasonable and the structural index should be constant over the entire area for which the response is anomalous.

3.6 Modelling of Aeromagnetic Anomalies

This involves making numerical estimates of the depth and dimensions of the sources of anomalies and this often takes the form of modelling of sources which could, in theory replicate the anomalies recorded in the survey. In other words, conceptual models of the subsurface are created and their anomalies calculated in order to see whether the earth-model is consistent with what has been observed, i.e. given a model that is suitable with the physical approximation to the unknown geology, the theoretical anomaly of the model is calculated (forward modelling) and compared with the observed anomaly. The model parameters are then adjusted in order to obtain a better agreement between observed and calculated anomalies.

The initial reason for graphical depth determination methods was the fact that exact modelling of anomalies in pre-computer days, is time consuming and it required tedious manual computation of anomaly forms, using different formulae. With the advent of computers and publication of a series of routines that allowed modelling by trial and error, curve-matching processes have become routine.

The most significant of the computer modelling algorithms are:

i. Computation of the magnetic field of a two-dimensional (infinite strike) body with an arbitrary polygonal shape (Talwani and Heirtzler, 1964). This method calculates the effect of the polygon by summing the magnetic effect of a series of horizontal sheets with sloping edges that correspond to the sides of the polygon. Modelling with the routine is commonly referred to as 2D modelling. This routine had been modified to a faster version that can handle situations where the magnetic body can be partly above the point of observation and where the observation point can be inside the magnetic body.

ii. Computation of the magnetic effect of arbitrarily shaped three-dimensional bodies by approximating them to horizontal polygonal laminae (Talwani, 1965). Good results can be produced with this routine, but the process of modifying the corners of the horizontal laminae to match a grid of observations, using a forward modelling process, can be very time consuming.

iii. Magnetic anomaly due to a dipping prism (Hjelt, 1972). This routine calculates the magnetic effect of prismatic bodies with parallel sides for cases where the top and bottom of the body are horizontal.

iv. Magnetic effect of a body with polygonal cross-section and limited strike length (Shuey and Pasquale, 1973 and Cady, 1980). This routine has a significant advantage over the Talwani and Heirtzler (1964) routine in that, it enables cross-sections of bodies with finite strike lengths to be modelled with a single profile. The routine assumes that equal portions of strike length occur on either side of the profile being modelled, and that the body being modelled has the same strike cross-section along its complete strike length. Modelling with the routine is commonly referred to as 2.5 - D modelling.

v. Magnetic anomaly of a finite-length right polygonal prism (Coggon, 1976). This routine calculates the magnetic field of a body arbitrary constant cross-section on a profile perpendicular to the body at any location along the length of the body. Modelling with this routine is commonly referred to as 2.75 - D modelling.

vi. Magnetic anomaly of a tri-axial ellipsoid (Clark, Saul and Emerson, 1986). This routine is extremely useful for modelling the response of a variety of ore bodies. It is capable of computing the effect of anisotropic susceptibility and demagnetization. Demagnetization is an effect whereby the magnetic effect of very magnetic bodies distort the ambient magnetic field such that the direction of the earth' s field changes and the computation of magnetic anomalies using simple induction relationship is no longer possible.

vii. A modelling package specifically designed to simulate structural problems (Valenta, Jessel, Jung and Bartlett, 1992; Jessel, Valenta, Jung, Cull and Geiro, 1993). Using this package it is possible to input a series of horizontal layers and then compute the magnetic effect on the stratigraphy after a specified sequence of folding, faulting and igneous intrusion. The routine is based on subdividing the under-formed magnetic units into small cubes. The magnetic effects of the original model and all deformed model are calculated by summing the magnetic effect on the cubes in their original or relocated positions. This package can give useful indications of the likely magnetic patterns in structurally complex areas.

viii. Computer model of the magnetic effect of arbitrarily shaped magnetic bodies by approximating their surface to a series of triangular facets (Bott, 1963 and Lee, 1980). These routine model virtually all situations; however, they depend upon having a routine that facilitates the translation of the shape of the body to the triangular facets. Lee's routine includes the possibility of correcting for the demagnetization effect if no remanence is present. Lee also addresses the problem of defining the triangular facets.

These computer routines have been incorporated into various proprietary and commercially available packages in windows-type environments. These packages allow the interpreter such option as definition of regional, computation of residuals multi-source model and inclusion of remanence, demagnetization and anisotropy. The algorithms used for each modelling exercise depend upon whether the anomalies being interpreted are sufficiently elongated for a two-dimensional or quasi-two-dimensional approximation to be used or whether a three-dimensional model is required. The type of three-dimensional algorithm used depends on the form of the magnetic source and the detail required. Such routines have become basic interpretation tools; however, they can be time consuming to apply. They are suited to detailed analyses of single anomalies and cluster of anomalies and cannot be realistically applied to area depth determination problem. The modelling technique used in this work is a two dimensional (2D) modelling. The program, Gravity/Magnetic Systems (GMSYS), is an extension available in Oasis montaj version 7.5 of 2011.

CHAPTER FOUR

4.0 RESULTS AND DISCUSSION

4.1 Qualitative Analysis/Interpretation of Aeromagnetic Data.

Qualitative interpretation of aeromagnetic surveys is usually undertaken as an aid to geological mapping, often using the property of magnetic surveys to reveal the magnetic signature of the crystalline bedrock, even where it is covered by superficial deposits and thus invisible to the conventional field photo-geologist.

Qualitative analysis is presented in order to establish trends within the study area. Much qualitative information may be derived from a magnetic contour map. This applies especially to aeromagnetic maps that often provide major clues as to the geology and structure of a broad region from an assessment of the shapes and trends of anomalies. Sediment covered areas with relatively deep basement are typically represented by smooth magnetic contours reflecting basement structures and magnetization contrasts. Igneous and metamorphic terrains generate far more complex magnetic anomalies, and the effects of deep geological features may be obscured by high frequency anomalies of near surface origin. Spatial variations in the total magnetic field over an area reflect the variations in the magnetization of the rocks below the magnetometer. All variations in magnetic intensity measurable at the surface would be a result from a topographic or lithologic changes associated with the underlying basement rocks (Reeves, 2005).

4.2 Results of Qualitative Analysis/Interpretation of Total Magnetic Intensity (TMI) Map

The total magnetic intensity (TMI) map of the study area (Figure 4.1) shows a colour range of total magnetic intensity anomaly values, with red as highs and blue as lows. The map has magnetic values ranging from 7655.2 nT to 7972.6 nT with an average value of 7820 nT (relative to 25, 000 nT). The figure shows that the south-western part and the north-eastern part of the map trend northeast–southwest, while the south-eastern part and the central region of the study area trend east-west direction. The north-western part however, trends northwest- southeast. The northeast–southwest dominates the study area as shown in Figure 4.2.

Several magnetic highs and lows dot the survey area. The closures of the magnetic highs were marked as '**H**' while the magnetic lows were marked as '**L**' in Figure 4.2. These features are largely supported by colour distribution of Figure 4.1. Prominent among these lows is the combination of northwest (N-W), northeast (N-E) and east-west magnetic trends, which lie between latitude 10^{o}N and 11.2^{o}N. It is bounded by the landward extension of the Romanche fracture zone, delineated with AA' and St Paul fracture zone, delineated with CC' (Ajakaiye, Hall, Asiekaa and Udensi, 1991; Udensi and Osazuwa, 2003 and Ojo, 1990) (Figure 4.3). The lineament CC' could be the separation between the Bornu Basin and the Upper Benue Trough, which was named as "Dumbulwa-Bage High" by Zaborski, Ugodulunwa, Idornigie, Nnabo and Ibe (1998). This feature was reported to be found by Zaborski, Ugodulunwa, Idornigie, Nnabo and Ibe (1998) at about latitude 11.00^{0}N.

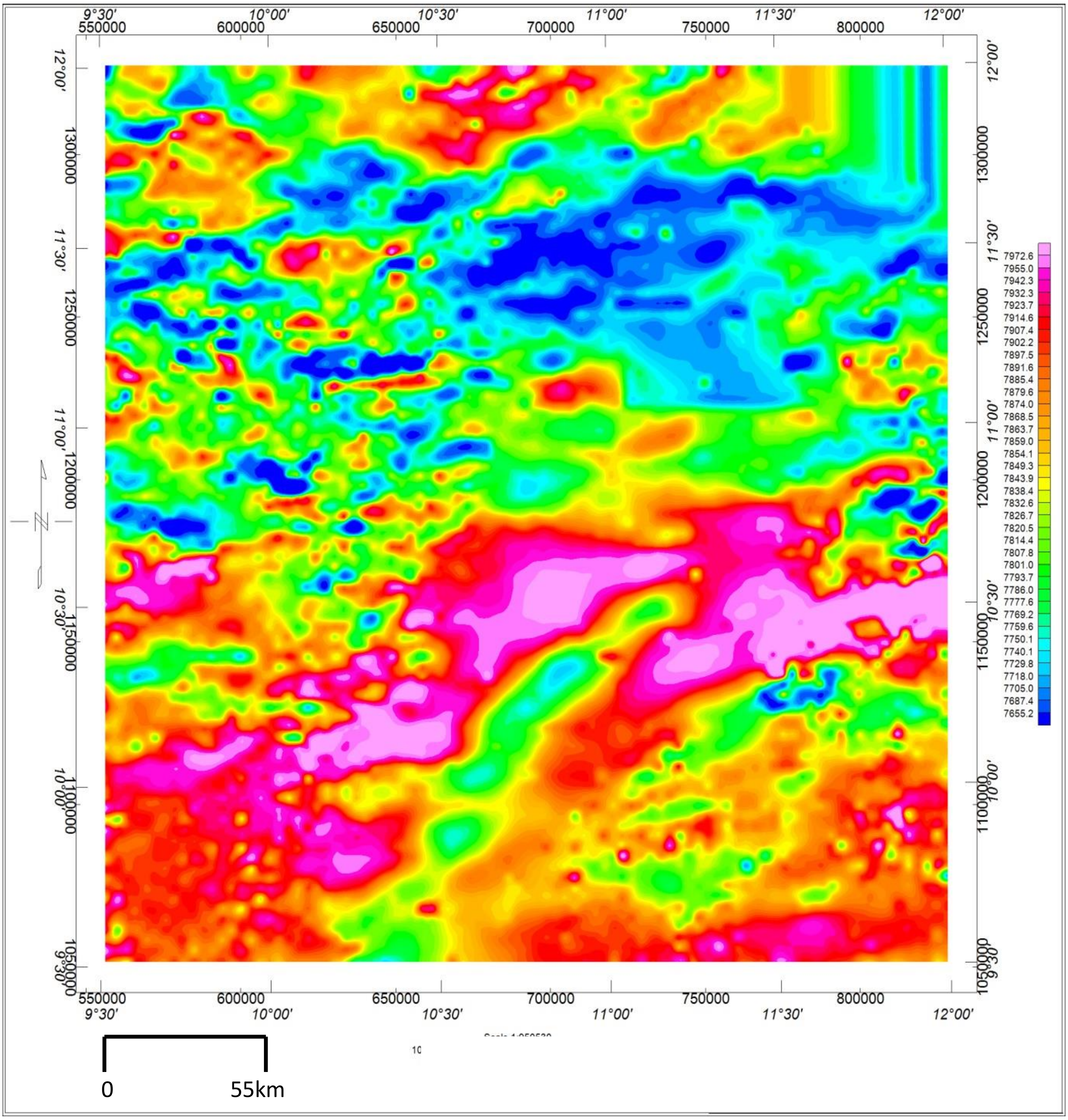

Figure 4.1: Colour-Shaded Total magnetic intensity map of parts of Upper Benue Trough and southern Bornu Basin. Unit of total magnetic intensity is nano tesla (nT). A value of 25000 nT must be added to get the total field value.

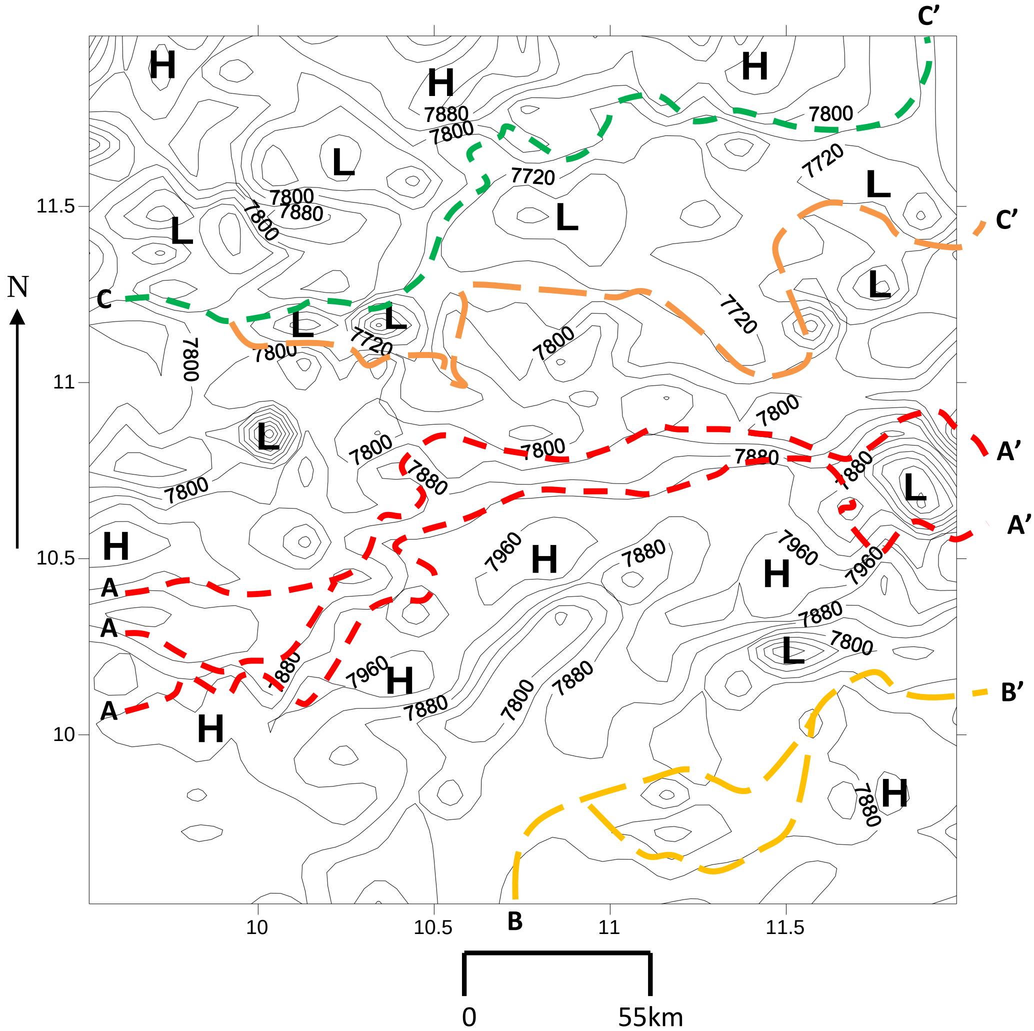

Figure 4.2: Total Magnetic Intensity Contour Map of parts of Upper Benue Trough and southern Bornu Basin. Magnetic 'Highs' and 'Lows' are depicted with 'H' and 'L' respectively. AA' BB', CC' are the landward extension of the Oceanic fracture zone noticed to have passed through the study area as postulated by Ajakaiye, Hall, Ashiekaa and Udensi (1991). AA', BB', CC' from their postulates, represents the Romanche, Chain and St. Paul paleo-structures respectively. (Contour Interval is 40 nT). A value of 25000 nT must be added to get the total field value.

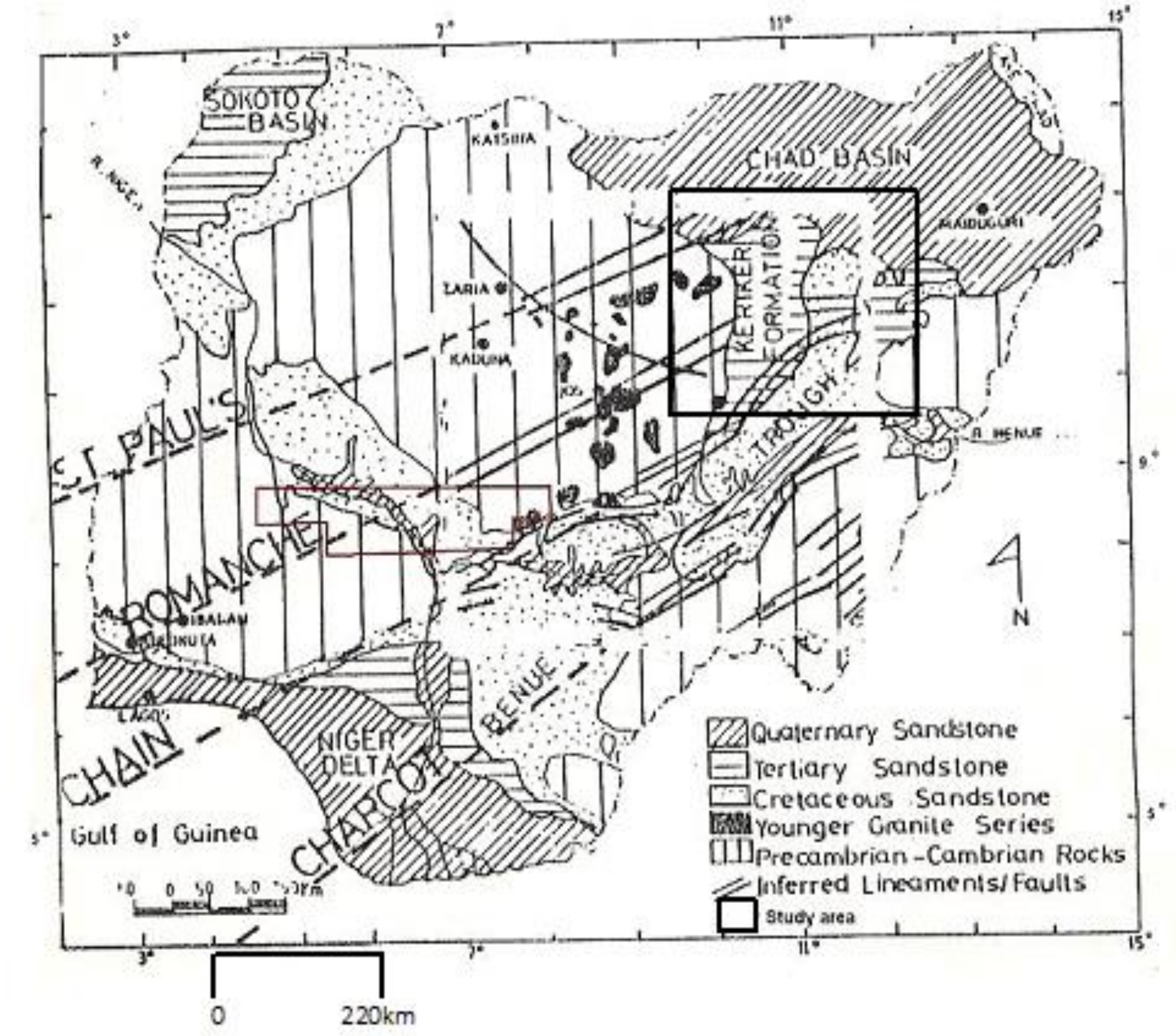

Figure 4.3: Structural map of Nigeria. The paleostructures St. Paul, Romanche, Chain and Charcot fracture zones were postulated to have passed through the study area (Source: (Ajakaiye, Hall, Ashiekaa and Udensi (1991) and Udensi, Osazuwa and Daniyan (2003).

Similarly, the southern parts dominated with highs were also bounded by both the postulated Romanche and Chain fractured zones, delineated by AA' and BB'. There are two other prominent closures of magnetic lows found in between AA' and BB' at the south-eastern part. Three other prominent highs could be found at the extreme northern part. The contours within the area are smooth at the boundaries.

The pattern of the magnetic lineaments across the Benue Trough is in agreement with the linear margins expected for a rift. The trough is characterised by sub-parallel magnetic anomaly belts trending ENE – WSW. The magnetic lineament (paleo-structures) interpreted by Ajakaiye, Hall, Ashiekaa and Udensi (1991), as St. Paul (CC'), Romanche (AA') and Chain (BB') ancient fracture zones were noticed as lineament passing through the survey area (Figure 4.2). These features were detected with about six distinct discontinuities that passed through the survey areas at different latitudes (AA', BB', CC' and CD'). Figure 4.4 is modified after Whiteman (1982), which also shows those paleostructures reported by Ajakaiye, Hall, Ashiekaa and Udensi (1991). The detection of these features has lent support to the view held by Ajakaiye, Hall, Ashiekaa and Udensi (1991), that the mid-Atlantic fracture zones have extension on-shore. It is observed that the two prominent magnetic closures within the study area are close to these lineaments (most especially, the Romanche and Chain fracture zones) and are aligned in the same direction. It is also observed that the composite magnetic map exhibits magnetic discontinuities close to the boundary at the northern part and south-eastern part of the map. These fractures are also identified as St Paul and Chain fracture zones respectively (i.e. CC' and BB') (Ajakaiye, Hall, Ashiekaa and Udensi, 1991; Udensi, Osazuwa and Daniyan, 2003 and Ojo, 1990).

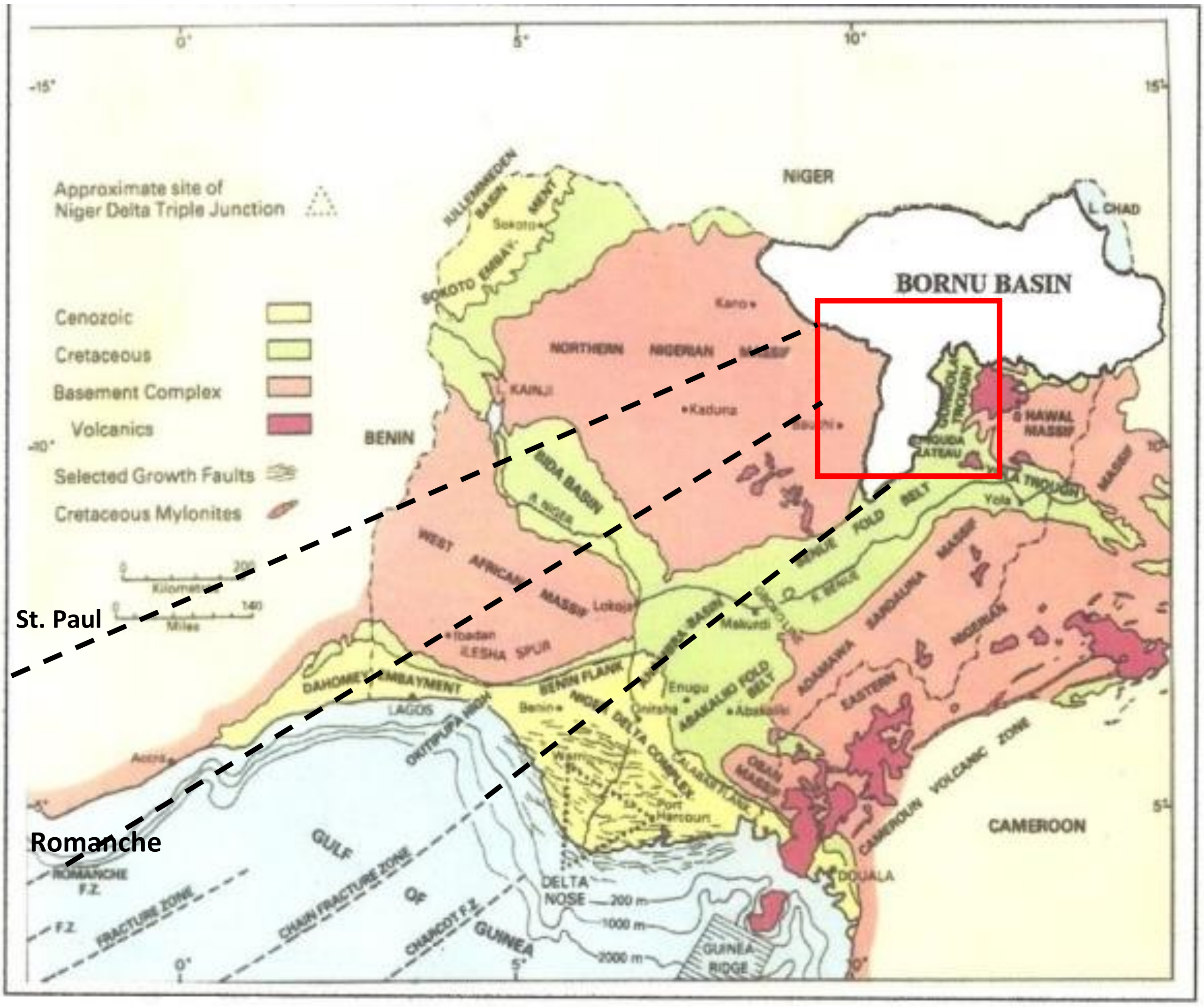

Figure 4.4: Generalised Geology map of Nigeria. The paleostructures: St. Paul, Romanche, and Chain fracture zones are postulated to have passed through the Upper Benue Trough and southern Bornu Basin. (Modified after Whiteman, 1982)

Located at the north-central portion of the map is a very big magnetic closure characterised with very low (L) contour values. This feature seems to be the lowest point of magnetic values, which extends towards the north-eastern part. It has a lateral distance of about 165 km and width of about 80 km. This feature will be analysed further in section 4.3.3. Another notable feature of southwest-northeast trends, found at the southern parts of the study area has large anomalies of as much as 7900 nT amplitude. These anomalies extend from longitude 10.00^{o}E to 12.00^{o}E (i.e. it has a lateral extent of about 200 km) and has a width of about 20 to 27 km. These anomalies were bounded by the Romanche and Chain fractures delineated as AA' and BB' respectively.

4.2.1 Surface Geologic Units Inferred from Total Magnetic Intensity Map (TMI)

Figure 4.5 shows the superposition of total magnetic intensity contour map over the geology map of the study area. This figure shows the relationships between the geology map and the TMI. From the figure, there are good correlations between the two maps. The highest magnetic contour values could be found around the basement complex area and the volcanic areas at the eastern part of the study area.

The sandstones (correspond to the Keri - Keri Formation) deposits found around Gombe, Ako-Gombe are characterised with relatively high magnetic values of amplitude 7880 nT to 7960 nT; this area corresponds to the highest magnetic value in Figure 4.1 with pink colouration. This sandstone deposit extends towards north of this figure (i.e. areas around Azare, Bulkachuwa, Damagum and Damaturu) where it is called the Chad Formation but with relatively low magnetic values of amplitude 7720 nT to 7800 nT. This area corresponds to the lowest magnetic value of Figure 4.1 (with blue colouration).

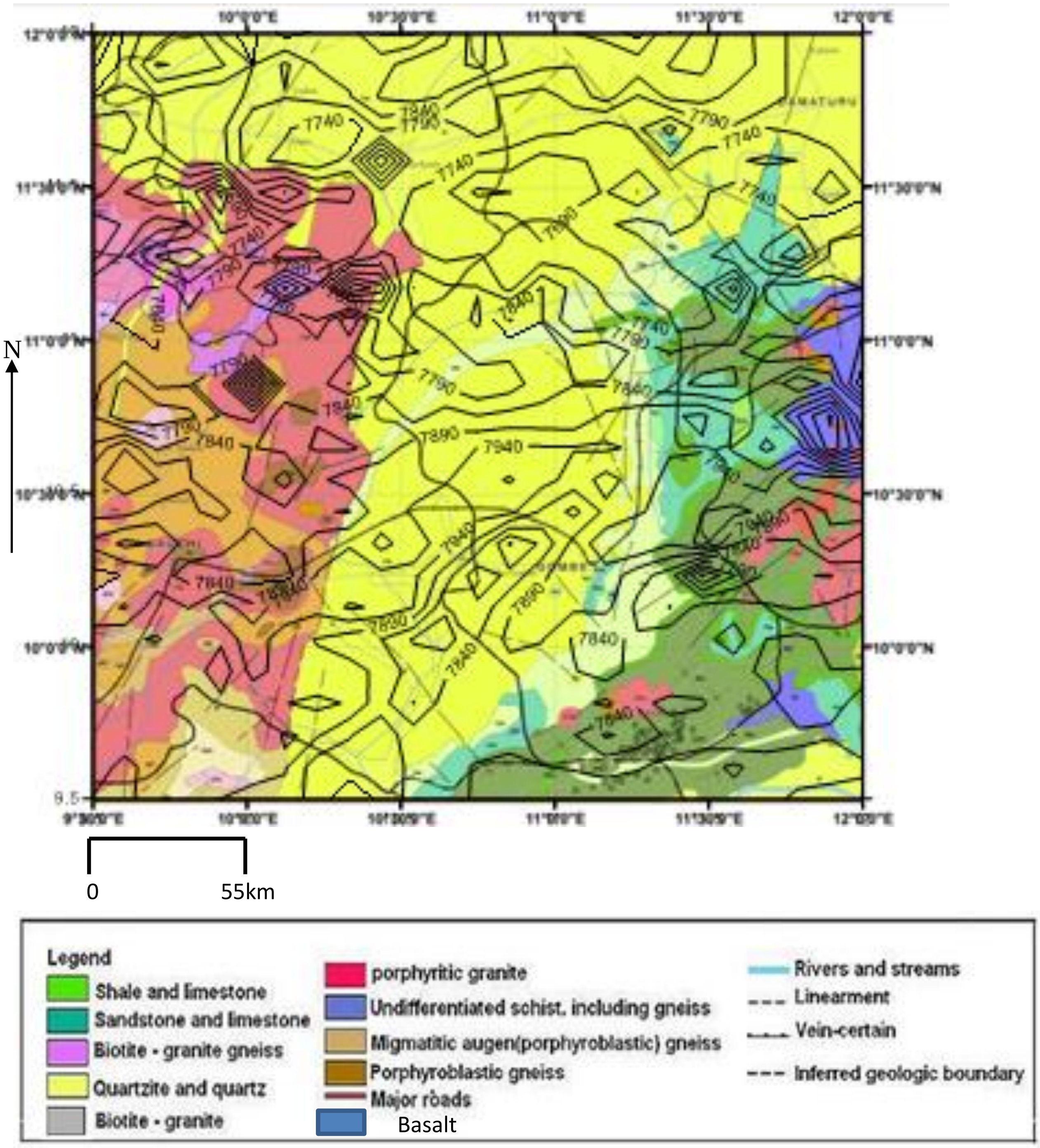

Figure 4.5: Total magnetic intensity contour map superimposed on the Geology map parts of Upper Benue Trough and southern Bornu Basin. Unit of total magnetic intensity is nano tesla.

4.2.2 Comparison of Lineament Map with Total Magnetic Intensity Map (TMI)

Figure 4.6 shows the relationship between the lineaments structure of the study area and the total magnetic intensity map. The dominant lineament trends in Figure 4.6 are northeast-southwest. There are however, mixtures of northwest-southeast and northeast-southwest trending structure to the northeast portion of Figure 4.6. Areas associated with volcanic nature as indicated (areas marked with "A") in Figure 4.6, are characterised with relatively high magnetic values between 7800 nT to 7960 nT. This area corresponds to Mazza, Meringa, Biu, Gandi, Buratai, Kwaya and Walama. The major fractured zone identified as Chain in Figures 4.2, 4.3 and 4.4 could be seen in Figure 4.6 at the southern part of the figure shown with oxblood dotted line. Another noticeable fractured line passes through Figure 4.6 at the north-western part corresponds to St. Paul of Figures 4.2, 4.3 and 4.4 delineated with red dotted line.

4.2.3 Comparison of Mineral resources Map with Total Magnetic Intensity Map (TMI)

There are different mineral resources scattered all over the study area. Figure 4.7 shows the relationship between the mineral resources distribution with the total magnetic field contour map of the study area. The Figure shows that areas like, Azare in the northwest is endowed with bromine (with relatively low magnetic values i.e. 7800 nT to 7880 nT); Damagum in north central (with magnetic values between 7720 nT and 7800 nT) is endowed with gypsum and phosphate, Gandi and Kwaya in eastern part are endowed with gypsum (with magnetic values between 7800 nT and 7960 nT). Gombe in southern part is endowed with feldspar; Kaltungo in the same region is endowed with Trona,

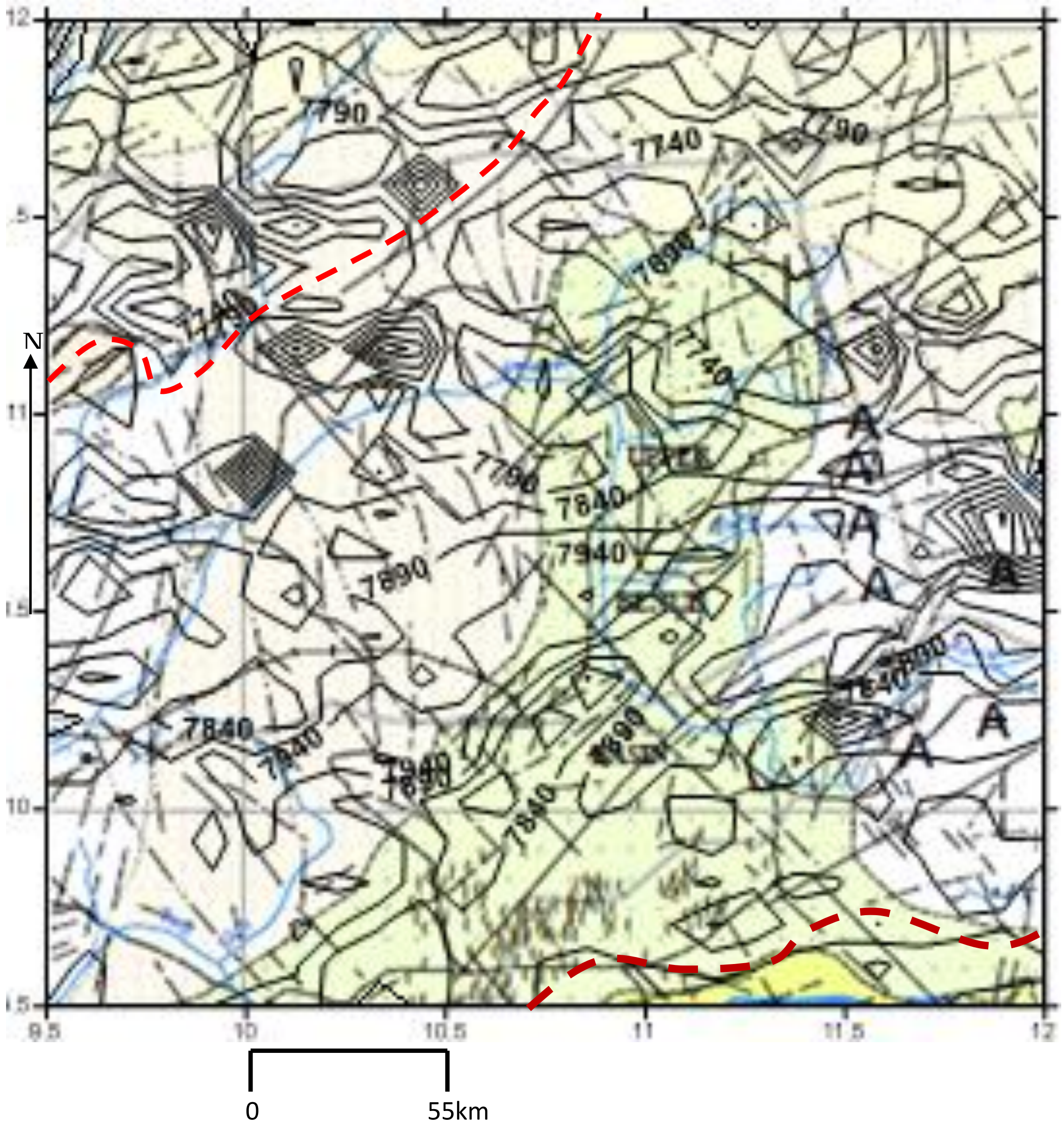

Figure 4.6: Total magnetic intensity contour map superimposed on the Lineament map of parts of Upper Benue Trough and southern Bornu Basin. Unit of total magnetic intensity is nano tesla. (Adapted from Nigeria Geological Survey Agency, 2006)

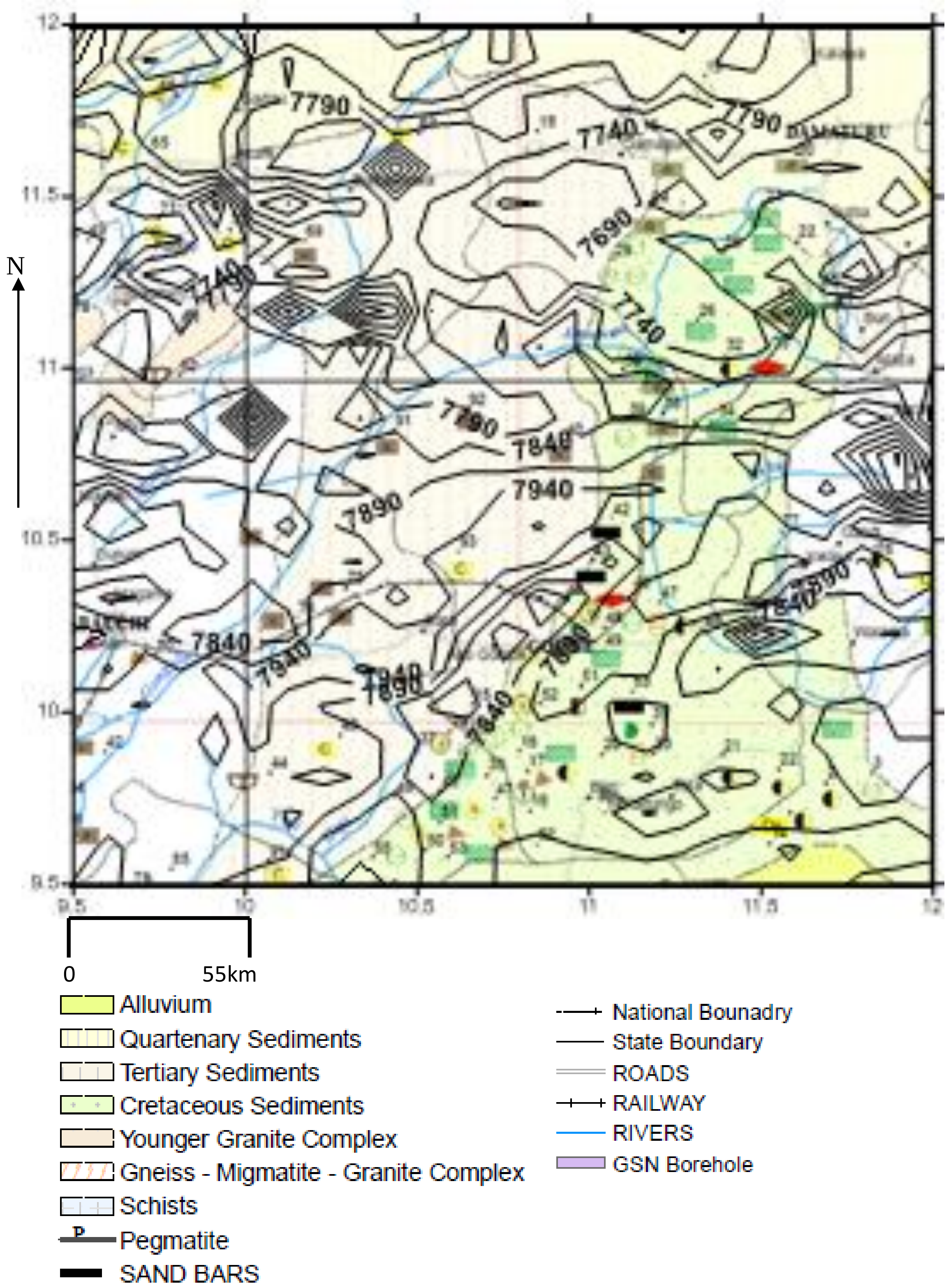

Figure 4.7: Total magnetic intensity contour map superimposed on the mineral map of parts of Upper Benue Trough and southern Bornu Basin. Unit of total magnetic intensity = nano tesla. (Adapted from Nigeria Geological Survey Agency, 2006)

gypsum, zinc, zircon, bromine and lead (Ford, 1981), the magnetic signatures around this region range between 7800 nT and 7880 nT. These minerals are less conductive or they have relatively low magnetic susceptibility values compared to magnetic minerals like, magnetite (Telford, Geldart, Sheriff and Keys, 2001).

4.3 Results of Filtering Process from Regional–Residual Separation and Upward Continuation

4.3.1 Regional Magnetic Field

Figure 4.8 is the map of the regional magnetic field data obtained from the separation of residual field data from the total field. The regional magnetic field values obtained range between 7761.3 nT and 7905.0 nT. The regional magnetic field map (Figure 4.8) shows contour lines trending in a general northwest–southeast direction.

The regional map (Figure 4.8) trend west-northwest – east-southeast could be attributed to effects of deeper heterogeneity of the earth crust. According to Figure 4.8, the dominant trend of the lineaments in Figure 4.6 is perfectly in agreement with the regional trend of the area. However, this trend disagreed with the deduction of Ajakaiye, Hall, Ashiekaa and Udensi (1991) who identified a system of northeast- southwest trending narrow magnetic lineaments along which are concentrated the alkaline ring complexes and suggested that the lineament represented pre-existing zones of weakness in the Pan- African crust. The disagreement might be due to the limitation or the extent of this survey area, which is smaller compared to the area covered by Ajakaiye, Hall, Ashiekaa and Udensi (1991).

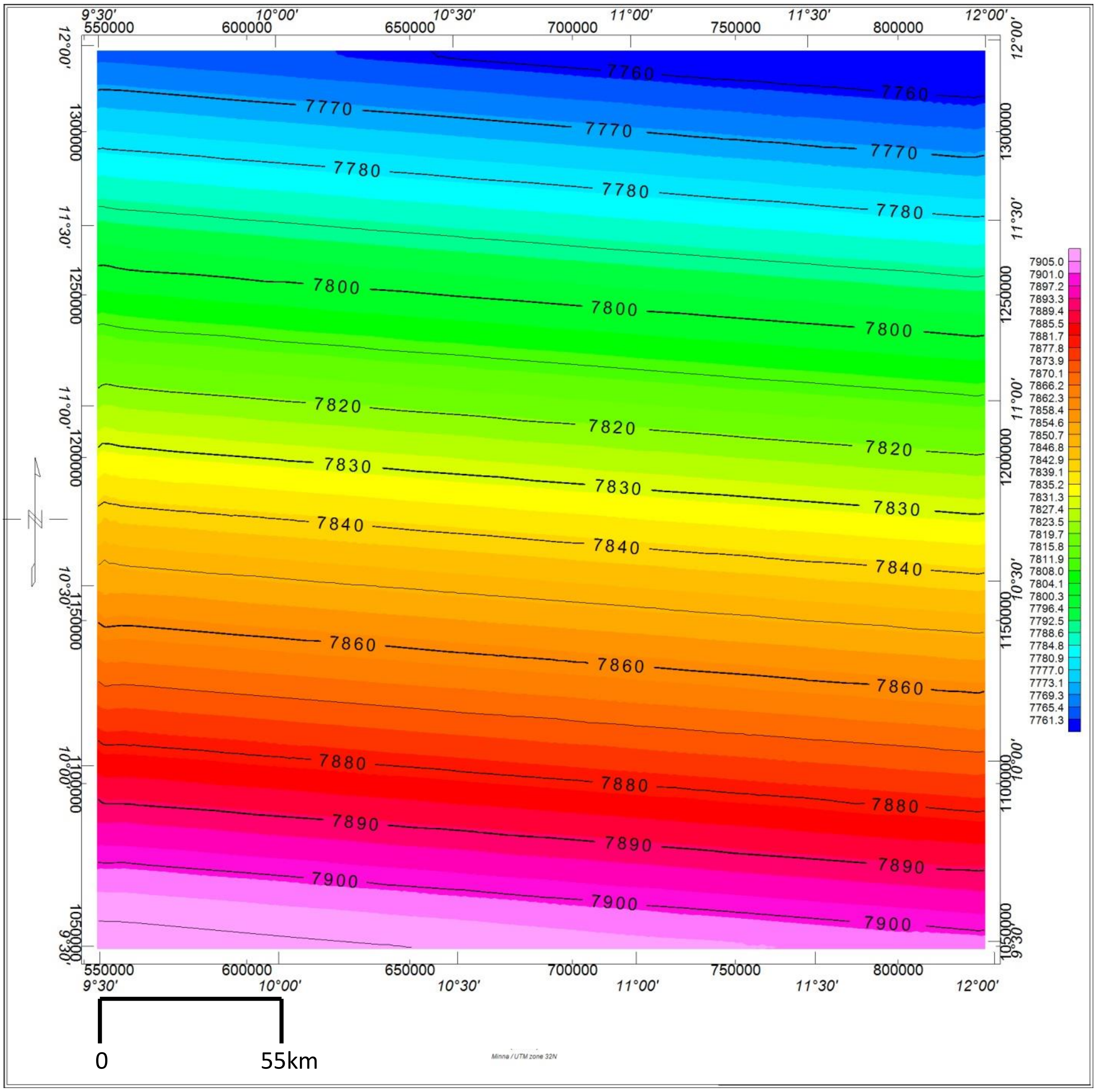

Figure 4.8: Regional-magnetic contour map of parts of Upper Benue Trough and southern Bornu Basin (Contour Interval is 10nT).

4.3.2 **Residual Magnetic Field**

The magnetic map shown in Figures 4.9 and 4.10 has magnetic values between -142.7 nT and 134 nT. These Figures are very similar to Figure 4.1 and 4.2. The Figures show that the southern part of the map and the north-eastern part trend in the NE – SW while the north-western part trends NW – SE. Typical of Figures 4.1 and 4.2, areas identified as highs were depicted in Figure 4.9 and 4.10 as relatively high (positive) magnetic contour values. Similarly, those areas identified as magnetic lows were also characterised with negative magnetic values. The fracture zones identified in Figures 4.1 and 4.2 were also noticed in Figures 4.9 and 4.10.

The results of regional-residual separation brought out another feature found below the larger magnetic anomalies described in section 4.1.1. The anomaly is marked as **K** in Figure 4.9. This anomaly could be characterised as low amplitude magnetic anomaly with magnetic values of -142.7 nT to -86.6 nT. It is bounded by the postulated extension of the Oceanic fracture zones known as Romanche and Chain fractures, delineated as AA' and BB' respectively. The anomaly could be found around Gombe and Ako Gombe area. It also trends in the southwest-northeast direction and extends from latitude 9.5^{o}N to 10.5^{o}N and longitude 10.25^{o}E to 11.0^{o}E. It has a mean width of about 25 km. Another notable low magnetic anomaly could be found at the north-eastern part of Figures 4.9 and 4.10, which is regional in nature. The anomaly is bounded by the Romanche (AA') and St. Paul (CC') as shown in Figure 4.10. It has a lateral distance of about 165 km and the thickness of about 100 km. This anomaly is marked as **M** in Figure 4.10. The anomaly could be found around Damaturu, Damagum and Gujba areas.

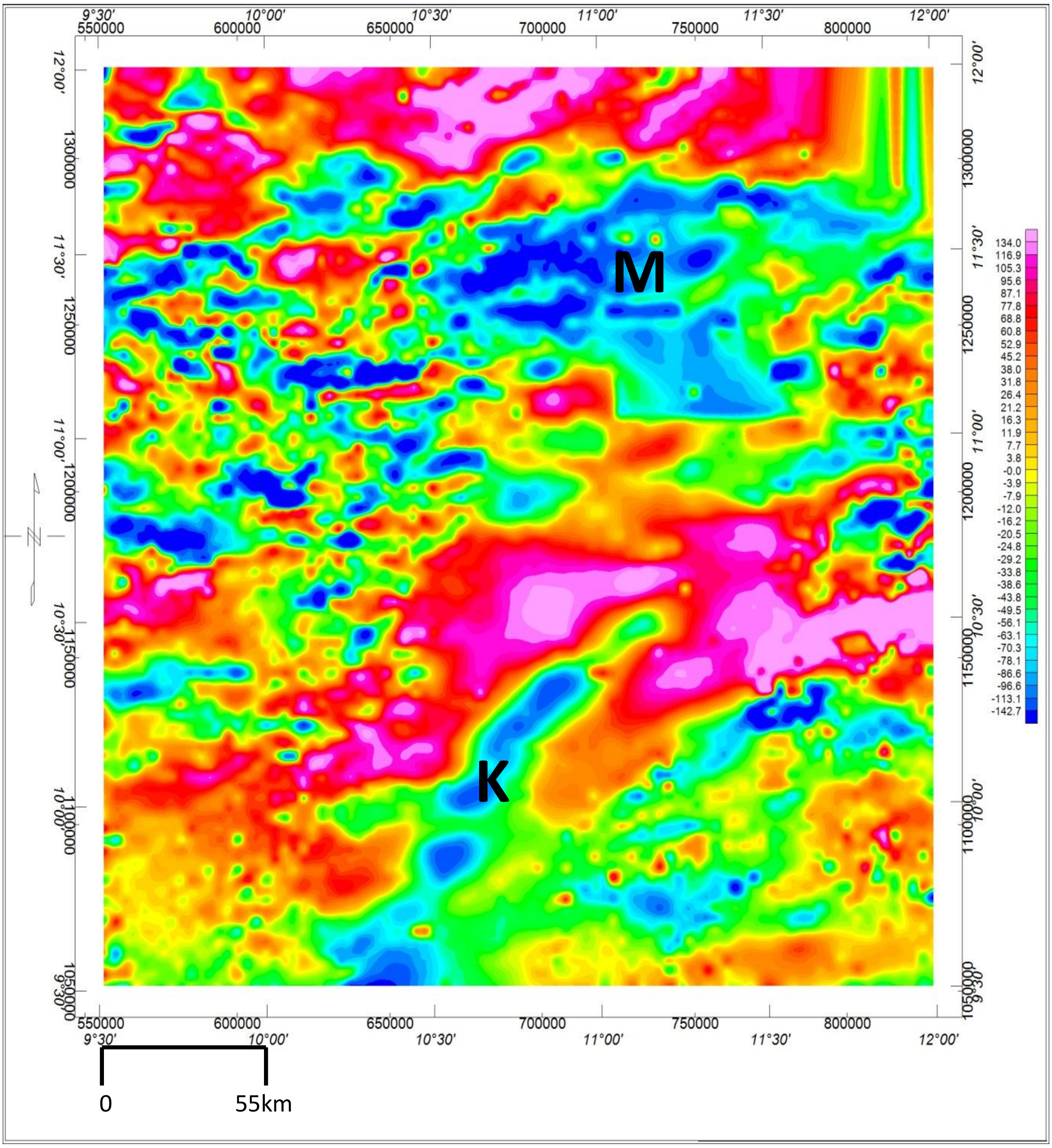

Figure 4.9: Residual-magnetic map of parts of Upper Benue Trough and southern Bornu Basin. Unit of total magnetic intensity is nano tesla. 'M' and 'K' represent prominent magnetic 'lows'.

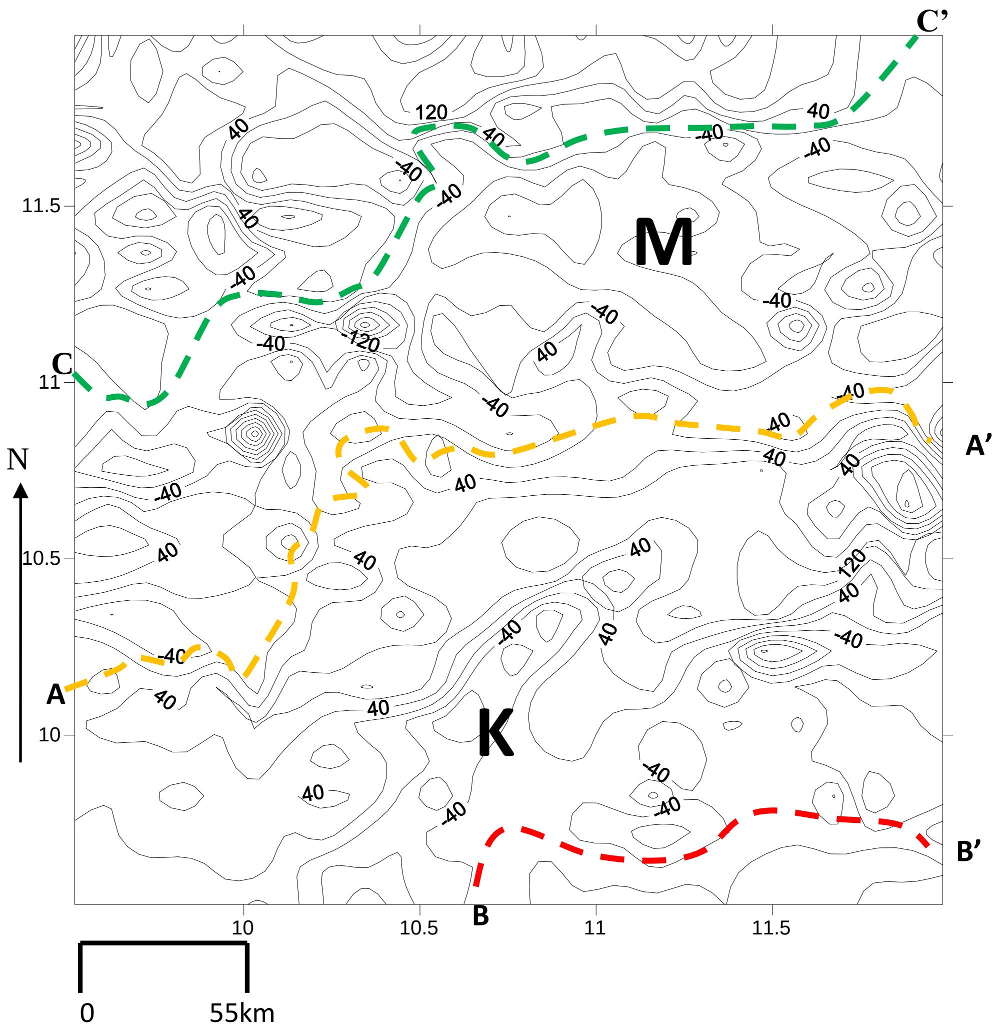

Figure 4.10: Residual-magnetic contour map of parts of Upper Benue Trough and southern Bornu Basin (Contour Interval is 40nT). ‘M’ and ‘K’ represent prominent magnetic ‘lows’.

4.3.3 Results of Filtering Process Using Upward Continuity Filter Control

Figures 4.11, 4.12, 4.13, 4.14 and 4.15 shows the upward continuation of total magnetic intensity (TMI) field at 2 km, 5 km, 10 km, 15 km and 20 km respectively. In Figure 4.11, the effect of near surface magnetic anomalies could be seen from the map as the map is not too different from Figure 4.1 and 4.9.

However, in Figure 4.12, the near surface anomaly has gradually disappeared leaving anomaly with relatively long wavelength. Similarly, in Figure 4.13 the effect of short wavelenght anomaly had been greatly removed leaving the anomaly with regional effect. At this level, the feature marked K in Figure 4.9, had dissappered. Figures 4.14 and 4.15 resemble the regional magnetic map of Figure 4.8, shows only the anomaly with regional effect and trends the same direction as the regional map. The direction of low magnetic trend in Figure 4.8 is towards the northern part which is in agreement with the upward continued filter results (Figures 4.14 and 4.15). Thus, Figures 4.14 and 4.15 are the result of the separation between the residual features (shortwave anomalies) and the regional effect (longwave anomalies). The persistent magnetic low, feature M, in Figure 4.15 might indicate intrusive body with low magnetic susceptibility.

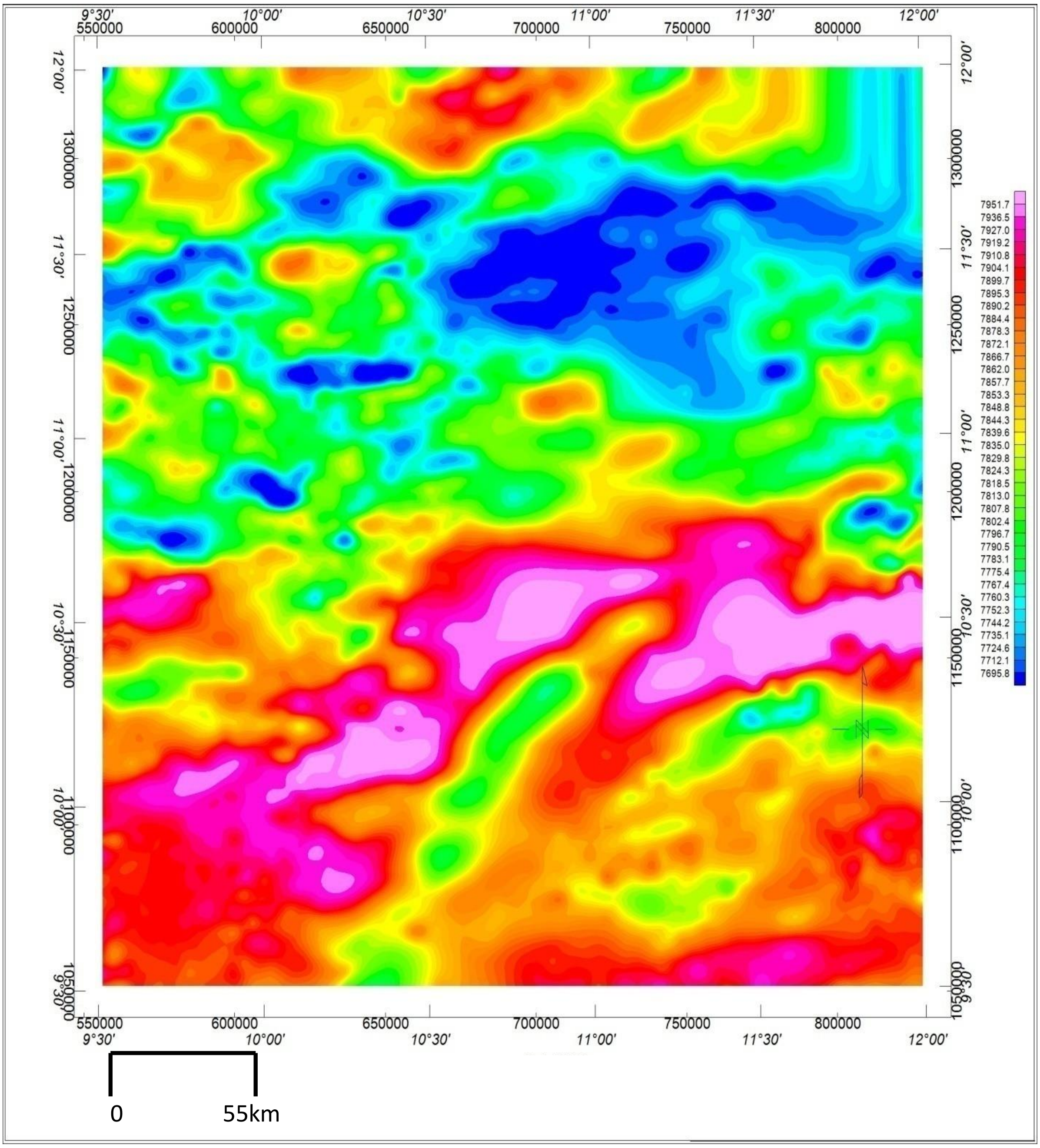

Figure 4.11: Total magnetic map of parts of Upper Benue Trough and southern Bornu Basin upward continued at 2 km.

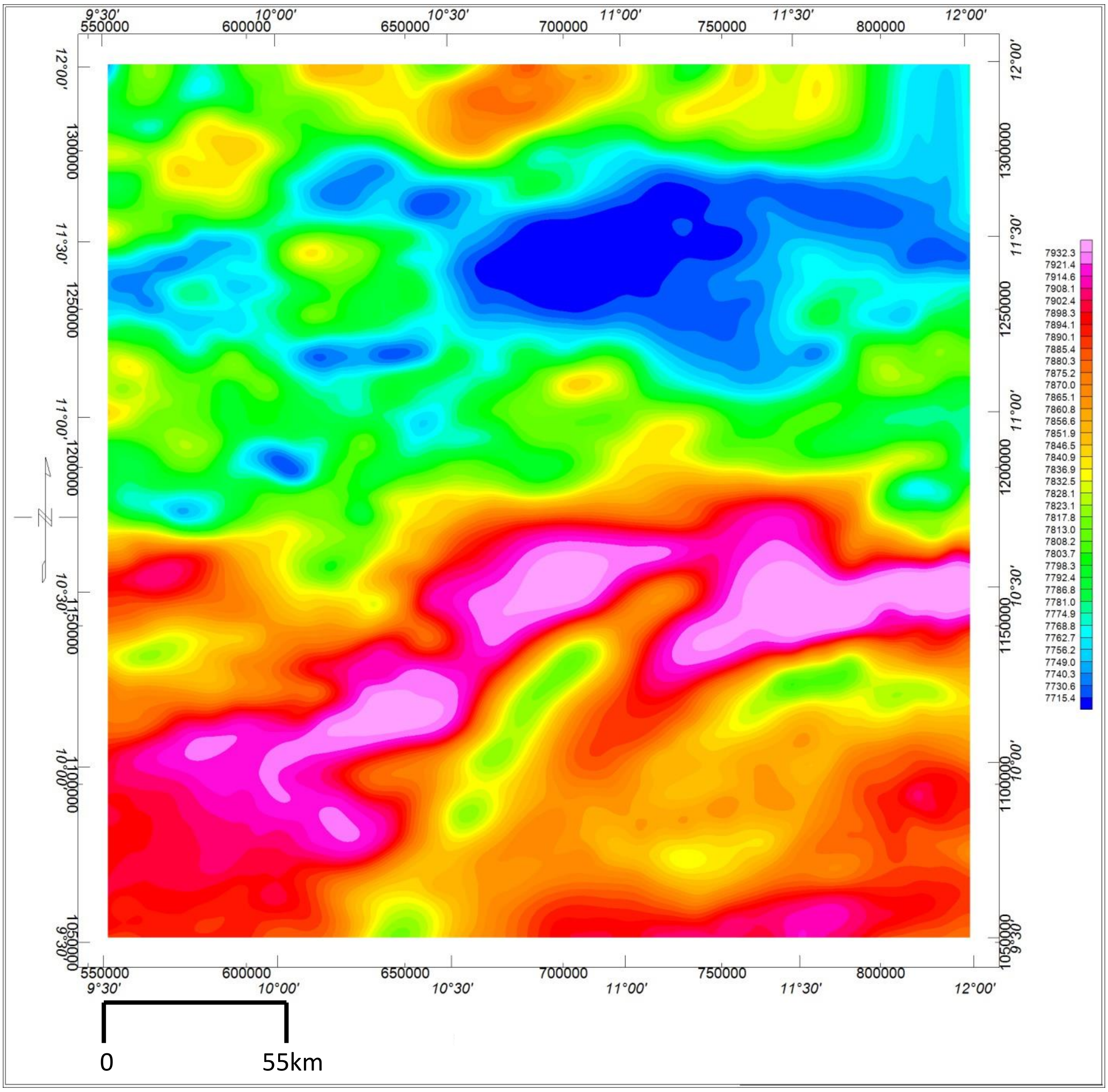

Figure 4.12: Total magnetic map of parts of Upper Benue Trough and southern Bornu Basin upward continued at 5 km.

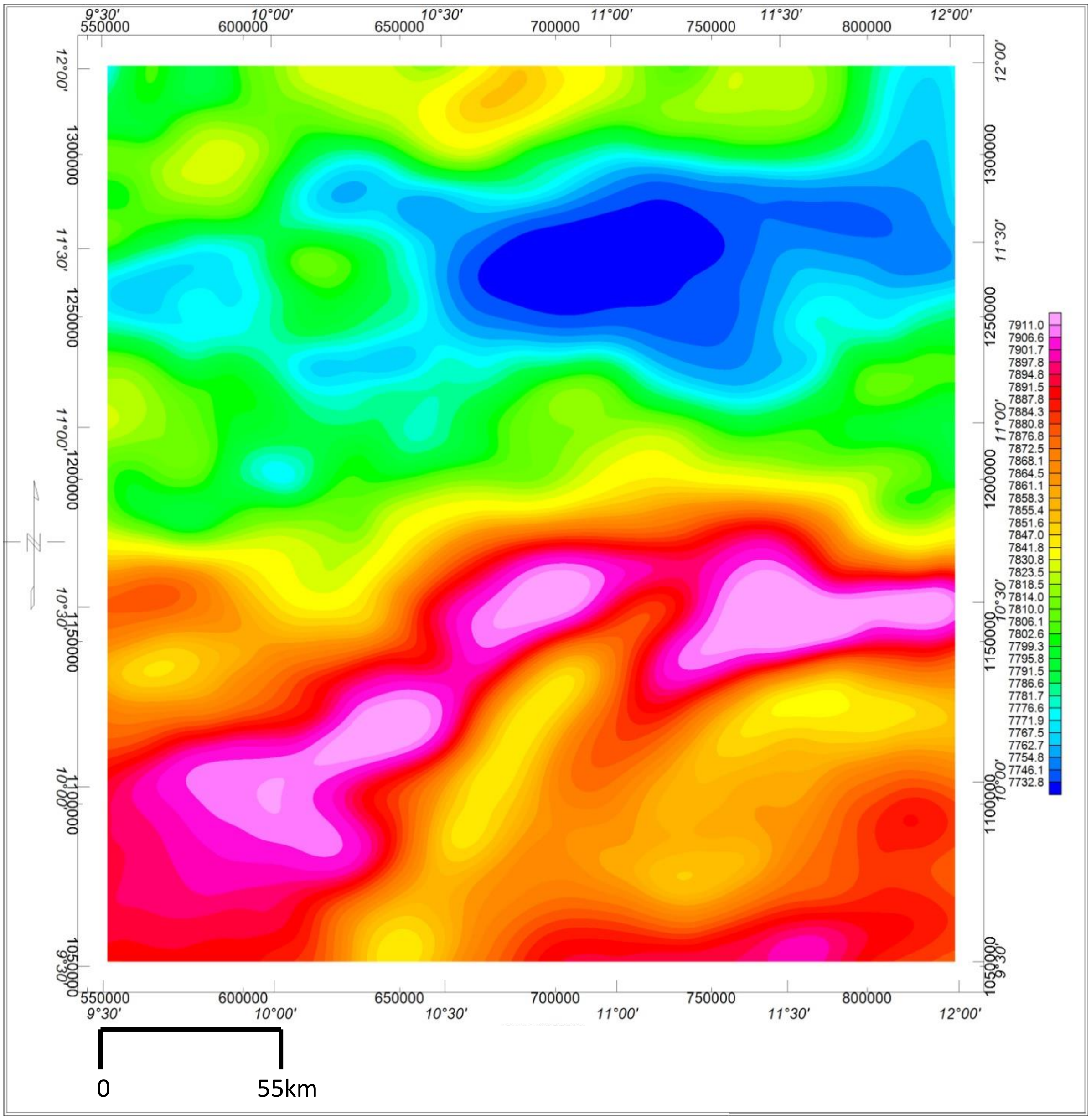

Figure 4.13: Total magnetic map of parts of Upper Benue Trough and southern Bornu Basin upward continued at 10 km.

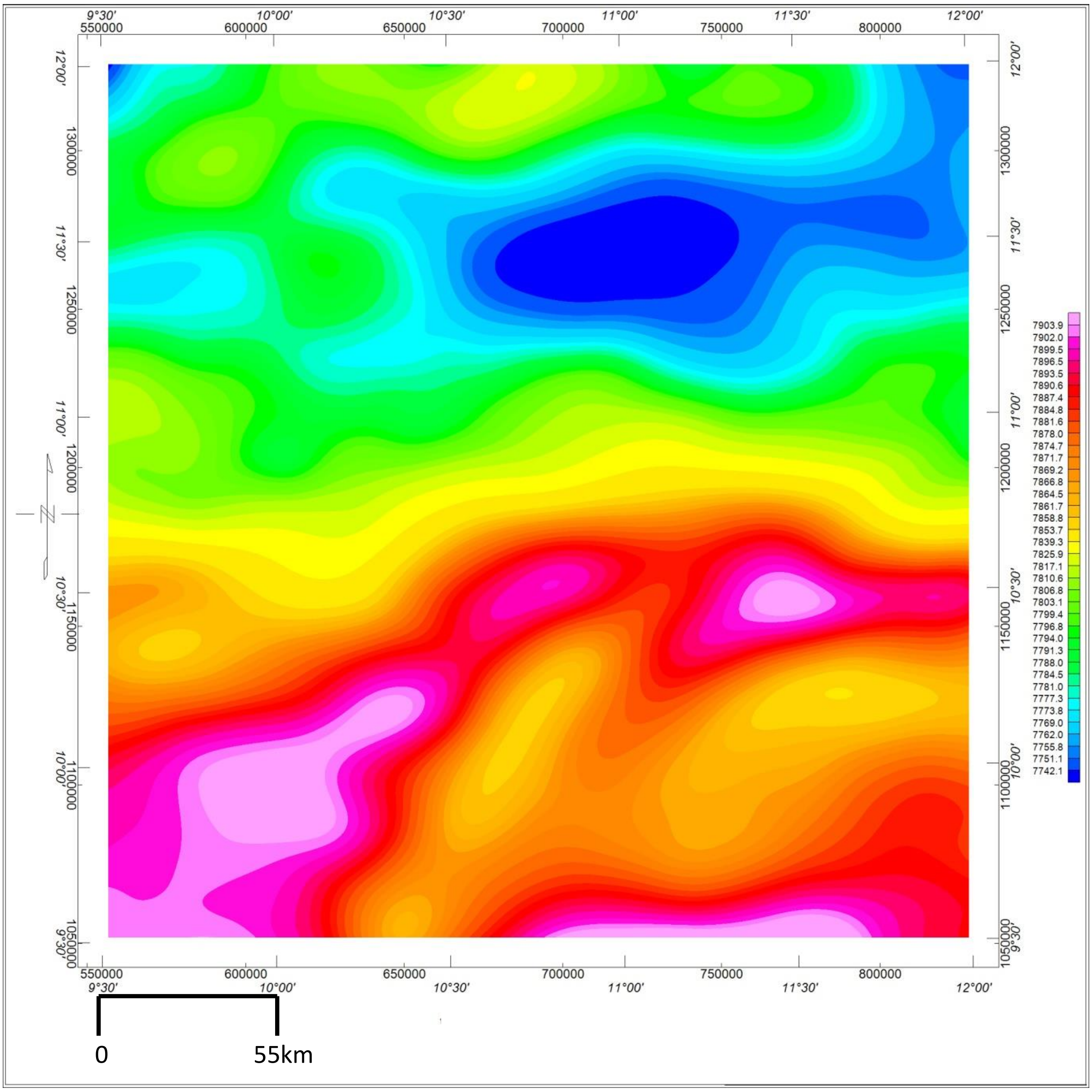

Figure 4.14: Total magnetic map of parts of Upper Benue Trough and southern Bornu Basin upward continued at 15 km.

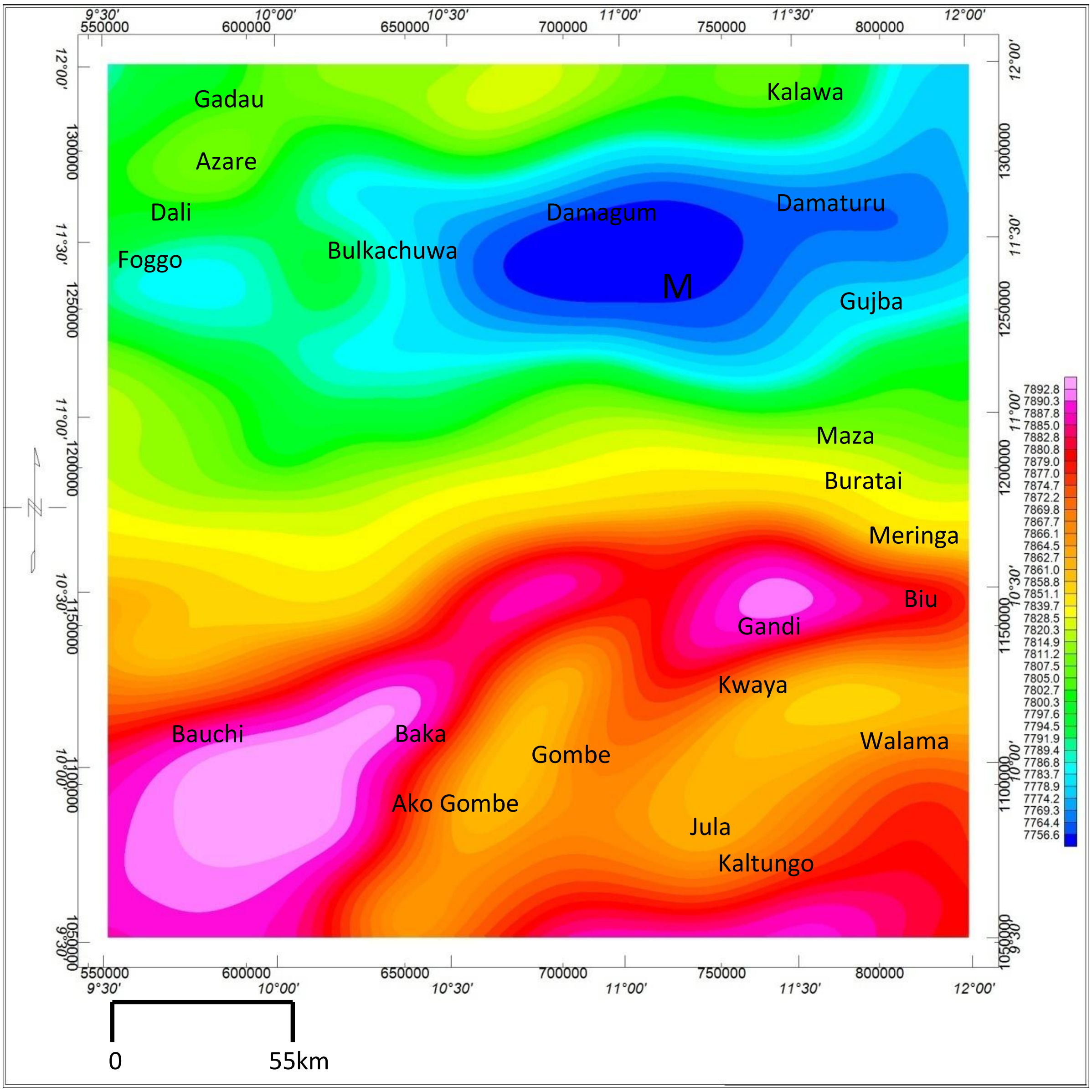

Figure 4.15: Total magnetic map of parts of Upper Benue Trough and southern Bornu Basin upward continued at 20 km.

The upward continued maps show that the north central parts towards the north eastern part of the maps has very low magnetic values which is in conformity with the total magnetic field in Figure 4.1 (i.e. those areas demarcated as lows conform with north-central part of Figure 4.15). The deduction here could be that the sedimentary cover is thick as the magnetic effect is been buried at deeper depth or that, there exist a large intrusive body with low magnetic susceptibilty. Also, the effect of magnetic low identified as K in Figure 4.9 can also be seen at greater. The highest magnetic amplitude could be found at south western part of Figure 4.15, with magnetic value of 7892.8 nT, which corresponds to the basement complex region of the study area.

4.4 **Results of Structural Analysis of the Residual Map using CET Grid Analysis**

The structural analysis is better done when the residual grid is reduced to the pole (RTP). The structures in the original data/grid if not transformed would not be well captured. The main advantage of this process to avoid the negative and positive component distortion associated with magnetic data. At the pole, magnetic anomalies are positive while at equator, they are negative; between these ends they are both positive and negative, which bring distortions. Thus, to avoid these distortions, the magnetic data could be transformed to either pole (RTP) or to the equator (RTE).

Figure 4.16 was obtained through the use of appropriate algorithm and the figure obtained is called reduce to equator (RTE). This Figure is not too different from the residual grid map of Figure 4.9.

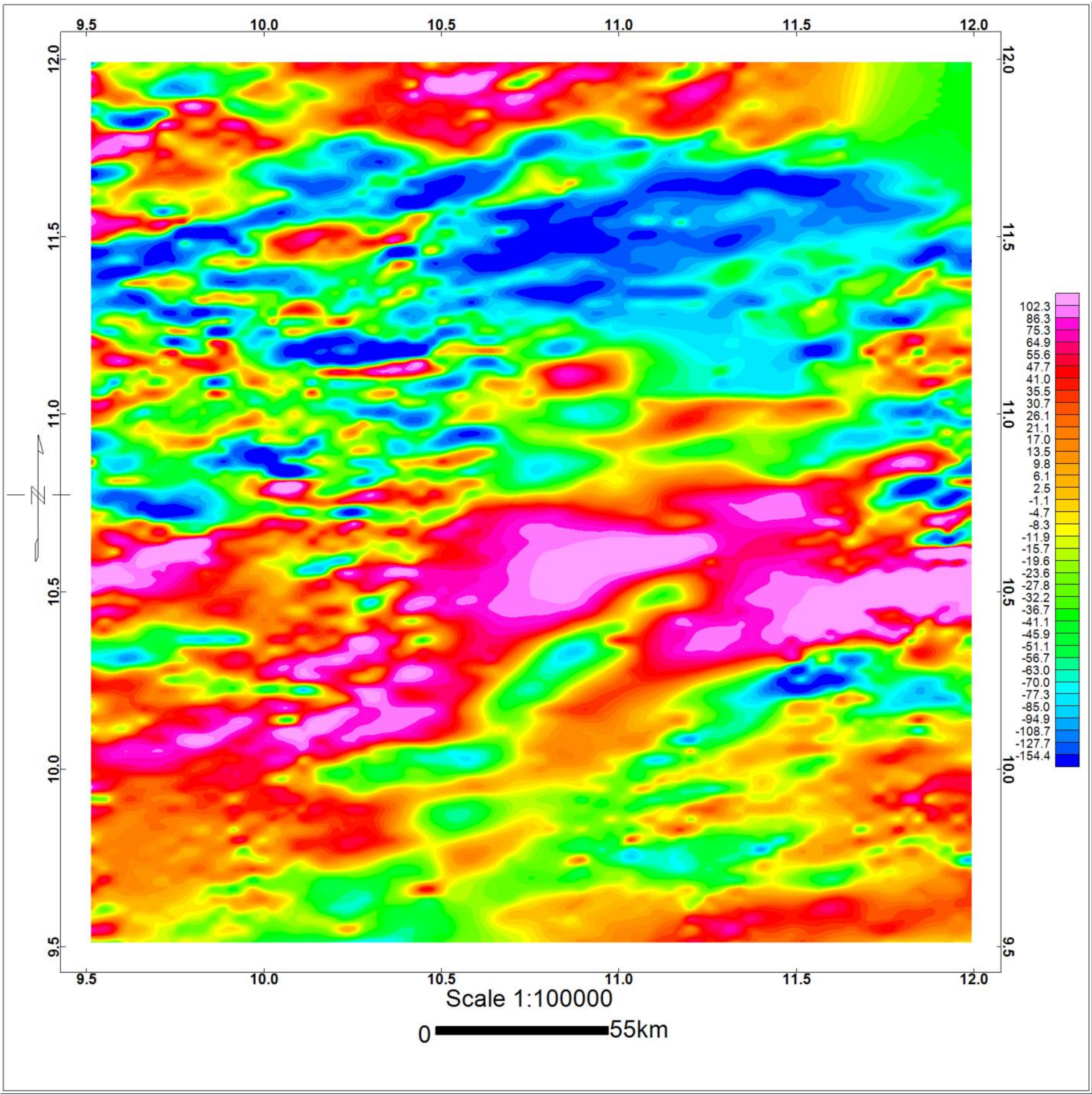

Figure 4.16: Residual grid map of Upper Benue Trough and southern Bornu Basin reduced to equator (RES_RTE).

The data obtained in Figure 4.16 were reduced to pole (RTP) to obtain Figure 4.17. The RTP data served as the input grid for the CET grid analyses.

Figure 4.18 shows the separation between the long wave anomaly and short wave anomaly. This is done by suppressing the short wavenumber anomaly and enhancing the long wavenumber anomaly. As part of the texture analysis among the CET grid algorithms, the locations of complex local textures were highlighted with respect to magnetic discontinuity. This process produced Figure 4.19.

The **lineation** algorithm uses the results of Figure 4.19 to **detect** and isolate any laterally continuous line-like regions of discontinuity by elongating or joining any line like structures to produce Figure 4.20.

The **lineation** vectorisation reduces the regions containing discontinuities detected by the phase symmetry in Figure 4.20 into skeletal structures detailed as a binary grid. This algorithm is able to define a direction for structures elongated in Figure 4.20 by straighten perfectly line-like structures identified in Figure 4.20. The result of this produced vectorised lineation map, Figure 4.21.

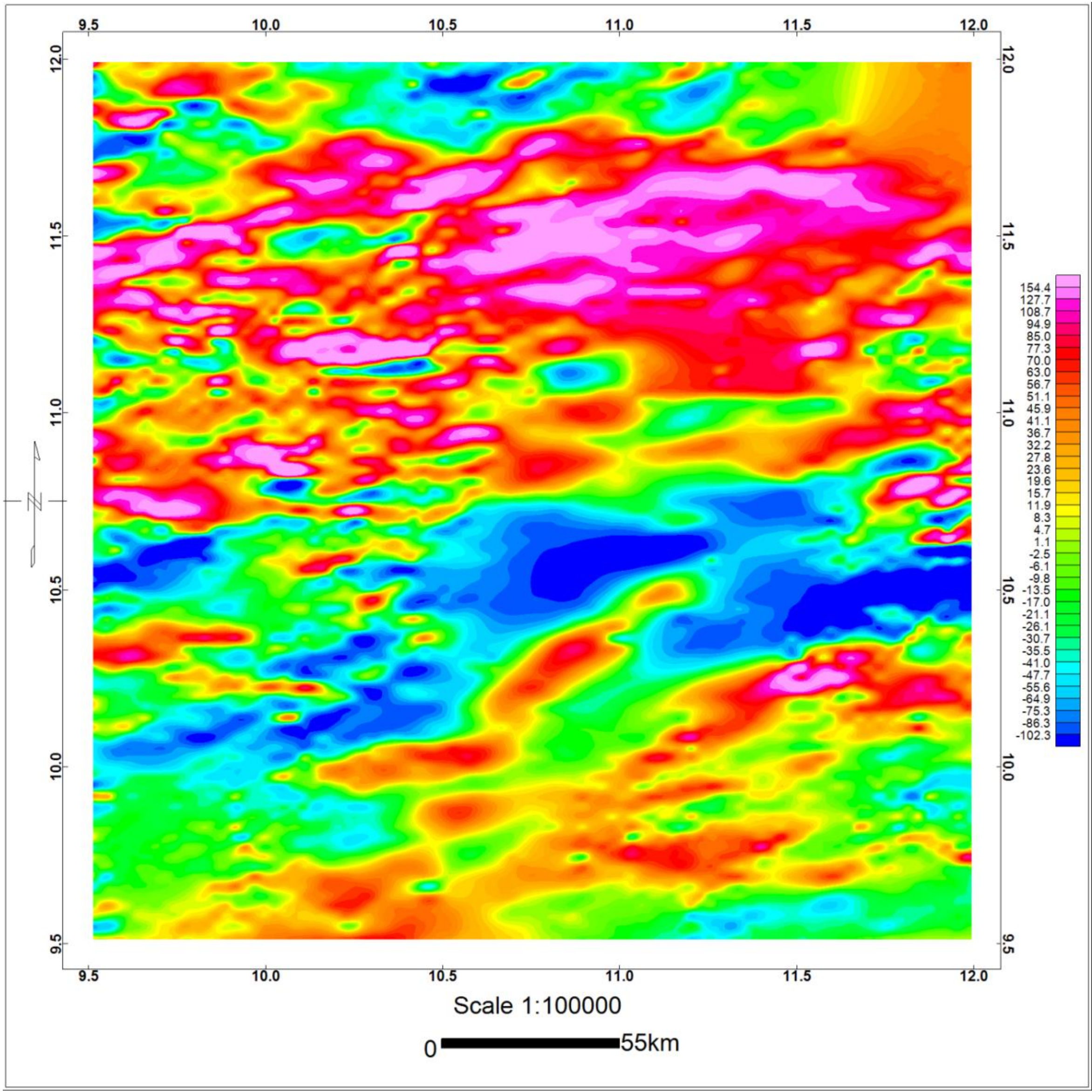

Figure 4.17: Residual grid map of Upper Benue Trough and southern Bornu Basin reduced to pole (RES_RTP).

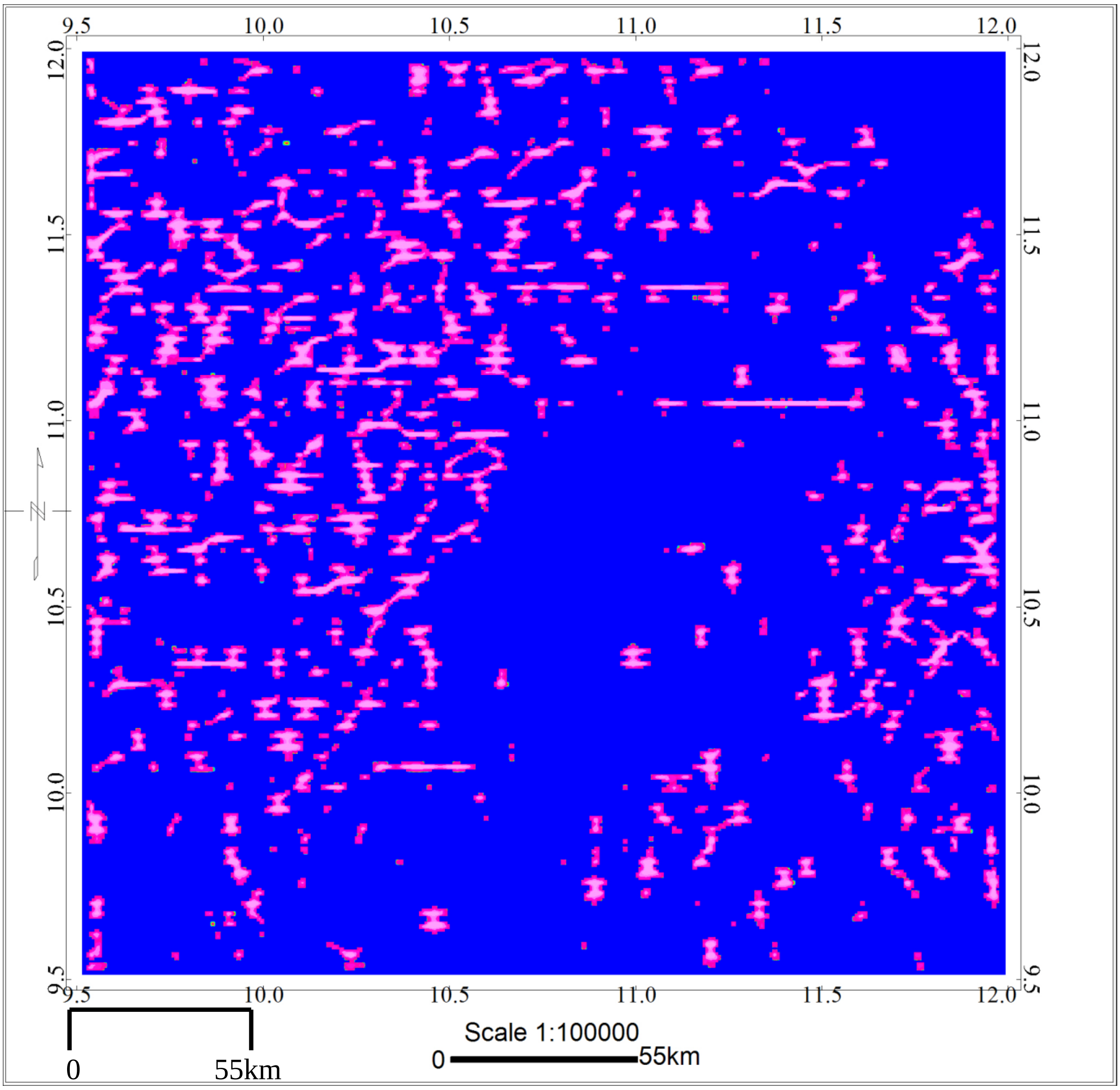

Figure 4.18: Separation between the long wave anomaly and short wave anomaly.

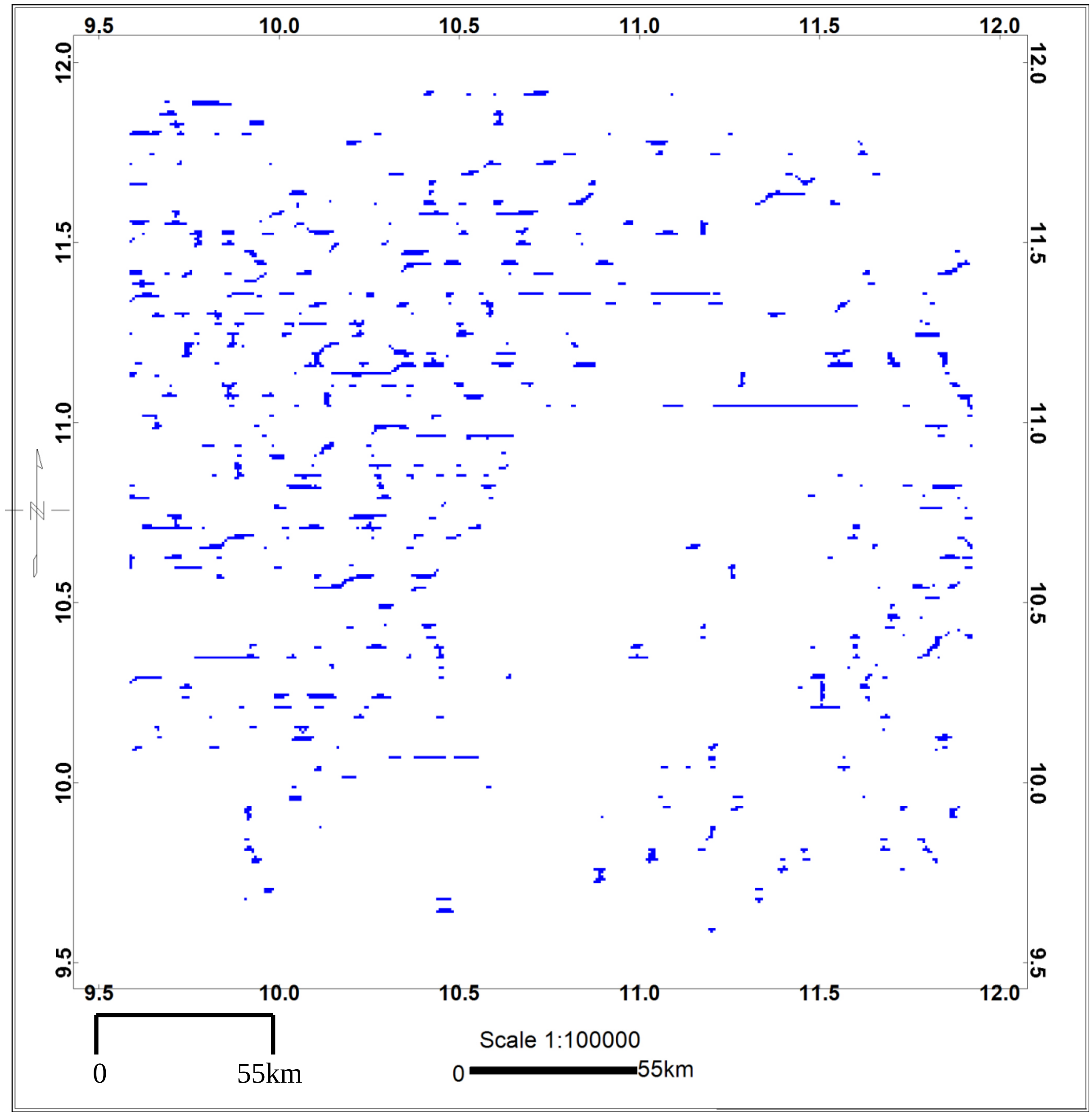

Figure 4.19: Locating area of complex local textures with respect to magnetic discontinuity.

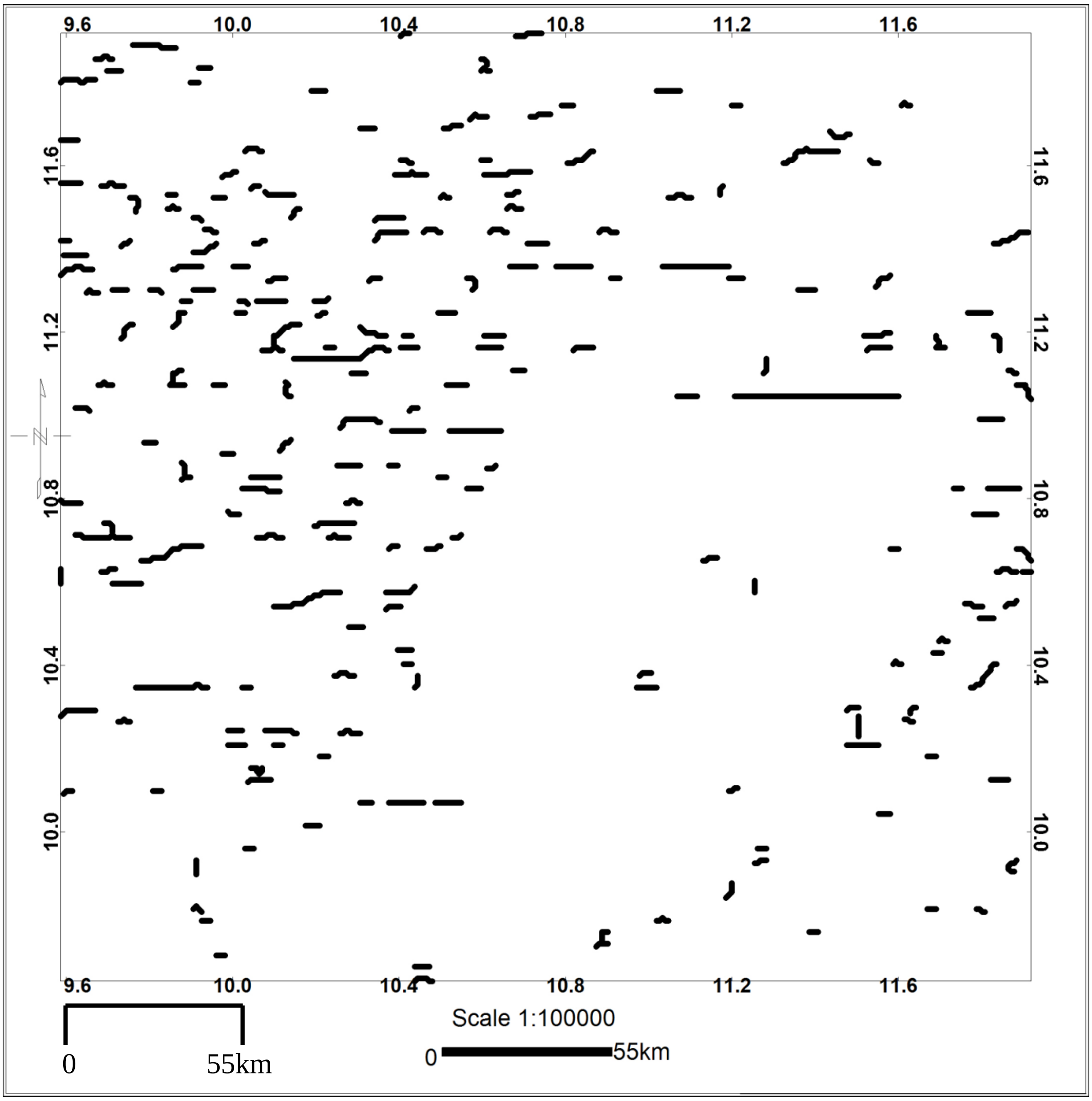

Figure 4.20: Detection, isolation and elongation of laterally continuous line-like structures.

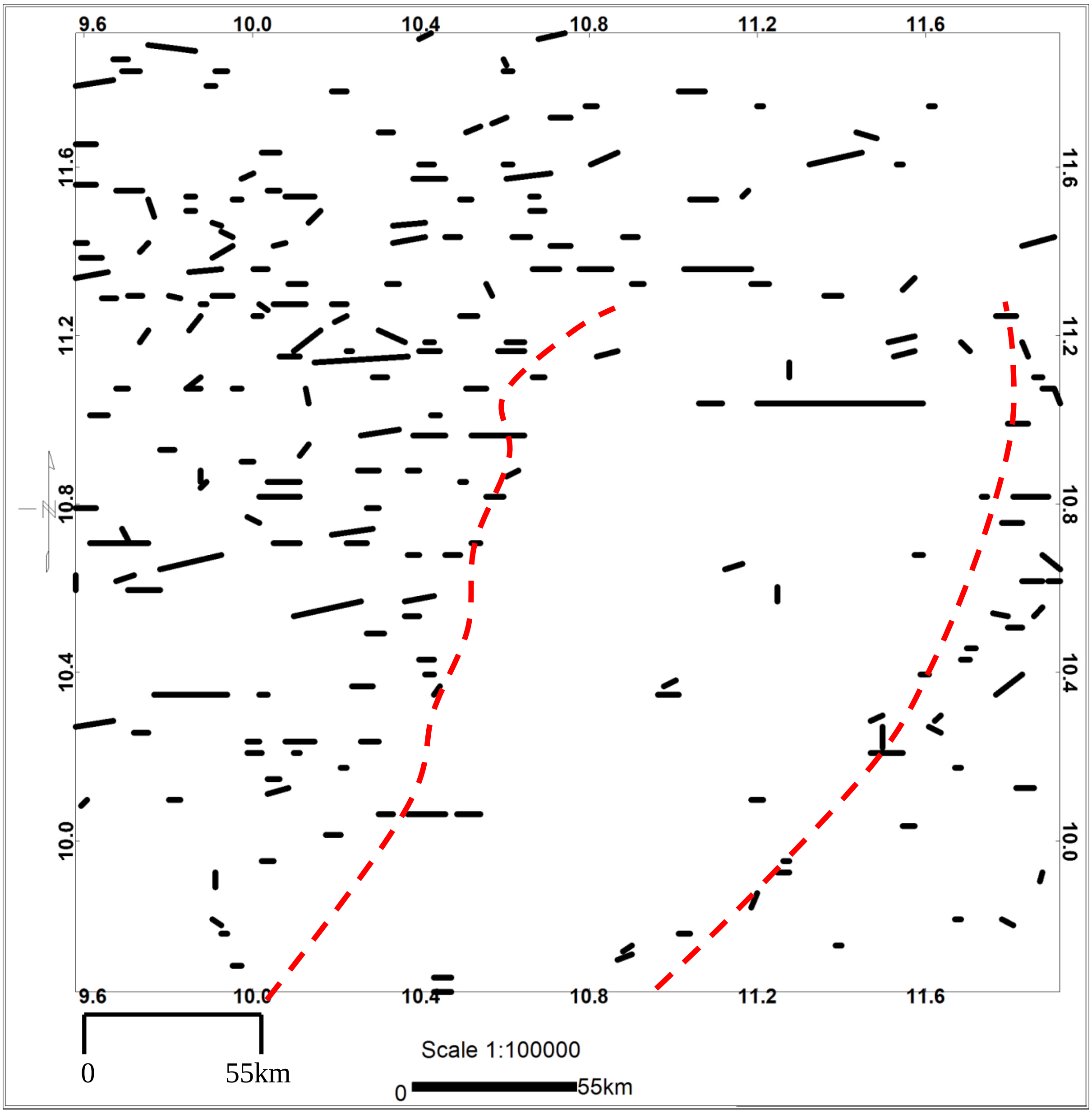

Figure 4.21: Vectorised lineation map of the study area.

Inferred Benue Trough delineation

4.4.1 **Comparison of the CET Grid results with the Geology**

Figure 4.22 shows the relationship between the results of subsurface structural analysis using CET grid plug-ins and the surface geology map. The Figure shows that the basement complex region of the geology map has several structures or contains more structural activities compared with the structural features in the sedimentary regions. The structures in the basement complex (Figure 4.22a) have the same coverage as that of the geology (Figure 4.22b). This similarity implies that the structural features obtained from CET grid analysis (Figure 4.22a) agreed with the geology settings of the area (Figure 4.22b).

Similarly, areas associated with volcanic activities from geologic map in the eastern part also contain some structural features. There are similarities in the structural activities in both the Benue Trough and Bornu Basin. However, it is worthwhile to note that there are more structural activities in Bornu Basin than as seen in the Benue trough. Structurally, there are great similarities in the structural settings obtained from CET grid structural analysis and the geology map of the area.

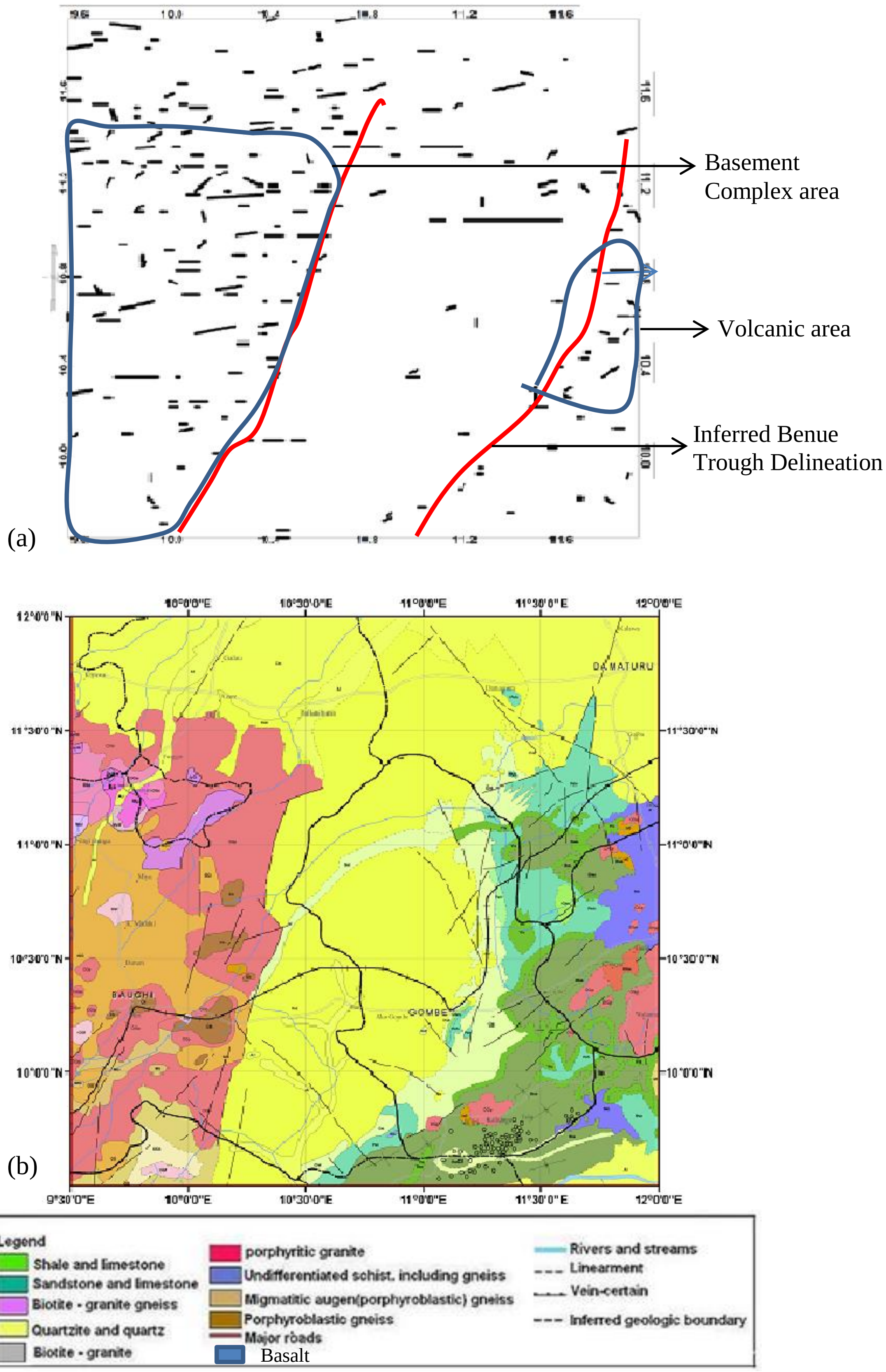

Figure 4.22: Relationship between (a) CET grid structural analysis and (b) the geology map of the study area. x and y are the coordinates in longitude and latitude respectively in degrees.

4.5 **Results of Depth Analysis**

4.5.1 **Spectral Depth Determination**

The residual map of the study area Figure 4.9 was divided into forty-one (41) blocks of overlapping magnetic sections. Twenty-five of the divisions (sections) covered 55 km^2 and sixteen other covers 110 km^2. The division of residual data/map into 41 spectral sections was done with Oasis montaj and the spectral energies were plotted within it. The *.SPC file obtained were later exported into the Microsoft Excel worksheets one after the other until the total number of 41 spectral (*.SPC) energy files were exported. The Microsoft Excel worksheets file obtained was later used as an input file into a spectral program plot developed with Matlab. The total numbers of 41 spectral energies were plotted in Matlab with the developed program. A typical plot of energy against frequency (wavenumber) is as shown in Figure 4.23. Other spectral energy plots are contained in the appendix.

Equation 4.1 shows the relationship between the depth (h) to the basement and the decay slopes (m) of the energy spectrum.

$$h = \frac{-m}{4\pi} \tag{4.1}$$

where m is the slope of the best line of fit. Equation 4.1 was used to generate the data in Table 4.1. Table 4.1 shows the estimated magnetic sources for both the shallow source (h_1) and deeper sources (h_2) from equation 4.1.

Typical of these estimates, the depth from magnetic deeper source could be found as follows:

$h_2 = -\frac{m_2}{4\pi}$, where m_2 is -34.50 cycle per km cycle from Figure 4.23

$h_2 = +2.75\ km$; while depth to magnetic shallow source could be found as:

$h_1 = -\frac{m_1}{4\pi}$, where m_1 is -11.00 cycle per km from Figure 4.23

$h_1 = 0.875\ km\ or\ 875\ m$

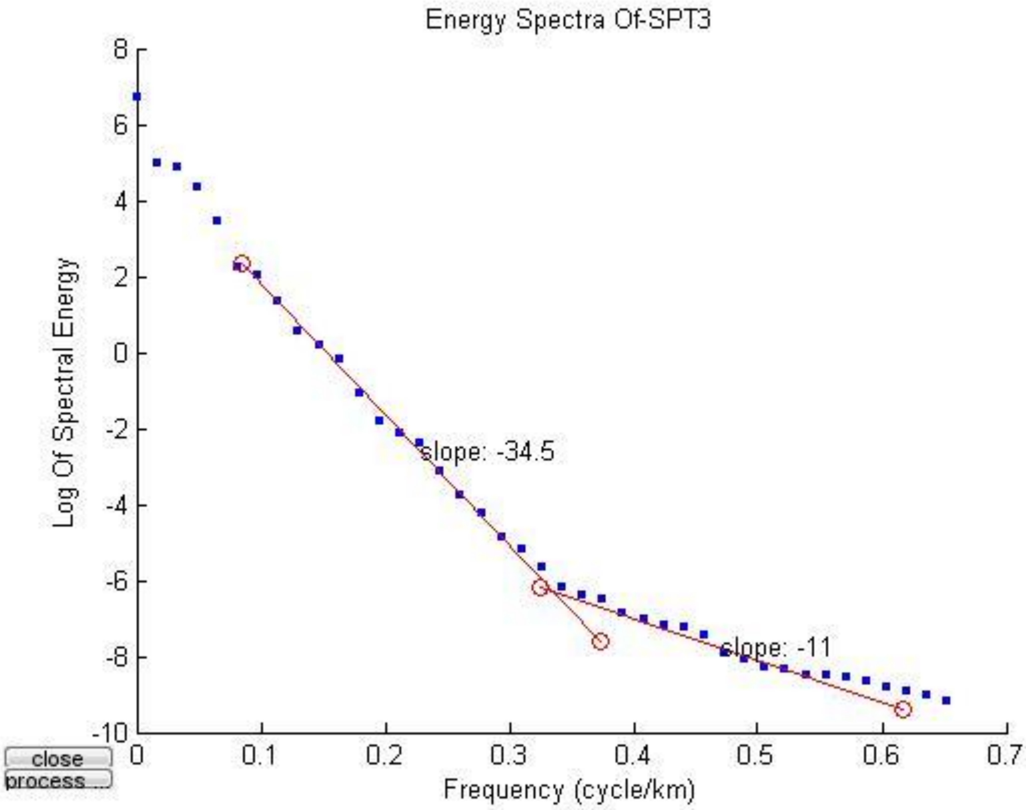

Figure 4.23: A typical plot of energy spectrum against frequency of section 3

Table 4.1: Estimated depth to the shallow (h_1) magnetic sources and deep (h_2) magnetic sources in km. M_1 and M_2 are the slopes 1 and 2 for the magnetic ensembles.

S/No.	Spectral Section	longitude	Latitude	M_1	M_2	h_1	h_2
1	SPT1	9.75	11.75	-10.00	-10.00	0.795672	0.795672
2	SPT2	10.25	11.75	-11.10	-11.10	0.883195	0.883195
3	SPT3	10.75	11.75	-11.00	-34.50	0.875239	2.745067
4	SPT4	11.25	11.75	-8.99	-36.70	0.715309	2.920115
5	SPT5	11.75	11.75	-9.57	-33.80	0.761458	2.68937
6	SPT6	9.75	11.25	-6.00	-6.00	0.477403	0.477403
7	SPT7	10.25	11.25	-7.50	-7.50	0.596754	0.596754
8	SPT8	10.75	11.25	-13.60	-40.60	1.082113	3.230426
9	SPT9	11.25	11.25	-15.40	-33.30	1.225334	2.649586
10	SPT10	11.75	11.25	-7.36	-37.40	0.0.58561	2.975812
11	SPT11	9.75	10.75	-9.27	-9.27	0.737588	0.737588
12	SPT12	10.25	10.75	-9.81	-9.81	0.780554	0.780554
13	SPT13	10.75	10.75	-8.43	-46.60	0.670751	3.707829
14	SPT14	11.25	10.75	-8.52	-42.00	0.677912	3.34182
15	SPT15	11.75	10.75	-4.86	-31.60	0.386696	2.514322
16	SPT16	9.75	10.25	-9.15	-9.15	0.728039	0.728039
17	SPT17	10.25	10.25	-7.08	-7.08	0.563335	0.563335
18	SPT18	10.75	10.25	-10.3	-37.3	0.819542	2.967855
19	SPT19	11.25	10.25	-3.88	-29.60	0.308721	2.355188
20	SPT20	11.75	10.25	-3.47	-29.70	0.276098	2.363144
21	SPT21	9.75	9.75	-3.92	-3.92	0.311903	0.311903
22	SPT22	10.25	9.75	-7.94	-7.94	0.631763	0.631763
23	SPT23	10.75	9.75	-7.90	-30.10	0.628581	2.394971
24	SPT24	11.25	9.75	-5.13	-29.90	0.40818	2.379058
25	SPT25	11.75	9.75	-5.26	-29.50	0.418523	2.347231
26	SPT26	10.0	11.5	-6.84	-6.84	0.544239	0.544239
27	SPT27	10.5	11.5	-7.35	-11.20	0.584819	1.225334
28	SPT28	11.0	11.5	-8.06	-39.70	0.641311	3.158816
29	SPT29	11.5	11.5	-8.67	-36.60	0.689847	2.912158
30	SPT30	10.0	11.0	-9.98	-9.98	0.79408	0.79408
31	SPT31	10.5	11.0	-6.35	-35.30	0.505251	2.808721
32	SPT32	11.0	11.0	-9.47	-40.20	0.753501	3.1986
33	SPT33	11.5	11.0	-7.14	-34.60	0.568109	2.753024
34	SPT34	10.0	10.5	-5.55	-5.55	0.441598	0.441598
35	SPT35	10.5	10.5	-9.34	-36.00	0.743157	2.864418
36	SPT36	11.0	10.5	-8.04	-34.40	0.639720	2.73711
37	SPT37	11.5	10.5	-7.32	-35.00	0.582432	2.78485
38	SPT38	10.0	10.0	-7.94	-7.94	0.631763	0.631763
39	SPT39	10.5	10.0	-8.59	-31.90	0.683482	2.538192
40	SPT40	11.0	10.0	-5.51	-30.80	0.438415	2.450668
41	SPT41	11.5	10.0	-6.49	-29.60	0.516391	2.355188

The primary sources that account for the first layer depth derived from the statistical spectral analysis are the magnetic rocks that intrude the sedimentary formation. An estimated depth of 0.268 km to 1.23 km could be observed from the first layer magnetic source's depth. The maximum depth of 1.23 km could be found at the north-central part while the minimum depth of about 0.27 km could be found in the south eastern and south western part of Figure 4.24.

The second layer depth may be attributed to magnetic rocks that are emplaced or intruded into the basement underlying the sedimentary basin. Also, intra-basement features such as fractures could equally contribute to sources that accounted for the second layer depth. The second layer depth thus invariably represents a depth to the underlying magnetic basement rock within the study area. This depth to the underlying magnetic basement as estimated from the statistical analysis ranges from 0.31 km to 3.71 km, and this also represent the average thickness of the sedimentary pile within the study area. The highest sedimentary thickness could be found at the central-eastern part of the study area. This area corresponds to the sedimentary part of the Upper Benue Trough at the top end of Gombe. Similarly, the minimum sedimentary thickness, however, corresponds to the basement complex region of the area (Figure 4.25).

This range of depth is very well in agreement with the work of the previous workers that have used several methods to estimate the thickness of the study area. According to Avbovbo, Ayoola and Osahon (1986), a thickness of over 10 km was obtained around Maiduguri depression, but less than 5 km was later proved from seismic reflection data. Nur, Onuoha and Ofoegbu (1994) obtained 1.6 km to 5 km for deeper sources around the middle Benue, while 60 m to 1.2 km were obtained for shallow magnetic sources; Nwogbo (1997) got 2 km to 2.62 km for deeper sources and 70 m to 0.63 km for

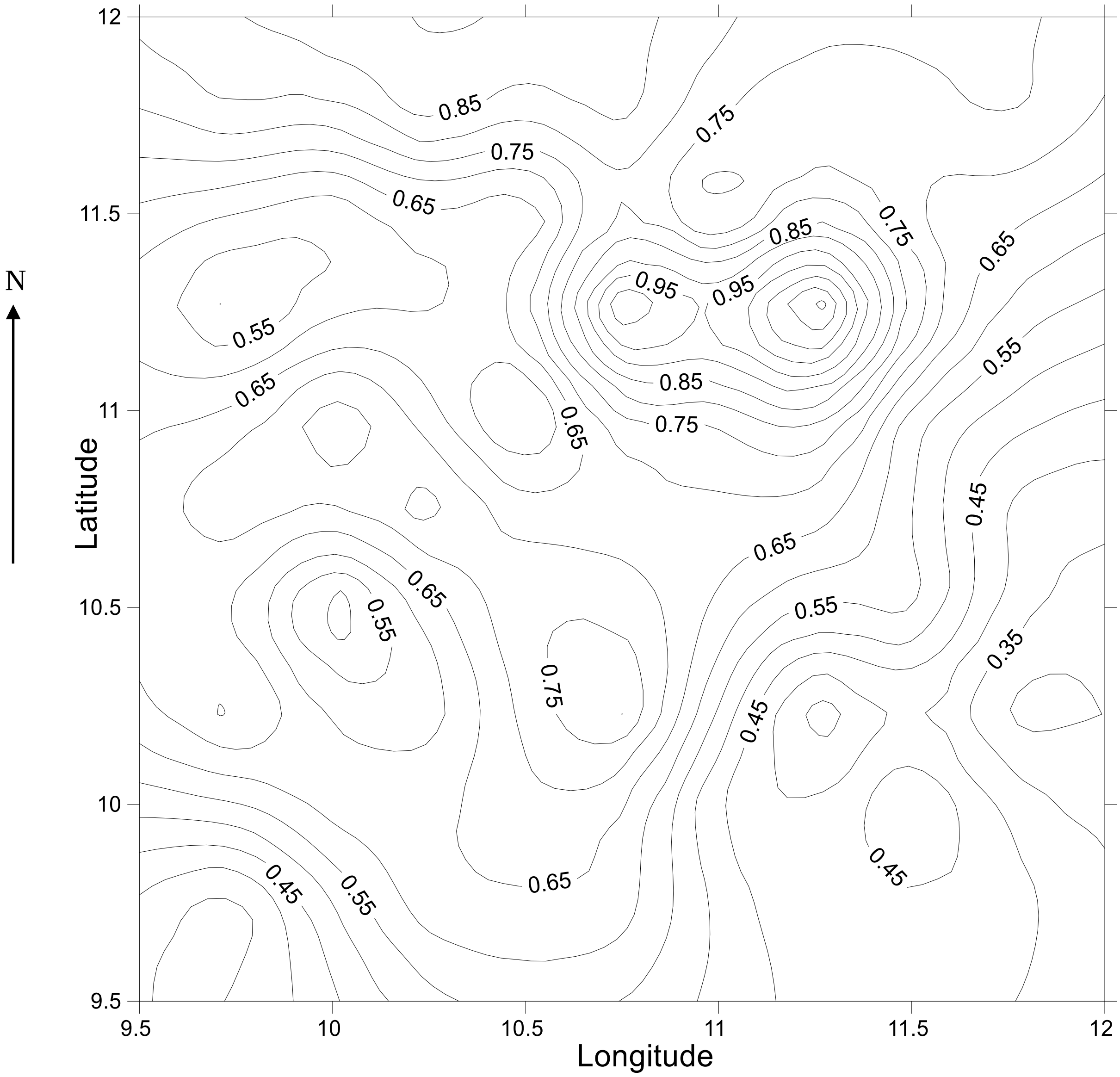

Figure 4.24: Contour map of first layer magnetic source. Contour interval is 0.05km.

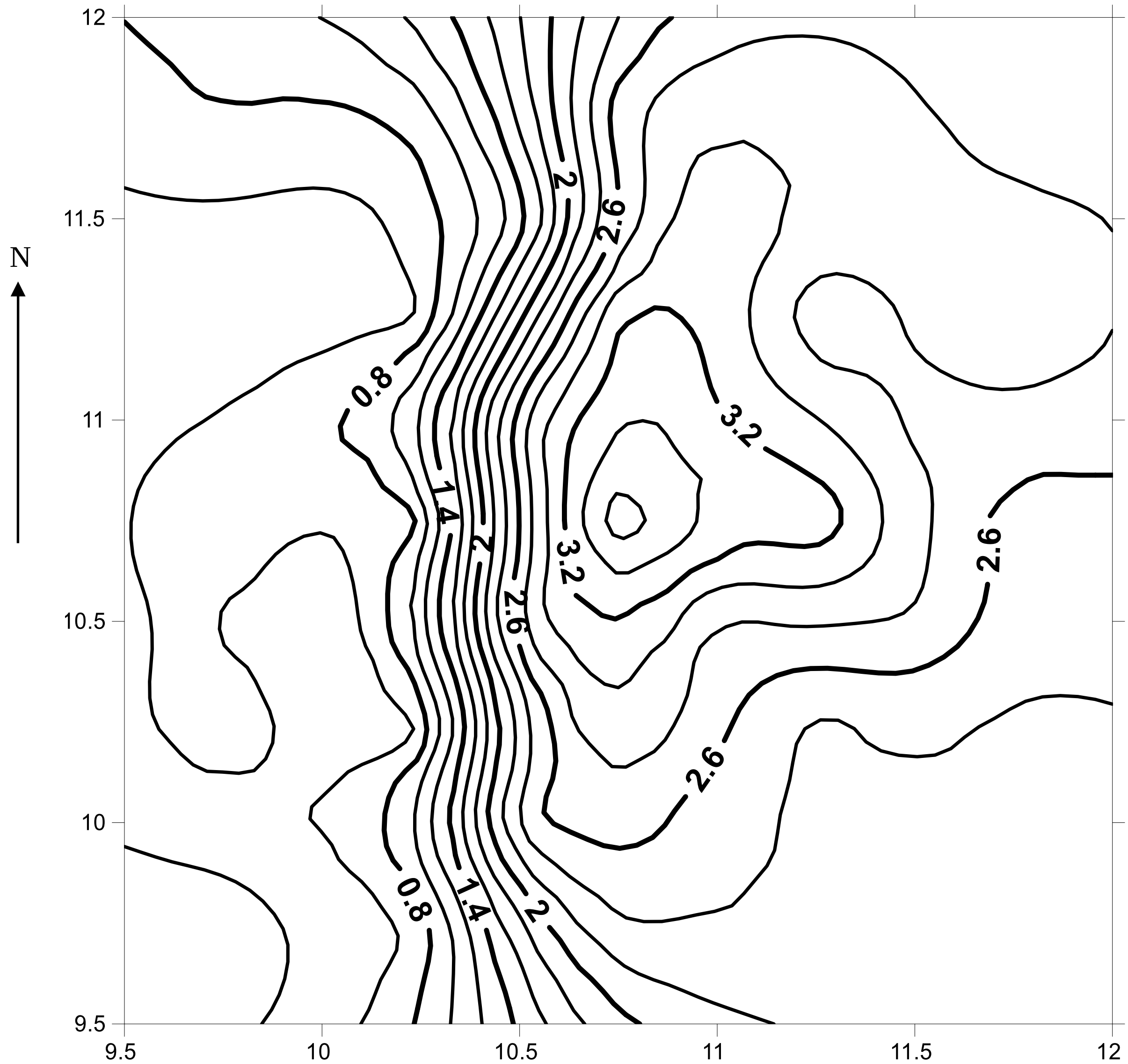

Figure 4.25: Contour map of second layer magnetic source of the Upper Benue Trough and Southern Bornu Basin (Contour interval is 0.2 km).

from spectral analysis of upper Benue trough; Udensi and Osazuwa (2003) obtained a maximum depth of 3.39 km in the Nupe Basin; Nur (2000) obtained a depth range of 625 m to 2.219 km for deeper sources and an average of 414 m for shallow sources at Upper Benue Trough; Nur (2001) got a depth range of 420 m to 8 km southwest of Chad Basin. Other workers whom this present work has largely corroborated include: Likkasson, Ajayi and Shemang (2005), Nur (2002), Nur (2001), Nur, Ofoegbu and Onuoha (2003), Osazuwa, Ajakaiye and Verheijen (1981) and Ofoegbu (1984 and 1988).

Figures 4.26 and 4.27 show the surface map of deep and shallow magnetic source depth in a coloured range respectively. From the figures, a prominent sedimentary reservoir can be found around the central part. It has a depth of 3.71km. This area corresponds to Baka, Ako Gombe and Gombe at the central part.

Figure 4.28 shows the superposition of the spectral depth contours of magnetic deep sources on geologic map. This Figure shows some similarities between the surface structures as delineated by geologists and the subsurface magnetic features. Figure 4.28 indicates that depth to basement is shallow in basement complex region (western region of the study area) and eastern region of the area where there are volcanic activities as indicated by the geological map.

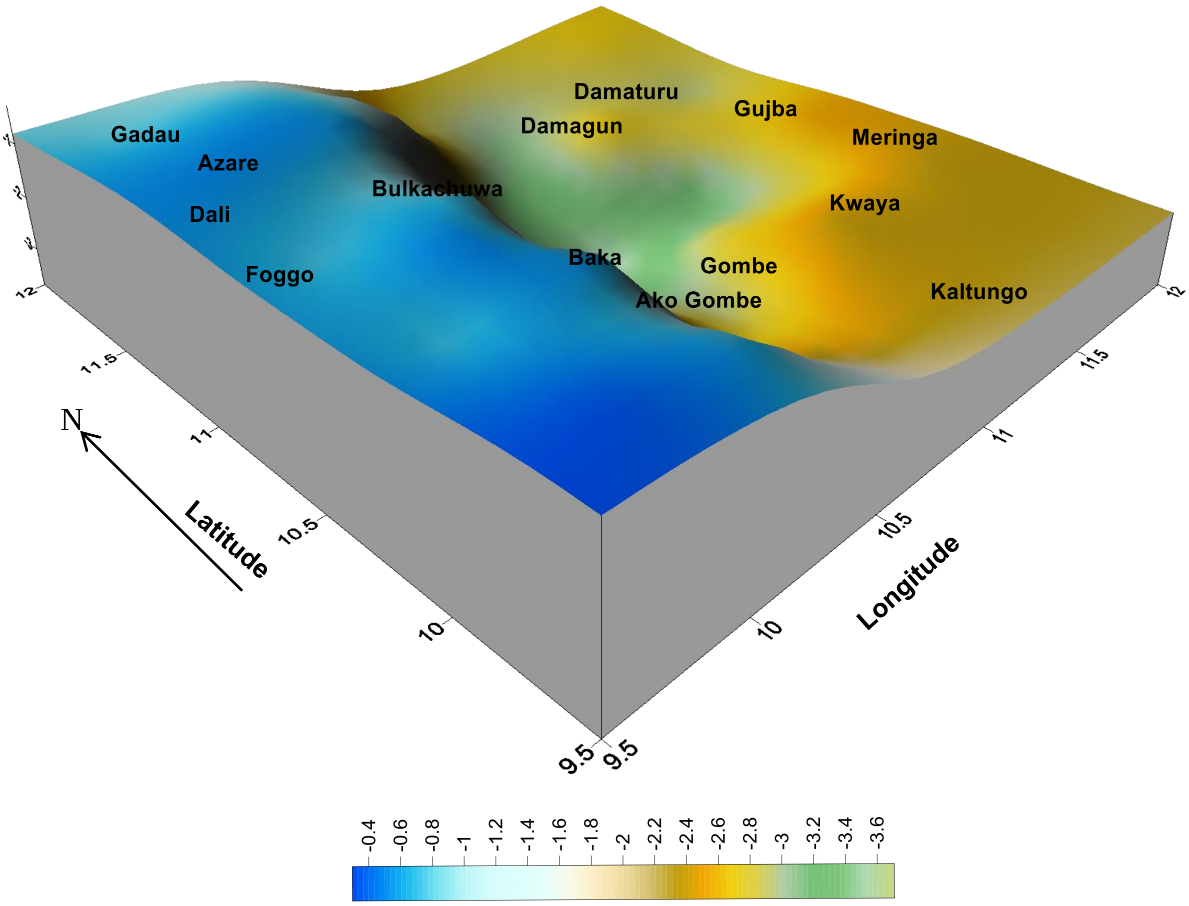

Figure 4.26: 3D Surface map of deeper magnetic source depth of the Upper Benue Trough and southern Bornu Basin.

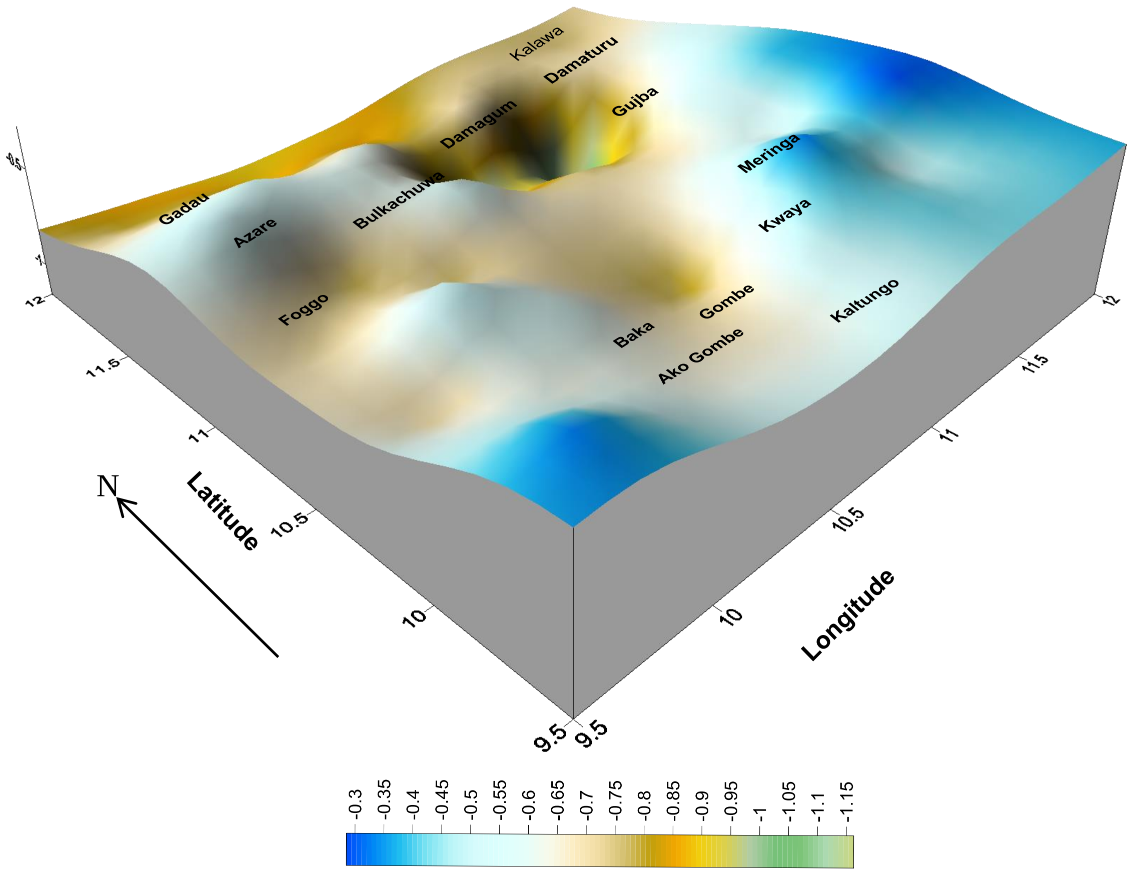

Figure 4.27: 3D Surface map of shallow magnetic source depth of the Upper Benue Trough and southern Bornu Basin.

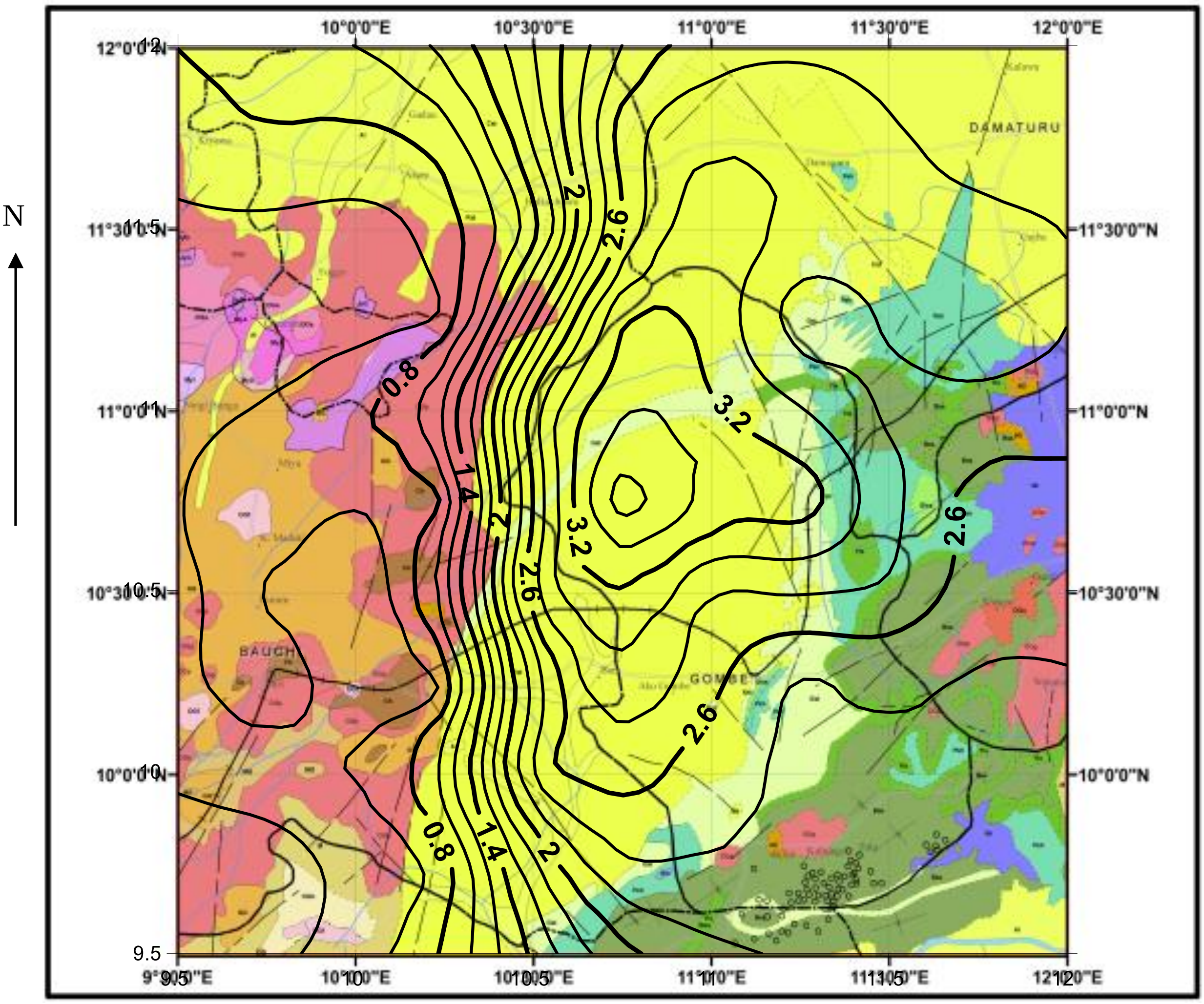

Figure 4.28: Depth to magnetic deep sources superimposed on the geologic map of the area (contour interval is 0.2 km)

4.5.2 **Determination from Source Parameter Imaging (SPI) Method**

The depths to magnetic sources were determined through several mathematical processing from various grids. The pre-processed grids from the residual grid as input grid are dx, dy and dz. These output grids were later served as input grids for SPI processing. First order derivative was adhered to, as the method (SPI) is much more sensitive to noise at higher derivative order. Therefore, careful filtering of data was ensured so as to have good estimates of the local wavenumber and hence the depth. Figure 4.29 shows the depth estimates obtained from the source parameter imaging (SPI).

The figure (Figure 4.29) shows the depth estimate of the upper basement depth (i.e. top of the sediment/basement interface) Smith, Thurston, Dai and Ian (1998). The white areas/ portion of Figure 4.29 are the areas where the derivative used to estimate the local wavenumber are so small that the SPI structural index cannot be estimated reliably. The model-independent local wavenumber had been set to zero in that portion. From Figure 4.29, the depth to sedimentary/basement interface varies between 0.96 km and 5.862 km. The smallest depth can be found in the south-central part to the north-eastern part. However, relatively large depths are also scattered around northern and southern parts.

The result from SPI agrees to a large extent with the result from spectral depth determination (Figure 4.25). Figure 4.30 shows the superposition of the second magnetic source depth (sedimentary thickness) obtained from spectral analysis with the SPI. Both the numeric values and the areas delineated are very much in agreement. That is, the shallowest region from both methods corresponds to the Basement complex in the area. Similarly, results from both depth estimate methods agreed largely with other published works in the study area, as earlier stated. The results from both spectral depth and SPI will be used as starting values for modelling in section 4.6.

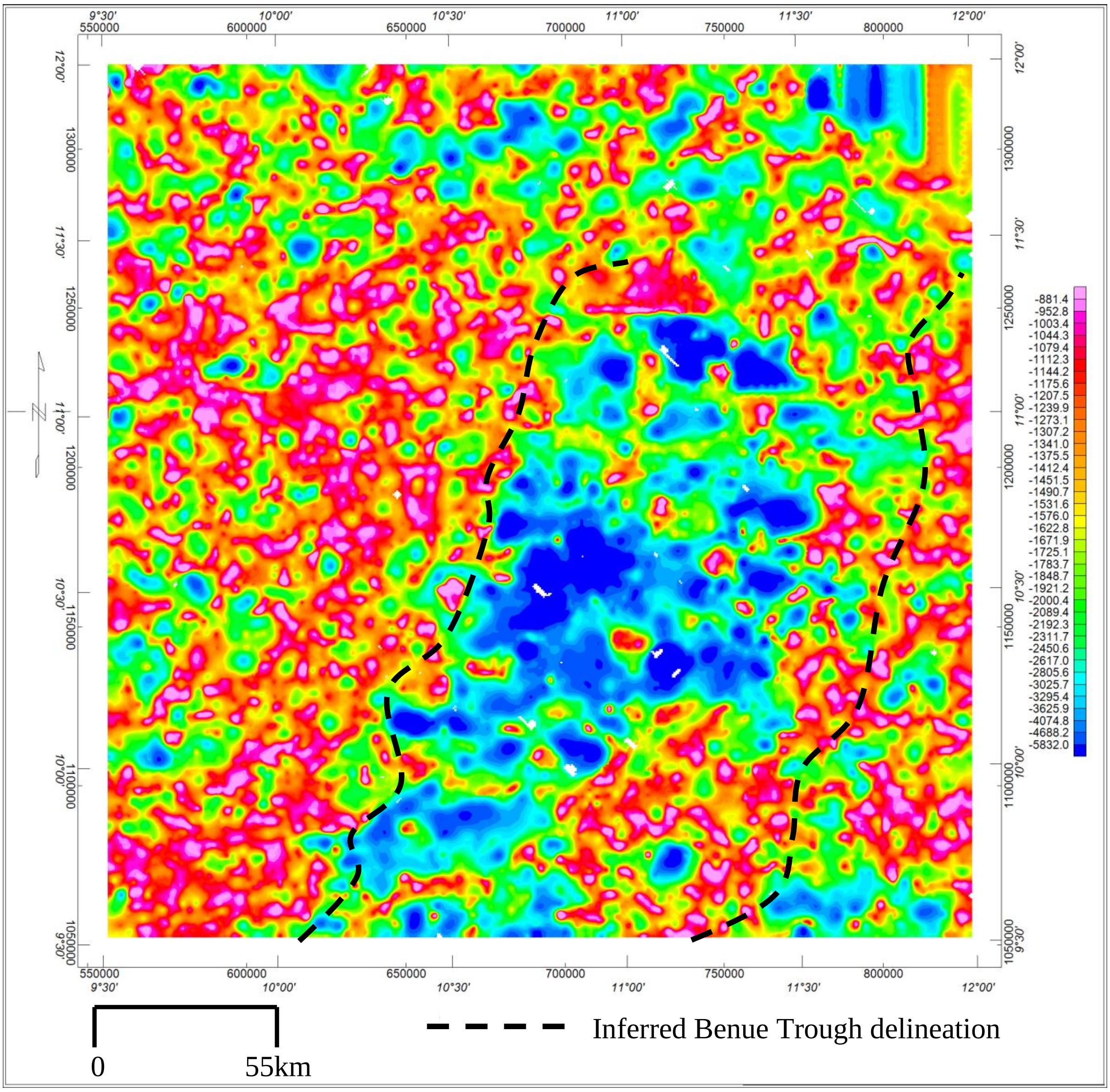

Figure 4.29: Depth determination from source parameter imaging (SPI). The colour bar shows the depth estimates in meters.

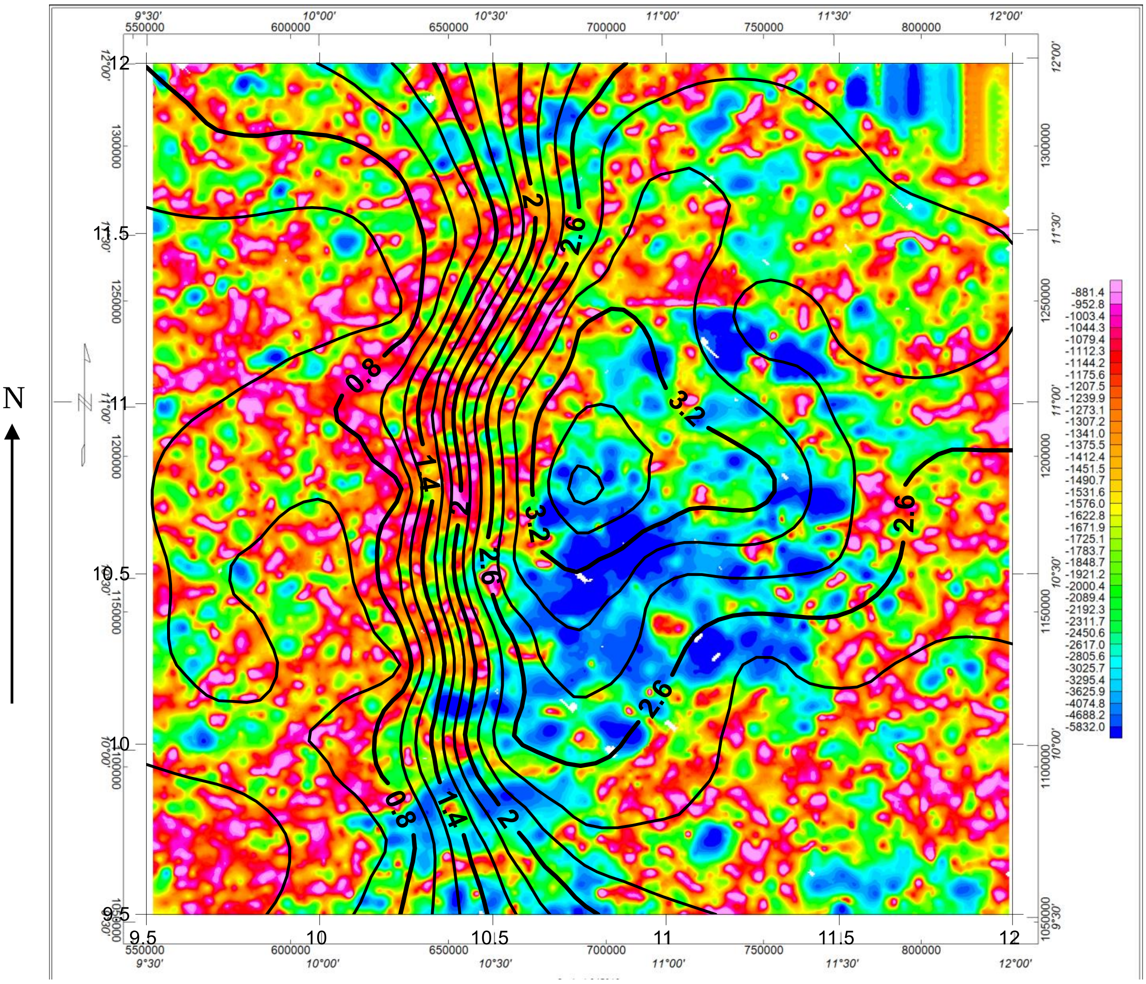

Figure 4.30: Depth to magnetic deep sources from spectral analysis superimposed on the results of the source parameter imaging (SPI) depth.

4.6 Two dimensional (2D) modelling of the residual magnetic field anomalies

Figure 4.31 shows the seven profiles AA^1, BB^1, CC^1, DD^1, EE^1, FF^1 and GG^1 that were modelled in this work. These profiles were drawn across the residual magnetic map (Figure 4.31) and on the geologic map (Figure 4.32). These profiles were carefully drawn with respect to Figure 4.21, which was used as a guide in drawing those profiles. These profiles were drawn perpendicular (not parallel) to the strike of the features identified in Figure 4.21. The profiles were drawn on the imported geologic map of 1:2000000 scale in Oasis, which was automatically transferred onto any map of interest like Figures 4.31 and 4.32.

The susceptibility values used for modelling the residual magnetic anomalies are: sedimentary rock section 0.0 c.g.s and basement rock section varies between 0.001 – 0.009 c.g.s. The remanence magnetization, magnetic inclination and declination could be calculated and or supplied as each models are opened for the first time. The TMI used for this work is 33235.26 nT; inclination is - 1935^0 and the declination is -4.763^0. These values were obtained from literature adapted from Ajakaiye, Hall and Millar (1985) and Ajakaiye, Hall, Ashiekaa and Udensi (1991), Ofoegbu (1985), Ojo (1990), Udensi and Osazuwa (2002) and Likkasson, Ajayi and Shemang (2005). These values fall within range of values for rocks and minerals (Telford, Geldart, Sherriff and Keys, 2001).

The depth to magnetic sources results obtained from the Source Parameter Imaging (SPI) was used as constraint depth for modelling the residual magnetic field anomalies. Each depth models were loaded as ‘Registered Backdrop’ in the GMSYS.

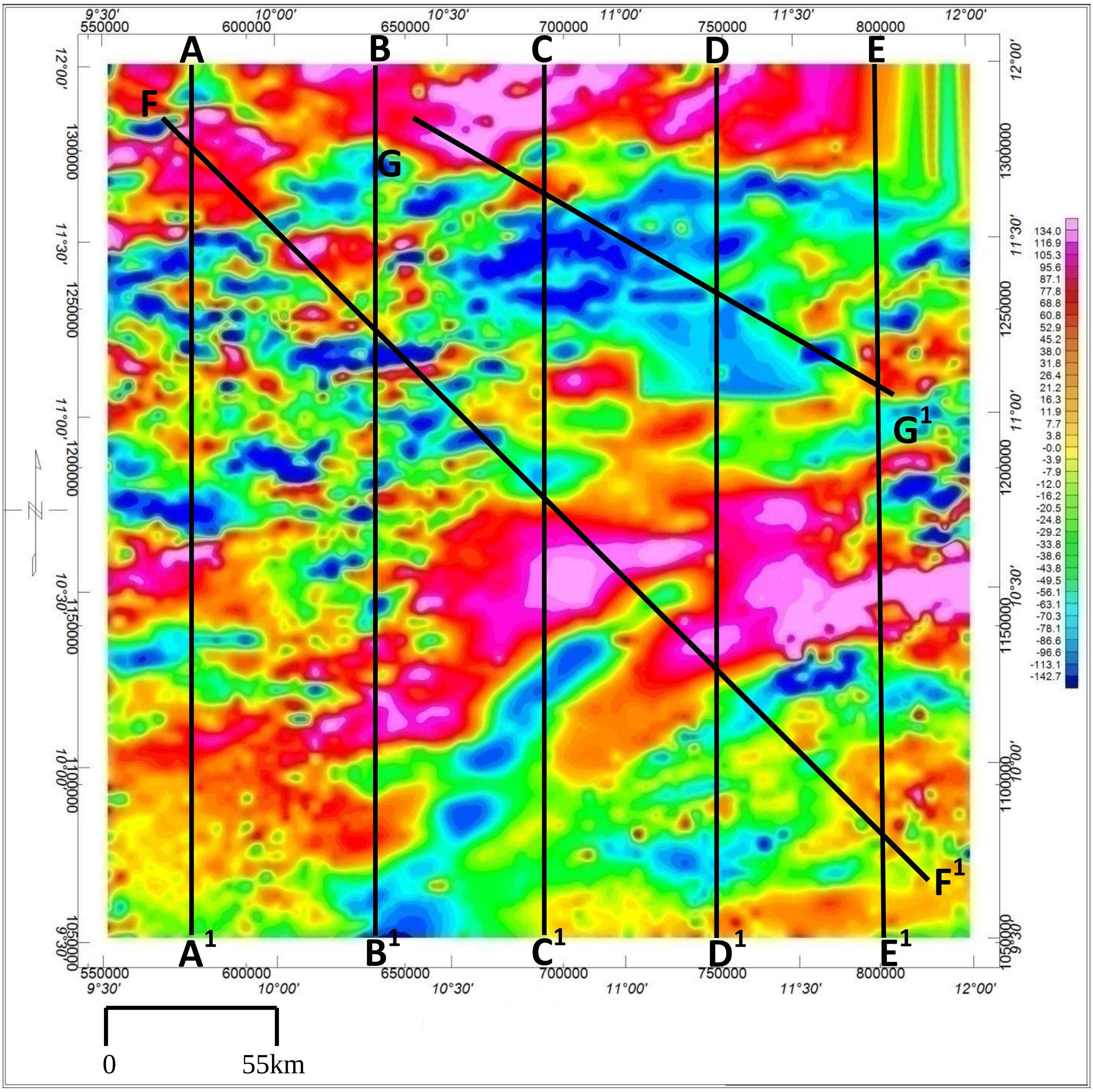

Figure 4.31: Residual magnetic map showing selected profiles for modelling. Unit of residual magnetic field = nano tesla.

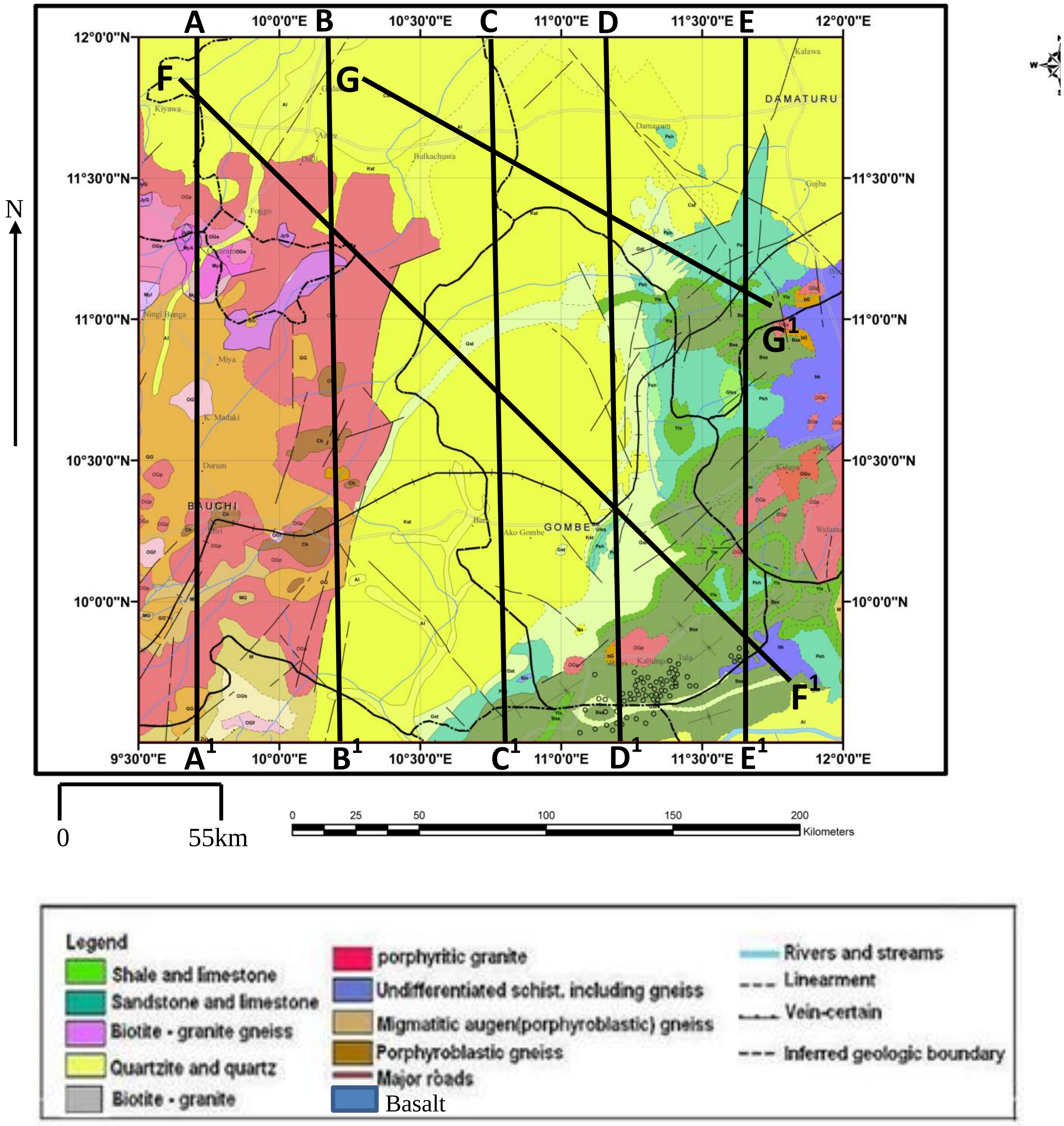

Figure 4.32: Selected profiles used for modelling displayed on the geologic map to scale 1:2000000.

The topographic data used for the models were adapted from the Shuttle Radar Topographic Mission (SRTM) (Figure 4.33) obtained from NGSA. The terrain clearance value used was 160 m which was obtained from the flight altitude used in collecting the aeromagnetic data. This value was added to the SRTM, which was used for the magnetic elevation control. This value thus serves as the total topographic value (called sensor) for the models and it is the value above the sea level.

The models or profiles were created from each selected database line. A database file was created for this purpose in Oasis and each profile line was drawn one after the other on one of the following grid files: the residual (as the magnetic grid file control) grid or the SRTM grid (as the topography grid file control). Once a profile line is drawn on any of those grid control files, the data from each of those grids would be sampled and stored accordingly in the created database file into their respective database line channels. The models were created from the database generated and each model was opened for modelling proper. It is worthwhile to note that, models generated or produced were within an acceptable error margin of 4% to about 12%, which is one of the lowest error margins obtained when compared with similar works in the literature.

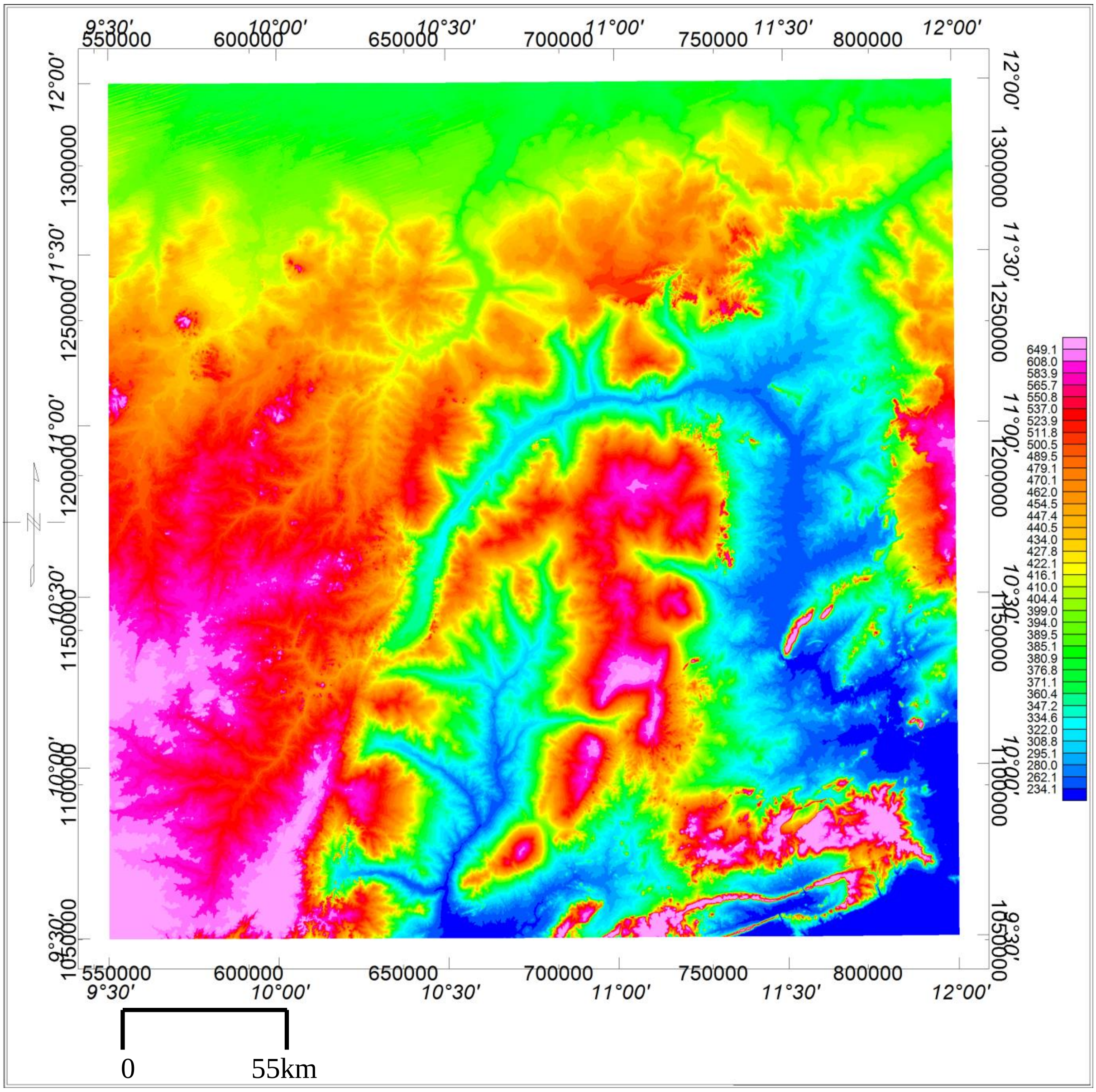

Figure 4.33: Topographical Map of the Study area (adopted from Shuttle Radar Topography Mission (SRTM) data, USA, obtained from Nigeria Geological Survey Agency, 2009.

4.6.1 Results from Profile AA[1]

Profile AA[1] (from Figure 4.31) is a north-south line drawn across a northeast-southwest and east-west trending anomaly. This profile passed through Foggo, Maya, Madaki, Magama and Bauchi in the basement complex of the study area. It also passed through Gadau, Durum and Azare in the northern part corresponding to the Chad Formation. The profile (Figure 4.34) cuts across the basement complex section of the study area and has a length of 270 km.

The model mainly consists of basement rocks outcropped over more than two-thirds of the profile length. The sedimentary rocks corresponding to the Chad Formation could be found in the northern part of the profile and has a length of about 50 km. Its thickness ranges from about 0.2 km to 1.6 km. From Figure 4.32, profile AA[1] passed through a tiny sedimentary body which is evident in Figure 4.34, is a sedimentary formation corresponding to Kerri-Kerri formation and has a depth of about 0.5 km.

The basement outcrops as delineated by the geological map are granite, biotite-granite, Younger Basalt and fine-grained-biotite- granite. The model has intrusive rocks in both the north and the southern parts. The intrusive rock to the north could be found at a depth of about 0.6 km and has a width of about 18 km and thickness of about 0.4 km. The intrusive rock to the south could be found at about 0.6 km depth. It has a lateral distance (or width) of about 40 km and a thickness of about 2.0 km. The intrusive rocks have similar magnetic properties; their susceptibility value is 0.002 c.g.s. The result of this model is in agreement with the depth to sources results obtained for both SPI (Figure 4.29) and the spectral models (Figure 4.25).

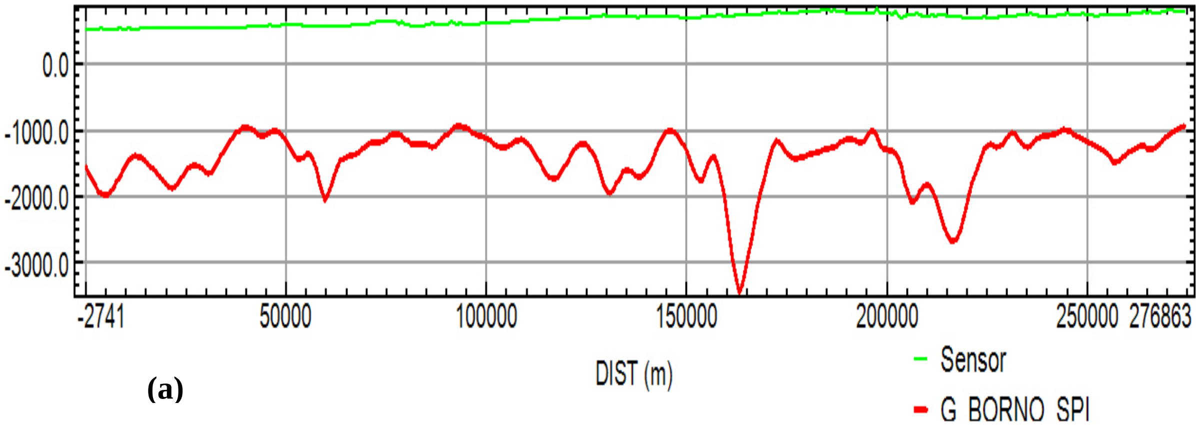

(a)

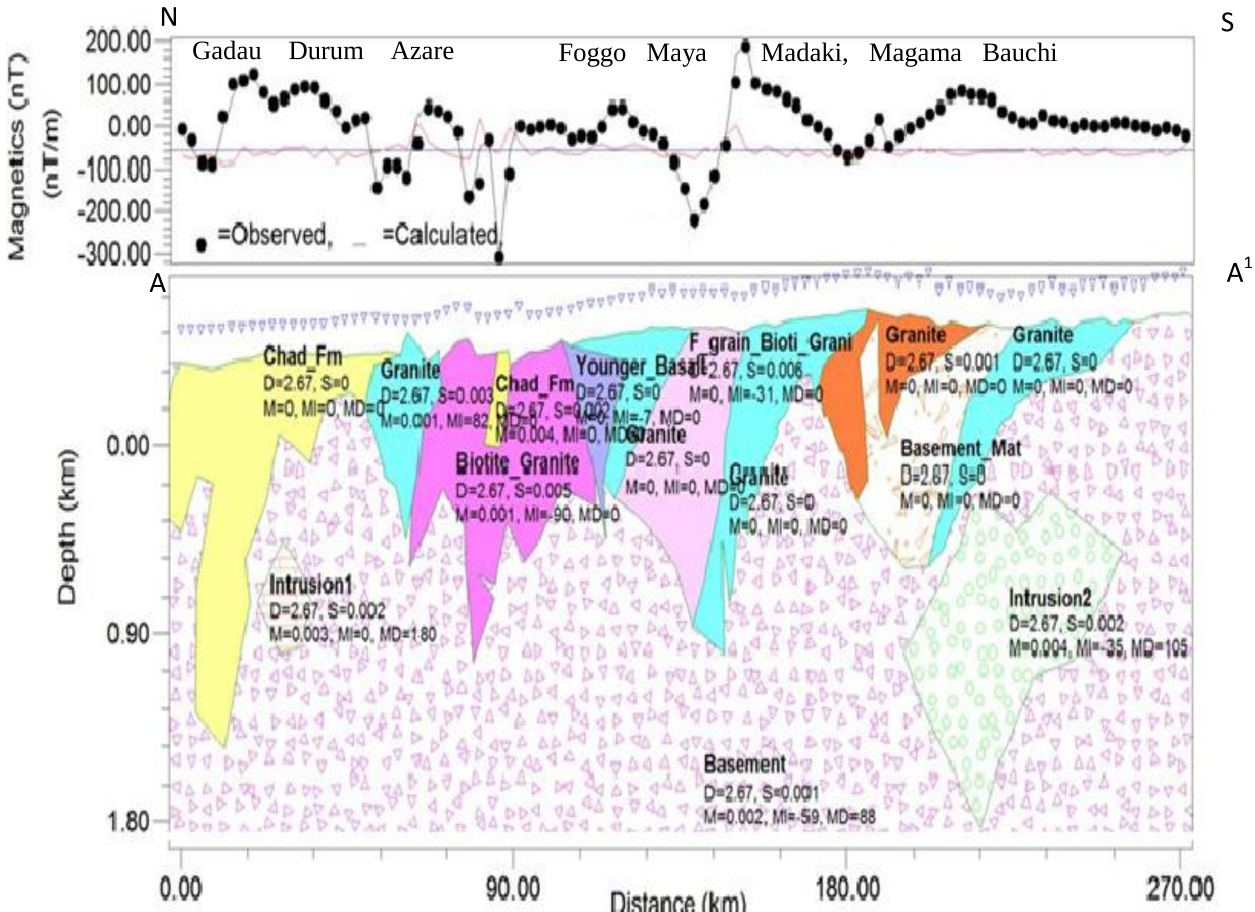

(b)

Figure 4.34: (a) SPI depth control and (b) model for profile AA[1]; S = susceptibility, M = Magnetization, MI = Magnetic Inclination, MD =Magnetic Declination

4.6.2 Results from Profile BB[1]

Profile BB[1] (from Figure 4.31) is a north-south traverse drawn across a northeast-southwest and east-west trending anomaly. This profile passed through Bulkachuwa in the north and west of Ako Gombe in the south. This profile also runs through the basement complex section of the study as shown in Figure 4.32. Figure 4.35 has a total distance of 270 km, the profile passes through the sedimentary region in the north, then through the basement complex in the middle of the profile and then through the sedimentary section in the south. The profile consists of sedimentary rocks underlain by the basement rocks. The basement material outcropped at about 90th km from the north which is evident from Figure 4.35, profile BB[1].

The thickness of the sedimentary formation in the north ranges from 0.18 km to about 1.30 km. The sedimentary thickness in the south ranges from 0.6 km to about 2.70 km in the south. The sedimentary formation to the north belongs to the Chad Formation and to the south; it belongs to the Kerri-Kerri Formation and Gombe Sandstones. The thickest sedimentary formation in the south could be found at about few kilometres west of Ako Gombe.

The basement is found outcropped as evident in Figure 4.33 in between the two sedimentary sections. It is named as basement material and corresponds to granite, biotite-granite and fine-grained- biotite-granite. The result of this model is in agreement with the depth estimates results obtained for both SPI (Figure 4.31) and the spectral models (Figure 4.26).

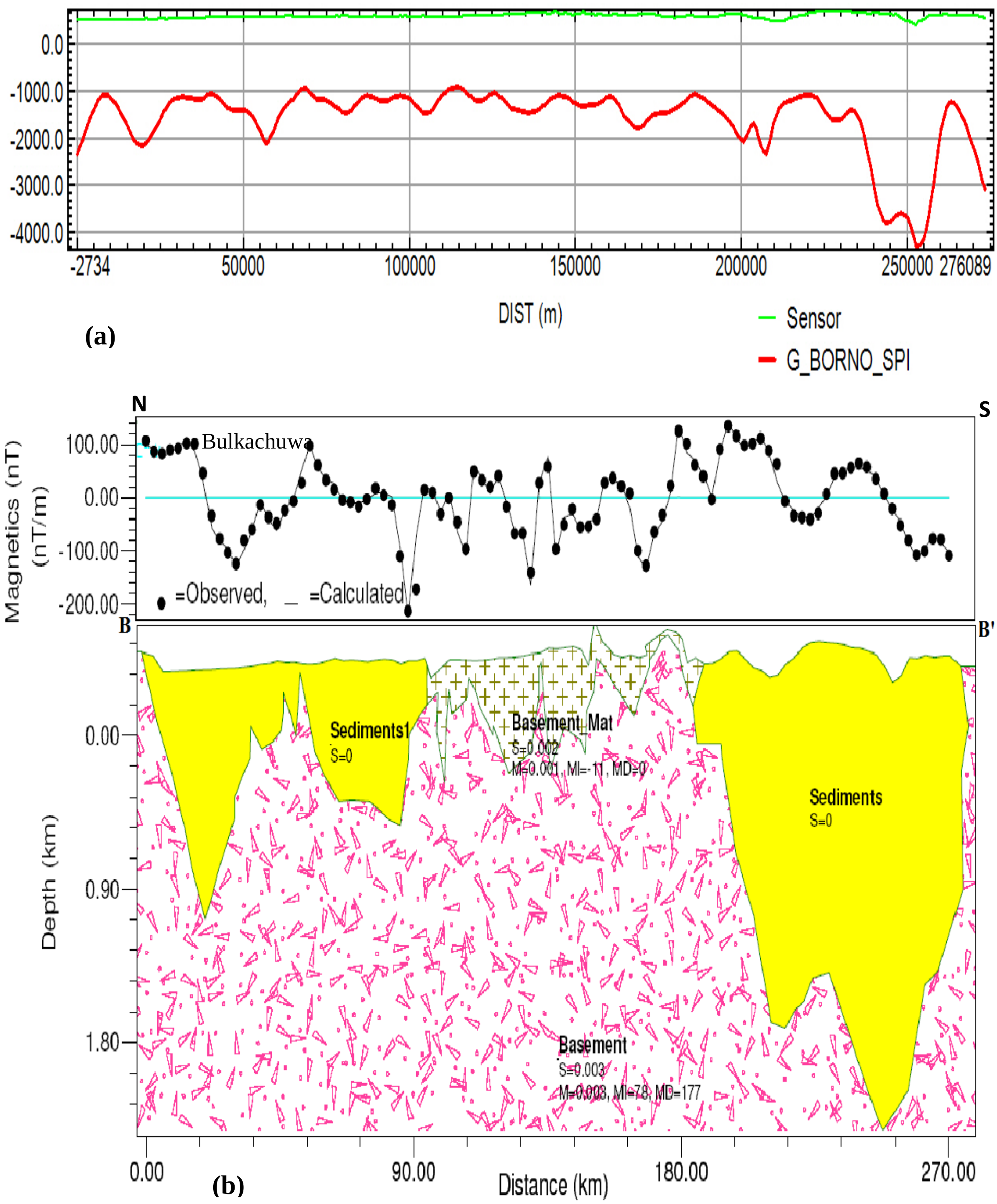

Figure 4.35: (a) SPI depth control and (b) model for profile BB[1]; S = susceptibility, M = Magnetization, MI = Magnetic Inclination, MD =Magnetic Declination

4.6.3 Results from Profile CC^1

Profile CC^1 (from Figure 4.31) is a north-south traverses across a northeast-southwest and east-west trending anomaly. This profile (Figure 4.36) passed through Gombe in the south and is 270 km long. The profile consists mainly of sedimentary sections. The sedimentary thickness varies from 0.60 km to about 4.60 km. The greatest sedimentary thickness is obtained at the southern part around Gombe axis. This sediment corresponds to the Kerri-Kerri Formation, Gombe Sandstones and Pindiga Formation in the south. In the north, the sedimentary thickness is about 2.40 km and it corresponds to the Chad Formation. The minimum sedimentary thickness is obtained at about 90^{th} km distance from the north (beginning) of the profile, which could be found at about Latitude of 11.0^0 N. The result of this model is in agreement with the depth estimates obtained for both SPI (Figure 4.29) and the spectral models (Figure 4.25).

4.6.4 Results from Profile DD^1

Profile DD^1 (from Figure 4.31) is a north-south traverse across a predominantly east-west trending anomaly. This profile passes between Damagun and Damaturu in the north, it also passed through Kaltungo area in the south. The profile (Figure 4.37) is 270 km long and passes through sedimentary section underlain by basement rocks. The basement is uplifted with about 0.20 km sediments. This minimum thickness occurs at about 54^{th} km distance from the north and corresponds to latitude 11.1^0 N. This area was reported by Zaborski, Ugodulunwa, Idornigie, Nnabo and Ibe (1998) that Chad Formation in Bornu Basin was separated from the Benue Trough sediments (Kerri-Kerri, Pindiga, Gombe Sandstones and Bima Formations). They described that the separation occurred between latitude 11.0^0 N to about 11.2^0 N, which corresponds to Dulbulwa-Bage High as cited by Zaborski, Ugodulunwa, Idornigie, Nnabo and Ibe (1998). The shallowness of basement to the south of the profile could also be ascribed

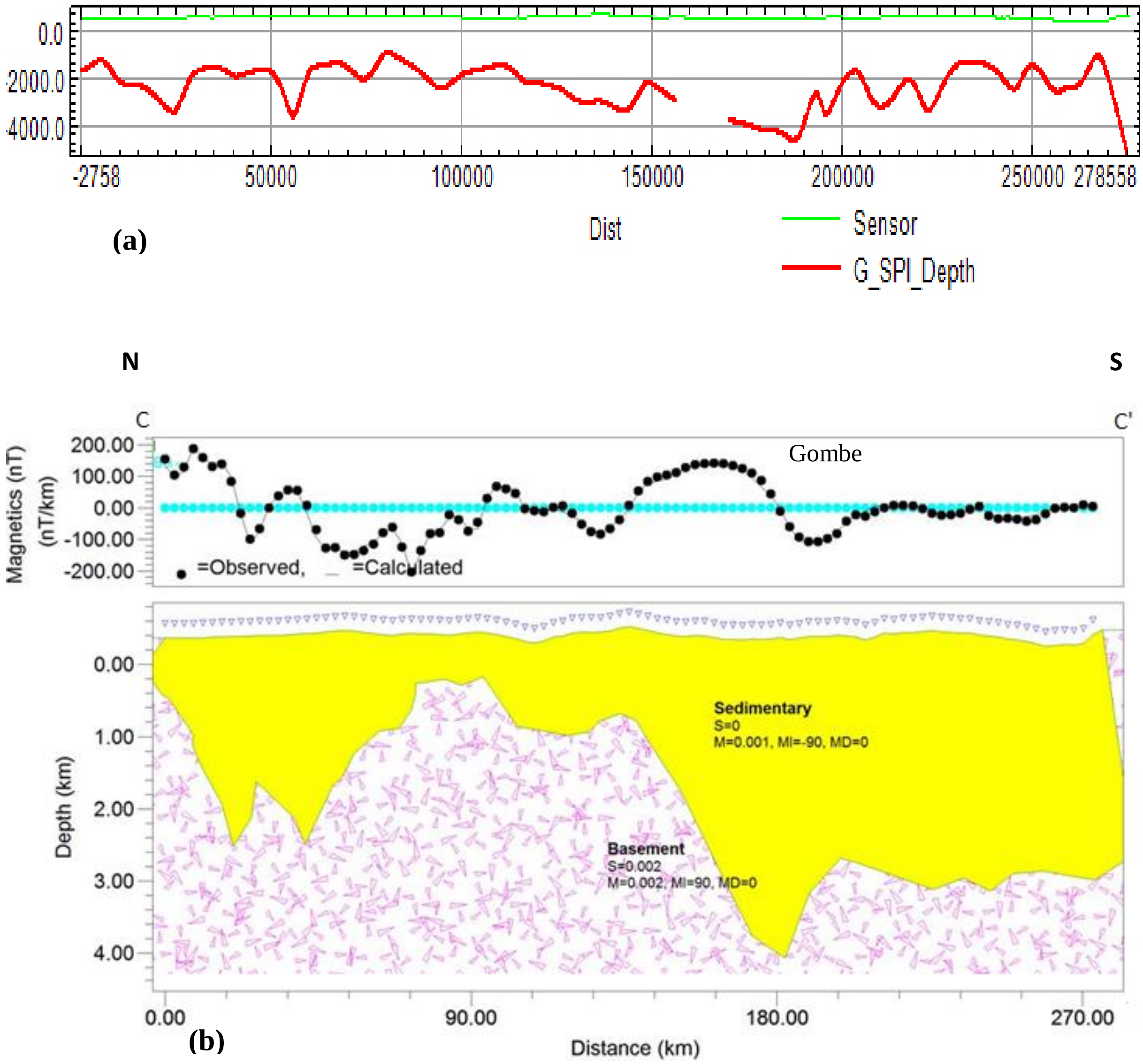

Figure 4.36: (a) SPI depth control and (b) model for profile CC^1; S = susceptibility, M = Magnetization, MI = Magnetic Inclination, MD =Magnetic Declination

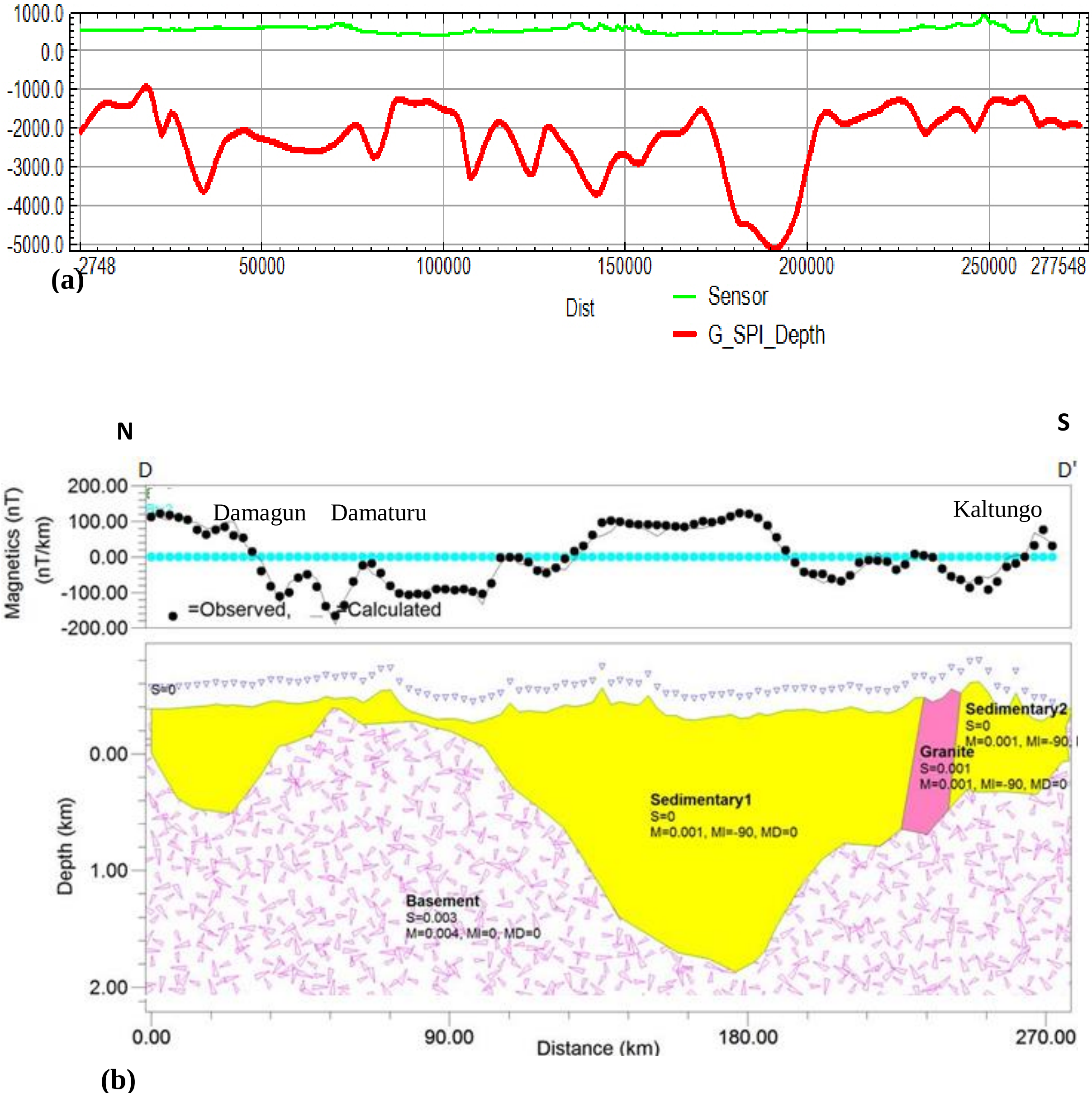

Figure 4.37: (a) SPI depth control and (b) model map for profile DD[1]; S = susceptibility, M = Magnetization, MI = Magnetic Inclination, MD =Magnetic Declination

to the Kaltungo Inlier, this was ascribed to thin sedimentary cover by numerous workers. The sedimentary thickness of about 1.0 km is obtained in this area.

The basement rock (granite) outcropped towards the southern part of the profile as found evident in Figure 4.32. The profile thus has a sedimentary thickness that ranges between 0.20 km to about 2.40 km towards south of the profile. The result of this model is in agreement with the depth estimates results obtained for both SPI (Figure 4.29) and the spectral models (Figure 4.25).

4.6.5 Results from Profile EE^1

Profile EE^1 (from Figure 4.31) is a north-south traverse drawn across a northeast-southwest and east-west trending anomaly. This profile (Figure 4.38) is 270 km long and passes through west of Bun, Maza, Burutai, Meringa, Biu, and Walama. Most of those town listed are located on basaltic rocks as delineated by the geologists (Figure 432). The profile is mainly sedimentary and has thickness that varies from 0.10 km to about 2.60 km. The maximum sedimentary thickness is obtained towards the southern part, around Walama while the minimum thickness is found in the north at about 90^{th} km from the north. The minimum sedimentary thickness occurred at about 11.1^0 N, which corresponds also to Dulbulwa-Bage High as cited by Zaborski, Ugodulunwa, Idornigie, Nnabo and Ibe (1998). This result is typical of the geology found in the area and thus in agreement with the depth estimates results obtained for both the SPI (Figure 4.29) and the spectral models (Figure 4.25).

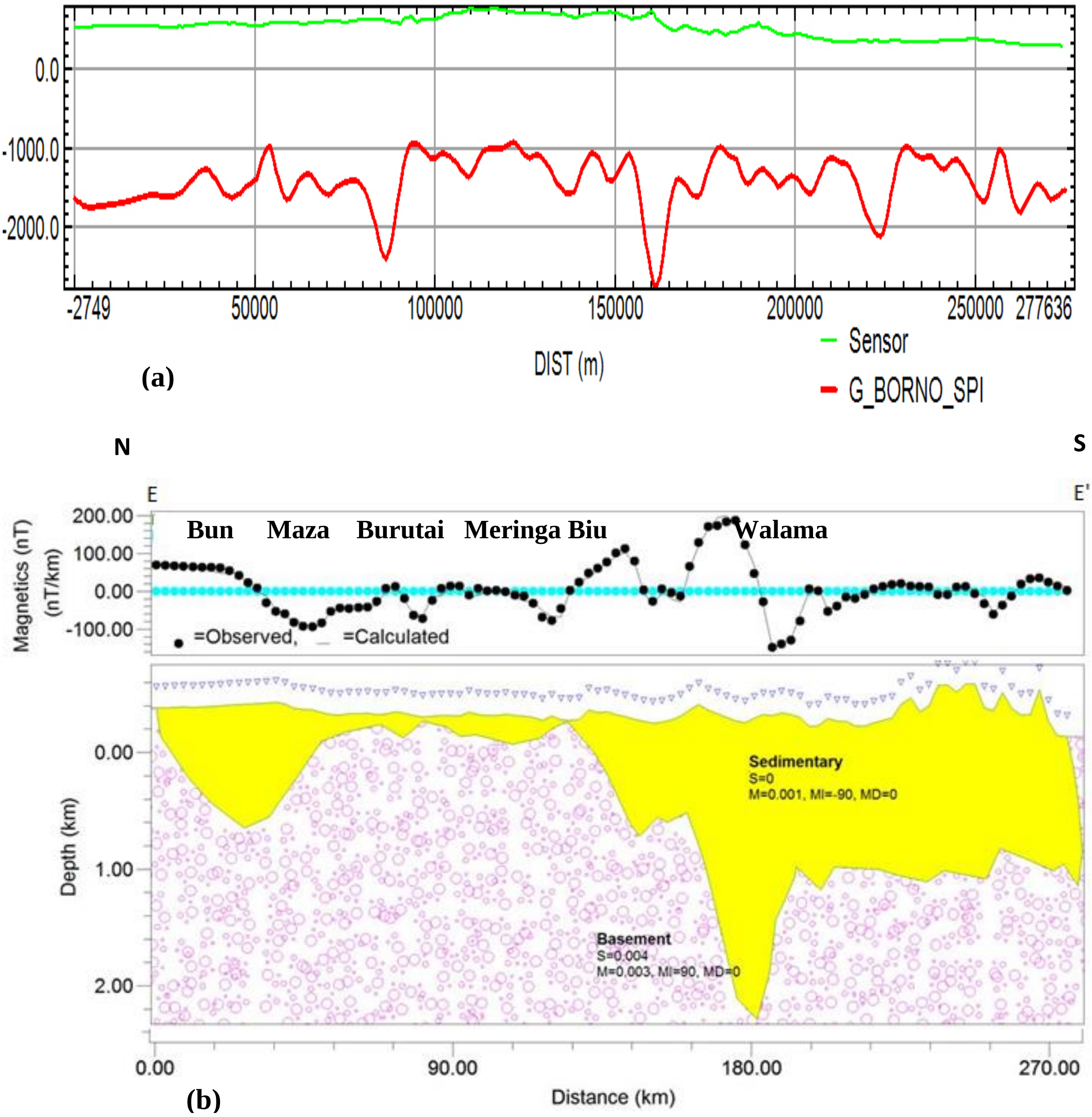

Figure 4.38: (a) SPI depth control and (b) model for profile EE[1]; S = susceptibility, M = Magnetization, MI = Magnetic Inclination, MD =Magnetic Declination

4.6.6 **Results from Profile FF^1**

Profile FF^1 (from Figure 4.31) is a northwest-southeast traverse drawn across a predominantly east-west and northeast-southwest trending anomaly. This profile (Figure 4.39) passed through Azare in the north and through southeast of Walama in the south. It is the longest profile with maximum length of about 355 km. The profile passes through the Chad Formation and some basement rocks in the north with sedimentary thickness of about 1.00 km; also through Kerri-Kerri and Gombe Sandstones in the middle where the sedimentary thickness is highest (3.00 km) and finally through Bima Sandstones, Pindiga Formation and Alluvium in the south where the sedimentary thickness is thin (about 1.60 km). The thin area in the south corresponds to Kaltungo inlier area, the information here corresponds to profile DD^1 and profile EE^1. As this profile cuts across the study area diagonally, it intersects with profile AA^1 in the north with sedimentary thickness of about 1.0 km; profile BB^1 also in the north with sedimentary thickness of about 1.0 km; profile CC^1 at the middle with sedimentary thickness of about 3.0 – 4.0 km; profile DD^1 towards south with sedimentary thickness of about 3.0 – 4.0 km and profile EE^1 in the south also with sedimentary thickness of about 1.0 km.

At about 50th km of the profile, there occurred an outcropped of granitic rock with thickness of about 50 km and width of about 1.40 km. Similarly, the profile landed on the basaltic rock in the south as shown in Figure 4.32. The deductions from those profiles are very much in agreement with the result obtained from profile FF^1. The sedimentary width of this profile is also about the length of the profile. The basement is shallow at about 140th km from the north of the profile and the sedimentary thickness there is about 0.20 km. This point corresponds to Dumbulwa-Bage High at about latitude 11.0^0 N.

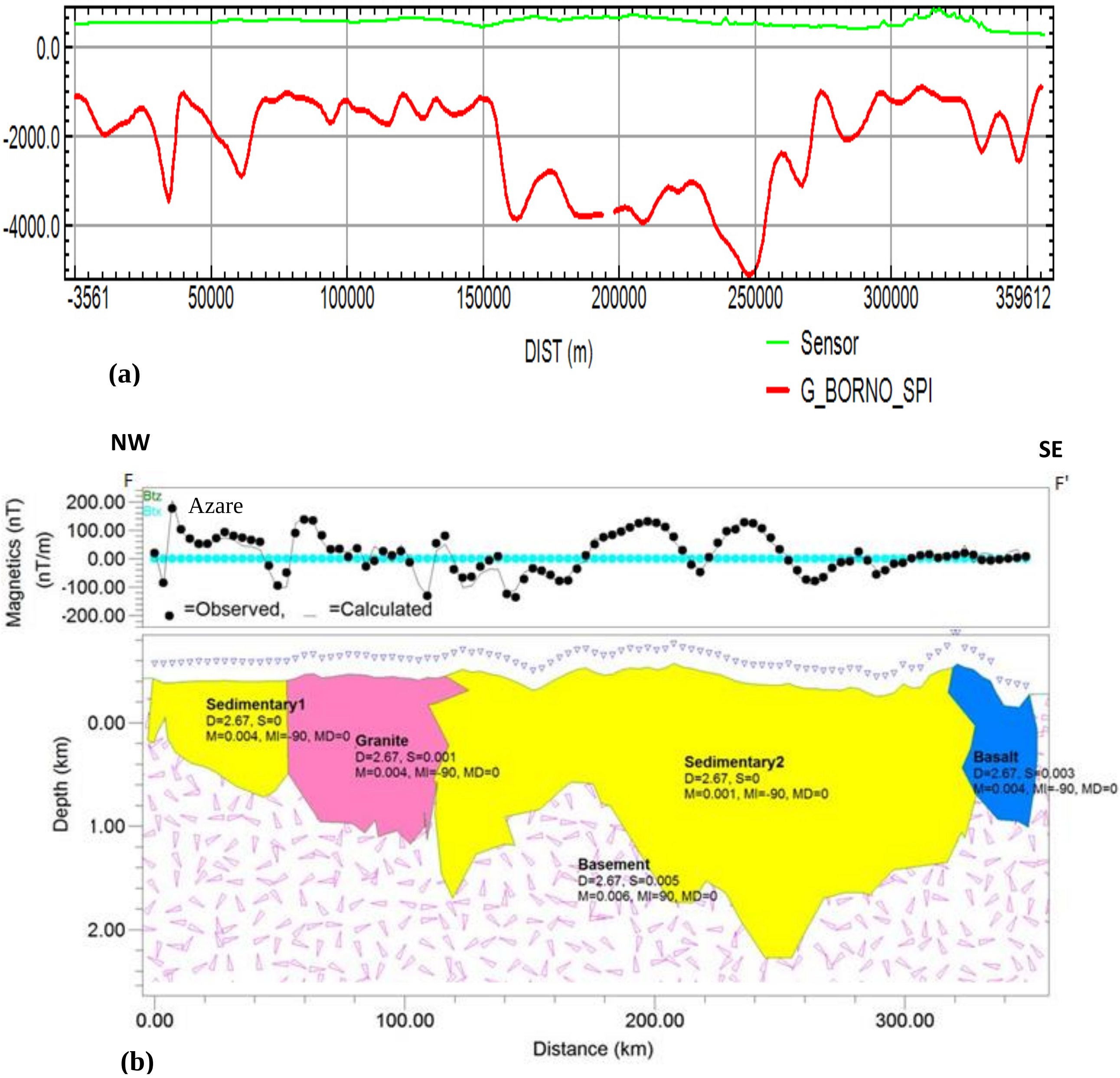

Figure 4.39: (a) SPI depth control and (b) model for profile FF[1]; S = susceptibility, M = Magnetization, MI = Magnetic Inclination, MD =Magnetic Declination

This point marked the point of intersection of profile FF^1 and profile CC^1. The result of this model is in agreement with the depth estimates results obtained for both SPI (Figure 4.29) and the spectral (Figure 4.25).

4.6.7 Results from Profile GG^1

Profile GG^1 (from Figure 4.31) is a northwest-southeast traverse drawn across a predominantly east-west and northeast-southwest trending anomaly. This profile (Figure 4.40) passed through east of Bulkachuwa and west of Damaturu in the north to Burutai in the eastern part of the profile. The profile length is about 180 km long and it consists of mainly sedimentary rocks. The sedimentary thickness varies from about 0.20 km to 4.60 km. The highest sedimentary thickness is obtained around Bulkachuwa and Damaturu and has a width of about 60 km before the sedimentary thickness decreases towards the eastern part of the profile where basaltic eruption is. This area lies around Dumbulwa-Bage High of Zaborski, Ugodulunwa, Idornigie, Nnabo and Ibe (1998). The area where the sedimentary thickness is thin corresponds to the points of intersection of this profile and profiles CC^1 and DD^1, where their sedimentary thicknesses were also thin.

A about 156^{th} km southeast of the profile, there exists an intrusive rock with susceptibility value of 0.006 c.g.s. It has a width of about 0.40 km and a thickness of about 12.00 km. The result of this model is also in agreement with the depth estimates results obtained for both SPI (Figure 4.31) and the spectral models (Figure 4.25).

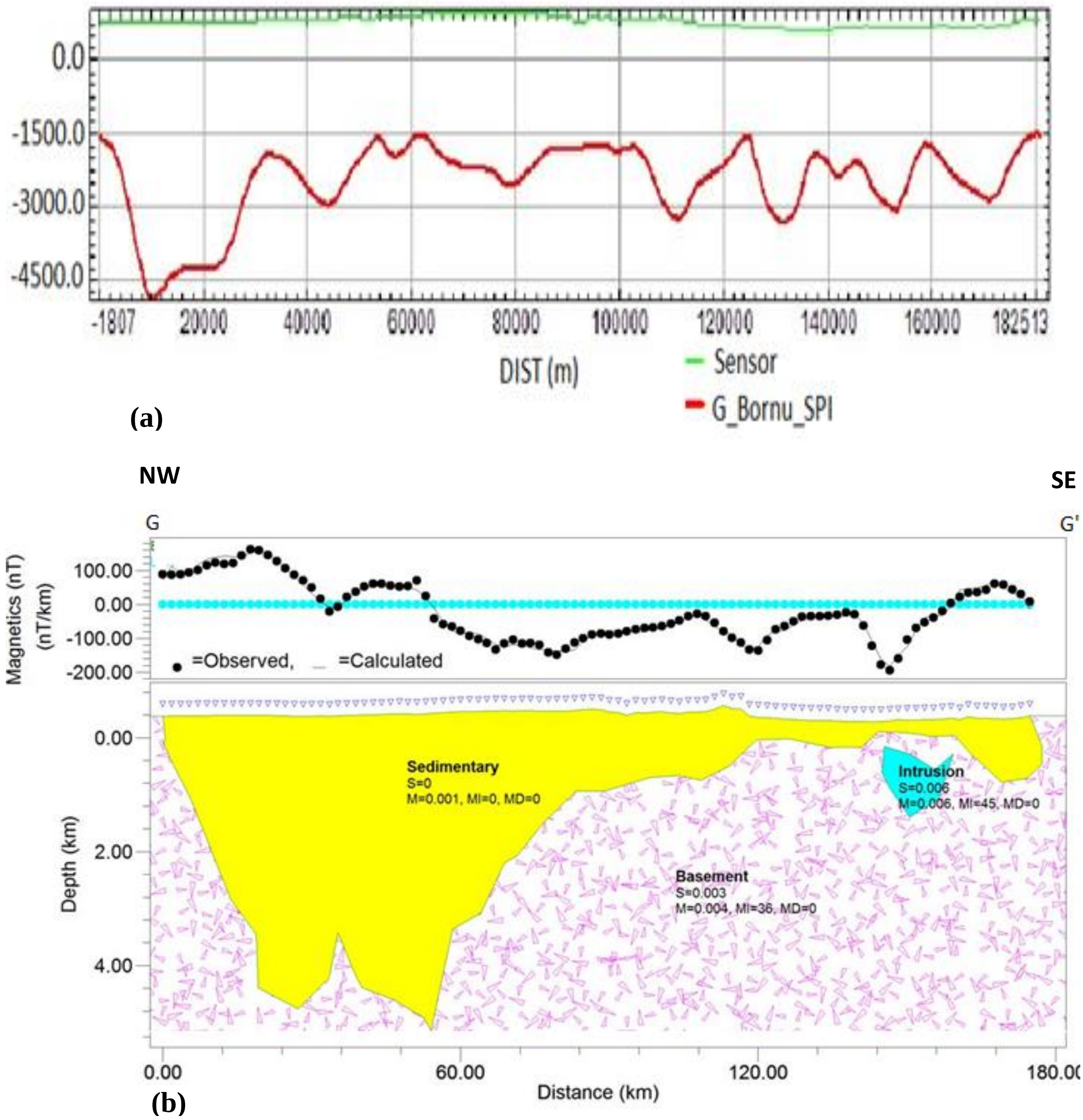

Figure 4.40: (a) SPI depth control and (b) model for profile GG[1]; S = susceptibility, M = Magnetization, MI = Magnetic Inclination, MD =Magnetic Declination

4.6.8 **Summary of the Depth Models from 2D Modelling**

Figures 4.41 and 4.42 show the depth estimate from the digitization of depth models obtained from Figures 4.34 to 4.40. Figure 4.41 is the contour map of the depth estimates from model AA^1 to GG^1. The maximum depth of 3.8 km is obtained at the southern part of the study area around Gombe and Ako Gombe. Similarly, the maximum depth of about 4.2 km is obtained at the northcentral part towards the nortwest of Damagun, Damaturu and to the northeast of Azare. The minimum depths between 0.00 km to about 0.40 km were obtained at the basement area in western part and in the east around volcanics area. Figure 4.42 is the surface map of the depth models. This figure agreed with the 3D map of second magnetic source depth, Figure 4.26.

The dashed lines in Figures 4.41 and 4.42 marked the supposed separation between the Benue Trough and the Bornu Basin. This line passes through the study area at about latitude 11.0^0N as noted by Zaborski, Ugodulunwa, Idornigie, Nnabo and Ibe (1998). They described the separation area to have occurred around Dumbulwa-Bage High at about latitude of 11.0^0. This area is described by Figures 4.41 and 4.42 to have shallow basement with maximum sedimentary thickness of about 1.4 km. However, to the either side of the area (north and south), the sedimentary thickness increases to about 3.80 km. Thus this area (Dumbulwa-Bage High) is an uplift that dips sediments to both the north (Bornu Basin) and the south (Benue Trough) of the study area.

Since the depth models obtained from both the SPI and spectral, were used as depth constrained for 2D modelling of the subsurface, the results obtained here (Figure 4.41) thus serve as the final depth model for this work.

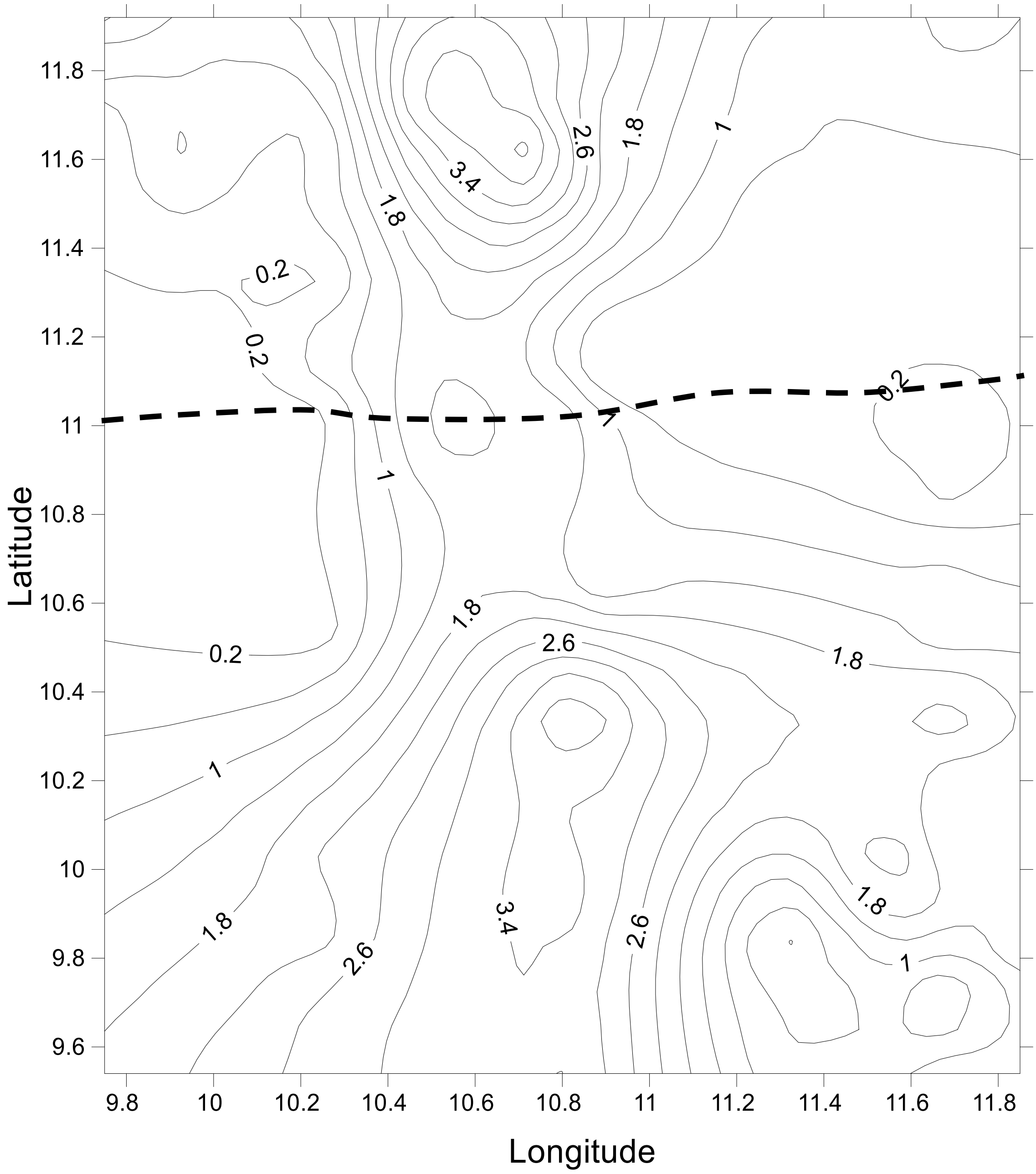

Figure 4.41: Contour map of sedimentary thickness obtained from 2D models of AA[1] to GG[1]. Contour interval is 0.4 km. The dashed line indicate the supposed separation between Upper Benue Trough and Chad Basin.

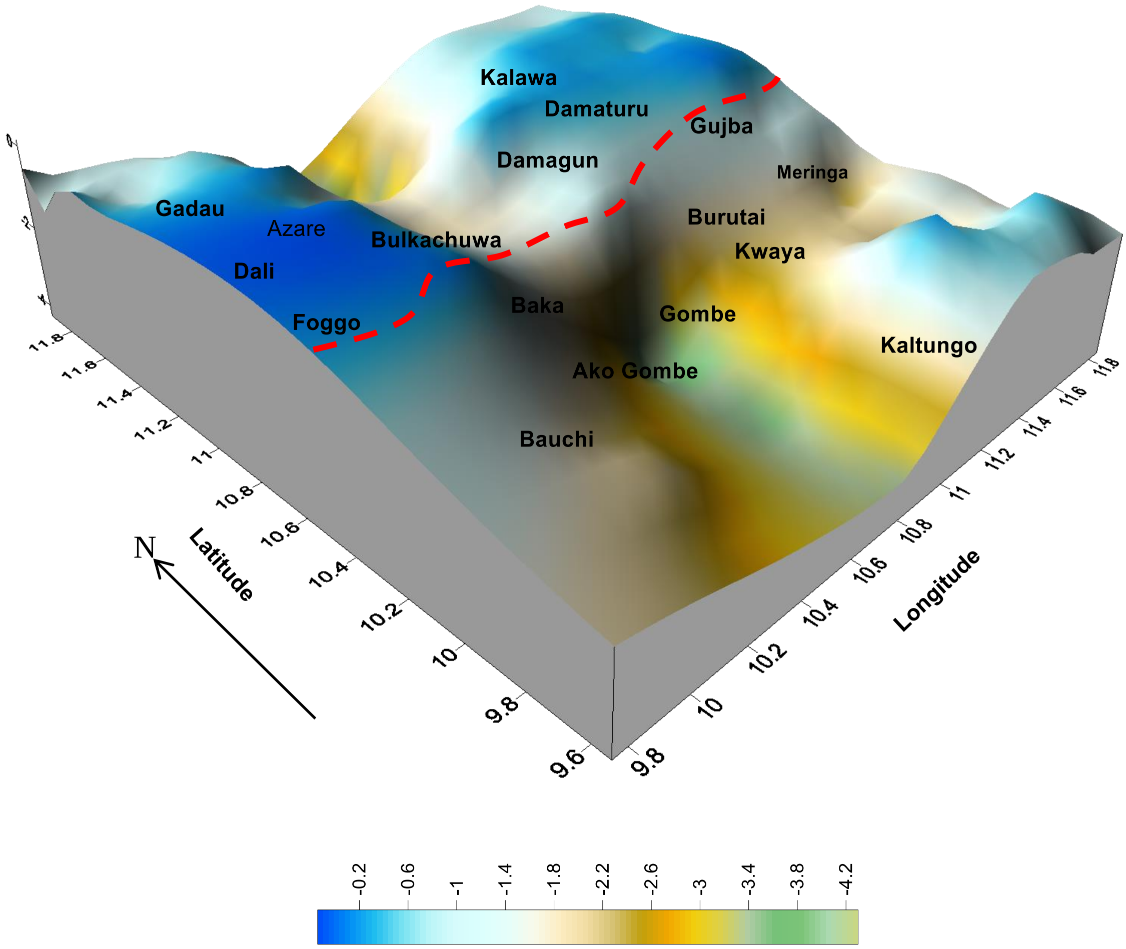

Figure 4.42: 3D surface map of profile depths obtained from 2D models of AA^1 to GG^1. The red dashed line indicate the supposed separation between Upper Benue Trough and Chad Basin.

CHAPTER FIVE

5.0 CONCLUSIONS AND RECOMMENDATIONS

5.1 Conclusions

The conclusions to be drawn from the results of filtering method (Upward continuation), CET grid analysis; depth analyses methods (spectral and source parameter imaging) and modelling of residual magnetic anomalies of the study area are as follows:

5.1.1 Trend Analysis of TMI and Filtering Processes

a. **Trend Analysis**: Figures 4.1 and 4.2 show that the south-western part of the map trends northeast–southwest; the north-eastern part, south-eastern part and central region of the study area trend east-west direction. The north-western part however, trends northwest-southeast, which dominate the study area as shown in Figure 4.2. Similarly, the regional map (Figure 4.8) has low contour value towards the northern part. The magnetic and or structural trends in the study area are east-west, northeast-southwest, and northwest-southeast trends. However, the dominating structural trend in the study area is northeast-southwest as shown in Figure 4.2.

The upward continuation filtering process performed on the total field successfully separated the deep seated (long wavelength) anomaly from the shallow (short wavelength) anomaly. The results from this method corroborates the total magnetic field map of the study area, as the area delineated with low magnetic values at the north central part of Figure 4.1 or 4.2 agreed largely with Figure 4.15 (Upward continued map at 20 km). This result also agreed with the result obtained from the separation of regional magnetic field from residual magnetic field. Figure 4.16 could also be regarded as the regional map of the study area.

b. **Paleo-structures:** There are various magnetic lineaments in the study area. These lineaments were traced to paleo-structures (Figure 4.3) identified by Ajakaiye, Hall, Ashiekaa and Udensi (1991); Udensi, Osazuwa and Daniyan (2003) and Ojo (1990). These lineaments labelled AA', BB', CC' and or CD' were believed to be landward extension of the Oceanic fracture zones namely: Romanche, Chain and St Paul respectively (Figure 4.2). These features were detected with about six distinct discontinuities that passed through the survey areas at different latitudes (AA', BB', CC' and CD'). The detection of these features has lent support to the view held by Ajakaiye, Hall, Ashiekaa and Udensi (1991), that the mid-Atlantic fracture zones have extension on-shore. The lineament CC' and or CD' could be the separation between the Bornu Basin and the Upper Benue Trough, which was named as "Dumbulwa-Bage High" by Zaborski, Ugodulunwa, Idornigie, Nnabo and Ibe (1998). This feature was reported to be found at about latitude 11.00^0N.

5.1.2 Structural Analysis with CET Grid Plug-Ins

The results of the subsurface structural analysis using CET grid plug-ins corroborated the surface geology of the study area and the lineation (structural) map of the area. It also showed that the two basins (Bornu and Benue Trough) had similar structural relationship, although, there are more structural activities in Bornu Basin than as seen in Benue Trough. The result of this analysis also showed that the basement complex region of the geology and the volcanic areas (eastern part) had more pronounced structural activities compared with the structural features in the sedimentary regions.

5.1.3 Sedimentary Thickness and Hydrocarbon Potential

Presence of hydrocarbon and its potential is enhanced by the thickness of the sediments of the basin, and also by the kind of geological structures existing within the basement that form traps for oil and gas.

The maximum sedimentary thickness obtained with spectral analysis is 3.72 km. The maximum sedimentary thickness was found at the northern part around Damaturu and Bulkachuwa. The basement rocks were exposed around Foggo and Bauchi axes in the basement complex region. The sedimentary thickness is thin around Kaltungo and volcanic area at the eastern part of the survey area. The results obtained here is in agreement with the result obtained with upward continuation filter.

The result of the Source Parameter Imaging (SPI) has its maximum sedimentary thickness of about 5.0 km around Gombe, Ako Gombe, Bulkachuwa and Damaturu areas. The minimum sedimentary thickness could also be found around basement complex and volcanic areas of the study area. Thus the results here agreed with the results obtained from spectral depth determination (Figure 4.26) and upward continued filter.

The results of the 2D modelling showed that the sedimentary thicknesses range from 0.0 km to the maximum of 4.60 km. The maximum sedimentary thicknesses were found around Gombe, Ako Gombe, Bulkachuwa and Damaturu areas, with a value of about 3.72 km to 4.60 km. Thus this result agreed with the results of spectral depth, SPI and even the upward continued filter.

The maximum sedimentary thicknesses obtained, which range between 3.72 km to about 4.60 km (Figure 4.41) are adequate for the hosting of hydrocarbons.

5.1.4 **Delineation of the two Basins and Lithologic Units within the Study Area**

The boundary between the Bornu Basin and the Upper Benue Trough was successfully delineated through: trend analysis of the total magnetic intensity, upward continuation filter and 2D modelling of the subsurface structures. The end results of these methods show that the Upper Benue Trough was separated from the Bornu Basin at about latitude 11.0^0 N. This area corresponds to "Dumbulwa-Bage High" of Zaborski, Ugodulunwa, Idornigie, Nnabo and Ibe (1998). This is defined in the depth contour map and 3D surface map in Figures 4.41 and 4.42 respectively.

However, the subsurface lithology obtained from subsurface 2D modelling of the residual field showed the presence of two lithological units. The sedimentary rock unit (consists of shales, sandstones, limestones, siltstones, clay and non-marine facies) and the Basement rock units (composed of pegmatite, granite gneiss and migmatites).

5.2 Recommendations

Detailed seismic survey should be carried out around Gombe, Ako Gombe, Damaturu and Bulkachuwa, these areas were suggested as having the highest sedimentary thickness of over 3.72 km, as this would determine the presence of hydrocarbon.

Detailed ground magnetic and gravity survey should be carried out around latitude 11.0^0 N to about 11.2^0 N so as to confirm further the supposed separation between Bornu Basin and Benue Trough, a follow up to St. Paul paleo-structure which was reported in this work to have aided the separation of the two basins.

REFERENCES

Abaneme, O. A. (1983). *Electrical Resistivity and Ground Magnetic Studies in Ishiagu Area of Imo State*. Unpublished M. Sc. Thesis, University of Nigeria, Nsukka.

Akubue, G. N. (1986). Model Geoelectric Study within the Obi Coal Field. *NMGS Abstract* 22, 12 - 13.

Aneke, U. J. J. (1984). *Geophysical Investigation of the Inyi Coalfield, Anambra State*. Unpublished M.Sc. Thesis, University of Nigeria, Nsukka.

Adighije, C.I. (1979). Gravity field of Benue Trough, Nigeria. *Nature,* 282, 199-201.

Adighije, C.I. (1981). Gravity study of the Lower Benue Trough. *Geology Magazine*, 118, 59-67.

Ajakaiye, D.E. (1970). Gravity Measurements over the Nigerian Younger Granite Province. *Nature*, 255, 50-52.

Ajakaiye, D.E. (1981). Geophysical Investigations in the Benue Trough- a review. *Earth Evolution Science*, 2, 100-125.

Ajakaiye, D.E. and Verheijen, P.J.T. (1983). An analysis of a possible episodic plume trace in West Africa. *Geophysics Research Letters,* 10: 424 - 427.

Ajakaiye, D.E., Hall, D.H., & Millar, T.W. (1985). Interpretation of Aeromagnetic data across the central crystalline shield areas of Nigeria. *Geophysical Journal of the Royal Astronomical Society*, London 83, 503-517.

Ajakaiye, D.E., Hall, D.H., Millar, T.W., Verhejen, P.J.T., Award, M.B., & Ojo, S.B. (1986). Aeromagnetic anomalies and tectonic trends in and around the Benue Trough, Nigeria. *Nature*, 319(6054), 582-584.

Ajakaiye, D.E. Hall, D.H., Ashiekaa J.A., & Udensi E.E. (1991). Magnetic Anomalies in the Nigerian Continental mass based on aeromagnetic surveys. *Tectonophysics,* 192, 211-230.

Ajayi, C.O. (1979). A Detailed Gravity Survey of the Middle Benue. Unpublished Ph.D. Thesis, Ahmadu Bello University, Zaria, Nigeria.

Ajayi, C.O., & Ajakaiye, D.E. (1981). The Origin and peculiarities of the Nigeria Benue Trough: another look from Middle Benue. *Tectonophysics*, 80, 285-303.

Ajibade, A.C. (1976). Provisional classification and correlation of the schist belts in north-western Nigeria. In C.A., Kogbe (2^{nd} Eds.), *Geology of Nigeria* (pp, 80-90). Elizabethan Press, Ibadan.

Ajibade, A.C. (1980). *Geotectonic evolution of the Zungeru Region*. Unpublished Ph.D Thesis, University College of Wales.

Ajibade, A.C., Woakes, M., & Rahaman, M.A. (1989). *Proterozoic crustal development in the Pan- African regime of Nigeria*. In C.A., Kogbe (Eds.), *Geology of Nigeria* (pp. 57-69). Rock View (Nigeria) Ltd., Jos, Nigeria.

Allix, P. (1983). Environmental Mesozoiques de la Partic Nord-Orientale du Fosse de la Benoue (Nigeria). *Stratigraphic, Sedimentologic, Evolution Geodynamique, Travaux Laboratoire Sciences Terre St.-Jerome Marseille,* (B) 21, iv + 200 pp.

Artsybashev, V.A., & Kogbe, C.A. (1974). Crustal structure of the Benue valley area. *Geologische Rundschau*, 64, 324-329.

Avbovbo, A.A., Ayoola, E.O., & Osahon, G.A. (1986). Depositional and structural styles in Chad Basin of northeastern Nigeria. *Bulletin American Association Petroleum Geologists*, 70, 1787-1798.

Barber, W. (1965). Pressure water in the Chad Formation of Bornu and Dikwa Emirates, northeastern Nigeria. *Bulletin Geological Survey of Nigeria,* 35, 1-138.

Bellion, Y.C. (1989). Histoire Geodynamique Post-Paleozoique de l'Afrique de l'ouest d'apres l'etude de quelques Bassins Sedimentaires (Senegal, Taoudenni, Iullemmeden, Tehad). *Publication Occasionnelle Centre International Formation Echanges Geologiques*, 17, 1 - 302.

Benkhelil, J. (1985). *Geological Map of Part of the Upper Benue Valley (Scale 1:100,000) (with explanatory note)*. Elf Nigeria Ltd., Lagos, Nigeria.

Benkhelil, J. (1986). *Structure et Evolution Geodynamique du Bassin Intracontinental de la Benoue (Nigeria)*. Unpublished Thesis Doctorat, Universite de Nice, France.

Benkhelil, J. (1988). *Structure et Evolution Geodynamique du Bassin Intracontinental de la Benoue* (Nigeria). *Bulletin Centres Recherches Exploration- Production Elf-Aquitaine*, 12, 29-128.

Benkhelil, J. (1989). The origin and evolution of the Cretaceous Benue Trough (Nigeria). *Journal of African Earth Sciences*, 8, 251-282.

Bird, D**.** (May, 1997). *Interpreting magnetic data: Geophysical corner*. EXPLORER, AAPG and SEG.

Black, R., Caby, R., Moussine-Pauchkie, A., Bayer, R., Bartrand J.M., Bovillier, A.M., Fabre, J., & Lesquer, A. (1979). Evidence for Late Precambrian plate tectonics in West Africa. *Nature*, 278, 223-227.

Bhattacharyya, B.K. (1966). A method for computing the total magnetization vector and the dimensions of a rectangular block – shaped body from magnetic anomalies. *Geophysics*, 31, 74 – 96.

Bott, M.H.P. (1963). Two methods applicable to computers for evaluating magnetic anomalies due to finite three dimensional bodies. *Geophysical Prospecting*, 11, 292-299.

Bowden, P., and Turner, D.C. (1974) Peralkaline and associated ring complexes in the Nigeria- Niger province, West Africa. In H. Sorensen, Ed. *The alkaline rocks*, 330-351. John Wiley, London.

Braide, S.P. (1992a). Studies on sedimentation and tectonics of the Yola Arm of the Benue Trough facies architecture and their tectonic significance. *Journal of Mining and Geology,* 28, 23-32.

Buchanan, M.S., Macleod, W.N., Turner, D.C., Berridge, H.G., and Black, R., (1971): The Geology of the Jos Plateau. *Bulletin Geological Survey of Nigeria* 32(2) 107p.

Cady, J.W. (1980). Calculation of gravity and magnetic anomalies of finite-length right polygonal prisms. *Geophysics*, 45, 1507-1512.

Carter, J.D., Barber, W., Tait, E.A., & Jones, G.P. (1963). The Geology of parts of Adamawa, Bauchi and Bornu Provinces in north-eastern Nigeria. *Bulletin Geological Survey of Nigeria*, 30, 1-99.

Clark, D.A., Saul, S.J., & Emerson, D.W. (1986). Magnetic and gravity anomalies of a triaxial ellipsoid. *Exploration Geophysics*, 17, 189-200.

Coggon, J.H. (1976). The magnetic and gravity anomalies of polyhedral. *Geoexploration*, 14, 93-105.

Cratchley C.R., & Jones, G.P. (1965). An interpretation of the geology and gravity anomalies of the Benue valley, Nigeria. *Overseas Geological Surveys Geophysical*, paper 1, 1-26.

Cratchley C.R., Louis, P., & Ajakaiye, D.E. (1984). Geophysical and geological evidence for the Benue-Chad Basin Cretaceous rift valley system and its tectonic implications. *Journal of African Earth Sciences*, 2, 141-150.

Dessauvagie, T.F.J. (1974). *Geological Map of Nigeria (scale 1:100,000)*. Nigeria Mining, Geological and Metallurgical Society, Ibadan, Nigeria.

Dessauvagie, T.F.J. (1975). Explanatory note to the geological map of Nigeria. *Journal Mining and Geology,* 9, 3-28.

Dobrin, M.B. (1976). *Introduction to geophysical prospecting* (3^{rd} Edition). McGraw Hill.

Eborall, A.C. (1976). Intermediate rocks from Older Granite Complexes of the Bauchi area, northern Nigeria. In C.A., Kogbe (Eds.). *Geology of Nigeria* (pp 65-74). Elizabeth Publication Company, Ibadan,

Eze, I. C. (1985). *Electromagnetic and magnetic survey of lead - zinc mineralization in the Wanakon area*. M. Sc. thesis, University of Nigeria, Nsukka.

Fairhead, J.D. (1986). Geophysical controls on sedimentation within the African Rift systems. *Spectral Publication Geological Society, London*, 25, 19-27.

Fairhead, J.D. (1988a). Mesozoic plate tectonics reconstructions of the central south Atlantic Ocean: the role of the West and Central African rift System. *Tectonophysics*, 155, 181-192.

Fairhead, J.D. (1988b). Late mesozoic rifting in Africa. In W. Manspeizer, (Eds.), *Triassic-Jurassic Rifting, Continental Break-up and the Origin of the Atlantic Ocean and passive Margins, part B* (pp 821-831). Elsevier, Amsterdam, Netherlands.

Fairhead, J.D., *&* Okereke C.S. (November, 1987). *A regional gravity study of the West African rift system in Nigeria and Cameroon and its tectonic interpretation*. Tectonophysics, 143, Issues 1-3, pages 141-159. Retrieved from: http//hinari-gw.who.int/whalecomwww.sciencedirect.com/whalecom0/science?

Fairhead, J.D. & Green, C.M. (1989). Controls on Rifting in Africa and the regional tectonic model for the Nigeria and East Niger rift basins. Journal of African Earth Sciences, 8, Issues 2-4, 1989, Pages 231-249 available online 24 January, 2006. http//hinari- gw.who.int/whalecomwww.sciencedirect.com/whalecom0/science?

Fairhead, J.D., & Okereke C.S. (1988). Depths to major density contrasts beneath the West African rift system in Nigeria and Cameroon based on the spectral analysis of gravity data. Journal of African Earth Sciences, Volume 7, Issues 5-6, 1988, Pages 769-777. Retrieved from: http//hinari-gw.who.int/whalecomwww.sciencedirect.com/whalecom0/science?

Fairhead, J.D., & Okereke C.S. (1990). Crustal thinning and extension beneath the Benue Trough based on Gravity studies. *Journal African Earth Sciences*, 11, 329-335.

Falconer, J.D. (1911). The *geology and Geography of Northern Nigeria.* MacMillan, London, UK.

Ford, S.O. (1981). The economic mineral resources of the Benue Trough. *Earth Evolution Sciences*, 1(2), 154-163.

Genik, G.J. (1992). Regional framework, structural and petroleum aspects of Rift Basins in Niger, Chad and the Central African Republic (C.A.R.). *Tectonophysics*, 213, 169-185.

Genik, G.J. (1993). Petroleum geology of the Cretaceous-Tertiary Rift Basins in Niger, Chad and the Central African Republic. *Bulletin American Association Petroleum Geologists*, 77, 1405-1434.

Geological Survey of Nigeria, (1956). Nigeria and the Cameroons. In R., Furon (4(3)), *Lexique Stratigraphique International* (pp 35-62). Centre National de la Recherche Scientifique, Paris, France.

Geological Survey of Nigeria, (1974). *Geological map of Nigeria. (Scale 1:2,000,000*). Geological Survey of Nigeria, Kaduna, Nigeria.

Grant, N. K. (1970). The South Atlantic Benue Trough and Gulf of Guinea Cretaceous Triple Junction. *Geological Society, American Bulletin*, 82, 2295 - 2298.

Grant, N.K. (1978). Structural distinction between a sedimentary cover and an underlying basement in the 600Myrs old Pan-African domain of northern Nigeria. *Geological Society, American Bulletin,* 89, 50-58.

Grant, F.S., & West G.F. (1965). *Interpretation theory in applied geophysics*. McGraw Hill.

Guiraud, M. (1989). *Geological map of part of the Upper Benue Valley (scale 1.150,000) (with explanatory note)*. Elf Nigeria Ltd., Lagos, Nigeria.

Guiraud, M. (1990a). *Mecanisme deformation du bassin sur Dechrochements multipless de la Haute-Benoue (Nigeria) . facies et geometrie des corps sedimentaires, microtectonique et deformations synsedimataires*. Memoir d'Habilitation, Universite de Montpellier, France.

Guiraud, M. (1991a). Mecanisme de fermation du bassin cretace sur decrochements multiples de la Haute-Benoue (Nigeria). *Bulletin Centres Recherches Exploration-Production Elf-Aquitaine* 15, 11-67.

Guiraud, M. (1993). Late Jurassic Rifting-Early Cretaceous Rifting and Late Cretaceous Transpressional inversion in the Upper Benue Basin (NE Nigeria). *Bulletin Centres Recherches Exploration-Production Elf-Aquitaine* 17, 371-383.

Guiraud, M. Binks, R.M., Fairhead, J.D., & Wilson, M. (1992). Chronology and Geodynamic setting of Cretaceous-Cenozoic Rifting in West and Central Africa. *Tectonophysics,* 213, 227-234.

Hartley, R.W., & Allen, P.A. (1994). Interior Cratonic Basins of Africa: Relation to Continental break-up and role of mantle convection. *Basin Research*, 6, 95-113.

Hjelt, S.E. (1972). Magnetostatic anomalies of a dipping prism. *Geoexploration*, 10, 239-254.

Holden, E., Dentith M., & Kovesi, P. (2008). Towards the automatic analysis of regional aeromagnetic data to identify regions prospective for gold deposits", *Computers & Geosciences*, 34(11), 1505–1513.

Holden, E., Kovesi, P., Dentith, M., Wedge, D., Wong J. C., & Fu, S. C. (2010). Detection of regions of structural complexity within aeromagnetic data using image analysis. *25th International Conference of Image and Vision Computing, New Zealand*.

Hsu, N. C., Herman, J. R., Bhartia, P. K., Seftor, C. J., Torres, O., Thompson, A. M., Gleason, J. F., Eck, T. F. and Holben, B. N. (1996). Detection of biomass burning smoke from TOMS measurements, *Geophysics Research Letters*, 23, 745– 748.

Huntings Geology and Geophysical Ltd (1976). *Airborne magnetometer survey contour of total intensity Map of Nigeria*. Airborne Geophysical Series.

Jessel, M.W., Valenta, R.K., Jung, G.,Cull, J.P., & Geiro, A. (1993). Structural geophysics. *Exploration Geophysics*, 24, 599-602.

Johnson, W.W. (1969). A Least-Squares method of interpreting magnetic anomalies caused by two-dimensional structures. *Geophysics*, 34, 65 – 74.

Jones, B. (1932). *The geology of southern Bornu*. Annual Report Geological Survey Nigeria 9-14.

Kearey, P, Brooks, M., & Hill, I. (2004). *An introduction to geophysical exploration*. 3rd edition, Blackwell Publications.

Keller, G.R., Wendlandt, R.F., & Bott, M.H.P. (1995). West and Central African Rift System. In. K.H., Olsen, *Continental Rifts. Evolution, Structure, Tectonics*, (pp 437-449). Elsevier, Amsterdam, Netherland.

Kovesi, P. (1991). Image features from phase congruency: *Videre: Journal of Computer Vision Research*, 1(3), *the MIT press*.

Kovesi, P. (1997). Symmetry and asymmetry from local phase, AI'97. *10th Australian Joint Conference on Artificial Intelligence*.

Lam, L., Lee, S.W., & Suen, C.Y. (1992). Thinning methodologies: a comprehensive survey, *IEEE transactions on pattern analysis and machine intelligence*, 14(9), 879.

Lee, T.J. (1980). Rapid computation of magnetic anomalies with demagnetization included, for arbitrary shaped bodies. *Geophysical Journal of the Royal Astronomical Society*, London, 60, 67-75.

Likkasson, O.K., Ajayi, C.O. and Shemang, E.M. (2005). Some structural features of the Middle Benue Trough, Nigeria, modelled from aeromagnetic anomaly data. *Science Forum, Journal of Pure and Applied Science*, 8, 100-125.

Madu, A. J. C., & Onuoha, K. M. (1984). Aeromagnetic anomalies, gravity, and ground magnetic studies in parts of north western Benue State, Nigeria. *Nigeria Journal of Mining Geology*, 21, 133 - 134.

Mareschal, J., (1983). Mechanisms of uplift preceeding rifting. *Tectonophysics*, 94, 51 - 66.

Matheis, G. (1976). Short review of the geology of the Chad Basin in Nigeria. In C.A., Kogbe, *Geology of Nigeria*, (pp 289-294). Elizabethan Publication Company, Lagos, Nigeria.

Maurin, J.C., & Guiraud, M. (1989). Relations entre tectonique et sedimentation dans les bassins barremo-aptiens du Nord Cameroun. *Comptes Rendus Academic Sciences Paris* 11 (308), 787-792.

Maurin, J.C., & Guiraud, M. (1990). Relationships between tectonics and sedimentation in the Barremo-Aptian intracontinental Basins of northern Cameroon. *Journal of African Earth Science*, 10, 331-340.

McCurry, P. (1976). The geology of the Precambrian to Lower Paleozoic rocks of northern Nigeria- a review. In C.A., Kogbe, *Geology of Nigeria*, (pp 15-39). Elizabethan Publication Company, Lagos, Nigeria.

Miller, R.E., Johnston, R.H., Oluwa, J.A.I., & Uzoma, J.U. (1968). *Groundwater hydrology of the Chad Basin in Bornu and Dikra emirates, northern Nigeria with special emphasis on the flow life of the artesian system.* Water supply United States Geological Survey, USA ,1957-1. 1-148.

Murthy K.S.R. & Mishra D.C. (1980). Fourier transform of the general expression for the magnetic anomaly due to a long horizontal cylinder. *Geophysics* 45, 1091 - 1093.

Nabighian, M.N. (1972). The analytic signal of two dimensional magnetic bodies with polygonal cross-section. its properties and use for automated anomaly interpretation. *Geophysics*, 37, 507-517.

Nabighian, M.N. (1974). Additional comments on the analytic signal of two dimensional magnetic bodies with polygonal cross-section. *Geophysics*, 39, 85-92.

Nigeria Geological Survey Agency (2009). Shuttle Radar Topography Mission (SRTM) data, *United States Geological Survey*.

Nigeria Geological Survey Agency (2006). Geological map of Nigeria, Mineral resources map of Nigeria and Lineament map of Nigeria.

Njoku, C. O. (1985). *Geophysical investigation of the Ndi Akparata area of the Abakaliki anticlinorium, Anambra States Nigeria*. Unpublished M. Sc. Thesis, University of Nigeria Nsukka.

Nur, A. (2000). Analysis of aeromagnetic data over the Yola arm of the Upper Benue Trough, Nigeria. *Journal of Mining and Geology*, 36, 77 – 84.

Nur, A. (2001). Spectral analysis and Hilbert transform of gravity data over the southwest of the Chad Basin, Nigeria. *Journal of Mining and Geology*, 37, 155 - 161.

Nur, A. (2003). A preliminary magnetic study over the Mandera – Lugh Basin, southwest, Somalia. *Journal of Mining and Geology*, 39, 117 – 120.

Nur, A., Onuoha, K.M., & Ofoegbu, C.O. (1994). Spectral analysis of aeromagnetic data over the Middle Benue Trough. *Journal of Mining and Geology*, 30, 211 – 217.

Nur, A., Ofoegbu, C.O., & Onuoha, K.M. (2003). Spectral analysis and Hilbert transform of aeromagnetic data over the Upper Benue Trough, Nigeria. *Global Journal of Geological Sciences*, 1(2), 129 – 142.

Nwodo, N. E. (1985). Electrical resistivity investigation for groundwater in the Nsukka area, Anambra State. Unpublished M. Sc. Thesis, University of Nigeria, Nsukka.

Nwogbo, P.O. (1997). Mapping the shallow magnetic sources in the Upper Benue Basin in Nigeria from aeromagnetic. *Spectra*, 4(3/4), 325-333.

Obaje, N.G. (2009). *Geology and mineral resources of Nigeria*. Springer Publishers, Germany, 1-203.

Obi, G.C. (1995). Stratigraphic succession and age of Cretaceous sedimentary rocks in the Hawal Basin, NE Nigeria. *Journal Mining and Geology*, 30, 195-203.

Obi, G.C. (1998). Upper Cretaceous Gongila Formation in the Hawal Basin, northeast Benue Trough. A storm and wave dominated regressive shoreline complex. *Journal of African Earth Sciences*, 26, 619-632.

Ofoegbu, C. O. (1984a). Interpretation of magnetic anomaly over the Lower and Middle Benue Trough of Nigeria. *Geophysical Journal of the Royal Astronomical Society*, 79, 813-823.

Ofoegbu, C. O. (1984b). An aeromagnetic study of the Lower Benue Trough, Nigeria. *Revista Brasiliera Geosciencias*, 14, 54-59.

Ofoegbu, C. O. (1984). Aeromagnetic anomalies over the Lower and Middle Benue Trough, Nigeria. *Journal of Mining and Geology*, 21, 103 - 108.

Ofoegbu, C. O., (1985). A review of geology of the Benue Trough, Nigeria. *Journal of African Earth Sciences*, 3(3), 281 - 291.

Ofoegbu, C. O. (1988). An aeromagnetic study of part of the Middle Benue Trough, Nigeria. *Journal of African earth Sciences*, 7, 77-90.

Ofoegbu, C. O., & Onuoha, K.M. (1990). A review of geophysical investigations in the Benue Trough. . In C.O., Ofoegbu, *The Benue Trough, Structure and Evolution*, (pp 203-216). Vieweg and Sohn, Braunschweig, Germany.

Ojo, O.M., & Pinna, P. (1982). Paleogeographical and structural evolution of the Benue Trough of Nigeria. *Cretaceous Research*, 3, 195-207.

Ojo, S.B., & Ajakaiye, D.E. (1976). Preliminary interpretation of gravity measurements in the Middle Niger Basin, Area, Nigeria. In C.O., Kogbe (2^{nd} Eds.), *Geology of Nigeria*, (pp 245-307). Elizabethan Publication Company, Lagos, Nigeria Lagos.

Ojo, S.B., & Kangkolo, D.E. (1997). Shortcomings in the determination of regional fields by polynomial fitting: A simple solution. *Journal Applied Geophysics*, 36: 205 – 212.

Okosun, E.A. (1992). Cretaceous ostracod biostratigraphy from Chad Basin in Nigeria. *Journal of African Earth Sciences*, 14, 327-339.

Okosun, E.A. (1995a). Review of the Geology of Bornu Basin. *Journal of Mining and Geology*. 31, 113-122.

Okoye, P. N. (1988). Electromagnetic terrain conductivity determination in Wanakom area of Cross River State. Unpublished M. Sc. Thesis, University of Nigeria, Nsukka.

Olugbemiro, O.R. (1997). Hydrocarbon potential, maturation and Paleoenvironments of the Cretaceous (Cenomanian-Santonian) series in the Bornu (Chad) Basin, NE Nigeria. *Tubinger Mikropaleontologische Mitteilungen*, 14, viii+150 pp.

Onuoha, K. M., & Aka, E. U. (1983). Resistivity prospecting for groundwater in the vicinity of Enugu, Anambra State, Nigeria. *Journal of Mining and Geology*, 20, 121-132.

Orajaka, S. & Nwachukwu, S. O. (1968). Combined electromagnetic and geochemical studies in the Ameri Lead - Zinc Ore. *Journal of Mining and Geology* 3, 49 - 51

Onwuemesi, A. G. (1995). One-dimensional spectral analysis of aeromagnetic anomalies and Curie depth isotherm in the Anambra Basin of Nigeria. *Journal of Geodynamics*, 23, 211-232.

Osazuwa, I.B., Ajakaiye, D.E., & Verheijen, P.J.T. (1981). Analysis of the structure of part of the Upper Benue rift valley on the basis of new geophysical data. *Earth Evolution Sciences*, 2, 126-135.

Oyawoye, M.A. (1964). The geology of Nigerian basement complex. *Journal of Nigeria Mining Geology and Metallurgical Society,* 1, 87-102.

Popoff, M. (1988). Du Gondwana a l'Alantique sud . Connexions du fosse de la Benoue avec les bassins du nord-est Bressilien Jusqu'à l'ouverture du golfe de Guinee au Cretace Inferieur. *Journal of African Earth Sciences*, 409-431.

Raeburn, C., & Jones, B. (1934). The Chad Basin. Geology and Water Supply. *Bulletin Geological Survey of Nigeria* 15. 1-61.

Reeves, C. (2005). *Aeromagnetic surveys: principles, practice and interpretation, training programme*, Nigeria Geological Survey Agency.

Reford M.S. (1964). Magnetic anomalies over thin sheets. *Geophysics* 29, 532 – 536.

Reford, M.S. & Sumner, J.S. (1964). Aeromagnetics. *Geophysics* 29, 482 - 516.

Reid, A.B. Allsop, J.M., Granser, H., Millet A.J., & Somerton, I.W. (1990). Magnetic interpretation in three dimension using euler deconvolution. *Geophysics*, 55, 80 – 91.

Reyment, R.A. (1965). *Aspects of the geology of Nigeria*. Ibadan University Press, Ibadan, Nigeria.

Reyment, R.A., & Tait, E.A. (1983). Resume on the geology of Nigeria. *In J. Fabre, Afrique de l'ouest Introduction Geologique et termes Stratigraphiques. Lexique Stratigraphique International, Nouvelle Serie 1,* (pp 127-135). Pergamon, Oxford, UK.

Russ, W. (1957). The geology of parts of Niger, Zaria and Sokoto provinces, with special reference to the occurrence of gold. *Bulletin Geological Survey of Nigeria*, 27, 1-42.

Sahagian, D.L. (1993). Structural evolution of African Basins: stratigraphic synthesis. *Basin Research* 5, 41-54.

Schneider, J.L., Wolff, J.P. (1992). Carte géologique et cartes hydrogéologiques à 1/500.000 de la République du Tchad. Mémoire explicatif. Document du BRGM 209, 2 volumes.

Sharma, P.V. (1987). Magnetic method applied to mineral exploration. *Ore Geology Reviews*, 2, 323 – 357.

Shemang, E.M, Jacoby, W.R., and Ajayi, C.O. (2005). Interpretation of gravity data over Gongola Arm of the Upper Benue Trough. *Global Journal of Geological Science* 3(1): 61-69

Shuey, R.T., & Pasquale, A.S. (1973). End corrections in magnetic interpretation. *Geophysics*, 38, 507-512.

Skeels, D.C. (1967). What is Residual Gravity? *Geophysics*, 32, 872 -876.

Spector, A. **(**1968). *Spectral analysis of aeromagnetic data.* Ph.D. Thesis, University of Toronto, Canada.

Spector, A. & Grant, F.S. (1970). Statistical models for interpreting Aeromagnetic data. *Geophysics, 35(2), 293-302*

Smith, R.S., Thurston, J.B., Dai Ting-Fan & Ian N.M. (1998). iSPI^{TM}- the improved source parameter imaging method. *Geophysical prospecting*, 46, 141-151.

Stuart, G.W., Fairhead, J.D., Dorbath, L., & Dorbath, C. (1985). A seismic refraction study of the crustal structure associated with the Adamawa Plateau and Garoua Rift, Cameroun, West Africa. *Geophysical Journal of the Royal Astronomical Society London*, 81, 1-12.

Talwani M. (1965). Computation with the help of Digital Computer, of Magnetic Anomalies caused by bodies of Arbitrary Shape, Geophysics, volume 30, pp 797 – 817.

Talwani, M., & Heirtzler, J.R. (1964). Computation of magnetic anomalies cuased by two dimensional bodies of arbitrary shapes. In G.A., Parks. (Eds.), *Computers in the Mineral Industries, Part I,* (9, 464 - 480). Stanford University Publishers, Geological Sciences.

Telford, N.W., Geldart, L.P., Sheriff, R.S., & Keys, D.A. (2001). *Applied geophysics*, Cambridge University Press.

Thurston, J.B., & Smith, R.S. (1997). Automatic conversion of magnetic data to depth, dip, and susceptibility contrast using the SPI^{TM} method. *Geophysics*, 62, 807-813.

Truswell,F.B. and Cope, R.N. (1963). The geology of parts of Nigeria and Zaria provinces, northwestern Nigeria. *Bulletin Geological of Survey of Nigeria.* 29, 1-72

Udensi, E.E., Osazuwa, I.B., & Daniyan, M.A. (2003). Production of a composite aeromagnetic map of the Nupe Basin. *Nigeria. Journal of Science Technology and Mathematics Educ*ation, 3(2) pp 150 – 159.

Udensi, E.E., & Osazuwa, I.B. (2002). Two and half dimensional modelling of the major structures underlying the Nupe Basin, Nigeria using aeromagnetic data. *Nigerian Journal of Physics* (NJP), 14(1), 55 – 61.

Udensi, E.E., Osazuwa, I.B. (2003). Spectral determination of the depths to the buried magnetic rocks under the Nupe Basin. *Nigerian Journal of Physics* (NJP), 15(1) 51 – 59.

Udensi E.E. (2000). *Interpretation of total magnetic field over the Nupe Basin in west central Nigeria using aeromagnetic data*. Unpublished Ph.D thesis A.B.U. Zaria Nigeria.

Valenta, R.K., Jessell, M.W., Jung, G., & Bartlett, J. (1992). Geophysical interpretation and modelling of three dimensional data in the Duchess area, Mount Isa, Australia. *Exploration Geophysics*, 23, 393-400.

Whiteman, A.J. (1982). *Nigeria: Its petroleum geology, resources and potential*. Graham and Trotman, London, UK.

Wright, J.B. (1976). Origin of the Benue Trough- A Critical Review, In. C.A., Kogbe, *Geology of Nigeria*, (pp 309-317). Elizabethan Publication Company, Lagos, Nigeria.

Zaborski, P. M. P. 1996. A compilation and short review of the literature on the Cretaceous of Nigeria. *Africa Geoscience Review, Paris,* 3: 491-523.

Zaborski, P.M., Ugodulunwa, F., Idornigie, A., Nnabo, P., & Ibe, K. (1998). Stratigraphy and structure of the Cretaceous Gongola basin, northeast Nigeria. *Bulletin Centres Recherches Exploration-Production Elf-Aquitaine,* 21(for 1997), 153-185.

Zaborski, P.M. (1998). A Review of the Cretaceous System in Nigeria. *African Geoscience Review*, 5(4), 385-483.

APPENDIX **Plots of Energy Spectrums against Frequency**

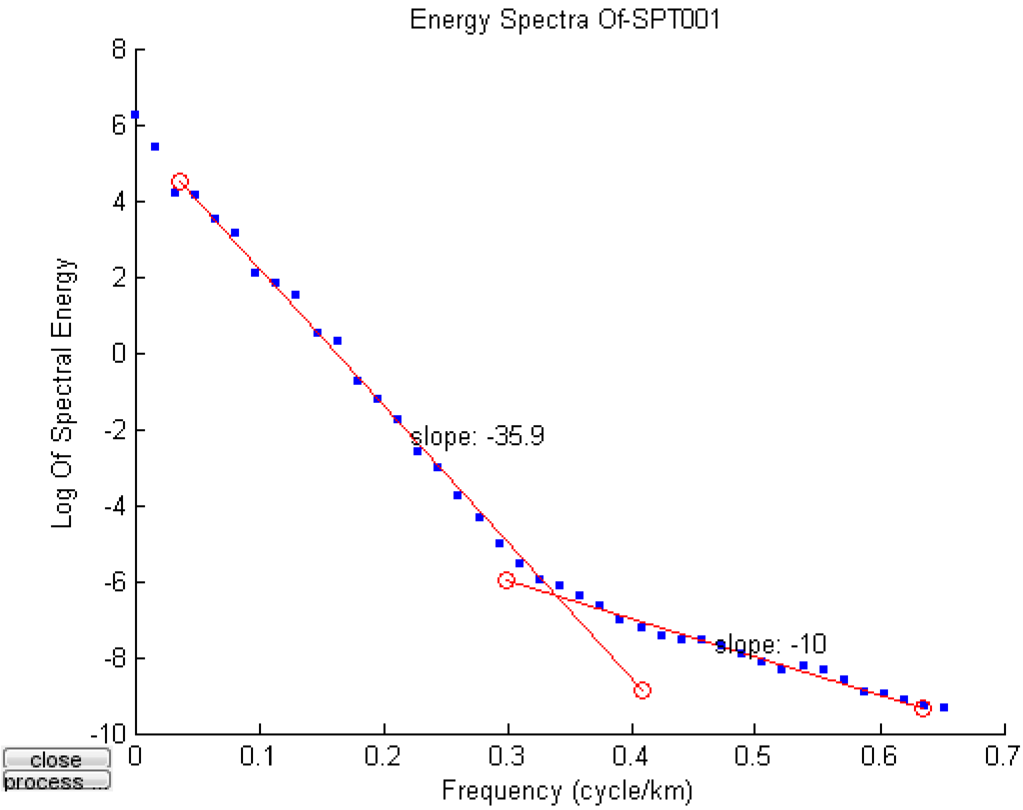

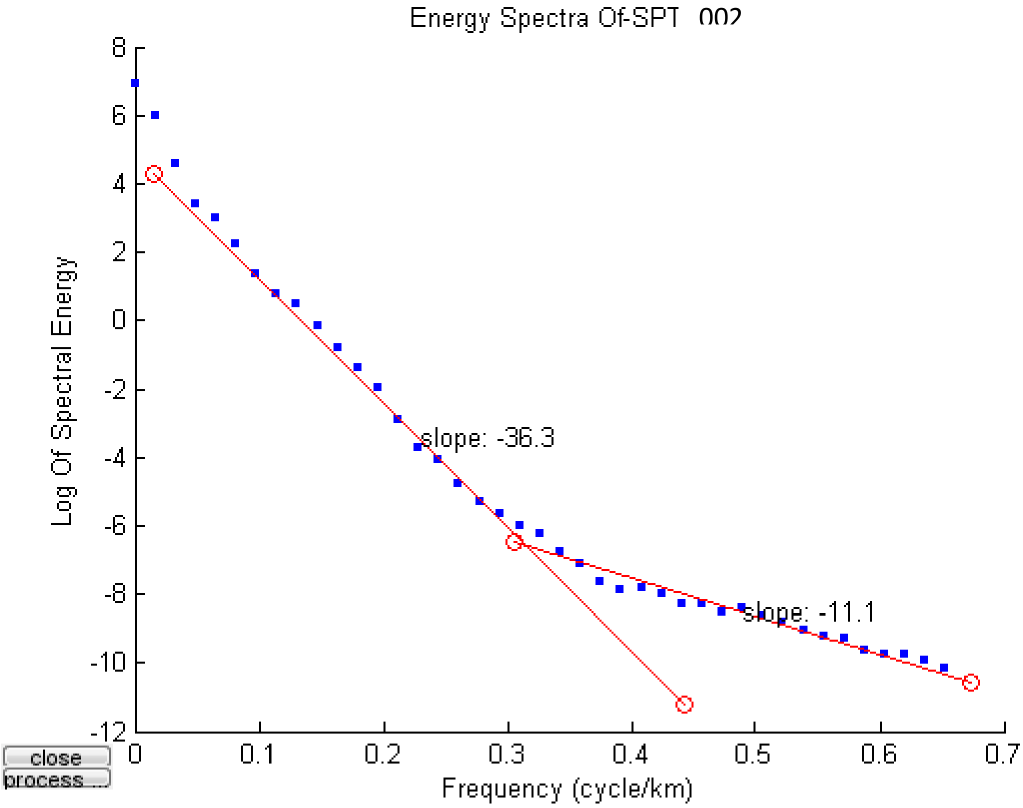

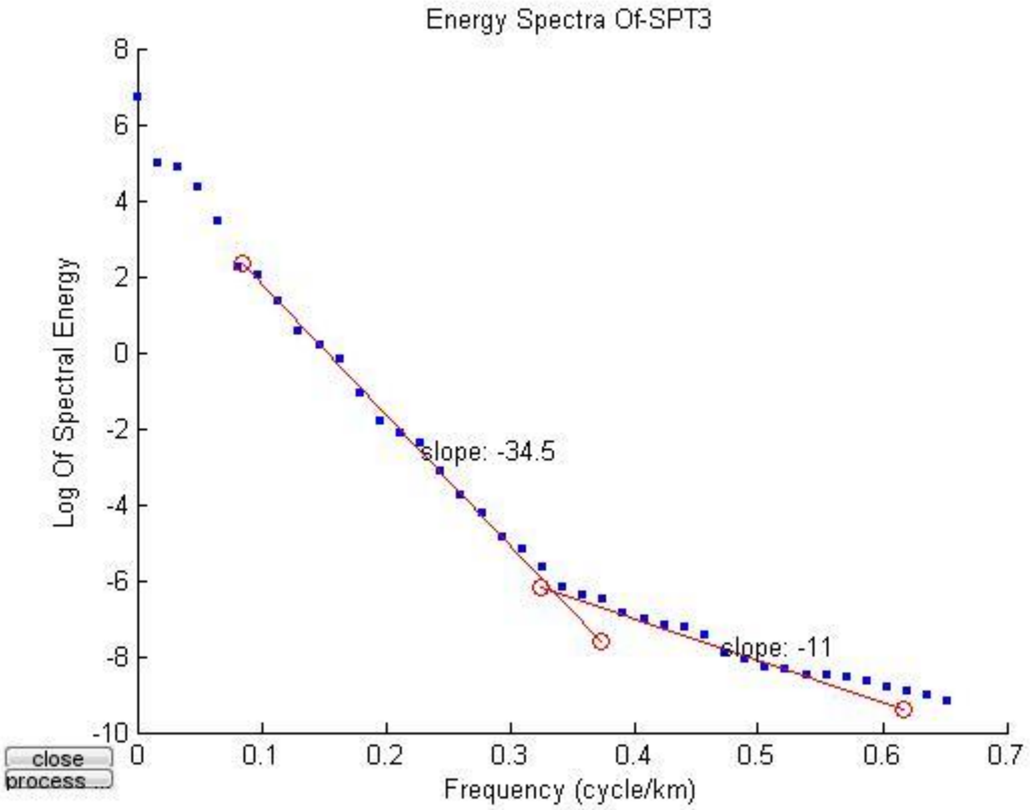
Energy Spectra Of-SPT3
Log Of Spectral Energy
slope: -34.5
slope: -11
close
process ...
Frequency (cycle/km)

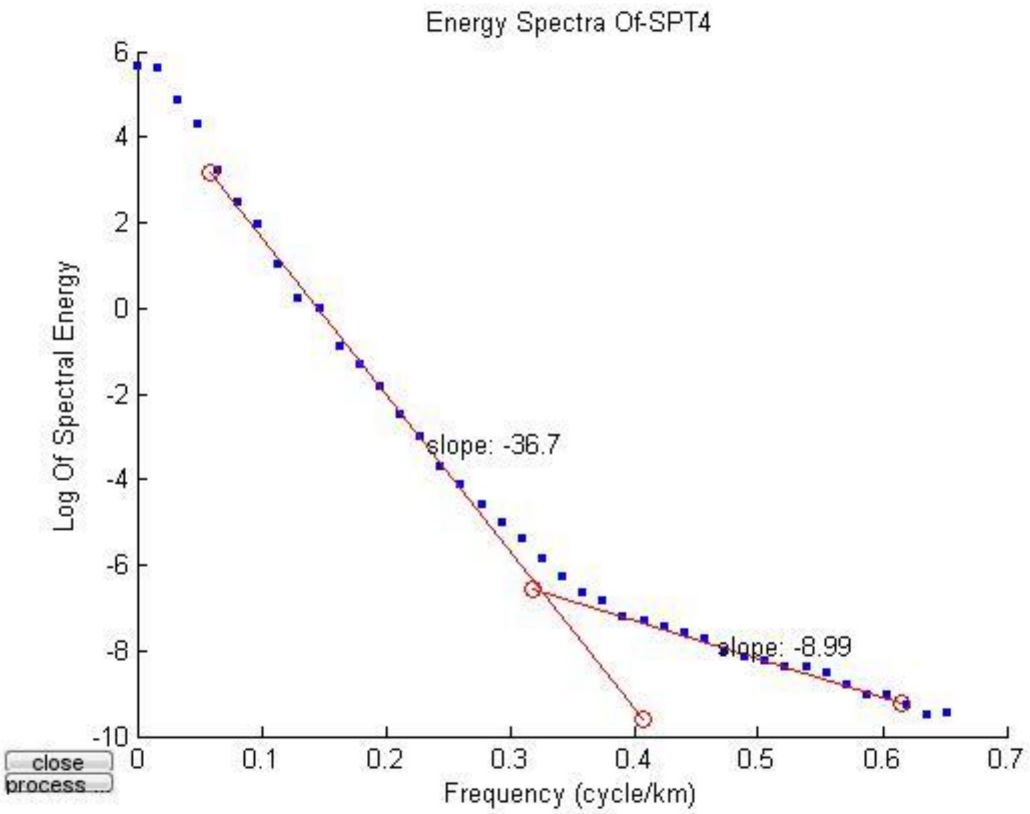
Energy Spectra Of-SPT4
Log Of Spectral Energy
slope: -36.7
slope: -8.99
close
process ...
Frequency (cycle/km)

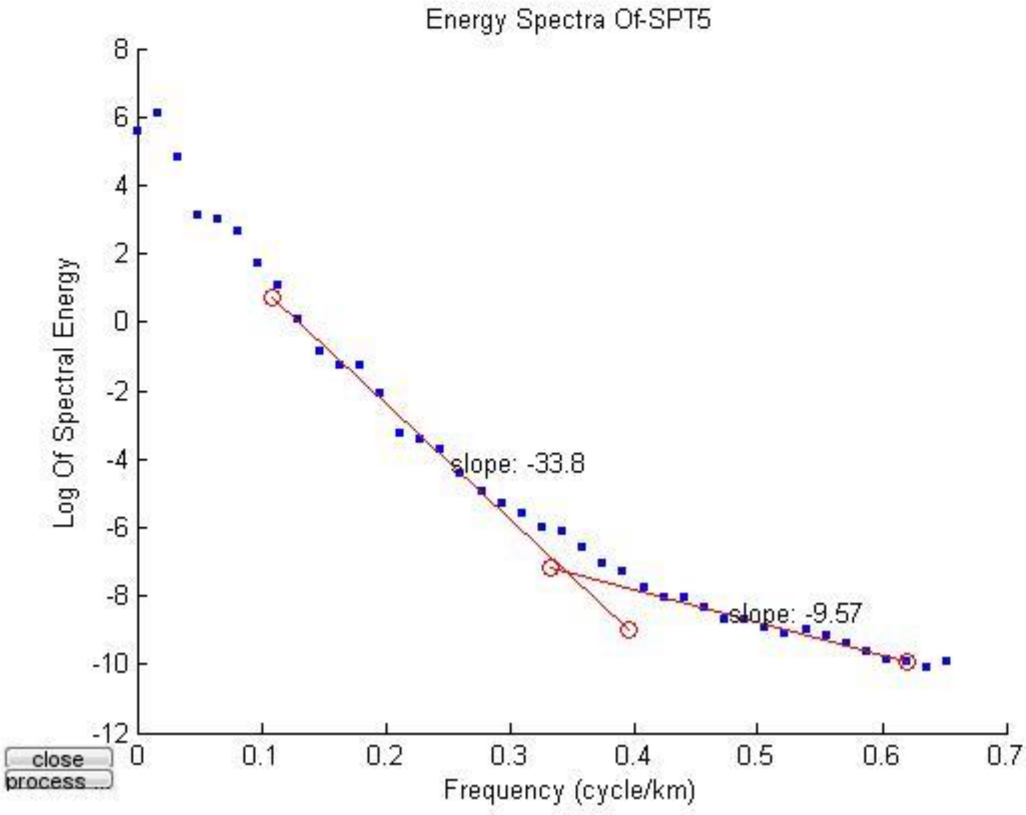
Energy Spectra Of-SPT5
Log Of Spectral Energy
Frequency (cycle/km)
slope: -33.8
slope: -9.57
close
process ...

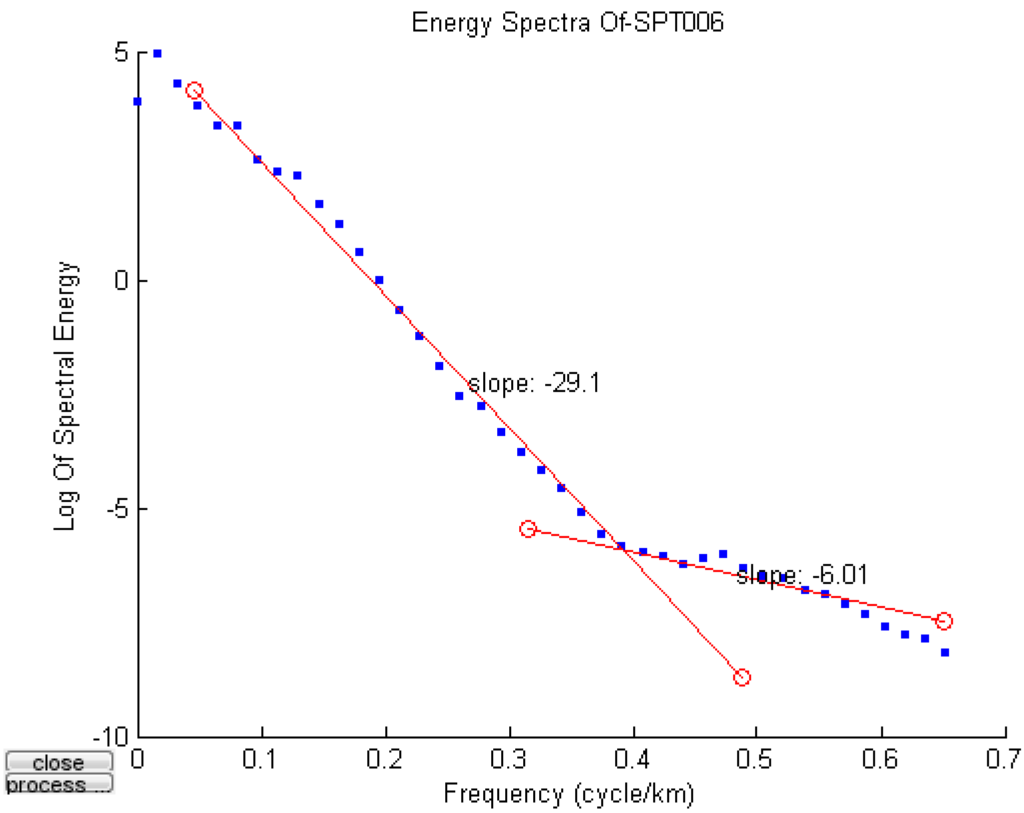
Energy Spectra Of-SPT006
Log Of Spectral Energy
Frequency (cycle/km)
slope: -29.1
slope: -6.01
close
process ...

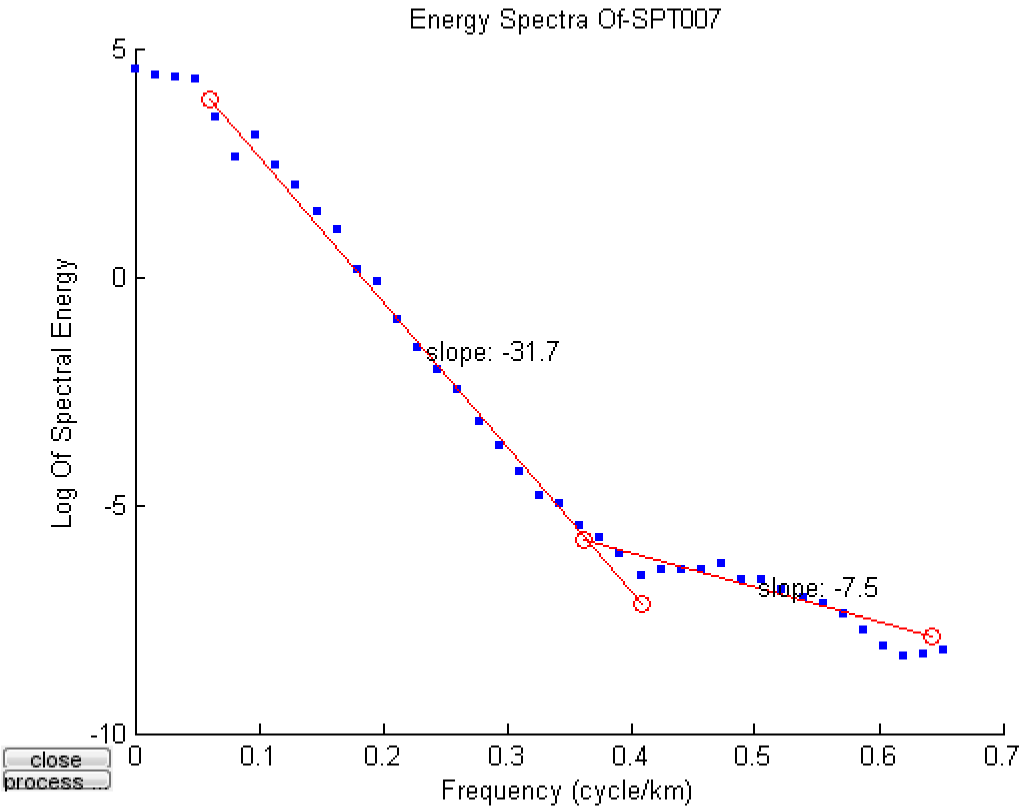
Energy Spectra Of-SPT007
Log Of Spectral Energy
Frequency (cycle/km)
slope: -31.7
slope: -7.5
5
0
-5
-10
0
0.1
0.2
0.3
0.4
0.5
0.6
0.7
close
process ...

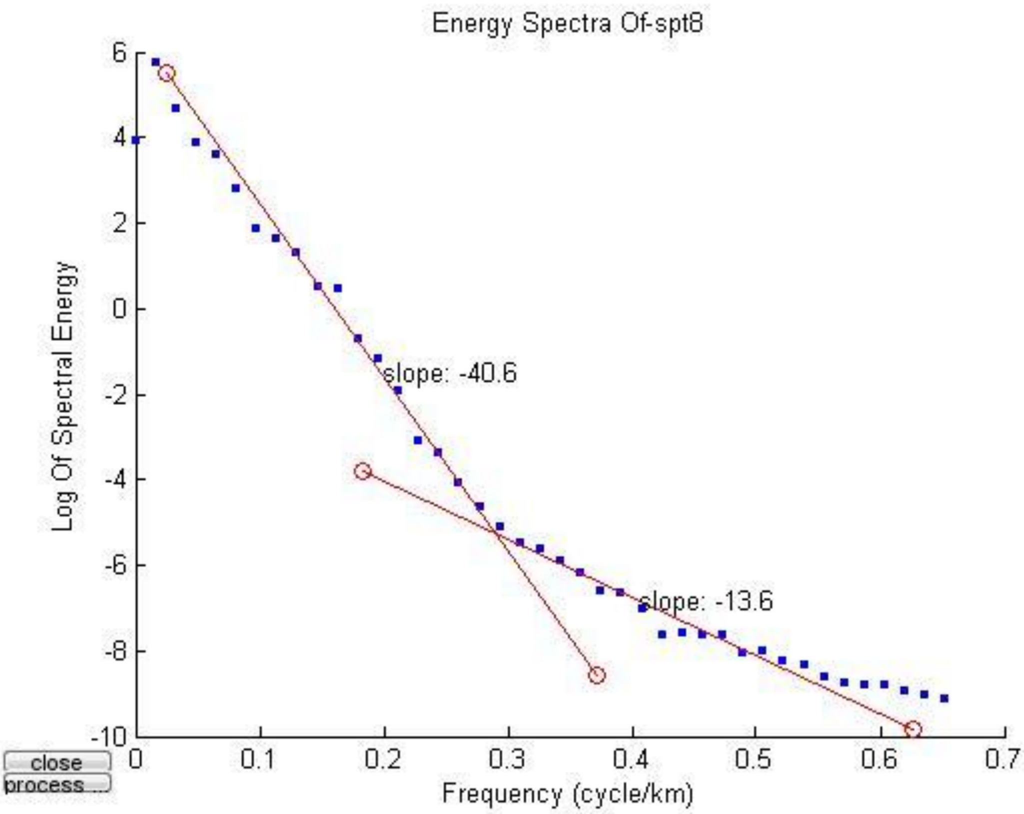
Energy Spectra Of-spt8
Log Of Spectral Energy
Frequency (cycle/km)
slope: -40.6
slope: -13.6
6
4
2
0
-2
-4
-6
-8
-10
0
0.1
0.2
0.3
0.4
0.5
0.6
0.7
close
process ...

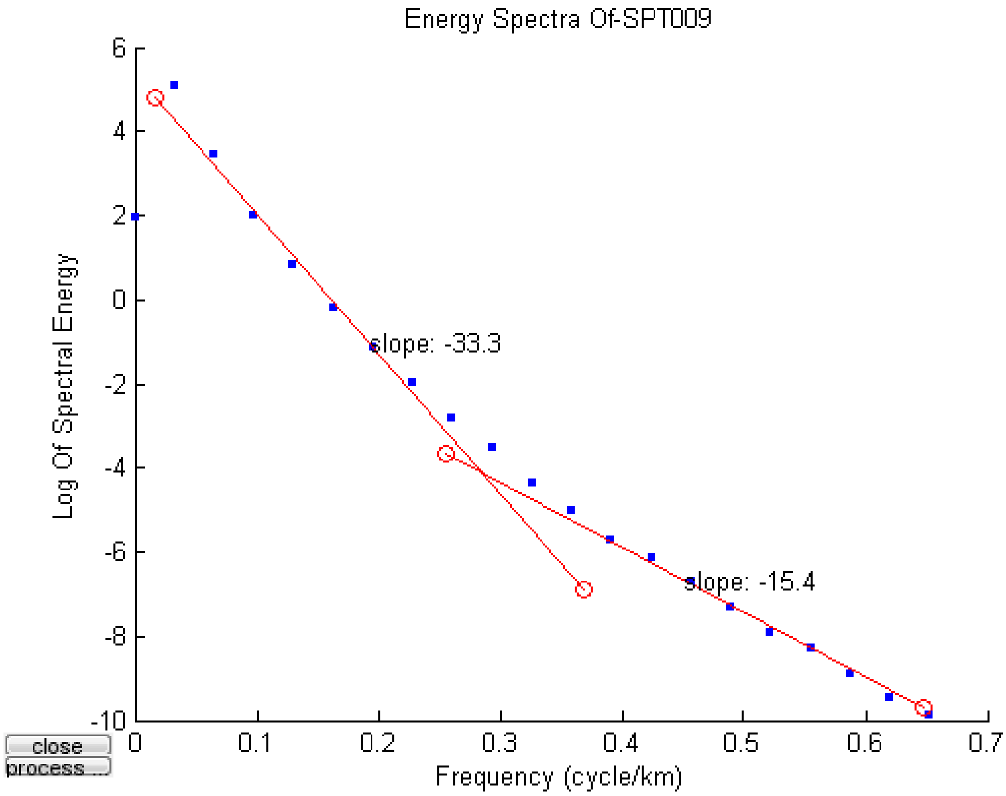
Energy Spectra Of-SPT009
Log Of Spectral Energy
Frequency (cycle/km)
slope: -33.3
slope: -15.4
close
process ...

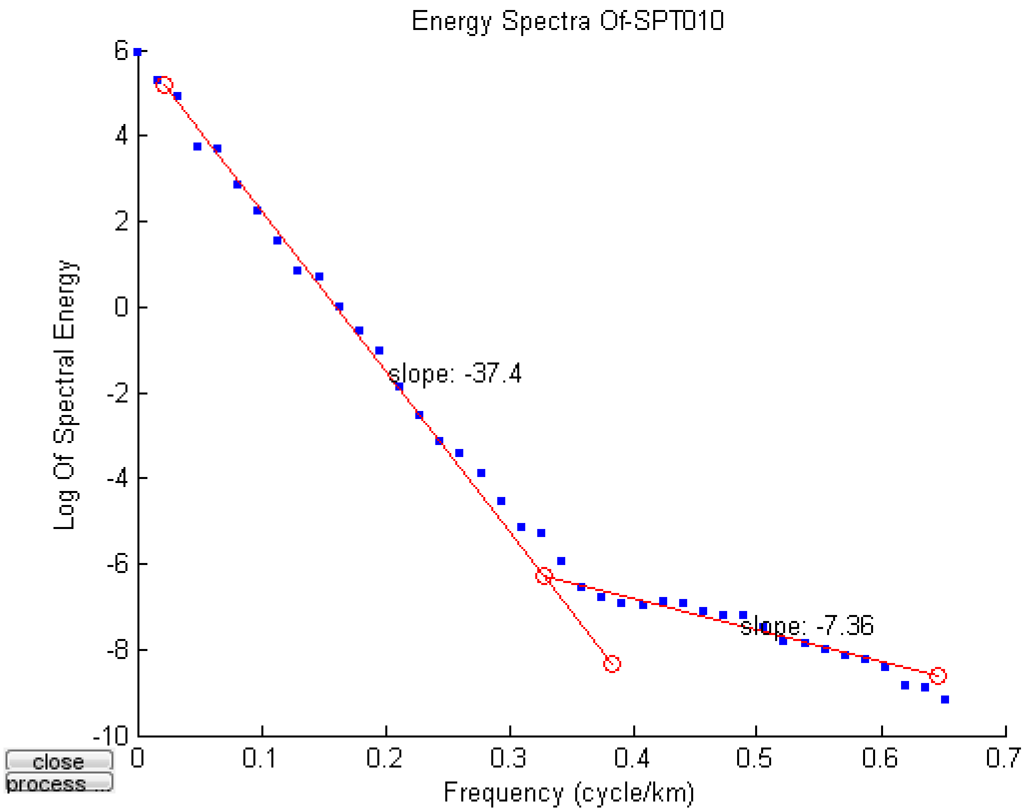
Energy Spectra Of-SPT010
Log Of Spectral Energy
Frequency (cycle/km)
slope: -37.4
slope: -7.36
close
process ...

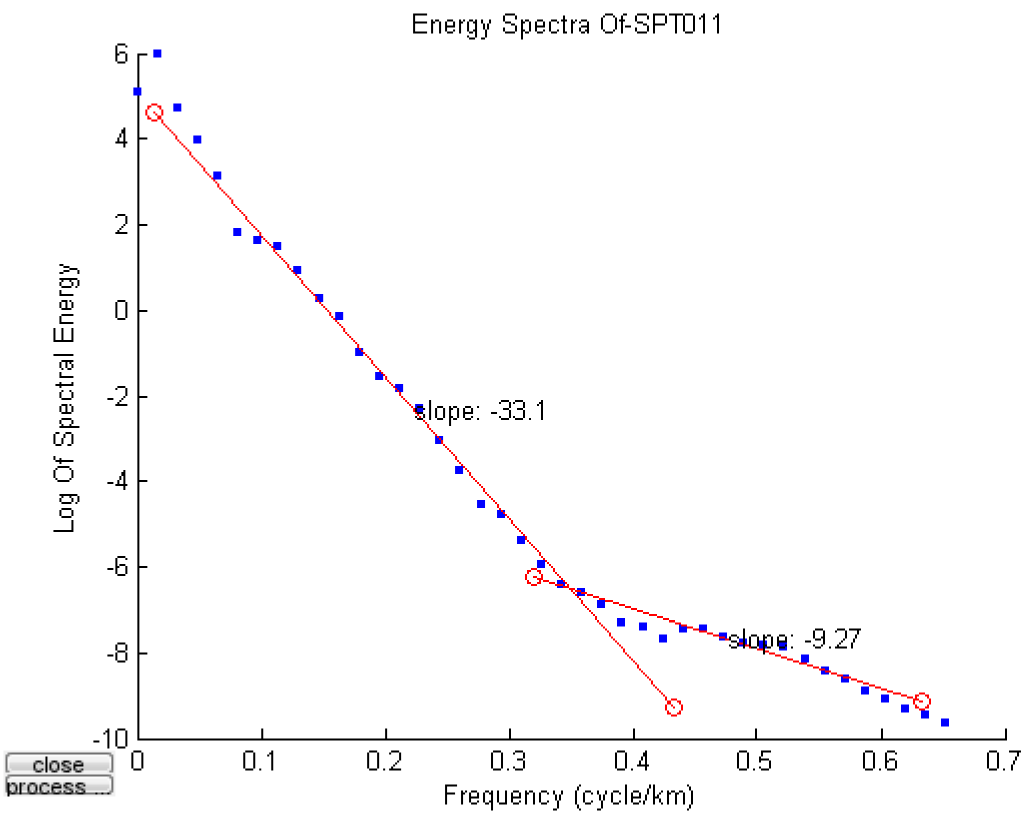
Energy Spectra Of-SPT011
Log Of Spectral Energy
Frequency (cycle/km)
slope: -33.1
slope: -9.27
6
4
2
0
-2
-4
-6
-8
-10
0
0.1
0.2
0.3
0.4
0.5
0.6
0.7
close
process ...

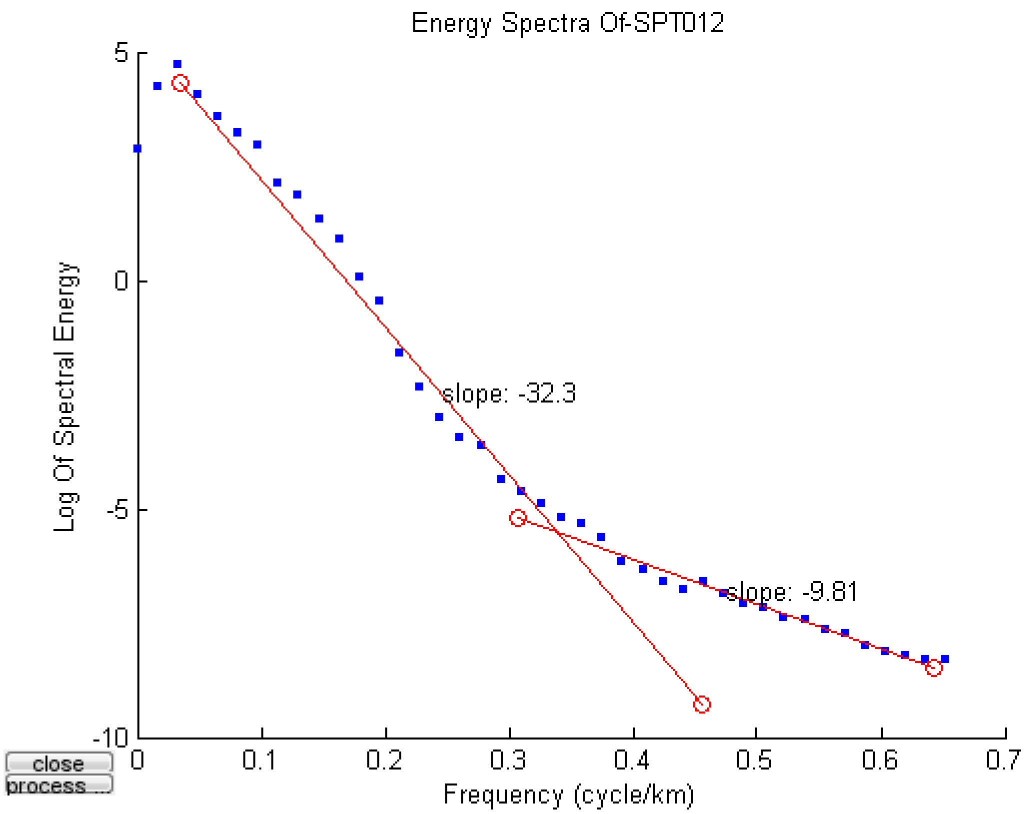
Energy Spectra Of-SPT012
Log Of Spectral Energy
Frequency (cycle/km)
slope: -32.3
slope: -9.81
5
0
-5
-10
0
0.1
0.2
0.3
0.4
0.5
0.6
0.7
close
process ...

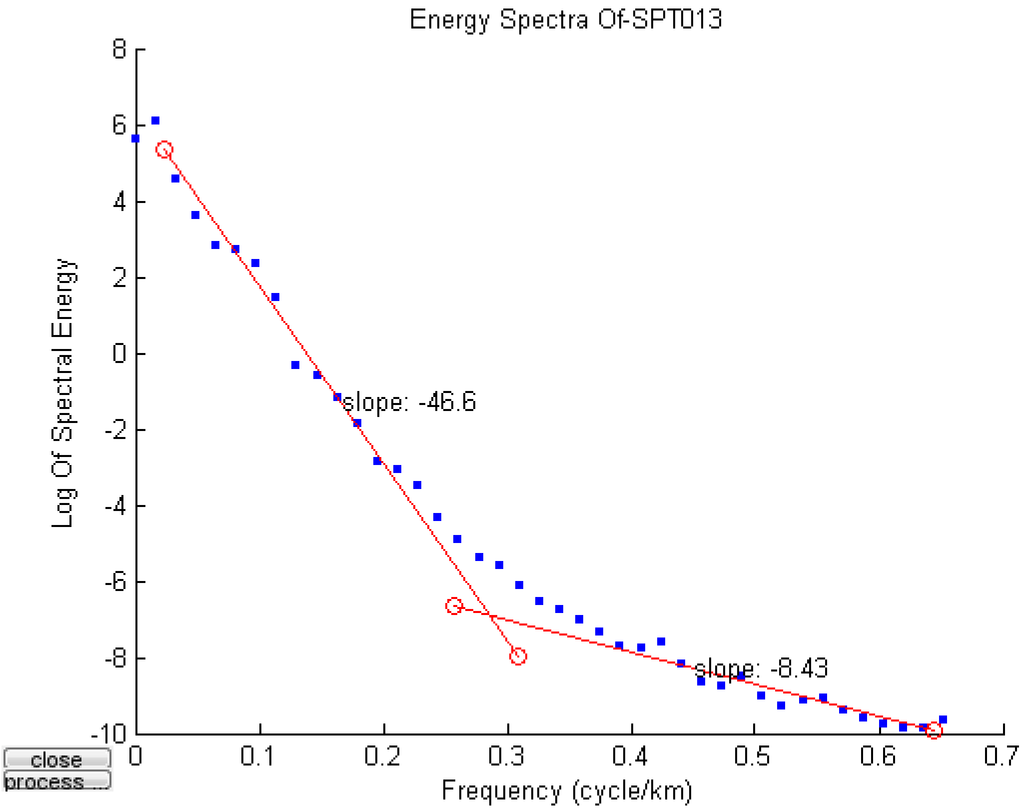
Energy Spectra Of-SPT013
Log Of Spectral Energy
Frequency (cycle/km)
slope: -46.6
slope: -8.43
close
process ...

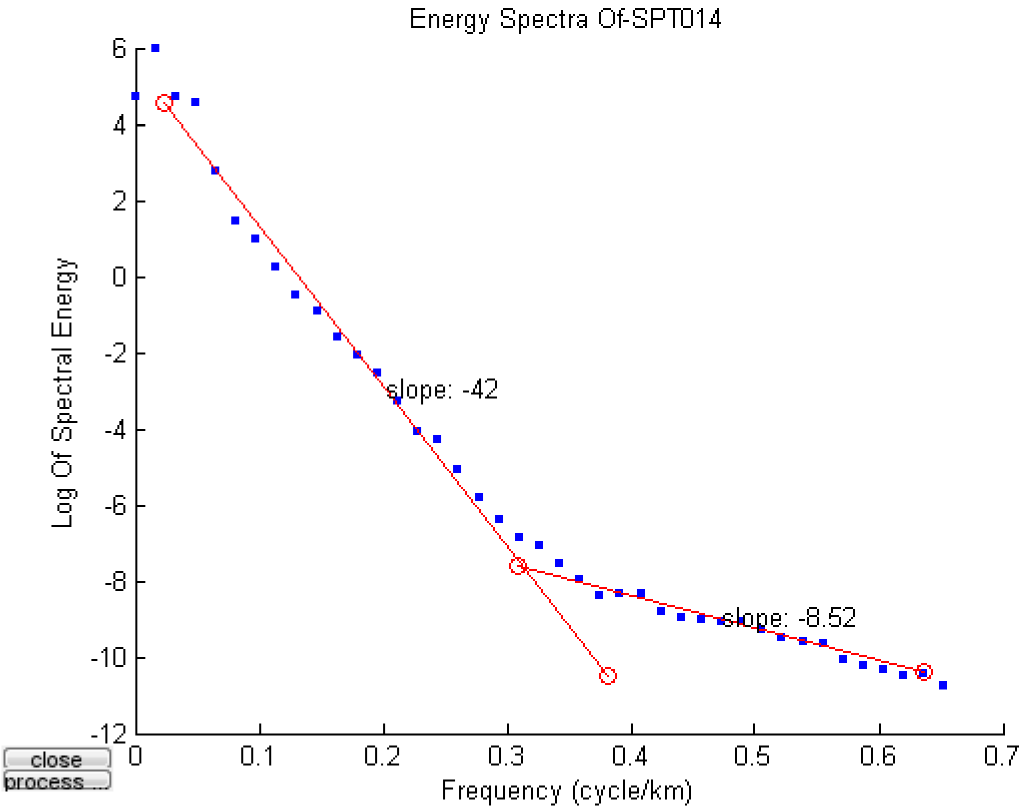
Energy Spectra Of-SPT014
Log Of Spectral Energy
Frequency (cycle/km)
slope: -42
slope: -8.52
close
process ...

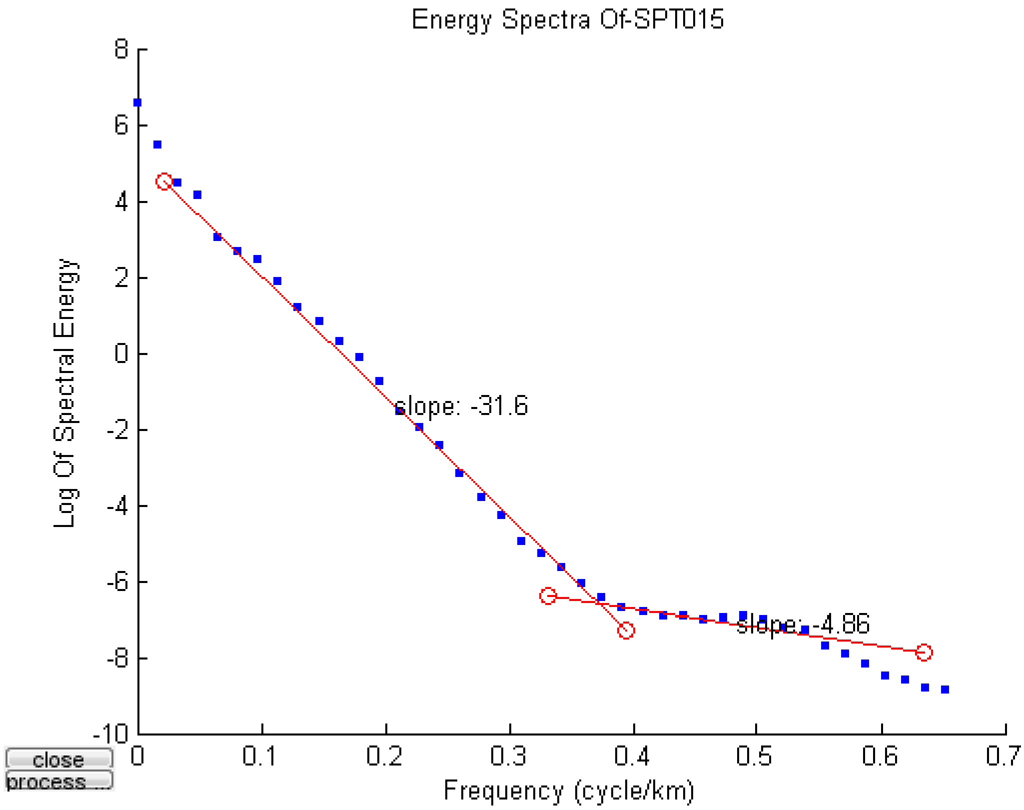
Energy Spectra Of-SPT015
Log Of Spectral Energy
Frequency (cycle/km)
slope: -31.6
slope: -4.86
close
process ...
8
6
4
2
0
-2
-4
-6
-8
-10
0
0.1
0.2
0.3
0.4
0.5
0.6
0.7

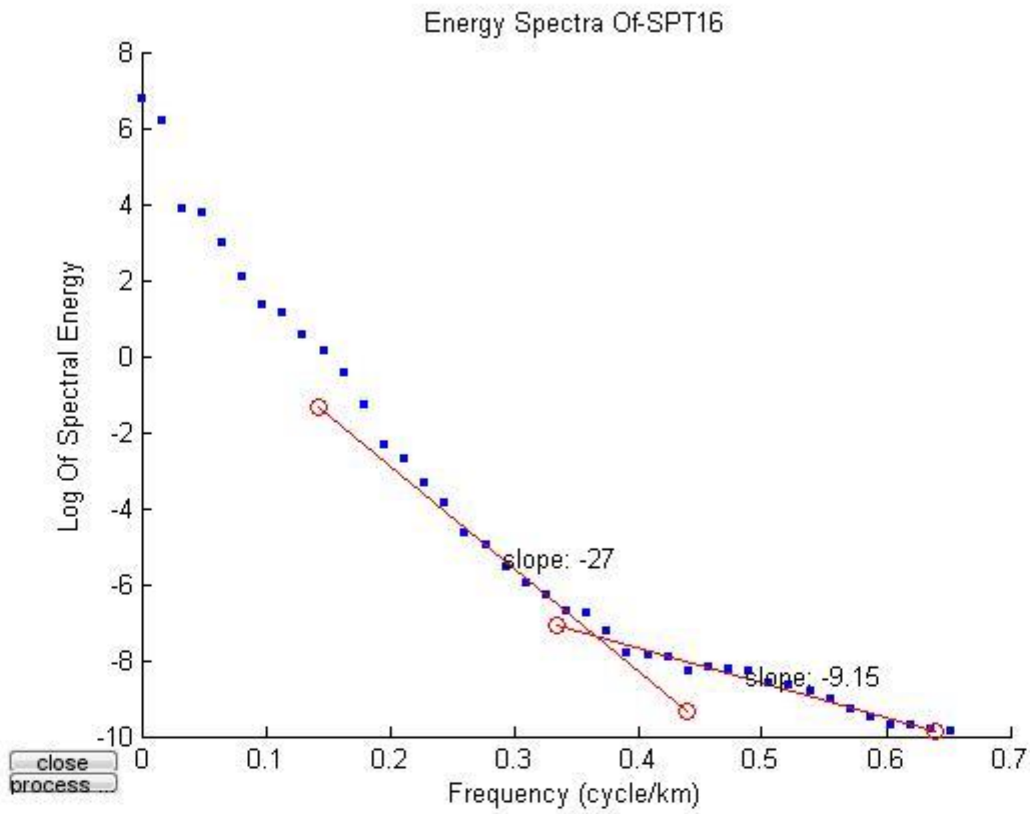
Energy Spectra Of-SPT16
Log Of Spectral Energy
Frequency (cycle/km)
slope: -27
slope: -9.15
close
process ...
8
6
4
2
0
-2
-4
-6
-8
-10
0
0.1
0.2
0.3
0.4
0.5
0.6
0.7

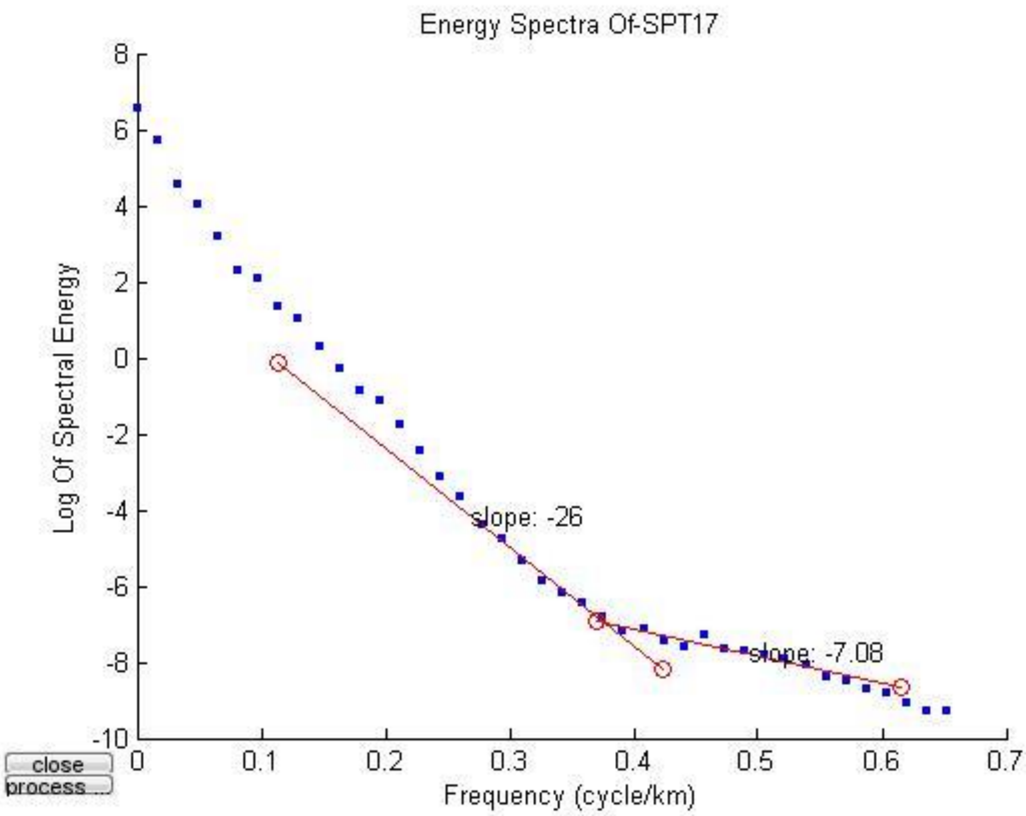
Energy Spectra Of-SPT17
Log Of Spectral Energy
Frequency (cycle/km)
slope: -26
slope: -7.08
close
process ...

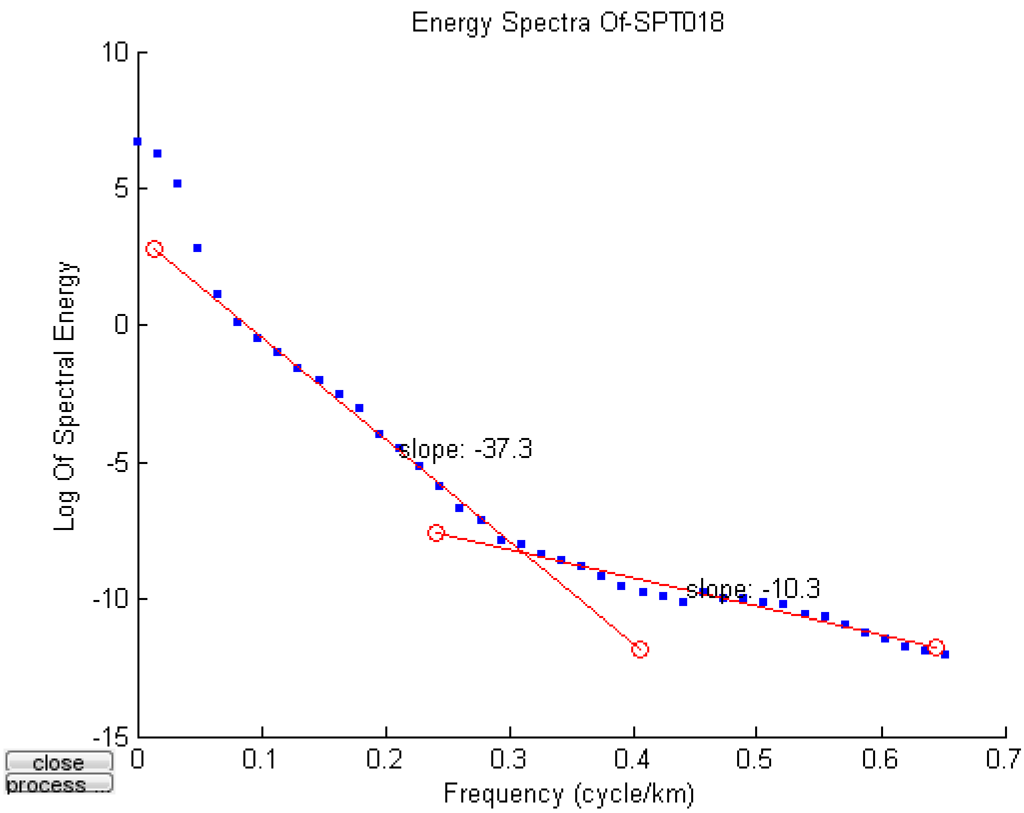
Energy Spectra Of-SPT018
Log Of Spectral Energy
Frequency (cycle/km)
slope: -37.3
slope: -10.3
close
process ...

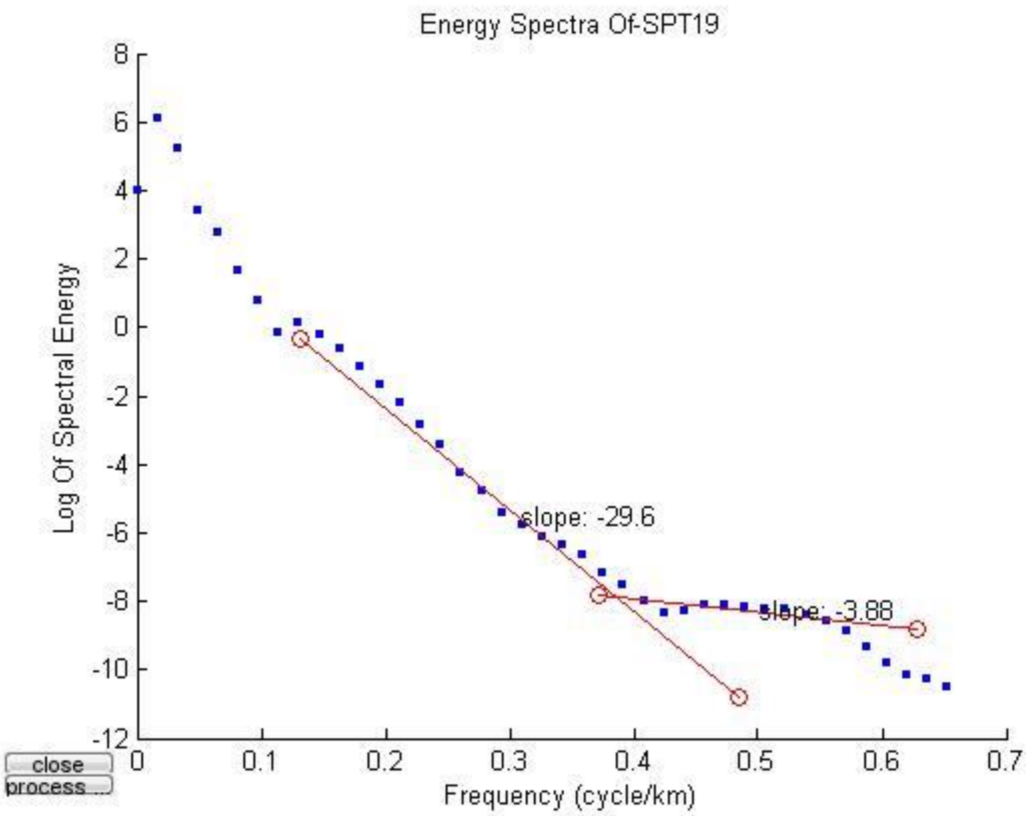
Energy Spectra Of-SPT19
Log Of Spectral Energy
Frequency (cycle/km)
slope: -29.6
slope: -3.88
close
process ...

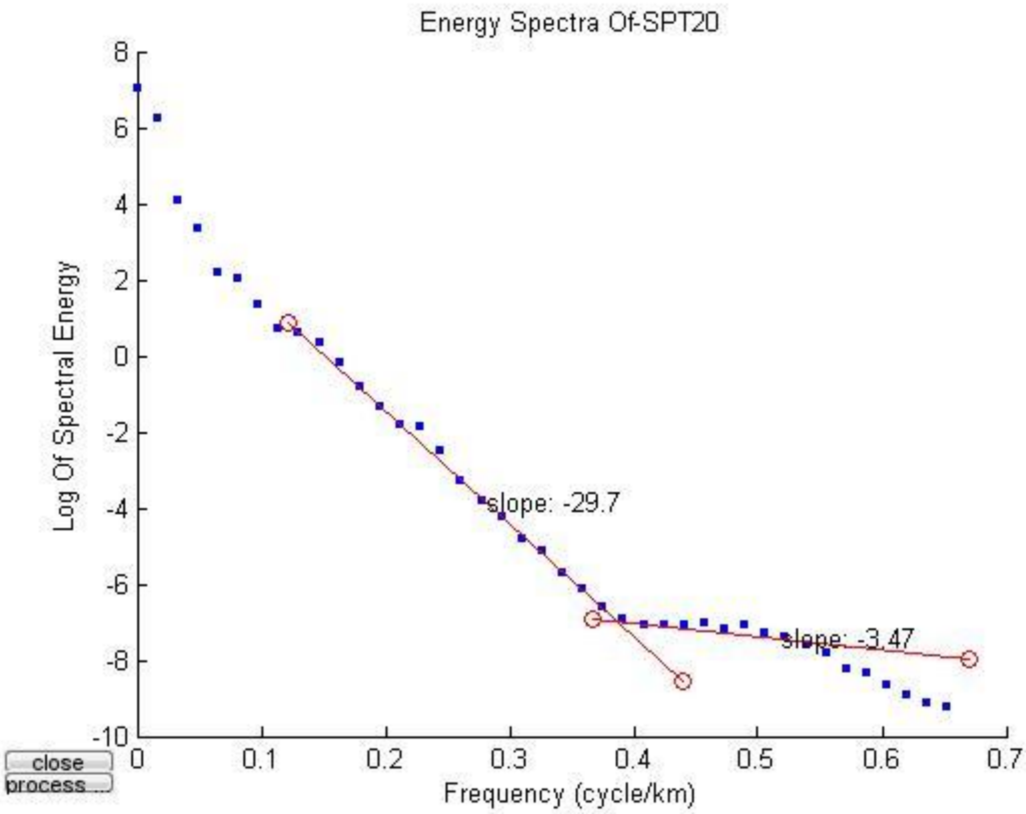
Energy Spectra Of-SPT20
Log Of Spectral Energy
Frequency (cycle/km)
slope: -29.7
slope: -3.47
close
process ...

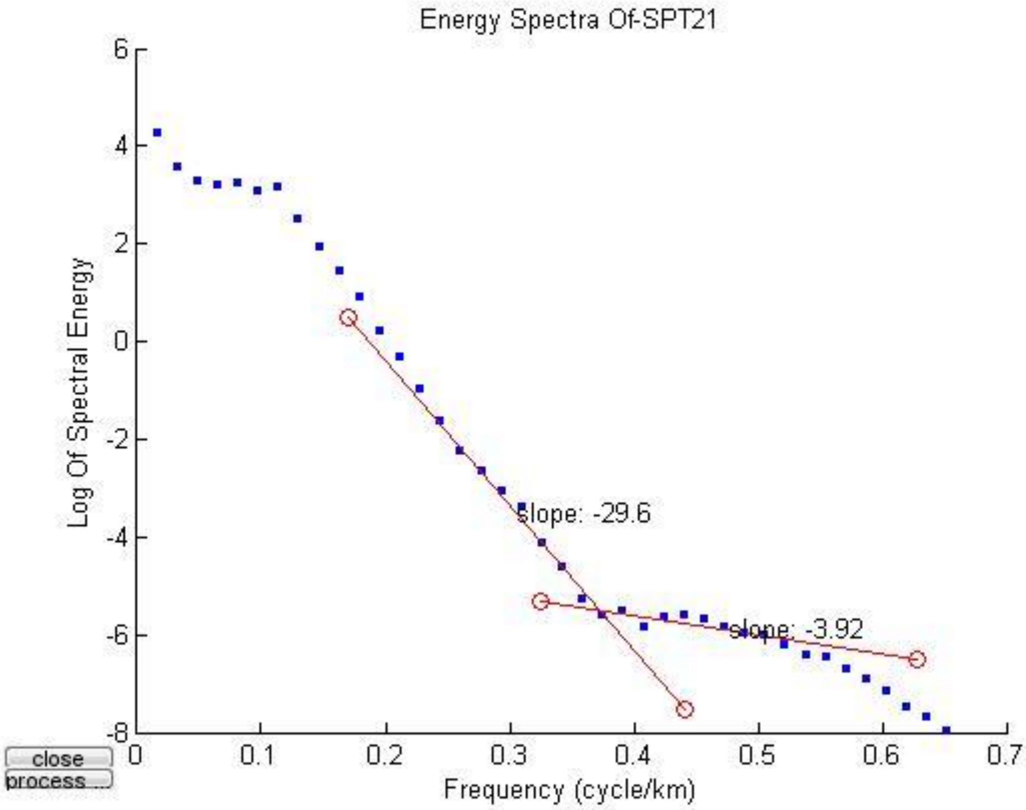
Energy Spectra Of-SPT21
Log Of Spectral Energy
Frequency (cycle/km)
slope: -29.6
slope: -3.92
close
process ...

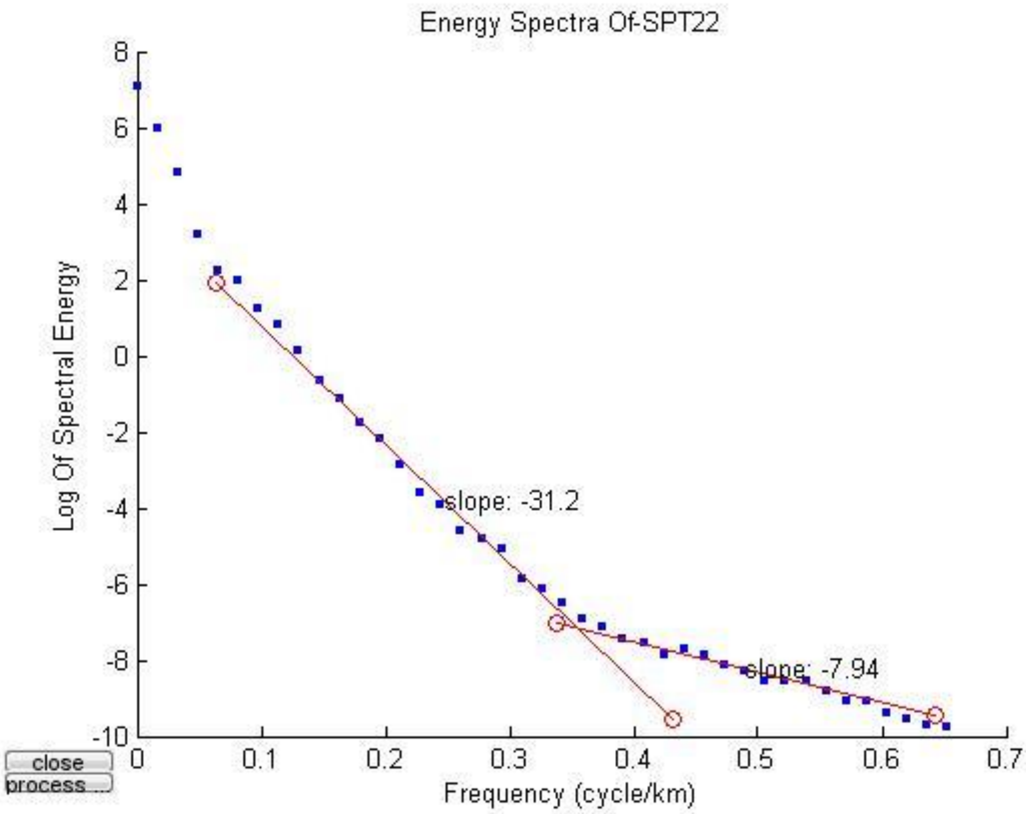
Energy Spectra Of-SPT22
Log Of Spectral Energy
Frequency (cycle/km)
slope: -31.2
slope: -7.94
close
process ...

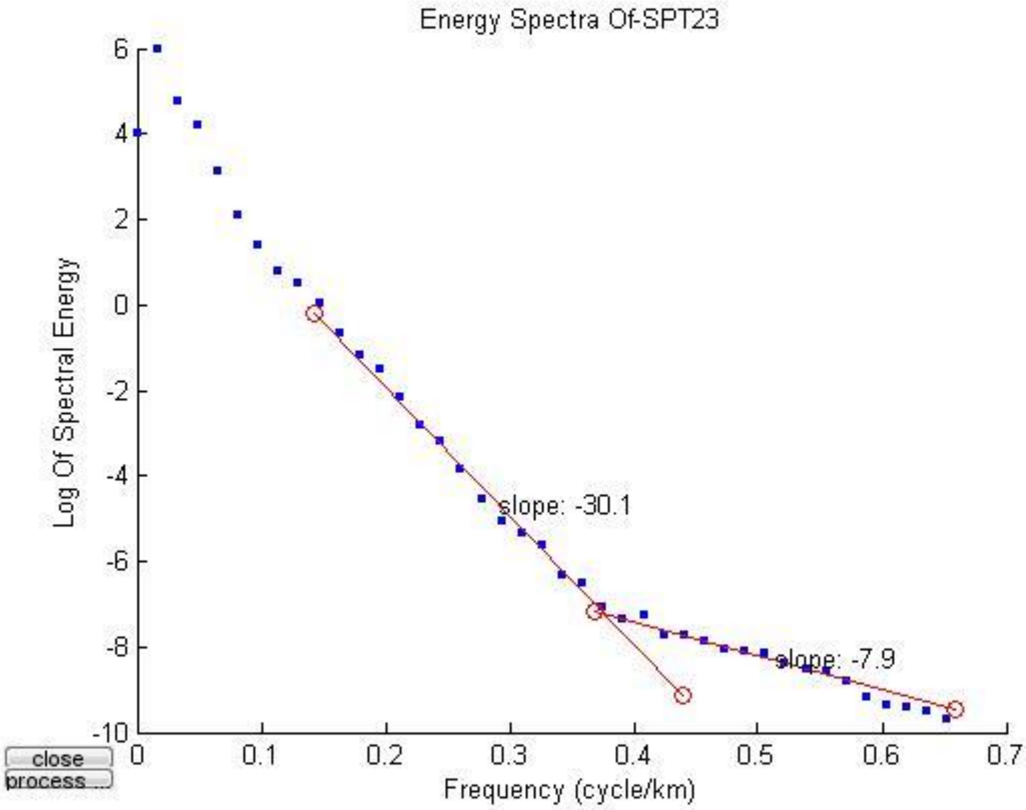
Energy Spectra Of-SPT23
Log Of Spectral Energy
Frequency (cycle/km)
slope: -30.1
slope: -7.9
close
process ...
6
4
2
0
-2
-4
-6
-8
-10
0
0.1
0.2
0.3
0.4
0.5
0.6
0.7

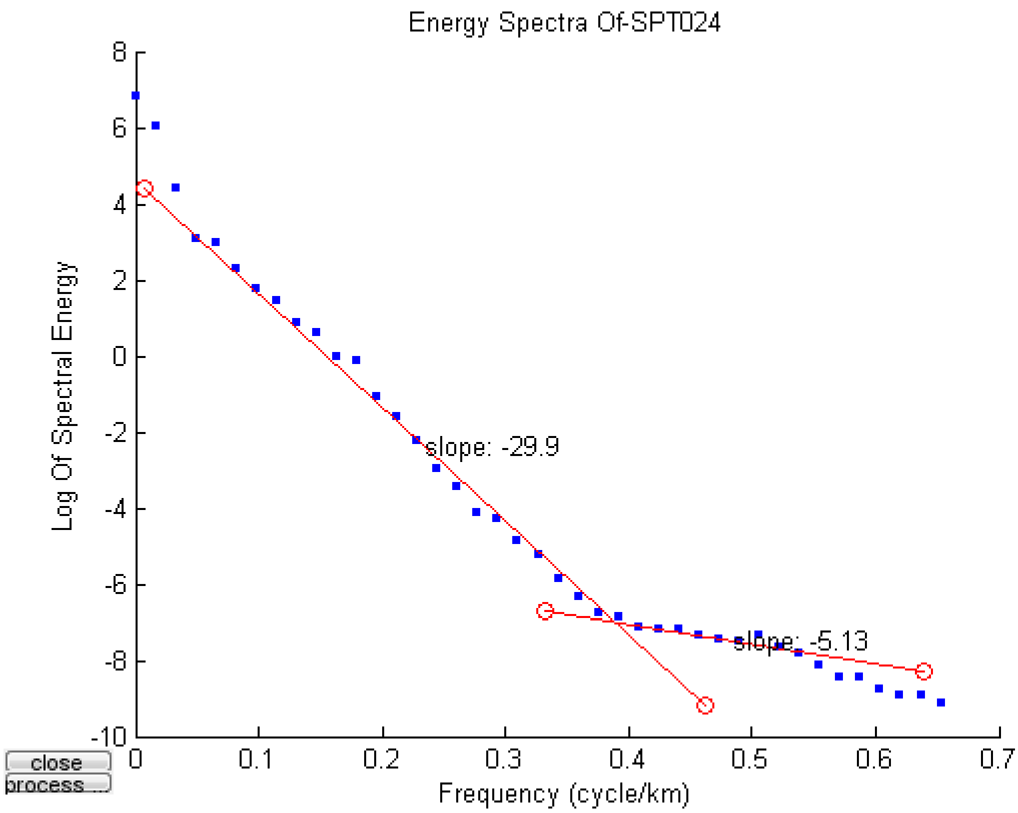
Energy Spectra Of-SPT024
Log Of Spectral Energy
Frequency (cycle/km)
slope: -29.9
slope: -5.13
close
process ...
8
6
4
2
0
-2
-4
-6
-8
-10
0
0.1
0.2
0.3
0.4
0.5
0.6
0.7

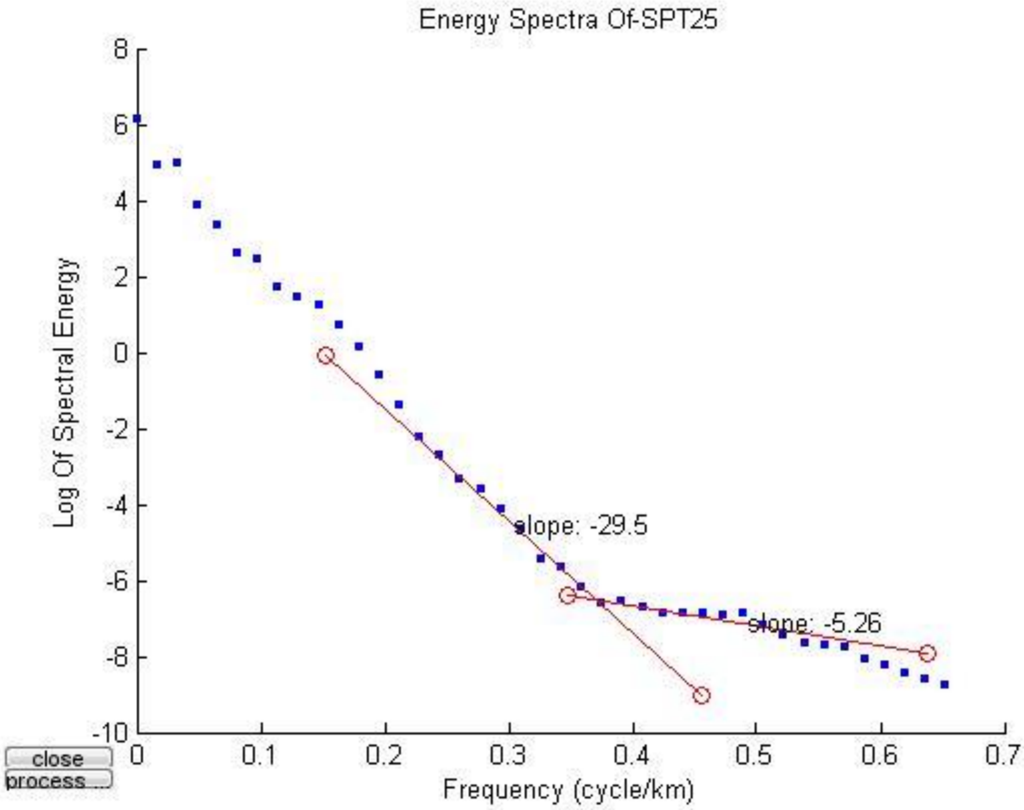
Energy Spectra Of-SPT25
Log Of Spectral Energy
Frequency (cycle/km)
slope: -29.5
slope: -5.26
close
process ...

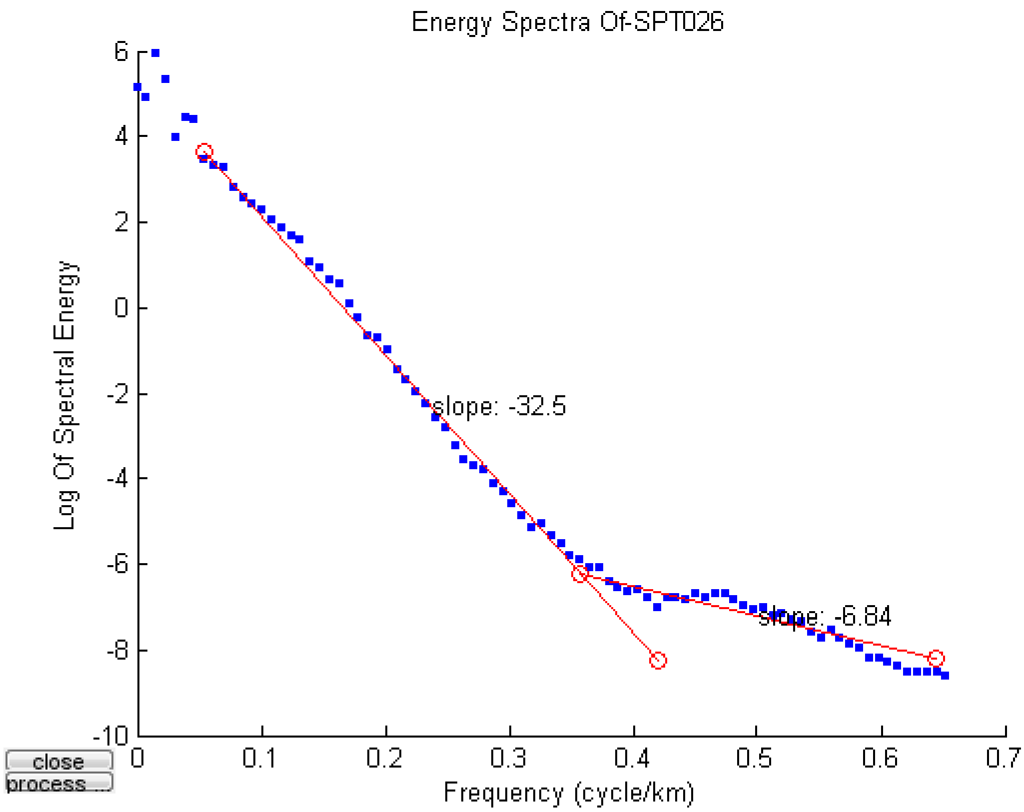
Energy Spectra Of-SPT026
Log Of Spectral Energy
Frequency (cycle/km)
slope: -32.5
slope: -6.84
close
process ...

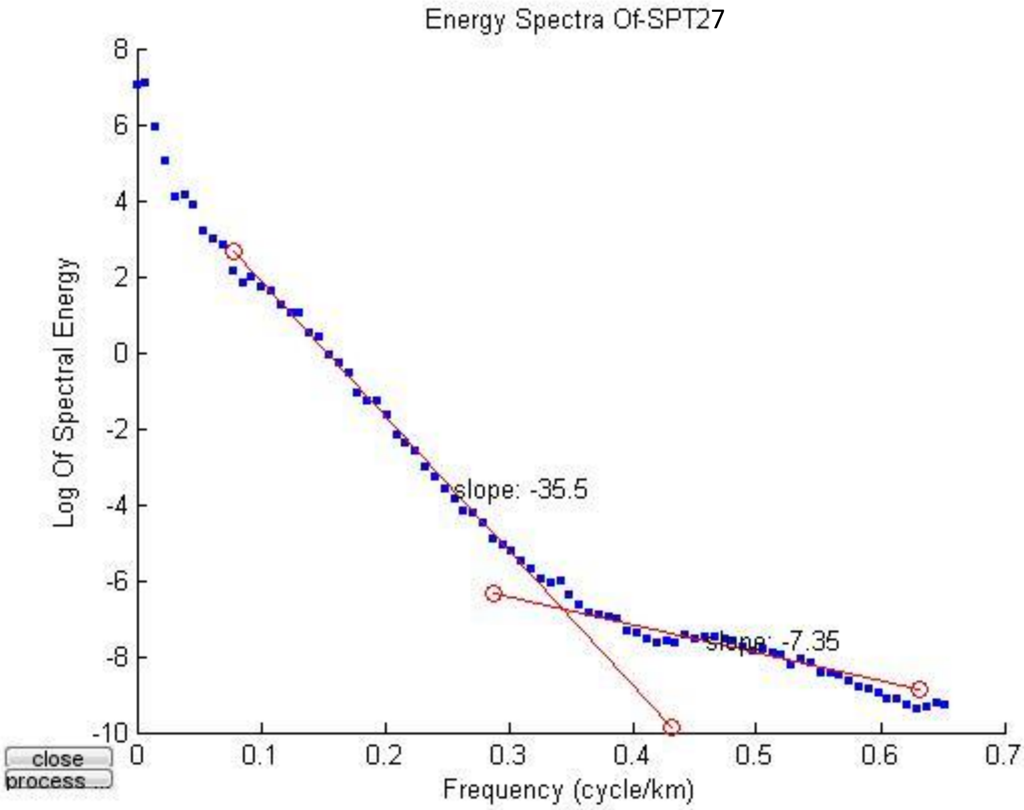
Energy Spectra Of-SPT27
8
6
4
2
0
-2
-4
-6
-8
-10
Log Of Spectral Energy
slope: -35.5
slope: -7.35
close
process ...
0
0.1
0.2
0.3
0.4
0.5
0.6
0.7
Frequency (cycle/km)

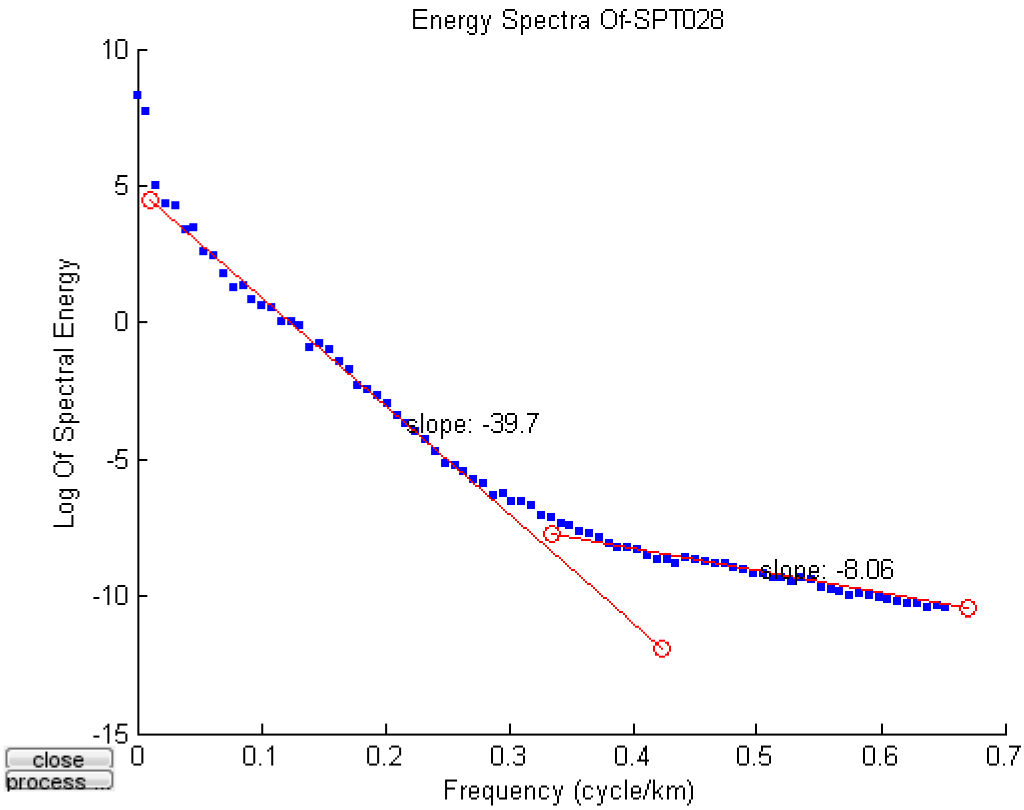
Energy Spectra Of-SPT028
10
5
0
-5
-10
-15
Log Of Spectral Energy
slope: -39.7
slope: -8.06
close
process ...
0
0.1
0.2
0.3
0.4
0.5
0.6
0.7
Frequency (cycle/km)

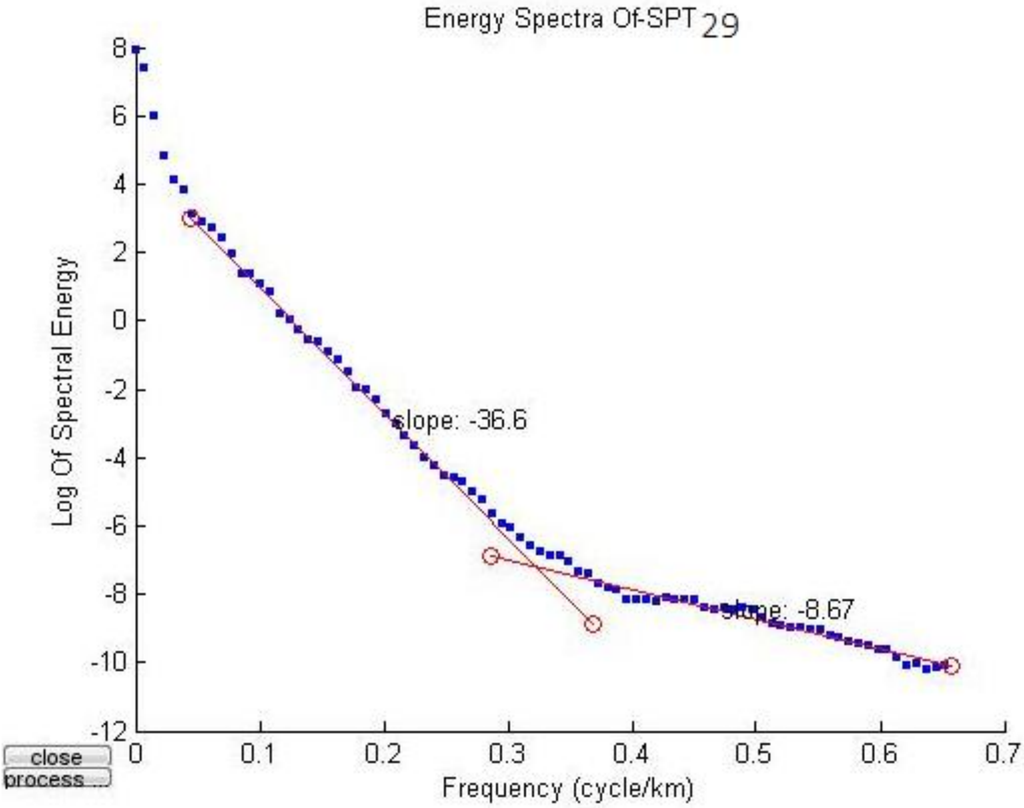
Energy Spectra Of-SPT 29
slope: -36.6
slope: -8.67
Log Of Spectral Energy
Frequency (cycle/km)
close
process

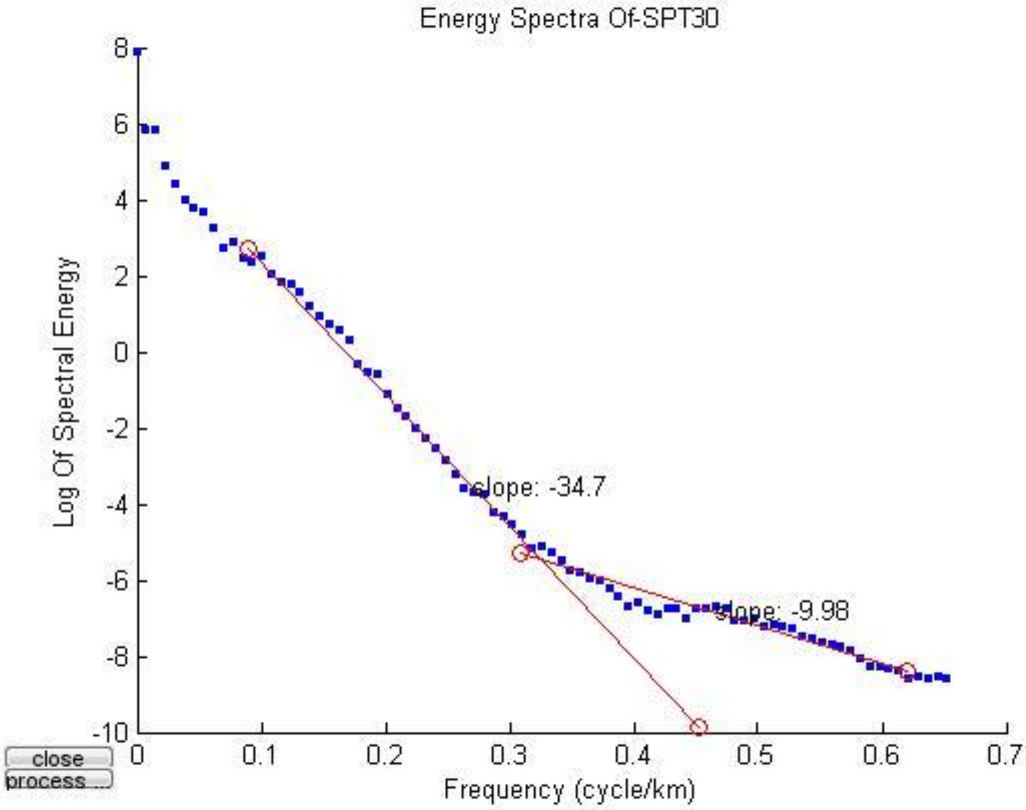
Energy Spectra Of-SPT30
slope: -34.7
slope: -9.98
Log Of Spectral Energy
Frequency (cycle/km)
close
process

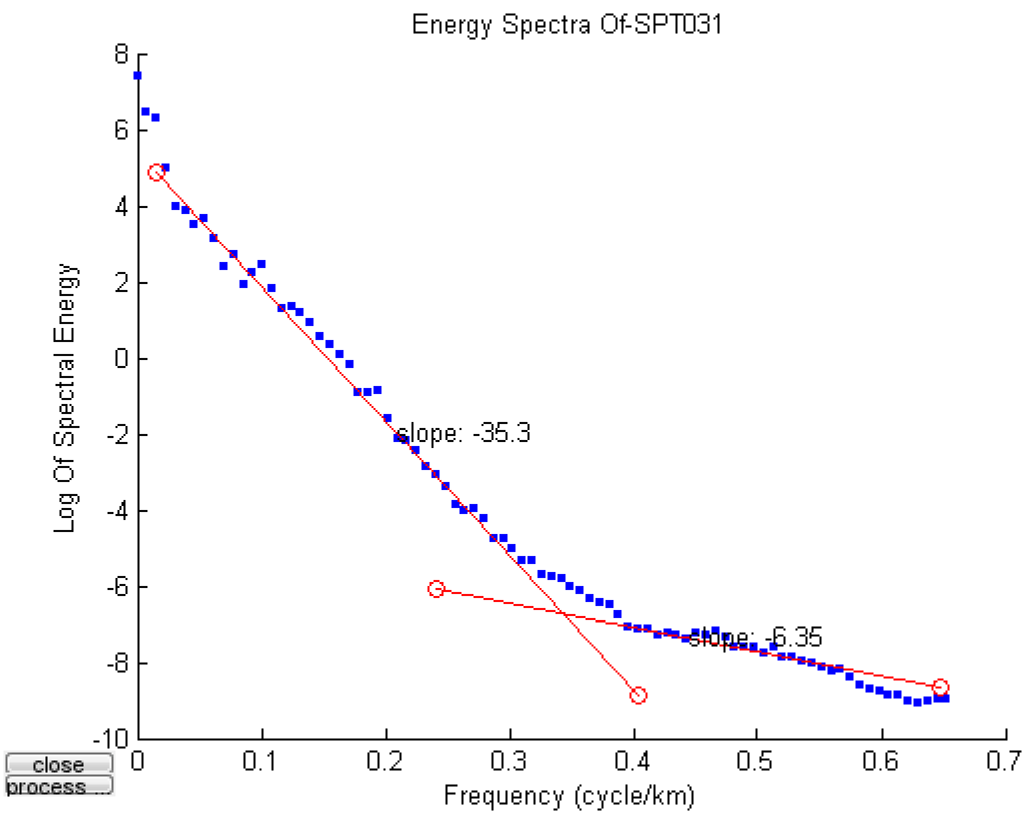
Energy Spectra Of-SPT031
Log Of Spectral Energy
Frequency (cycle/km)
slope: -35.3
slope: -6.35
close
process ...

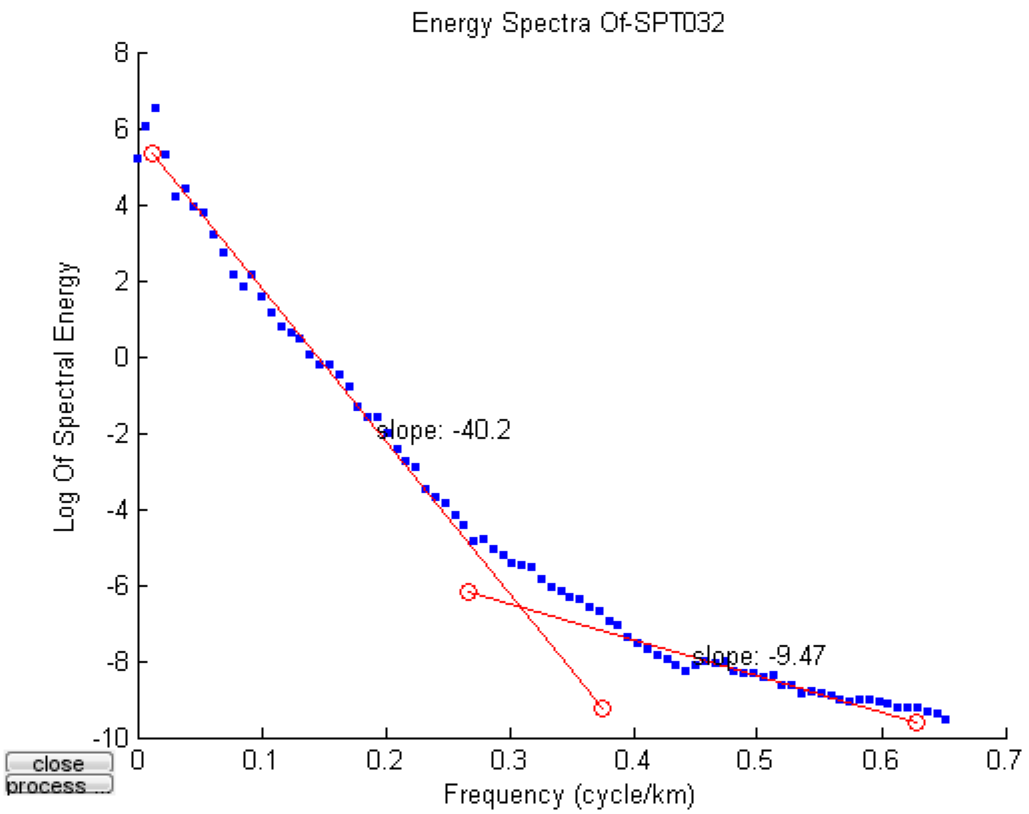
Energy Spectra Of-SPT032
Log Of Spectral Energy
Frequency (cycle/km)
slope: -40.2
slope: -9.47
close
process ...

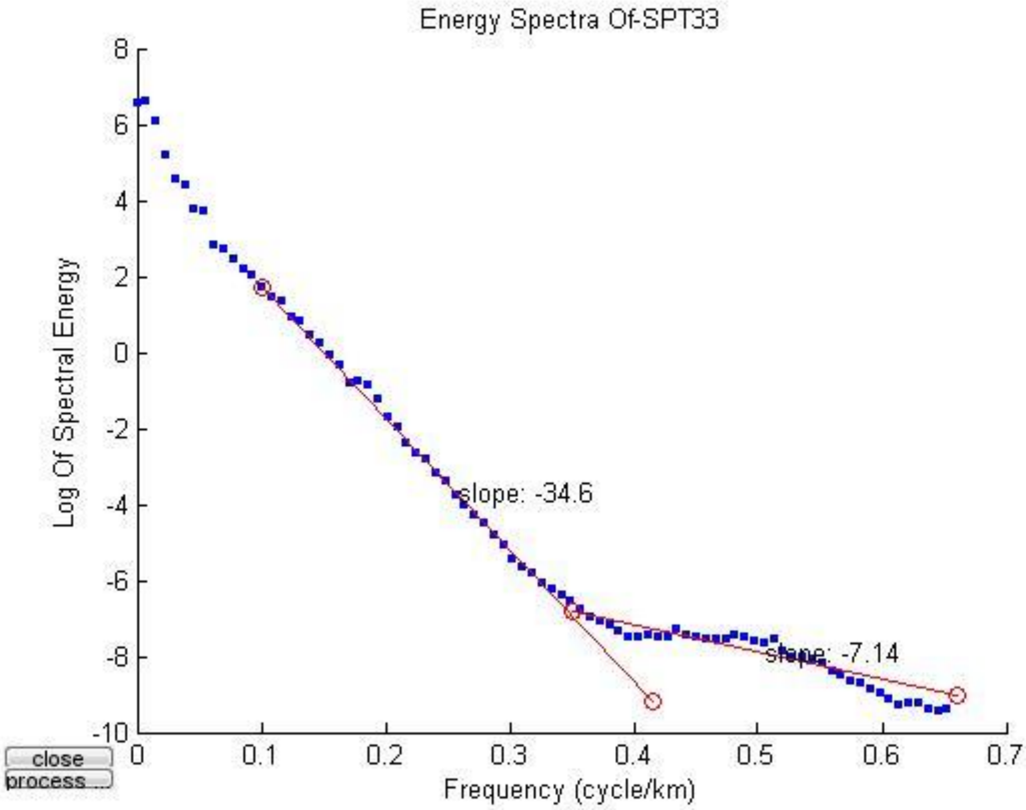
Energy Spectra Of-SPT33
Log Of Spectral Energy
Frequency (cycle/km)
slope: -34.6
slope: -7.14
close
process ...

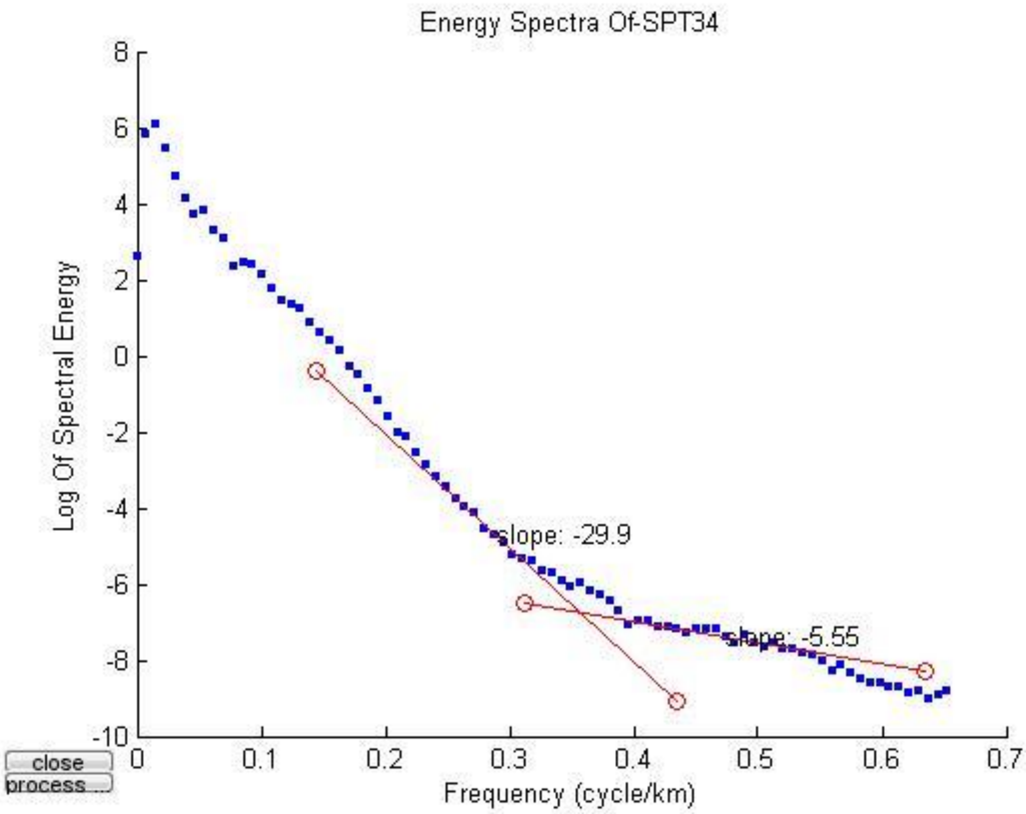
Energy Spectra Of-SPT34
Log Of Spectral Energy
Frequency (cycle/km)
slope: -29.9
slope: -5.55
close
process ...

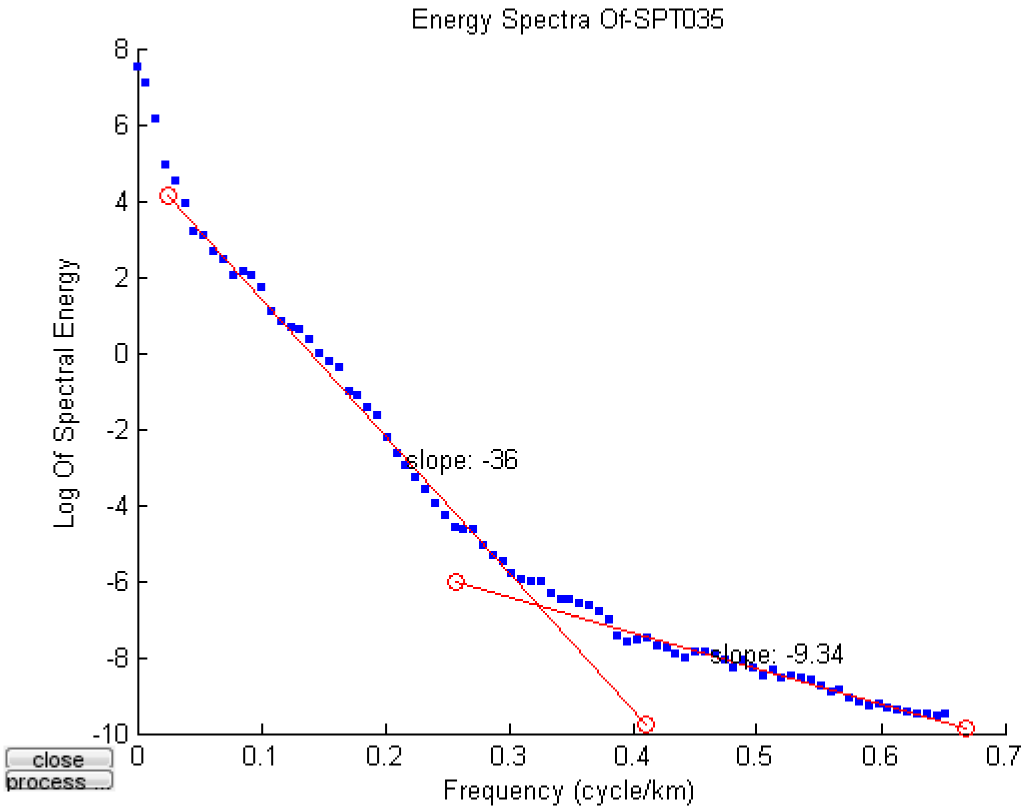
Energy Spectra Of-SPT035
Log Of Spectral Energy
Frequency (cycle/km)
slope: -36
slope: -9.34
close
process ...
8
6
4
2
0
-2
-4
-6
-8
-10
0
0.1
0.2
0.3
0.4
0.5
0.6
0.7

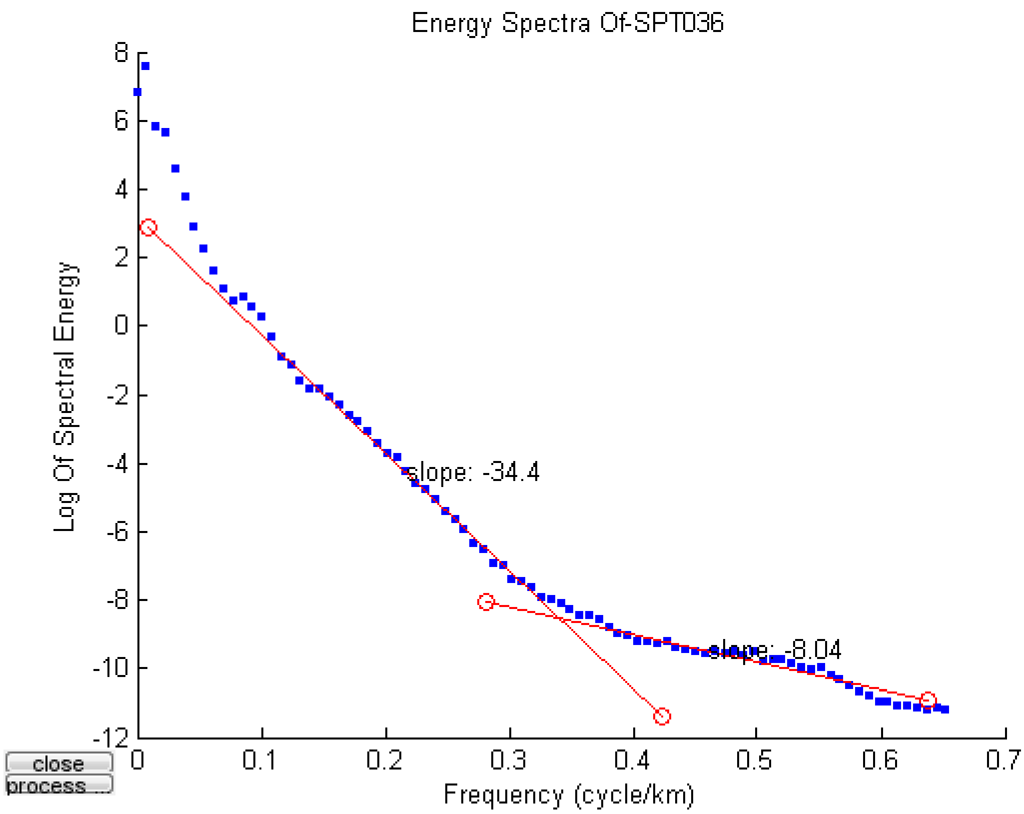
Energy Spectra Of-SPT036
Log Of Spectral Energy
Frequency (cycle/km)
slope: -34.4
slope: -8.04
close
process ...
8
6
4
2
0
-2
-4
-6
-8
-10
-12
0
0.1
0.2
0.3
0.4
0.5
0.6
0.7

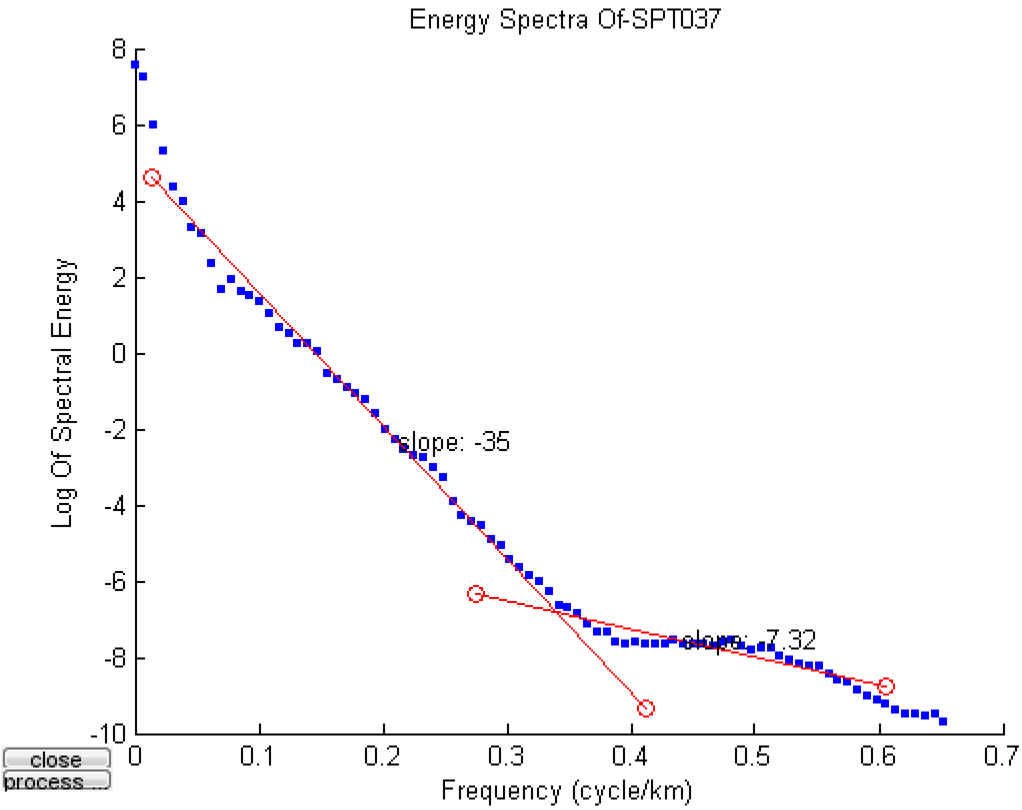
Energy Spectra Of-SPT037
Log Of Spectral Energy
Frequency (cycle/km)
slope: -35
slope: -7.32
close
process ...

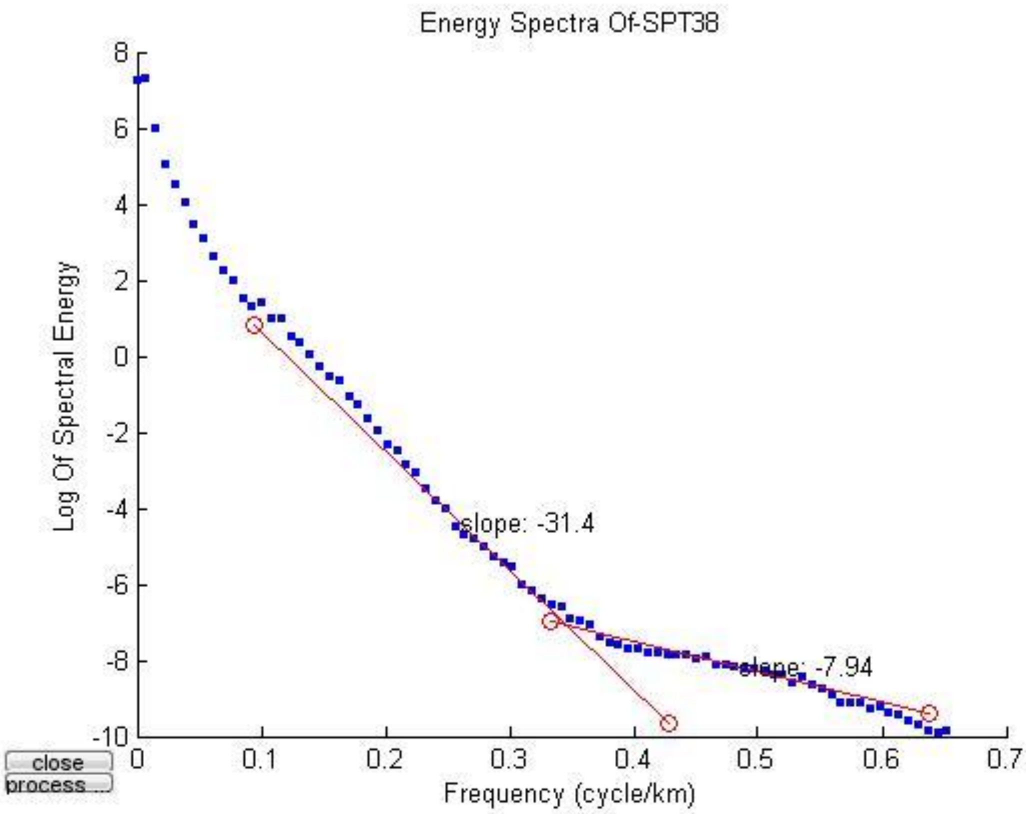
Energy Spectra Of-SPT38
Log Of Spectral Energy
Frequency (cycle/km)
slope: -31.4
slope: -7.94
close
process ...

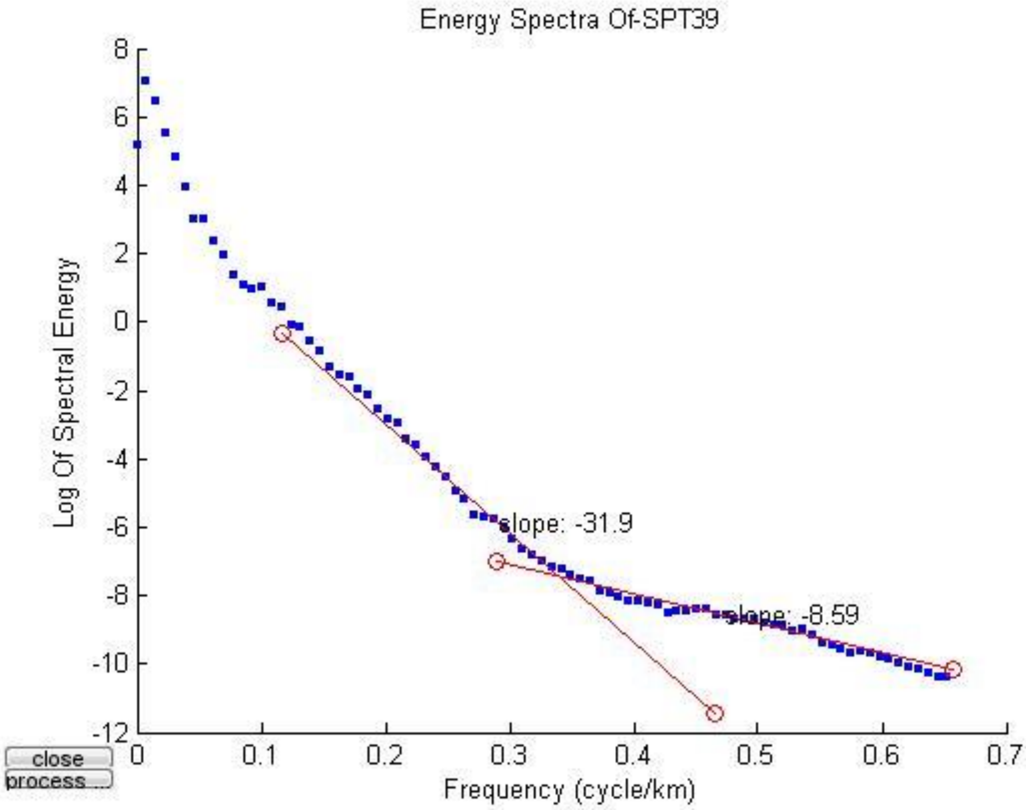
Energy Spectra Of-SPT39
Log Of Spectral Energy
Frequency (cycle/km)
slope: -31.9
slope: -8.59
close
process ...

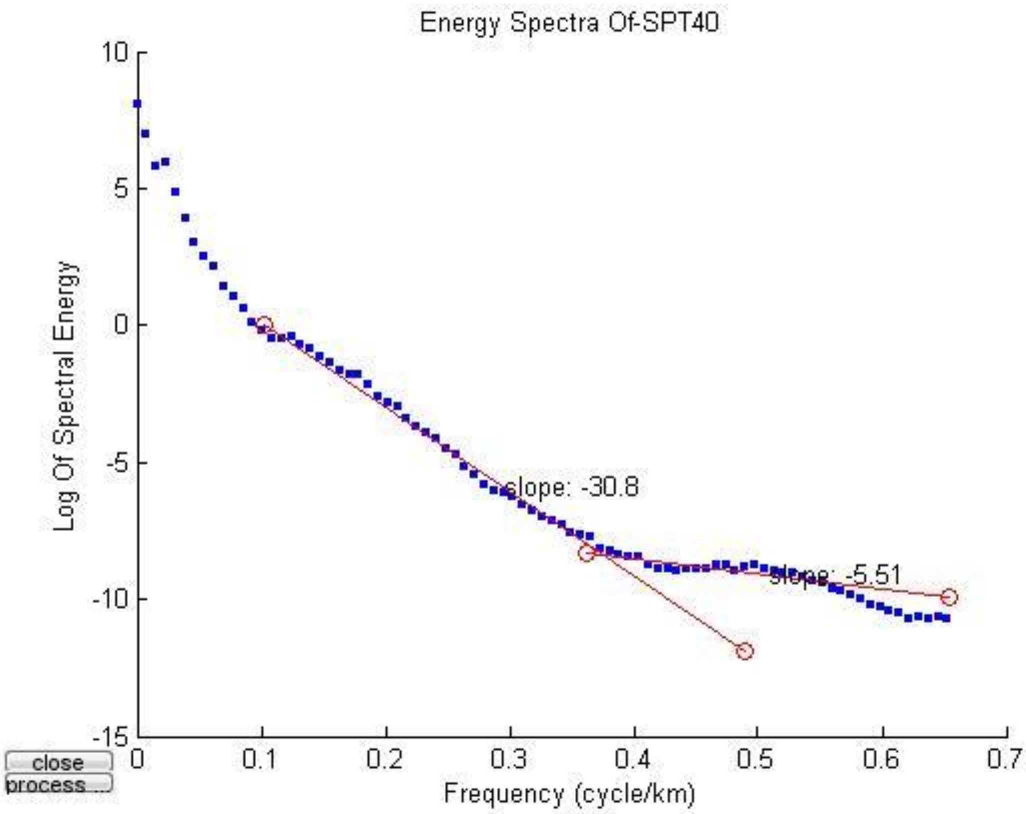
Energy Spectra Of-SPT40
Log Of Spectral Energy
Frequency (cycle/km)
slope: -30.8
slope: -5.51
close
process ...

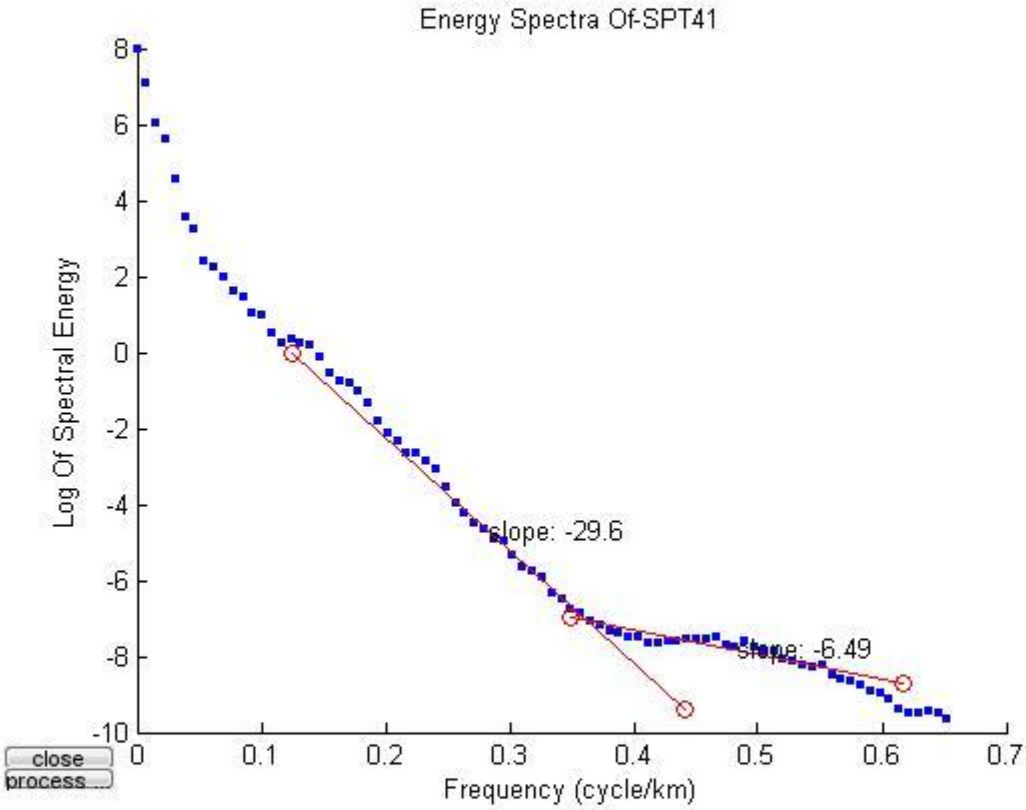

Energy Spectra Of-SPT41
Log Of Spectral Energy
8
6
4
2
0
-2
-4
-6
-8
-10
slope: -29.6
slope: -6.49
0
0.1
0.2
0.3
0.4
0.5
0.6
0.7
Frequency (cycle/km)
close
process ...